UNIVERSITÉ DE GENÈVE FACULTÉ DES SCIENCES

Professeur M. Stoffel

Section des sciences de la Terre et de l´environnement

Institut des sciences de l'environnement

Deciphering natural hazard histories based on tree-ring analyses in contrasting tropical ecosystems of Costa Rica

THÈSE

présentée à la Faculté des sciences de l'Université de Genève

pour obtenir le grade de Docteur ès Sciences, mention sciences de l'environnement

par

Adolfo QUESADA ROMÁN

de

San Vito (COSTA RICA)

Thèse N° -5518-

GENÈVE

2020

Deciphering natural hazard histories based on tree-ring analyses in contrasting tropical ecosystems of Costa Rica

UNIVERSITÉ DE GENÈVE

FACULTÉ DES SCIENCES

DOCTORAT ÈS SCIENCES, MENTION SCIENCES DE L'ENVIRONNEMENT

Thèse de Monsieur Adolfo QUESADA ROMAN

intitulée :

«Deciphering Natural Hazard Histories Based on Tree-Ring Analyses in Contrasting Tropical Ecosystems of Costa Rica»

La Faculté des sciences, sur le préavis de Monsieur M. STOFFEL, professeur ordinaire et directeur de thèse (Département F.-A. Forel des sciences de l'environnement et de l'eau), Monsieur J. A. BALLESTEROS-CANOVAS, docteur et codirecteur de thèse (Institut des sciences de l'environnement (ISE) de l'Université de Genève), Monsieur S. ST GEORGE, professeur (Department of Geography, University of Minnesota, Twin Cities, United States of America), Monsieur C.CORONA, docteur (CNRS Géolab, Université Clermont-Auvergne, Clermont-Ferrand, France), autorise l'impression de la présente thèse, sans exprimer d'opinion sur les propositions qui y sont énoncées.

Genève, le 4 décembre 2020

Thèse - 5518 -

Le Doyen

N.B. - La thèse doit porter la déclaration précédente et remplir les conditions énumérées dans les "Informations relatives aux thèses de doctorat à l'Université de Genève".

Copyrights

Compliance with Ethical Standards

All authors declare that they have no conflict of interest. This thesis does not contain any studies with animals or human participants performed by any of the authors.

Acknowledgements

First, I want to thank God for giving me peace in my moments of struggle as well as keeping me focused on my goal. To Markus Stoffel, I give all my gratitude for having trusted in me and having given me the opportunity to join his marvellous group in Geneva, I will be eternally grateful. I would like to pay my special regards to Juan Ballesteros who guided me along the Doctoral Program and has become a true friend. I wish to thank Scott St. George and Christophe Corona for being part of the Examination Committee and for giving me important imprints to improve the final manuscript. I would like to thank to my parents Gerardo and Rosa Elena, and my brother Isaac for giving me the strength and determination needed to accomplish this important goal in my life. I would also like to say thank you to all my family who supported me through the time. A special gratitude to my brother Leonardo Quesada who assisted me many times on the field and supported me as no one else could on this Earth. To my best friends Ricardo Quesada and Gustavo Pineda who have been always there.

To Isabel Avendaño and Luis Guillermo Brenes for their confidence in me. Also, to Christian Birkel, Pascal Girot, Deilyn Porras, Sebastián Granados, Paula M. Pérez, Manuel Camacho, Alfredo Alvarado, Eric Alfaro, Hugo Hidalgo, Mauricio Mora, Giovanni Peraldo, Jorge Alpízar, and Diego Hidalgo from University of Costa Rica who always were present and supported me during this time. To Lilliam Quirós, Marilyn Romero, Meylin Alvarado, Daniel Avendaño, Consuelo Alfaro, Daniela Campos, Marjorie Vargas, Ana Vargas, Jenny Diaz, Mauricio Vega, Ricardo Sánchez, and Germain Esquivel from the National University of Costa Rica, thank you. To Russell Lee Losco and Daria Nikitina, dear friends and colleagues from the University of West Chester in Pennsylvania. To Sergio Feoli of the National Company of Force and Light for his great support before and during the Doctoral Program in many ways. To my botanical friends Marco Cedeño, Isler Chinchilla, Esteban Jiménez and Junior Porras for their assistance during fieldwork and woody plants species recognition.

To all the C-CIA team members and friends: Sébastien, Clara, Victorine, Lina, Laura, Alberto (*los deliciosuras*), Virginia, Gary, Simon, Jaime, Jérôme, Neema, Lianne, Guoxiong, Adrien, Loic, Sandra, Theo, Alejandra and Gabriel for giving me a terrific place to work, their support when I needed it and your friendship. To my friends at ISE: Alejandro, Pablo, Pierre, Chloe, Charlotte for great moments during my stay in Geneva. To different friends in Geneva as Mirza, Farik, Tela, Verónica, David, Michelle, Myke, Allan, Pedro, Marcela, Gisela, Paula, Cecilia and Daniel who were present during this nice time in Switzerland. I want to thank different employees from national public institutions (CNE, ICE, MINAE, SINAC) and universities (UCR, UNA, TEC) in Costa Rica who facilitated me important information and support for the different analyses for this research. To all the journals editors and reviewers who improved the manuscripts. To all that who have not been mentioned, I would like to recognize the invaluable assistance that you all provided during my study.

This study has benefitted from grants of the Swiss Federal Commission for Scholarships (ESKAS-Nr 2017.1072), Ministry of Science and Technology of Costa Rica (N°MICITT-PINN-CON-2-1-4-17-1-002), the University of Costa Rica (OAICE-187-2017), and an Assistantship of the Environmental Sciences Institute of the University of Geneva for three years from September 2017 to 2020.

Summary

Climatic and anthropogenic changes are contributing to the degradation of different ecosystems in Costa Rica, thereby altering climatic, ecological, and geomorphic conditions. The hypothesis of this PhD thesis is that high tropical biodiversity of Costa Rica and the tropics is suitable to improve the understanding of hydrogeomorphic process dynamics and to generate baseline data on past disasters in a limited-data region. The principal motivation to link natural hazards and dendrochronology in this low-latitude region is the persisting scarcity of data on past hydrogeomorphic processes and the desire to define methods that can reduce its exposure and vulnerability. The principal research aim of this study therefore was to provide reference data that can improve the understanding of hydrogeomorphic processes as well as to explore the potential of tropical tree species in dendrochronological applications. This study thus combines remote sensing, meteorological assessments and tree-ring techniques with statistical analyses, hydraulic modelling, and risk assessments. The innovative nature of this research described the very limited experience available in terms of tree-ring analysis in Costa Rica and the clear lack of understanding on past disasters and their linkage to climate. This study will likely contribute to the implementation of new methodologies in disaster risk research and will hopefully contribute to future adaptation strategies in the tropics, the most biodiverse region of the world.

Résumé

Le Costa Rica est une des régions du monde les plus exposées au réchauffement climatique. Les impacts du changement climatique auront une incidence sur les écosystèmes et la biodiversité, mais ils risquent également d'exposer un nombre plus importants de personnes à des aléas hydro-météorologiques, probablement plus fréquents et intenses, au cours des prochaines décennies. Les processus hydro-géomorphologiques (crues éclairs, glissements de terrain, laves torrentielles) qui découlent de ces épisodes hydro-météorologiques sont à l'origine de nombreuses victimes et de nombreux dégâts matériels, chaque année, mais restent paradoxalement assez peu étudiés au Costa Rica. Le manque de données historiques, d'inventaires systématiques recensant les évènements hydro-géomorphologiques passés ont jusqu'à présent empêché les collectivités locales de mettre en place des mesures efficaces pour réduire l'exposition et la vulnérabilité des populations. Cette thèse de doctorat a pour objectif de fournir des données de référence afin d'améliorer la compréhension des processus hydro-géomorphologiques. Ce travail repose sur l'utilisation de la dendrogéomorphologie, une discipline étudiant le rythme de croissance des arbres pour reconstituer les aléas naturels passés – une approche rarement utilisée dans les tropiques. Cette methode a été couplée à d'autres disciplines telles que la climatologie, la télédétection, les statistiques et la modélisation hydraulique. Cette approche pluri-disciplinaire a permis de mettre en place un ensemble de méthodes qui seront utiles à la mise en œuvre de nouvelles politiques de mitigation des risques naturels au Costa Rica mais aussi plus généralement dans d'autres pays des tropiques.

TABLE OF CONTENTS

FIGURES

TABLES

CHAPTER 1

1. Overall introduction

1.1. Natural hazards worldwide

A natural hazard is a likely damaging physical event, phenomenon or human activity that possibly will cause the loss of life or injury, property damage, social and economic disruption or environmental degradation (UNDRR, 2019). Whether or not a natural hazard process will become a risk or even turn into a disaster will depend on the exposure of people and their assets as well as on their vulnerability. Accordingly, exposure is defined as the situation of people, infrastructure, housing, production capacities and other tangible human assets located in hazard-prone areas, whereas vulnerability is the relative and dynamic diminished capacity of an individual or group to anticipate, cope with, resist and recover from the impact of a natural or anthropic hazard. Therefore, disaster risk is the combination of the severity and frequency of a hazard, the numbers of people and assets exposed to the hazard, and their vulnerability to damage (UNISDR, 2015).

In the literature, risk is defined as the combination of hazard, exposure and vulnerability where death, loss and damage is the function of the context of hazard, exposure and vulnerability (UNDRR, 2019). Risk is therefore highest in a context where people or their assets are directly exposed to a natural hazard process and where there capacity to adapt to the situation is limited or inexistent, so that they are very vulnerable (and not protected at all) whenever an event should occur. To avoid the worst, risk management strategies always aim at reducing risk, casualties and losses (UNISDR, 2015). A risk assessment can be achieved by implementing integrated economic, structural, legal, social, health, cultural, educational, environmental, technological, political, and institutional actions in order to prevent and reduce hazard, exposure, and vulnerability under climate change conditions (IPCC, 2014; UNISDR, 2015). Therefore, natural hazards must be considered based on the risks they pose so as to understand linkages and interdependencies between the geodynamic nature of natural hazard processes and the socio-economic context/consequences. For risk management approaches to be effective, they require baseline data on past events and/or detailed information on likely future process activity (UNDRR, 2019).

In general terms, natural hazards can be geological or hydrometeorological in nature (UNDRR, 2019). Among the geological (or tectonic) hazards, earthquakes, tsunamis, volcanic activity and (coseismic) landslides are most common (Shi and Karsperson, 2015). By contrast, then most common hydrometeorological hazards (also known as weather-related, climatological, meteorological, or hydrological hazards) include floods, rain-triggered landslides (mass movements), droughts, extraordinary storms (e.g. monsoon and tropical cyclones), and wildfires (UNISDRR, 2009). Weather-related disasters tend to sum most casualties and economic losses every year at a worldwide level (Fig. 1). The focus of this thesis is on the incidence of hydrometeorological hazards, and in particular on rain-triggered landslides and floods.

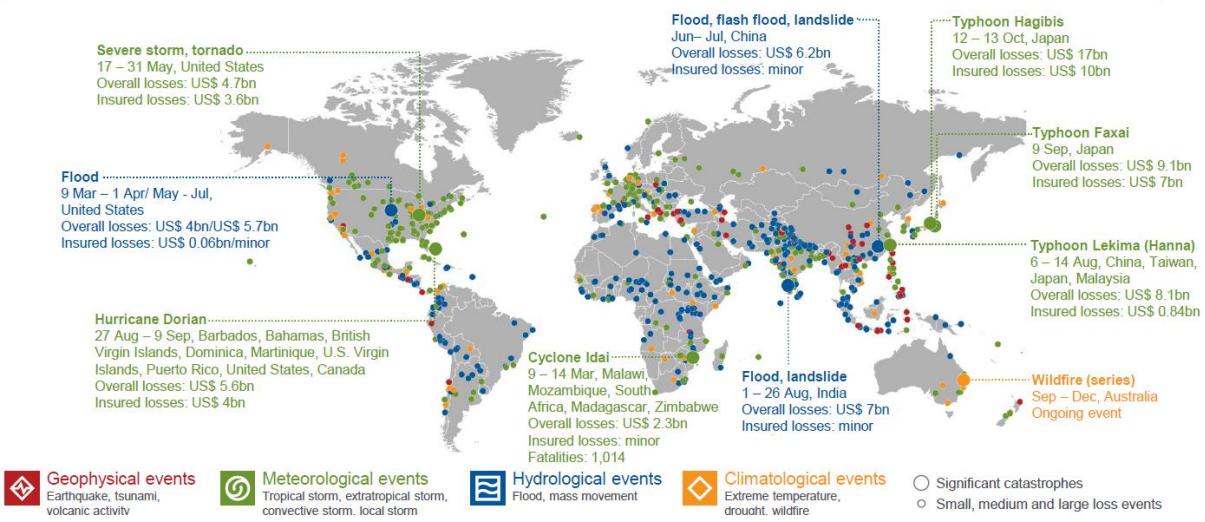

Fig. 1. Overview of relevant natural disasters that occurred in 2019 with indications on the losses caused (Source: Munich RE, 2020).

Landslides are one of the main causes of global human and economic losses in hilly regions, and vulnerability of people and their assets to landslides has increased due to expanded land urbanization in areas with high landslide susceptibility (Aristizábal et al., 2015). The highest numbers of landslides are observed in the major mountain regions, especially in the Alpine–Himalayan mountain tectonic belt, the Pacific Rim, and the Great Rift Valley (UNISDRR, 2009). Rain-induced landslides are mainly observed in humid areas with intricate terrains, such as the windward slope of the southern Himalayas, the Alps, and the Andes. The highest risk to die from a landslide is found in China, Brazil, Iran, Uganda, Philippines, Indonesia, India, Nepal, Paraguay, Bolivia, Burundi, and Colombia (Shi and Karsperson, 2015). Landslides have various drivers, and applying a probabilistic global model is not practical. They can be triggered by precipitation, change in air pressure or seismic activity. Determination of landslide mechanisms is key when it comes to the design of actions for risk mitigation. Urbanization often extends on unstable slopes and ancient landslides. This is predominantly true for informal settlements. Therefore, landslides frequently affect the poorest parts of urban areas, whose growth is constrained to land that would not withstand simple engineering tests (UNIDRR, 2019).

Similar to landslides, also flood frequency, flood-induced mortality and affected population have increased globally over the past decades (Hu et al., 2018). Higher mortality and loss rates are found in Bangladesh, China, India, Cambodia, Pakistan, Brazil, Netherlands, Indonesia, United States, Vietnam, Burma, Thailand, Nigeria, and Japan. Forecasting hydrometeorological hazards remains challenging despite improved knowledge of potential triggers and sophisticated climatological models. Moreover, climate change will affect the occurrence and the nature of processes, rendering accurate predictions even more challenging in data-scarce regions (Fig. 2). Global warming is expected to lead to an increase in flooding over the decades to come, with delicate consequences on livelihoods (UNDRR, 2019). More research is therefore critically needed to reduce uncertainties of climate change scenarios related to climate and hydrological models (Kundzewicz et al., 2018).

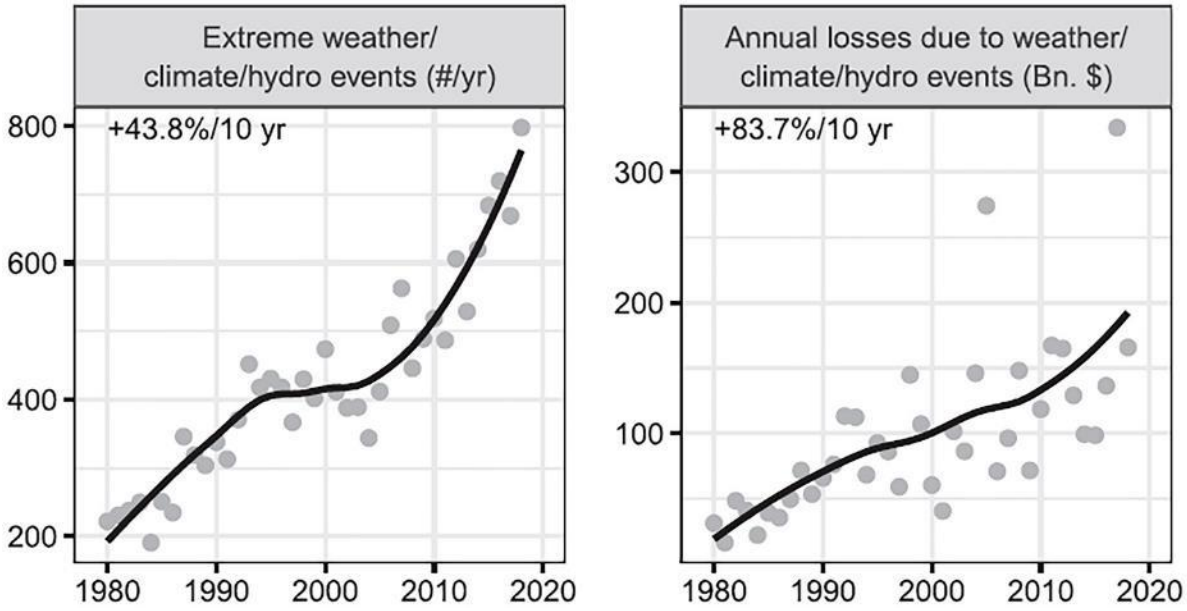

Fig. 2. Increase in extreme weather/climate/hydrological events and related annual losses in US dollar billions during the last four decades (Source: Ripple et al., 2019).

1.2. Natural hazards in the tropics

Worldwide assessments have shown that the combination of intense tectonics, volcanism, extraordinary rainfall, and active coastal processes may control hazard dynamics in the tropics. Moreover, tropical regions are commonly home to developing countries and thus have a much smaller Gross Domestic Product (GDP) than their temperate region counterparts.

Even if the tropics count for only 19% of the global land surface (Peel et al., 2007), they host between 40-50% of the global population (Tatem, 2017), and are affected by substantial land-use changes from forested and non-forested areas to croplands (Hettig et al., 2016). Moreover, over 80% of the global GDP is produced in cities, but cities also have substantial annual direct losses from natural disasters in the order of USD 314 billion (Sharifi, 2019). Another key element of developing countries is their fast urbanization and increasing population density, resulting in greater vulnerability (Mitchell et al., 2015). Consistently, low-latitude regions usually present high values for expected socio-economic losses due to earthquakes, volcanic risks, landslides, floods, storm surges, and tropical cyclones (Fig. 3). This fact is even more relevant in emerging countries and smaller economies located in the tropics as they often face difficult economic situations after a disaster and during recovery (Noy, 2009).

Tropical regions are often densely populated, and land-use changes have led to increased susceptibility of populations to geological (i.e. earthquakes or volcanism) and extreme weather-related hazards such as landslides and floods (Lawrence and Vandecar, 2015). Land-use changes enhance streamflow and sediment yields, changing sediment dynamics, with negative impacts on bed and bank stability and channel geometry, thereby favoring instability (Wohl, 2006). Concordantly, global tendencies indicate that disaster risk have been exacerbated by climate change, increasing the frequency and intensity of disasters in the tropics (UNDRR, 2019).

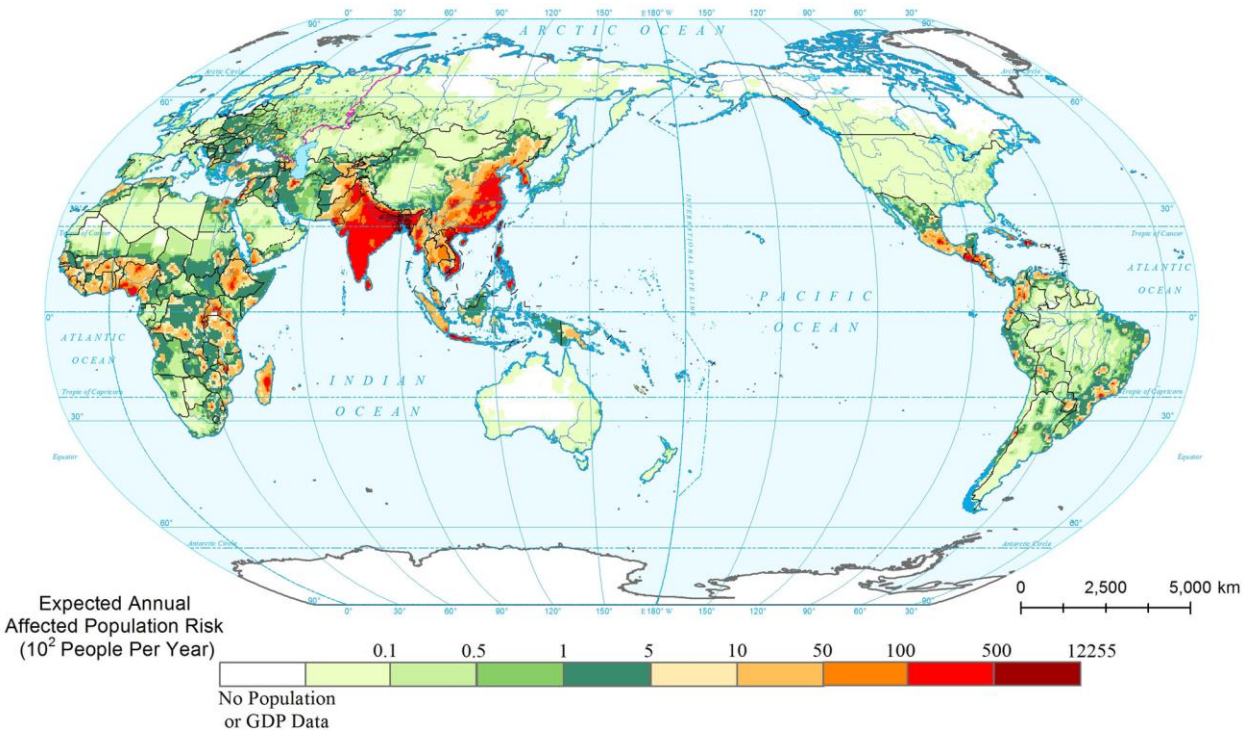

Fig. 3. Global expected annual affected population risk for multiple natural hazards (2020–2030; 0.5° x 0.5°; Shi et al., 2016).

1.2.1. Hydrometeorological hazards in the tropics

The seasonally or perennially barotropic conditions that dominate tropical climates are the Intertropical Convergence Zone where the trade winds, cold fronts, ENSO, cyclonic systems, and orographic uplift converge (Wohl, 2008). The most common hydrometeorological hazards on tropics are landslides, floods, tropical storms and droughts (UNISDR, 2009). In the case of floods, these events have caused a significant portion of the all-natural catastrophic economic impacts over the past decades worldwide (Aerts et al., 2018). In addition, extreme floods in the tropics have increased due to climate change (IPCC, 2018), and in many tropical countries, the highest number of natural disasters are caused by hydrometeorological events, including landslides and floods (Alcántara-Ayala, 2002).

High seismicity and extreme rainfall usually trigger gravitational processes. Many types of mass movements are present in the tropics, from slides (rotational or translational), falls, flows, spreads, and complex movements (Hungr et al., 2014). Landslides occur globally but the tropical regions are hotspots due to their geophysical dynamics (Lin et al., 2017). Closely coupled fluvial and gravitational processes (Savi et al., 2013) characterize mountain tropical areas. Mass movements starting at higher elevations may affect distant lower areas not only directly, but also through cascading effects involving rivers (Schauwecker et al., 2019), or through the amplification of processes by entrainment of material (Stoffel and Huggel, 2012). Landslides have been widely related to rainfall intensity-duration relations (Segoni et al., 2018) or to seismic activity (Reichenbach et al., 2018). Moreover, coupled earthquake-rainfall dynamics predispose unstable

slopes to landslides triggering (Quesada-Román et al., 2019). Fatalities related to landslides are greater in tropical and developing countries (Kirschbaum et al., 2015). The projected global mortality risk of landslide around the world shows a close link with mountain regions of both hemispheres located at latitudes <30° (Shi and Karsperson, 2015).

The occurrence of extreme climatic events and flood frequency have increased during the last decades, whereas natural forest cover has declined across the tropics (Lawrence and Vandecar, 2015). Floods in the tropics are controlled by the combined interaction between land-use changes, floodplain occupation and climatological dynamics associated with intense seasonal and extraordinary rainfall events (Syvitski et al., 2014). Accelerated deforestation rates in tropical rainforests have dramatic impacts on local public health, agricultural productivity, and again on global climate change (Vargas-Zeppetello et al., 2020). There is evidence of Atlantic Multidecadal Oscillation (AMO) relations with sea surface temperature (SST) variations in the tropics (Knight et al., 2006; Kayano and Capistrano, 2014; Sun et al., 2017). Hence, ENSO conditions are enhanced and monsoon/tropical cyclones activity increase (Wang et al., 2013). Extreme La Niña and El Niño events control the occurrence of intense dry or wet years along the tropics (NOAA, 2019). The effect of ENSO denotes that during the La Niña phase a greater possibility exists for tropical storms development than during an El Niño event (Goldenberg et al., 2001). Therefore, greater inputs and faster rates of change in the tropics have recently caused more extreme floods (Wohl et al., 2012). Many tropical countries present high mortality as well as economic and social losses projected rates during the next decades such as India, Cambodia, Argentina, Brazil, Indonesia, Vietnam, Thailand and Nigeria (Fig. 4).

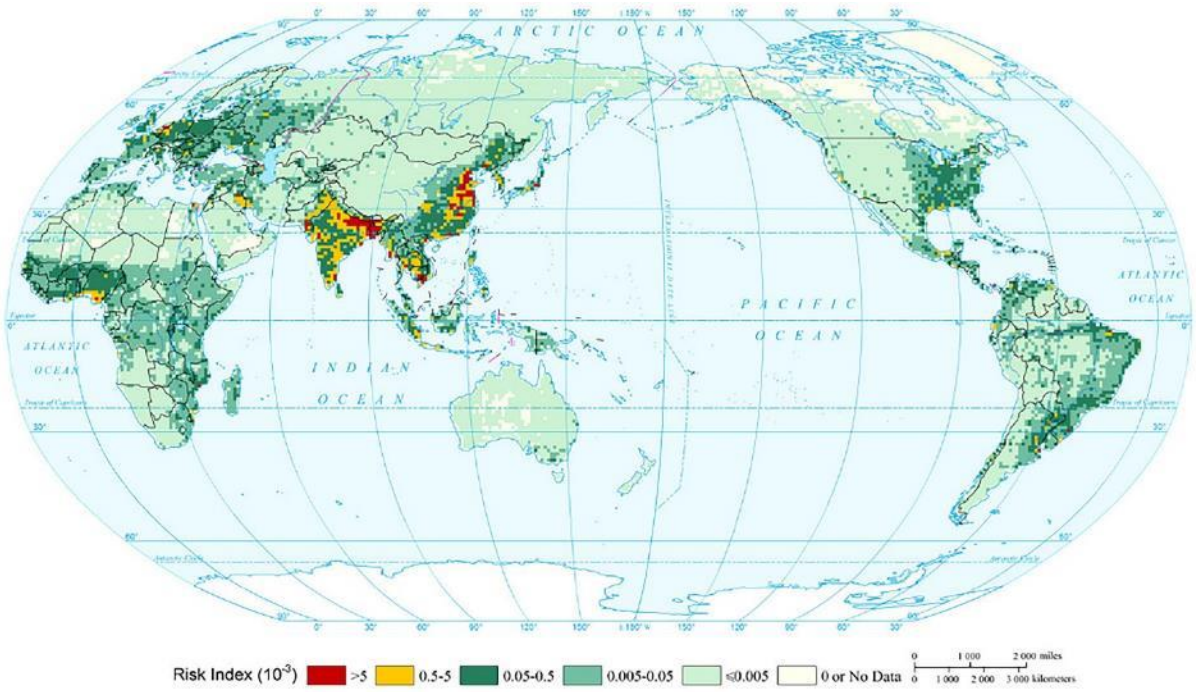

Fig. 4. Expected annual affected population risk of flood of the world (2020-2030; 1°x1°; Shi and Karsperson, 2015).

1.2.2. Challenges in the characterization of hydrogeomorphic processes in the tropics

Hydrogeomorphology is an interdisciplinary discipline focusing on interactions of hydrologic with geomorphic processes in their temporal and spatial dimensions (Sidle and Onda, 2004). Depending on the scale, climate, topography, soils, vegetation and land use affect differentially hydrogeomorphic processes. Most catchment studies still lack the information to measure runoff, erosion processes, and sediment transport processes. There is a necessity to perform these studies at different scales, combined with long-term catchment monitoring to generate field data to parameterize, test, and accurately calibrate numerical models (Sidle et al., 2017). Nonetheless, such information is often scarce and of poor quality in tropical countries (Wohl et al., 2012).

Accurate estimates of flood frequency and magnitude are an important element of any effective national, regional and local flood risk management (Nguyen et al., 2014). Flood flow frequency analysis depend on several data sources such as systematic records, historical data, paleoflood data and botanical information, regional statistics, and precipitation and climate data (England Jr et al., 2019). Determination of flood quantiles probability is required for many engineering works and flood risk management projects (Díez-Herrero and Garrote, 2020). Based on statistics, flood-frequency analysis acquire the relationship among flood quantiles and their nonexceedance probability to quantify the risk that a flood with a given discharge in the future develop (Wilhelm et al., 2019). The extrapolation of series based on short systematic records lead to misestimated hydrogeomorphic processes risk. Historical, geological (speleothems, lake and fluvial sediments), and botanical (tree rings) archives are recognized as valuable sources of extreme flood event information (Fig. 5; Wilhelm et al., 2019; Bodoque et al., 2020). The use of historical information can be of great value in the reduction of the uncertainty in flood quantiles estimators, though many have raised concerns with measurement and recording errors (Benito et al., 2015). Otherwise, despite geological archives have a good time and spatial window they also present more dating uncertainties.

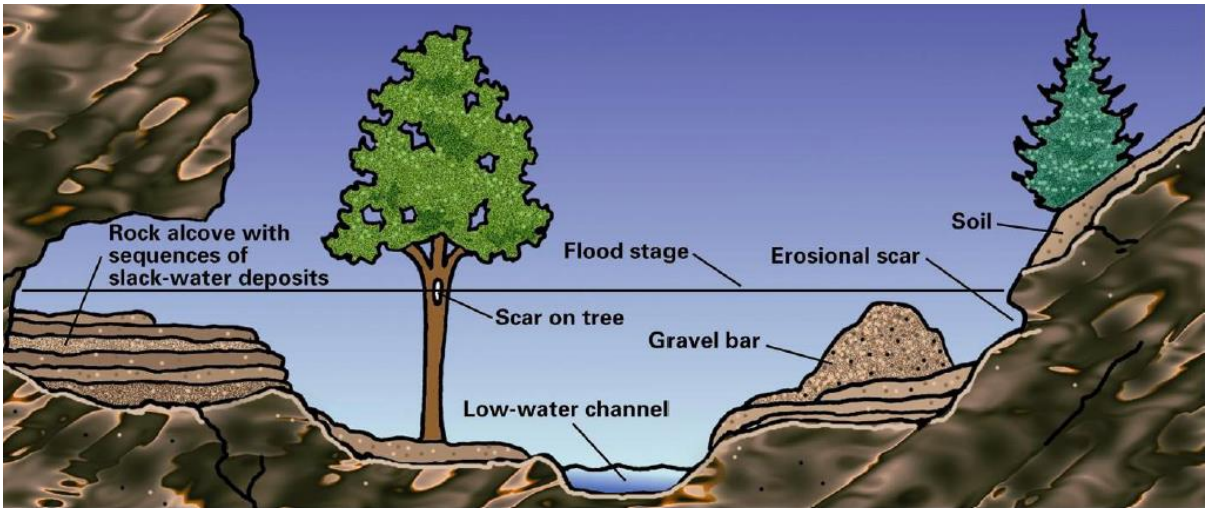

Fig. 5. Paleoflood features used as paleostage indicators (Jarret and England, 2002; England Jr et al., 2019).

The use of dendrochronology to assess paleo and/or recent floods have been widely used in temperate regions (St. George, 2010; Ballesteros et al., 2015). Moreover, tree rings are a critical proxy to determine the magnitude and frequency of hydrogeomorphic processes, e.g. landslides and debris flows (Stoffel et al., 2013; Stoffel and Corona, 2014). Dendrogeomorphic applications provide results that can reduce the information gaps of regions with data scarcity. A key implication of the vegetation–hydrogeomorphology linkage is that woody plants can allow reconstruction of ecological and hydrogeomorphic processes over several decades to centuries (Stoffel and Wilford, 2012). The hydrogeomorphic process information gathered by means of dendrogeomorphic techniques can certainly improve model uncertainties, event reconstruction and hazard zonation (Allen et al., 2018). Due to the fact that data on past events is critically lacking in tropical regions, this PhD thesis investigates the potential of tropical dendrochronology to assess hydrogeomorphic processes and to reduce uncertainties for risk assessments. Slow-energy marks after hydrogeomorphic processes such as soils, slack deposits or high-water marks do not remain preserved more than a few weeks. Tropical mountains are dynamic regions with energetic torrents that commonly comprise dense vegetation, making possible the dendrogeomorphology implementation as a reliable method to assess hydrogeomorphic processes.

1.3. Tropical dendrochronology

Dendrochronology is the science of dating annual growth layers (rings) in woody plants (Fritts, 1971). Dendrochronological analyses provide valuable insights into diverse fields of Earth sciences (Schweingruber, 1996). Among the study fields where dendrochronology analysis proved efficiency are climatology (Hughes, 2002), ecology (Fritts and Swetnam, 1989), geomorphology (Shroder, 1980), and archaeology (Kuniholm, 2002). Over more than a century, dendrochronology researches have covered all the continents except Antarctica, with chronologies development especially in the mid and high latitudes of the Northern Hemisphere (Fig. 6; Zhao et al., 2019). This is the result of a combination between the availability of trees to record climate and environmental changes (Esper et al., 2016). In addition, the extended usage of long-lived trees as well as the tree-ring laboratories location and researchers' interests (Pearl et al., 2020). Even recently, the annual growth-ring assumption of tropical species was not widely accepted (Worbes et al., 2017).

Fig. 6. Spatial representation of the International Tree-Ring Data Bank (ITRDB; modified from Zhao et al., 2019).

Over recent decades, tropical dendrochronology has gained in relevance due to its application in several scientific fields (Worbes, 2002). Despite the focus of tree-ring research on temperate and cold regions, several studies confirmed tropical species form growth zones with an annual layering driven by the species' sensitivity to climate, ecological, or geodynamic variations (Worbes, 1989; Schöngart et al., 2017). Thus, in repeated times rainfall demonstrated to have a great impact on annual ring growth (Fichtler, 2017; Silva et al., 2019). Therefore, the seasonality of growth may reflect the effects of predictable, moderately long rain-free periods in tropical forests that develop annual rings out of these growth layers (Fichtler et al., 2003).

Tropical dendrochronology has expanded recently to include studies focusing on geomorphic, climatological and ecological analyses (Worbes, 2002) thereby contributing substantially to the broadening of our current knowledge of tropical forest ecosystem functioning (Worbes, 2010). Certainly, many studies have already highlighted the nature of growth periodicity in tropical plants, growth-climate relations, drought and fire histories, flood dynamics, and/or climate variations (e.g., Boninsegna et al., 2009; Rozendaal and Zuidema, 2011; Fichtler, 2017). Nevertheless, and as tropical species show greater variations and complexity in the makeup of growth rings, they are still characterized by a greater diversity and lower identification accuracy (Silva et al., 2019). Hence, detailed knowledge of wood-anatomical structures and the variability of growth zones is vital to conduct successful dendrochronological studies in tropics (Worbes, 1995). Moreover, numerous species around the tropics produce annual rings. This is the case of trees growing in drier areas of the tropics or at higher altitudes, where pronounced seasonal climates are present (García-Cervigón et al., 2020), which will ultimately help in filling the geographic gap with more tree-ring studies (Zuidema et al., 2013).

The need to fill large geographic gaps in dendrochronological data has driven rapid expansion of testing previously unstudied species (Fig. 7; Pearl et al., 2020). Increasing and enhancing tropical dendrochronology can help to close the knowledge gap in regions without sufficient tree-ring chronologies and thereby support Earth system sciences (Babst et al., 2017).

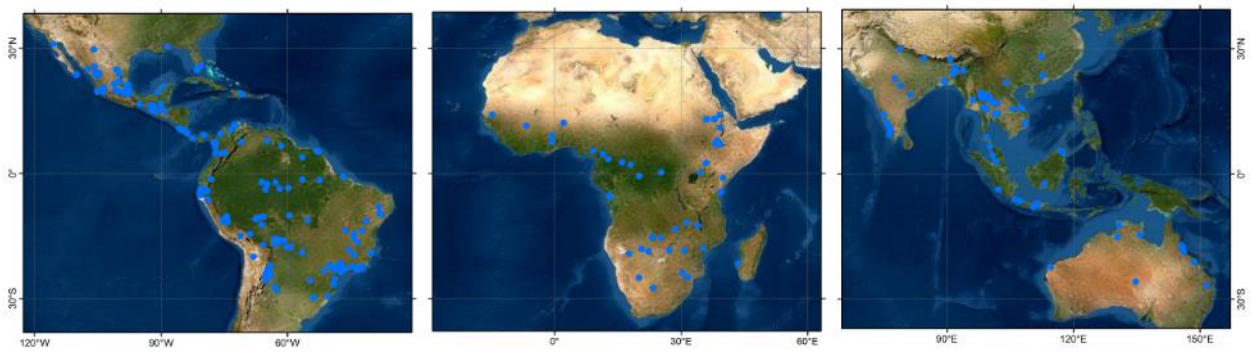

Fig. 7. Distribution of tropical dendrochronology studies along the tropics.

The direct link between natural hazards and their analyses with dendrochronological tools is called dendrogeomorphology. Dendrogeomorphic studies have interpreted signs of past earth-surface

processes found in the increment rings of trees and have hence been used to characterize past, current and potential future process activity. The technique has been widely used in the analysis of snow avalanche, debris flow, landslide or flood analysis (Stoffel and Bollschweiler, 2008). Due to the nature of tropical regions, landslides, floods, and erosion are the most frequently occurring processes; studying their activity through dendrogeomorphology can therefore be key to understand their connections with past or recent climatic, ecologic and geomorphic dynamics better. Stoffel and Corona (2014) identified a series of growth disturbances that can record past geomorphic process activity in trees. Among these, injuries/callus tissue, tangential rows of traumatic resin ducts, tracheid and vessel anomalies, reaction wood, growth reductions, growth releases, as well as germination and kill dates are some of the common disturbances reported for mass movement processes (Stoffel et al., 2013; Wistuba et al., 2019; Šilhán, 2020).

Flood marks left in the field can help to approximate the extent and magnitude in the days and weeks after an event. However, these marks are highly fragile and often vanish within a few months (Borga et al., 2014). Botanical indicators cover longer periods and can hence serve as an appropriate source of signal to date floods and to quantify their magnitude in rivers with scarce or nonexistent gauge records (Sigafoos, 1964; Ballesteros-Cánovas et al., 2015a). Scars in trees are the most reliable proxy of past floods as they allow precise dating of the event as well as a determination of water stages during floods (Gottesfeld, 1996; Ballesteros et al., 2011a, b). The use of tree-ring records in river corridors has allowed the extension of flood records back in time in several rivers, but past research has fixated mostly on temperate mountain environments (Sigafoos, 1964; McCoord, 1990; Ballesteros-Cánovas et al., 2015b; Wilhelm et al., 2019). The nature of the most suitable locations (e.g. alluvial terraces) for the sampling of scars that would allow the minimization of deviations between real and reconstructed flood heights have been identified in the past (Ballesteros-Canovas et al., 2015a; Victoriano et al., 2018).

Dendrogeomorphic research has been restricted largely to the neotropics, with a clear geographic focus on mass movements, erosional processes and floods and a geographic focus on Mexico (Franco-Ramos et al., 2020; Sánchez-Asunción et al., 2020), Brazil (Bovi et al., 2018) and Argentina (Paolini et al., 2005). With the ongoing climate warming and intensification of rainfall events, weathering rates are increasing across the tropics. These processes exacerbate further by the fact that tropical regions also are hotspots of tectonic activity, and changing land use, resulting in an intensification of erosional processes and the occurrence of natural disasters. Growth rings in trees and roots have been applied repeatedly to quantify erosion (and the evolution of erosion rates in extratropical settings) (Ballesteros-Cánovas et al., 2013; Stoffel et al., 2013), and have just lately been applied to tropical species as well (Bovi et al., 2019).

1.4. Dendrochronology in Costa Rica

In the Central American region, the future climatic projections indicate extreme warming and less precipitation (Giorgi, 2006; Hidalgo et al., 2013). Understanding past climate variations with higher spatial resolution can be useful to improve future climate projections (Cabos et al., 2019). Dendrochronology is one of the best proxies to determine annual and intra-annual oscillations due to climatic changes at local and regional scales. These interactions act jointly with surface characteristics (vegetation and orography) to shape climate at regional and local scales, subject to the variability imposed by modes such as El Niño-Southern Oscillation (ENSO).

Costa Rica hosts approximately 6% of the worldwide biodiversity (Kappelle, 2016), this makes the country an ideal tropical laboratory to develop dendrochronological records and to fill the knowledge gaps in dendrochronology. In Costa Rica, the application of dendrochronology have been limited to few studies (e.g. Worbes, 1989; Enquist and Leffler, 2001; Fichtler et al., 2003; Anchukaitis and Evans, 2010; Worbes and Raschke, 2012), despite the high potential to find new species that mark tree rings and the possible applications in ecology, climatology and geomorphology. A recent study demonstrated that *Hypericum irazuense*, a shrub species endemic to the Costa Rican páramo can be used to characterize broad-scale hydroclimatic variability (associated with ENSO) and climate reconstructions in a region where climatological records remain scarce (Horn, 2007; Lachniet et al., 2017; Quesada-Román et al., 2020b). Moreover, a dendrogeomorphic approach calculated the flood peak discharges related with a tropical storm using scarred trees (Quesada-Román et al., 2020a).

Dendrochronology can be applied to other regions of Costa Rica where warming conditions during the last decades have caused droughts such as the Central American Dry Corridor in Guanacaste (Quesada-Hernández et al., 2019), or to understand ENSO variations in different Costa Rican ecosystems (Muñoz-Jiménez et al., 2018). Moreover, there is a significant time gap in the continuity of climate or extreme events information in Costa Rica. Geological timescales are useful to study past climate, while present climate uses historical meteorological records. However, the decadal to centennial climate variability is largely unknown due to the lack of archives covering these timescales.

1.5. Costa Rica: a geodynamic study region

1.5.1. Tectonic and geological context

The Cocos-Caribbean plate's subduction margin, the Panama microplate, and the Cocos volcanic range subduction favor Costa Rican tectonic activity (Alvarado et al., 2017). This dynamic has formed three morphotectonic units: a forearc, a volcanic front, and a backarc that controlled the lithological distribution in the country (Fig. 8; Marshall, 2007). The forearc extends along the Pacific coast with an abrupt topography of Cretaceous-Quaternary age (Denyer and Alvarado, 2007). The volcanic front includes the Guanacaste, Tilarán, Aguacate, Central, and Talamanca cordilleras composed mainly of volcanic and sedimentary rocks of Paleogene-Quaternary age (Alvarado, 2011). The backarc extends from the Caribbean plains of the Tortuguero lowlands in northeastern Costa Rica to the rugged emergent morphology of the southern Caribbean (Quesada-Román and Pérez-Briceño, 2019). The main geomorphic environments in Costa Rica are fluvial, volcanic, and coastal landscapes, but also contain some glacial and karstic environments (Quesada-Román and Pérez-Umaña, 2020).

The high seismicity and volcanism of Central America and Costa Rica are due to the tectonic complexity of the region and make it particularly susceptible to geological hazards (Alvarado et al., 2017). Roughly, 10% of all natural disasters in the country are of geological origin and include earthquakes, volcanic activity, and coseismic landslides (LA RED, 2018). Nonetheless, their occurrence causes important economic losses every year. In Costa Rica, seismicity is abundant along the Pacific coast, particularly between the coastline and the Mesoamerican Trench, where

the Cocos, Caribbean, and Panama plates meet (Godínez-Rodríguez et al., 2018). Other major tectonic features include the Panama Fracture Zone (PFZ), the North Panama deformed belt (NPDB), and the Central Costa Rica deformed belt (CCRDB) (Linkimer et al., 2018). These crustal deformation broad zones are the proposed boundaries between the Caribbean plate and the Panama microplate (Marshall et al., 2000).

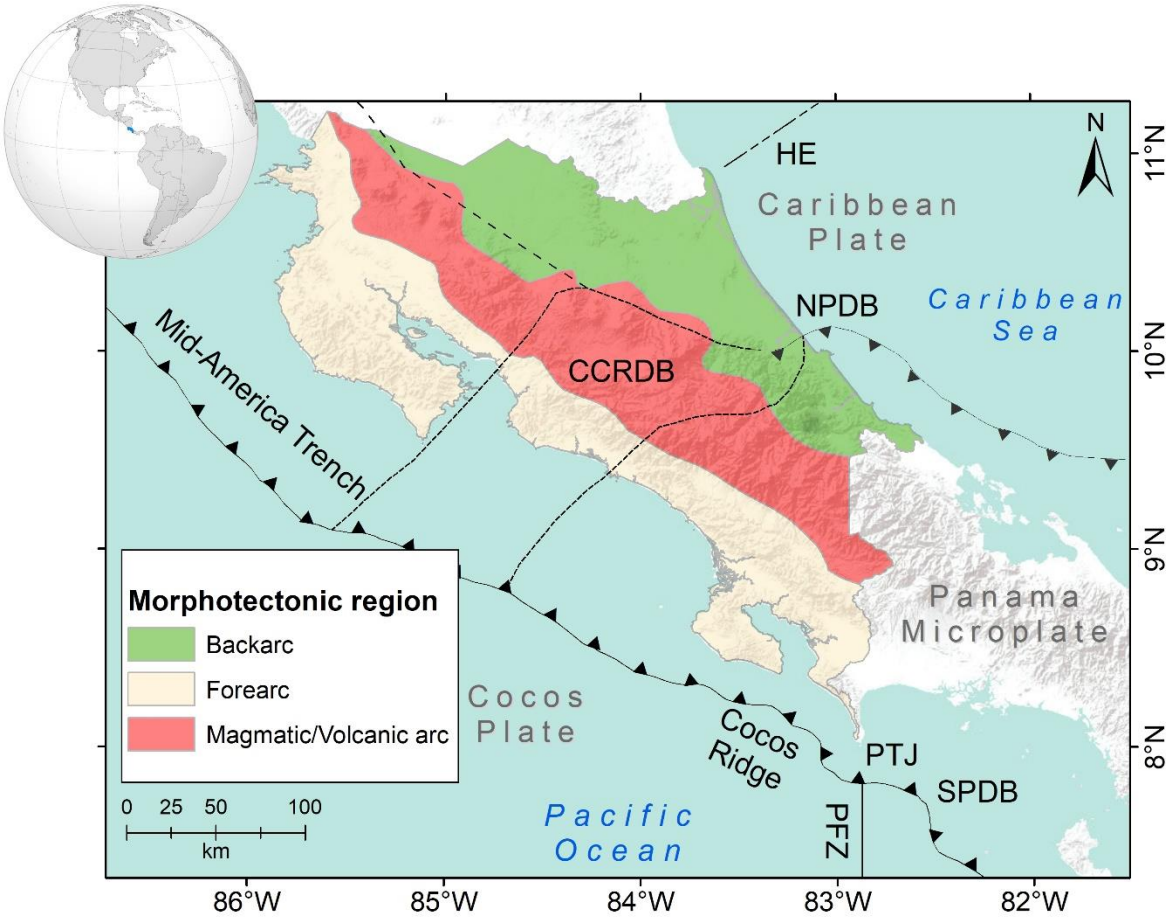

Fig. 8. Morphotectonic framework of Costa Rica (Source: ArcGIS Online Basemap; Projection GCS; Datum WGS84). HE: Hess Escarpment; ND: Nicaragua Depression; CCRDB: Central Costa Rica Deformed Belt; NPDB: North Panama Depression Belt; SPDB: South Panama Depression Belt; PFZ: Panama Fracture Zone; PTJ: Point Triple Junction (DeMets et al., 2010; Morell et al., 2012).

1.5.2. Climatological context

A continuous chain of cordilleras crosses Costa Rica with an NW-SE orientation to define the Pacific and Caribbean basin. This topographic barrier also controls the amount of rainfall in each basin, along with the latitudinal migration of the Intertropical Convergence Zone, El Niño Southern Oscillation, northeast trade winds, cold fronts, and tropical cyclones (Amador et al., 2010). As a result, their interaction with topography results in two climatic types known as Pacific and Caribbean climates. The Pacific side presents a bimodal rainfall distribution, while it is

difficult to define a dry season for the Caribbean side (Fig. 9; Maldonado et al., 2018). Whereas on the Caribbean side annual rainfall totals are up to 3000 mm, they are generally below 3 m on the Pacific side. The tropical climatic conditions also explain the fact that more than 90% of all disasters in Costa Rica are hydrometeorological. Among the latter, 60% are floods and 30% are landslides (LA RED, 2018).

In terms of impacts of tropical cyclones, a positive and statistically significant linear trend has been observed in the annual number of intense hurricanes in the Caribbean Sea since the 1970s (Saunders and Lea, 2008; Alfaro and Quesada-Román, 2010; Alfaro et al., 2010). Out of all tropical cyclones that formed in the Atlantic basin, 14% caused indirect effects in Costa Rica, but the probably for a direct impact in the country were <6% during the 20th century (Alvarado and Alfaro, 2003). Costa Rica has been impacted indirectly by various tropical cyclones, especially on the Pacific slope, but none of these made direct landfall until 2016 when Hurricane Otto hit the country (Quesada-Román and Villalobos-Chacón, 2020). During the rainy season, smaller disasters occur regularly; whereas tropical cyclones are typically the reason for the extraordinary occurrence of landslides and floods in Costa Rica (Quesada-Román et al., 2020d).

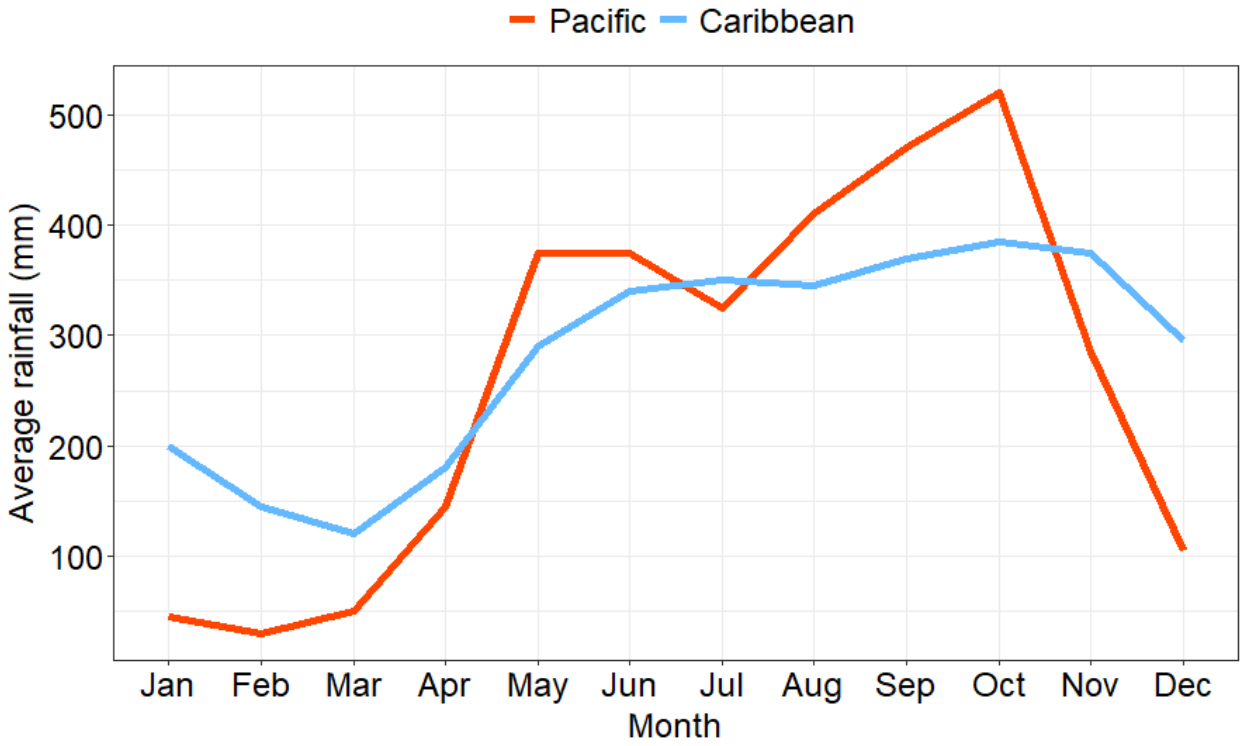

Fig. 9. Costa Rican Pacific and Caribbean basins rainfall regimes (Méndez et al., 2019).

1.5.3. Land use and natural hazards in Costa Rica

The high number of species and endemic organisms position Costa Rica as a megadiverse country composed of mountain cloud forests, evergreen moist forests, seasonal forests, dry forests, páramos, coastal, and wetlands ecosystems (Kappelle, 2016). The large altitudinal range, important topographic barriers, and soil diversity explain the presence of several and diverse ecosystems in the region (Antonelli et al., 2018). Deforestation and landscape fragmentation dominated in the region from the 1950s until the mid-1980s. Afterwards, a series of environmental

policies reversed deforestation together with the rise of ecotourism and the development of more sustainable production alternatives, such that the country nowadays has again a forest cover of 51% (Keenan et al., 2015).

In 2018, Costa Rica's population reached five million inhabitants and, during the last three decades, its population shifted from a marked rurality to a clear urban trend reaching 75% of the population in 2011. Currently, the Greater Metropolitan Area (or GAM) accounts for 65% of the population (approximately 3 million inhabitants) of Costa Rica occupying 14% of its surface (Van Lidth de Jeude et al., 2016). This urban sprawl poses the GAM as exposed and vulnerable region to the impacts of landslides and floods every year (Quesada-Román et al., 2020d). The study of landslide and flood processes has been extensive in Costa Rica. However, the hazard maps' output scale and its integration with vulnerability and risk analysis has been limited (Quesada-Román, 2017; Quesada-Román et al., 2018).

Every year, Costa Rica uses ~86 million USD (~1% of the national gross domestic product, GDP) to repair and rehabilitate the effects of natural disasters (Astorga, 2010). Disaster impacts due to the natural hazards are clear examples of the increasing national vulnerability. The cost of recovery from Limón Earthquake (1991) was 4.2%, Cinchona Earthquake (2009) equaled 1.5%, while Hurricane Otto (2016) represented 0.4%, and tropical storm Nate (2017) summed 1.3% of the GDP. These disaster consequences were predominantly related to reparations of road infrastructure (bridges and roads) where Costa Rica has a clear development delay (Brenes and Girot, 2018).

1.6. Research aims, hypothesis and outlines

The research aim of this thesis is to provide reference data for an improved understanding of hydrogeomorphic processes as well as to explore the potential use of tropical species for natural hazards and dendrochronological applications in Costa Rica and the tropics. Consequently, this study intends to develop a methodological approach that allows the gathering of baseline data of past hydrogeomorphic processes so as to understand associations amid climatic, ecological and geomorphic responses. This PhD thesis is the product of a multidisciplinary research combining climatology, geomorphology and dendrochronology and targets at closing important research gaps in the fields of natural hazards and dendrochronology in Costa Rica with a series of study cases.

The principal motivation to link natural hazards and dendrochronology in low latitudes is the repetitive scarcity of baseline data to perform practical hydrogeomorphic process analyses and approaches that could ultimately help to reduce the negative effects of disasters in vulnerable tropical regions or in developing countries in more general terms. To achieve these goals, the PhD thesis has been organized around five studies with particular hypotheses and research questions (Fig. 10).

Deciphering natural hazard histories based on tree-ring analyses in contrasting tropical ecosystems of Costa Rica

Chapter 1

Overall introduction

- Natural hazards worldwide
- Natural hazards in the tropics
- Tropical dendrochronology
- Dendrochronology in Costa Rica
- Costa Rica as a geodynamic country
- Research aims, hypothesis and outlines

Research aim:

Provide reference data in the understanding of hydrogeomorphic processes as well as to explore the potential use of tropical species for natural hazards and dendrochronological applications in Costa Rica and the tropics

	Chapter 2	Chapter 3	Chapter 4	Chapter 5	Chapter 6
Subject	Relationships between earthquakes, hurricanes, and landslides in Costa Rica	Tropical dendroecology: approaches, applications, and future prospects	Neotropical Hypericum irazuense shrubs reveal recent ENSO variability in Costa Rican páramo	Dendrogeomorphic reconstruction of floods in a dynamic tropical river	Improving regional flood risk assessment in mountain catchments impacted by tropical cyclones
Publication	Quesada-Román et al. 2019. Relationships between earthquakes, hurricanes, and landslides in Costa Rica. Landslides 16(8), 1539-1550	Quesada-Román et al. 2020. Tropical dendroecology: approaches, applications, and future prospects. Submitted to Earth-Science Reviews	Quesada-Román et al. 2020. Neotropical Hypericum irazuense shrubs reveal recent ENSO variability in Costa Rican páramo. Dendrochronologia 61, 125704	Quesada-Román et al. 2020. Dendrogeomorphic reconstruction of floods in a dynamic tropical river. Geomorphology 359, 107133	Quesada-Román et al. 2020. Regional flood risk assessment in mountain catchments impacted by tropical cyclones. Submitted to Journal of Hydrology: Regional Studies
Data	Satellite images, high-resolution rainfall data, topographic data	Qualitative and quantitative analysis of previous findings based on literature	Wood samples and climatological models	Scarred trees, UAV flights	Hydrological data, dendrogeomorphic data, topographic data, and social indexes and data
Methods	Geomorphic assessment, climatological analysis, Generalized Linear Model	A review paper of 344 papers on dendrochronology on the tropics	Wood anatomy, dendroclimatology and dendroecology	Dendrogeomorphic assessment, hydraulic models, statistical models	Regional flood frequency analysis, flood risk assessment
Results	Coupled earthquake-hurricane dynamics with higher landslide densities close to the epicenter and larger rainfall totals	Review of the current knowledge and assessments of future prospects	Climate-growth relationships of Hypericum irazuense and its relationship with ENSO events	Scarred trees in cut banks were better candidates for flood peak reconstruction	Regional flood risk determination in the biggest watershed of Costa Rica

Chapter 7

Overall conclusions

- Principal results synthesis
- Research limitations
- Future research lines

Main conclusions:

- Earthquakes can weaken volcanoes hillslopes prior a hurricane and provoke compound effects in tropical regions
- Tropical dendrochronology requires more geographical coverage, methods adaptation, and local participation
- ENSO events control rainfall and growth rate on an endemic shrub species in Costa Rican páramo
- Scarred trees in cut banks were better candidates for flood peak reconstruction in tropical rivers
- A regional flood risk assessment is feasible for mountain catchments impacted by tropical cyclones

Fig. 10. Thesis structure and content outlines.

The first research paper (Chapter 2) deals with the analyses of the impacts of the co-occurrence of an earthquake and high intense rainfalls on hydrogeomorphic processes. The specific hypothesis here was that tropical cyclone rainfall on volcanic slopes that were weakened previously by earthquakes may enhance the triggering of debris flows and landslides. By doing so, the study attempted to answer the question whether such connections can be found in data-scarce regions.

Whereas the research was useful in providing insights into the co-occurrence of landslides and debris flows after the passage of a tropical cyclone on a volcanic slope that was weakened by earthquakes, it become also obvious that data on past events is still scarce. For that reason, in Chapter 3, a review was performed on existing work on tropical dendrochronology, with the aim to explore the potential of trees to serve as recorders of past hydrogeomorphic process activity. To this end, we identified tree growth patterns of tropical species, the most studied regions, families, genera and thereby also the most suitable species. Likewise, we investigated the approaches and techniques that were most commonly used in tropical tree-ring research, different applications, limitations, and further research prospects. The specific hypothesis of the review paper was that dendrochronology has potential to increase climatological, ecological and geomorphic responses in low-latitude environments.

Based on these insights, Chapter 4 tests the suitability of dendrochronology on an endemic shrub species at the highest elevations of the Costa Rican páramo. The study hypothesizes that short-lived shrub species produces growth annual rings with widths depending on climatic variability and oscillations in the rainy season. This study thereby also searched to identify the climatological and environmental variables driving annual growth of an endemic shrub páramo species growing in the Costa Rican highlands.

With the knowledge that Costa Rican species are suitable for dendrochronological purposes, Chapter 5 was designed to apply dendrogeomorphic methods to determine peak discharges in a Costa Rican river after the passage of tropical cyclones. This research hypothesized that the reconstruction of flood peak discharges following tropical cyclones is possible in ungauged catchments if a dendrogeomorphic approach is used.

Chapter 6 finally merges hydrological, hydraulic and a dendrogeomorphic approaches to perform a regional flood risk assessment in a Costa Rican basin. The key aspect here is the return period of events as this information is key for land use planning and disaster risk reduction in data-scarce catchments. Therefore, this study aimed to answering the question of whether flood-frequency models coupled to dendrogeomorphic approaches defining peak discharges can help in determining flood risk at regional scales after the passage of tropical cyclones.

Multidisciplinary in nature, this study merges remote sensing, geospatial applications, meteorological assessments, historical data, and dendrochronological methods, as well as hydraulic modelling, flood-frequency analysis and risk assessments. The outputs of this PhD will enhance the implementation of different methodologies and future adaptation strategies in regions with data scarcity and in a tropical region that is among the most biodiverse in the world. Chapters 2 to 6 have been published (or submitted) as research papers to peer-reviewed, ISI indexed journals and provide answers to the research questions and hypothesis outlined above.

CHAPTER 2

2. Relationships between earthquakes, hurricanes and landslides in Costa Rica

Adolfo Quesada-Román [a,b], Berny Fallas-López [c], Karina Hernández-Espinoza [d], Markus Stoffel [a,e,f], Juan Antonio Ballesteros-Cánovas [a,e],

[a] Climatic Change Impacts and Risks in the Anthropocene (C-CIA), Institute for Environmental Sciences, University of Geneva, Geneva, Switzerland
[b] School of Geography, University of Costa Rica, San José, Costa Rica
[c] Hydrology Department, Costa Rican Institute for Electricity
[d] Climatology and Applied Research Department, Costa Rican National Meteorological Institute
[e] Department of Earth Sciences, University of Geneva, Geneva, Switzerland
[e] Department F.-A. Forel for Environmental and Aquatic Sciences, University of Geneva, Geneva, Switzerland

Landslides 16 (8), 1539-1550. https://doi.org/10.1007/s10346-019-01209-4

Landslides are a common natural hazard in Costa Rica, recurrently triggered by seismicity and extraordinary rainfall. Here, we investigate the coalescence of both processes and their ability to trigger massive landslides and debris flows in Costa Rica. The study focuses on Miravalles volcano, affected by an earthquake of 5.4Mw on July 2, 2016, and by intense rainfalls related to the Hurricane Otto only four months later, on November 24, 2016. During the passage of Hurricane Otto, ~300 mm of rain were recorded in the study region. We use logistic general linear regression models (GLM) to represent the statistical relationships between the factors controlling landslides (such as epicenter distance, rainfall during Hurricane Otto, altitude and slope). The compound 2016 event triggered 942 landslides, of which 62% were located within 3–6 km from the Bijagua earthquake epicenter, and on the eastern, southeastern and southern slopes of Miravalles volcano, i.e. in the zone where the density of local faults is highest and rainfall reached maximal values during the hurricane. The statistical analysis supports the existence of coupled earthquake-hurricane dynamics with higher landslide densities close to the epicenter and at sites receiving larger rainfall totals, but also showing higher slopes and altitudes. Debris flows affected an area of ~27 km^2 and moved down the river systems, leaving eight casualties around the volcano and ca. 103 million US$ of losses in Upala and Bagaces. Results of this study can be useful for the assessment and understanding of geological and hydrometeorological hazards in Costa Rica and other tropical countries.

2.1. Introduction

Mountain areas are characterized by closely coupled fluvial and gravitational processes (Savi et al., 2013). Mass movements starting at higher elevations may impact distant lower areas not only directly, but also through cascading effects involving rivers (Schauwecker et al., 2019), or through the amplification of processes by entrainment of material (Korup et al., 2010; Stoffel and Huggel, 2012). Given the geographical location and characteristics of Costa Rica, the Pacific and Caribbean slopes are influenced by differing climatic dynamics which in turn facilitate the occurrence of extreme hydrometeorological phenomena related to the El Niño Southern Oscillation (ENSO), or more specifically during the passage of cold fronts and tropical cyclones. The occurrence of such extremes have been demonstrated to trigger landslides and floods in the region (Campos-Durán and Quesada-Román, 2017). Since the 1970s, a positive and statistically significant linear trend has been observed in the annual number of intense hurricanes in the Caribbean Sea (Saunders and Lea, 2008; Alfaro and Quesada-Román, 2010; Alfaro et al., 2010). Of the total number of tropical cyclones formed in the Atlantic basin, 14% produced indirect effects in Costa Rica, but the chances of a direct impact to the country were less than 6% during the 20th century (Alvarado and Alfaro, 2003). Costa Rica has been impacted indirectly by various tropical cyclones, especially along the Pacific slope, but none of these events impacted land directly (Alfaro and Pérez-Briceño, 2014). This situation changed drastically in November 2016 when Hurricane Otto made landfall in northern Costa Rica.

Landslides have been widely related to rainfall intensity-duration relations (Guzzetti et al., 2008; Sidle and Bogaard, 2016; Segoni et al., 2018) or to seismic activity (Lacroix et al., 2014; Reichenbach et al., 2018). Nonetheless, the probability that rainstorms and earthquakes affect the same area is small (Sassa et al., 2007; Lin et al., 2008b; Chen and Hawkings, 2009). Landslide events that were triggered through the combination of both processes have been intensively described for the 2008 Mw 7.9 Wenchuan Earthquake in Sichuan, China (Zhang et al., 2016; Fan et al., 2018). Understanding the combined effect of both processes on landslide triggering thus could contribute to an improved forecasting and early warning in the case of future compound events (Leonard et al., 2013; Zscheischler et al., 2018).

The passage of Hurricane Otto in 2016 caused 10 fatalities and serious damage due to flooding and landsliding in Costa Rica. According to the National Commission for Risk Prevention and Emergency Management (CNE), 10,831 people were affected or isolated, 69 shelters were activated to host 3,655 evacuated people. Some 461 communities reported damage after the passage of the hurricane, namely on 280 road sections, 48 bridges, 14 dikes, 6 aqueducts, and 27 educational centers. In addition, 1610 private homes were affected, of which 262 were destroyed completely. The approximate economic losses caused by Hurricane Otto were in the order of 187 million US$ (CNE, 2017a).

The understanding of such extraordinary phenomena is important to anticipate cross-sectorial impacts and to reduce economic losses and casualties (UNISDR, 2015). Therefore, the aim of this paper is to analyze the compound effects of seismic activity at Miravalles volcano (5.4 Mw) on July 2, 2016, the subsequent passage of Hurricane Otto on November 24, 2016, and the resulting occurrence of at least 942 landslides and debris flows that affected different communities on the NE and SW slopes of Miravalles volcano.

2.2. Study area and landslide triggering

2.2.1. Geological and geomorphic setting

Located in northern Costa Rica, the Guanacaste Volcanic Arc was formed by the subduction of the Cocos under the Caribbean plate at relative plate movements of ~8 cm yr^{-1}. This subduction has resulted in active volcanism and the faulting of a chain of Quaternary shield-like stratovolcanoes (Marshall, 2007; DeMets et al., 2010). Miravalles volcano (2028 m asl) is one of these and has been described by Alvarado (2011) as a very complex stratovolcano (160-187 km^2, 60-120 km^3) with six volcanic craters, of which five are aligned in a NE-SW direction. The highest point of the volcano is a remnant cone and next to its southwestern base is Miravalles crater (600 m in diameter). To the NE of the volcano's peak, a double cone can be found, dissected by a NW orientation fault. Whereas one of these two cones is much eroded, the other (with a peak at ~2000 m asl) is better conserved. Both cones show crater vestiges, but at the NW are relics of a very antique, eroded crater. The last major activity at Miravalles volcano dates back to 8000-8200 years BP; this event left lava flows, debris avalanches and subsequent lahars. In historic times, only a small steam hydrothermal explosion has been noted on the SW flank of Miravalles volcano in 1946, as well as minor, secondary type activity in the form of thermal sources, fumaroles, and mud pots (Cigolini et al., 2018). The volcanic massif mainly consists of Pleistocene lavas, tuffs as well as deposits from debris avalanches and debris flows (Denyer and Alvarado, 2007). Soils of Miravalles volcano are typical *hapludands*, volcanic non-crystalline soils with depths ranging from 10-55 cm. They contain predominantly sandy clay textures with bulk density of ~0.68 g/cm^3, with diffuse plane limits (Cervantes, 1977; Méndez, 1977; Sáenz et al., 1993). At higher elevations, the volcanic massif is part of a protected zone (since 1976) with mountain-cloud forests with trees reaching up to 30 m in height (Lawton et al., 2016).

2.2.2. Seismic activity and the 2016 Bijagua earthquake

Central America is one of the most active zones worldwide in terms of seismicity due to the interaction of five tectonic plates. In the case of Costa Rica, tectonic activity is favored by the Cocos-Caribbean subduction margin, the Panama microplate, and the Cocos volcanic range subduction (Alvarado et al., 2017b). According to Taylor et al. (2016), tectonics are particularly complex in northern Costa Rica and seismicity controlled by strike-slip, normal and inverse faults. Around Miravalles volcano, 5 and 6 Mw earthquakes have been recorded in 2002, 2011, and 2016. The substantial seismic activity in our study region has been confirmed by a minimum 1D velocity model that was applied to the Guanacaste Volcanic Arc, as it identified one of the main seismicity clusters on the basement of Miravalles volcano (Araya et al., 2016). Furthermore, Montero et al. (2017) proposed that the Hacienda-Chiripa fault system would serve as the northeastern boundary of the Guanacaste Volcanic Arc Sliver motion related with the regional seismicity. The Bijagua earthquake occurred on July 2, 2016 at 7:58 PM with a Mw=5.4 and a focal depth of 7 km. The epicenter of the earthquake was located 4 km north of Bijagua de Upala (Fig. 11). The main shock was followed by two aftershocks of Mw≥4.0 within 30 minutes after the main event. The earthquake was triggered by a dextral strike-slip NW-SE fault running parallel to the Caño Negro fault and had a Modified Mercalli scale (MM) intensity of VI in the towns of Las Armenias, Aguas Claras and Bijagua in Upala canton (Taylor et al. 2016; Porras et al. 2017). According with the

EEL-UCR the peak ground acceleration registered in Upala at 19 km north was of 159.73 cm/s^2, it is unknown for the Miravalles volcano. Noteworthy, the September 5, 2012 7.6 Mw earthquake occurred in Samara (Nicoya), ~110 km away from our study site and with a MM=VI at Miravalles volcano (Linkimer et al., 2013).

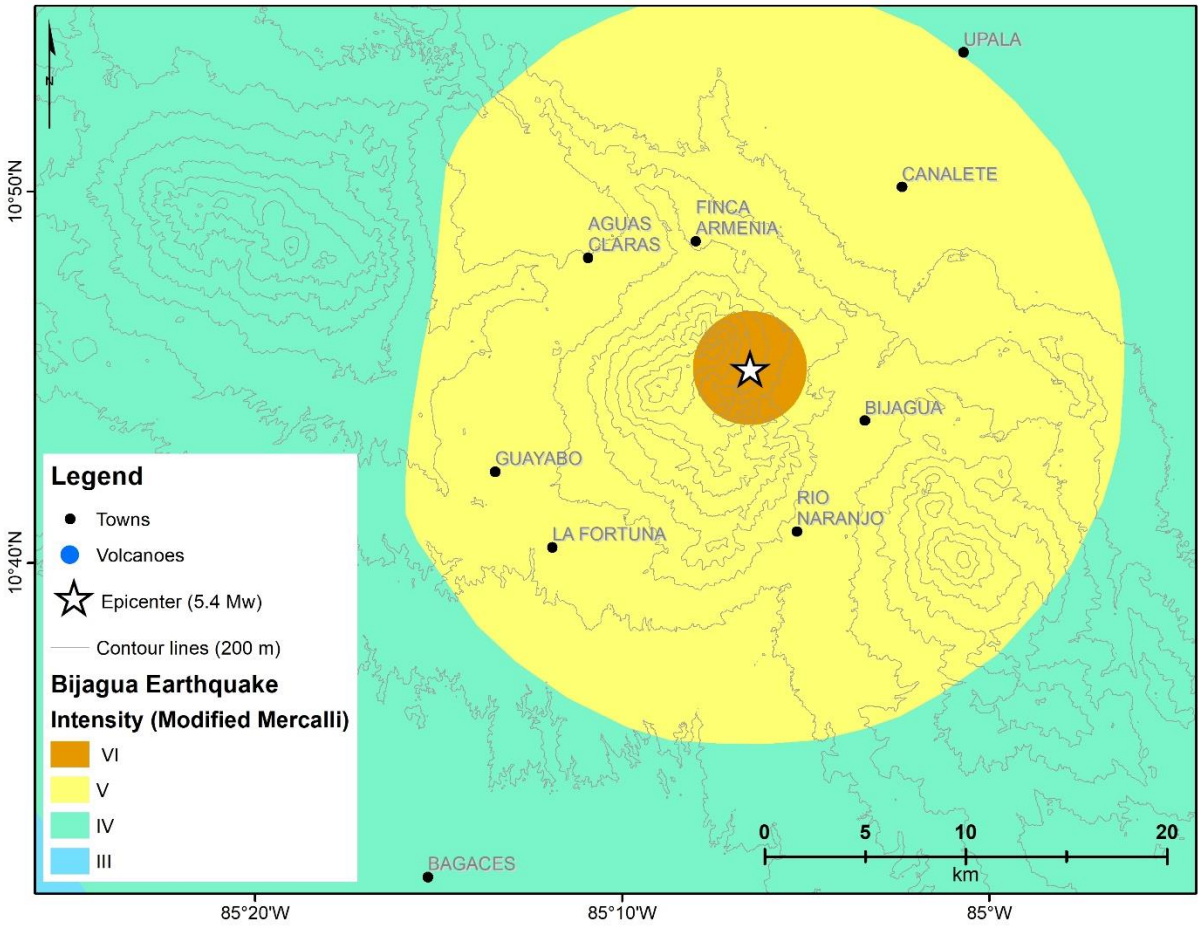

Fig. 11. Bijagua earthquake epicenter with its Mercalli Modified Intensity distribution.

2.2.3. Dynamics of Hurricane Otto

On November 21, 2016, tropical depression # 16 was recorded off the coast of the Caribbean Sea, towards the NE of Costa Rica and Panama. In the early morning hours of that day, the system entered warm waters with favorable atmospheric conditions for its intensification, so that by the night convection developed further into a tropical storm with sustained winds of 95 km/h – Otto was born. By November 22, it continued to intensify to such an extent that by 3 PM it is officially named the seventh hurricane of the season with wind speeds of 120 km/h and an atmospheric pressure in its center of 984 mb. During the morning of November 23, the system weakened temporarily, becoming a tropical storm again, however, late that same day, its intensity increased considerably to reach wind speeds of 140 km/h (NOAA, 2017). By November 24, Otto continued to produce a deep convection area as part of a rapid intensification process until it made landfall south of San Juan de Nicaragua, as a category 3 hurricane with winds of 185 km/h and an

atmospheric pressure at sea level of 975 mb (Fig. 12). During the night of that day, the eye of the hurricane was still discernible and well organized, as it passed over the border area between Costa Rica and Nicaragua. By the time the depression passed over Upala, Otto maintained its category 1 hurricane intensity. While over land, it moved between 15 and 20 km/h in a westerly direction, and wind speeds dropped to ~110 km/h, so that it became a tropical storm in the night from November 24-25. By November 25, wind speeds decreased further to 95 km/h, before they decreased to 35-45 km/h during the following night. By November 26, Otto officially dissipated in the Pacific Ocean (NOAA, 2017).

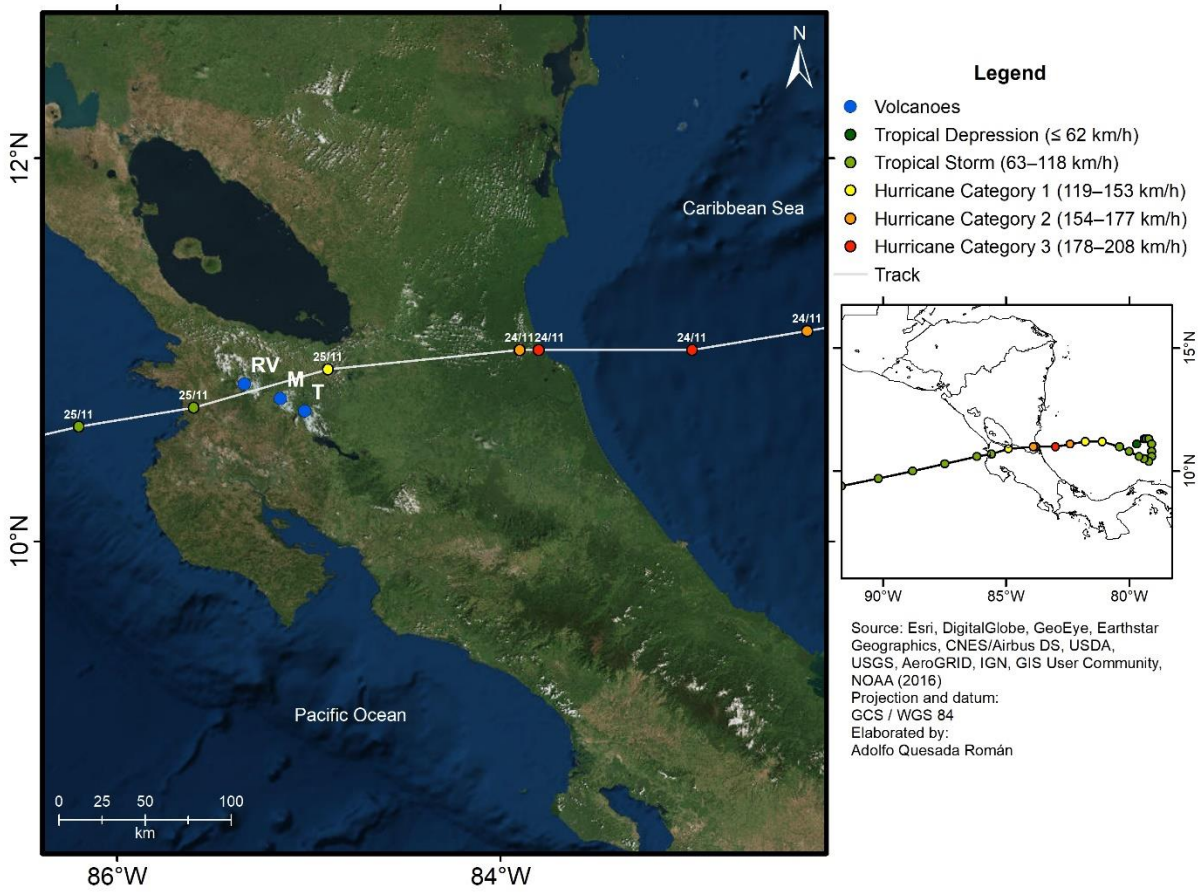

Fig. 12. Track, dates, and categories of Hurricane Otto as it passed over Costa Rica between November 24 and 25, 2016. RV: Rincón de la Vieja volcano, M: Miravalles volcano, T: Tenorio volcano.

2.3. Materials and methods

2.3.1. Rainfall patterns

For the analysis and mapping of rainfall accumulated during the passage of Hurricane Otto at Miravalles volcano on November 24, 2016, we used weather records from 14 stations of the Costa Rican National Meteorological Institute (IMN) and 21 records of the Costa Rican Institute for Electricity (ICE). These stations are either mechanical or automatic, presenting either daily or hourly precipitation totals, respectively. The rainfall information for November 24, 2016 was then

interpolated using a multivariate and multidimensional Nearest Neighbor approach, because the spatial distribution of rainfall was best represented by this approach for the study area and as the method has also been proven to have a smaller bias when it comes to landslides and debris flows triggered by rainfall (Nikolopoulos et al., 2015; Destro et al., 2017). Historical data (1975-2017) from the closest meteorological stations of Miravalles volcano were then used to contrast the cumulative rainfall information with the precipitation during 2016 event and to put rainfall totals recorded during the passage of Otto into perspective.

2.3.2. Geomorphic impacts

The ground effects of Hurricane Otto around Miravalles volcano were mapped with 30-cm resolution WorldView-3 and WorldView-4 imagery taken after the passage of Hurricane Otto (in February and March 2017), and with 5-m RapidEye satellite imagery available for 2010 (CNE, 2017b). The high-resolution WorldView images were made available from the National Commission for Risk Prevention and Emergency Management (CNE). To prevent misinterpretation and/or the inclusion of landslide scars predating the passage of Hurricane Otto, landslide mapping was restricted to clear, bare areas from which dense vegetation was clearly removed very recently and for which freshly eroded soil was clearly distinguished. In addition, immediately after the passage of the hurricane, the CNE realized several fieldworks to verify the impacts of Otto on the slopes of Miravalles volcano and in the river's plains. This post-event inventory was used further to validate the satellite-based landform mapping and the distinction between landslides and debris flows.

Data of similar quality does not unfortunately exist for other periods, which prevented analysis of similar detail prior to the passage of Hurricane Otto. Miravalles volcano is one of the most difficult areas in Costa Rica when it comes to obtain imagery as it acts as a natural barrier between the Caribbean Sea and the Pacific Ocean, forming a continuous cloud cover along the year, preventing any analyses of similar quality for the pre-Hurricane situation. For the pre-Hurricane period, analyses were based on four 10-m resolution Sentinel-2A satellite images (T16PFT, T16PFS, T16PGT, T16PGS) to detect the occurrence of landslide scars that existed already before the Bijagua earthquake (taken on February 4 and April 14, 2016), those newly seen on imagery after the seismic event (October 10, 2016), as well as those existing after the passage of Hurricane Otto (March 30, 2017). Analyses were realized for the three volcanoes were the highest rainfall totals were registered, namely Tenorio, Miravalles, and Rincón de la Vieja (see Fig. 13 for details).

2.3.3. Triggering analysis

We used a generalized linear model (GLM) to describe linkages between landslide occurrence (L) and co-variables such as the distance of landslides from the Bijagua earthquake epicenter (D), altitude (A), slope (S) or rainfall totals recorded during the passage of Hurricane Otto (R). To this end, we created a mesh with a cell size of 100 × 100 m covering the entire study region and estimated the centroid for each mapped landslide. For each cell, we also computed mean values for each co-variable, as well as the number of landslide centroids falling inside each cell using geostatistical tools from ArcGIS 10. Based on the Akaike Information Criterion (AIC) (Samia et al., 2018), we contrasted the null hypothesis (i.e. L ~1) against the alternative hypothesis (i.e. L~D+A+S+R). We also evaluated possible interaction effects between co-variables. Model

parameters were then used to evaluate the weight of each co-variable explaining the occurrence of landslides. All co-variables were first standardized using z-score. Debris flows triggered around Miravalles volcano were analyzed in terms of process morphometry, area, distance of landslide occurrences from the epicenter, elevation, slope, and aspect.

2.4. Results

2.4.1. Dynamics of Hurricane Otto

Hurricane Otto arrived to Costa Rica at Los Chiles around 2 PM of November 24, 2016 where the three weather stations recorded a daily rainfall total of 108, 116, 166.2 mm, respectively. The hurricane then moved on to Upala to result in 131 to 137.2 mm of rainfall recorded for the 7 to 10 hrs during which the depression remained in the area. Other regions in northern Costa Rica reported high rainfall totals as well for the same day, as for instance at the stations located in Liberia and La Cruz with 109.4 and 353.2 mm during 5 to 7 hours. The closest meteorological stations to Miravalles volcano reported 179.8 (Canalete), 235 (Bijagua), 180.9 (Guayabal), 178.1 (Río Naranjo), 224.8 (Fortuna), 299 (Casa Máquinas Miravalles), 131.8 (Casa Vieja), and 225.3 mm (Pozo 29). The distribution of the stations and interpolated rainfall patterns are presented in Fig. 13.

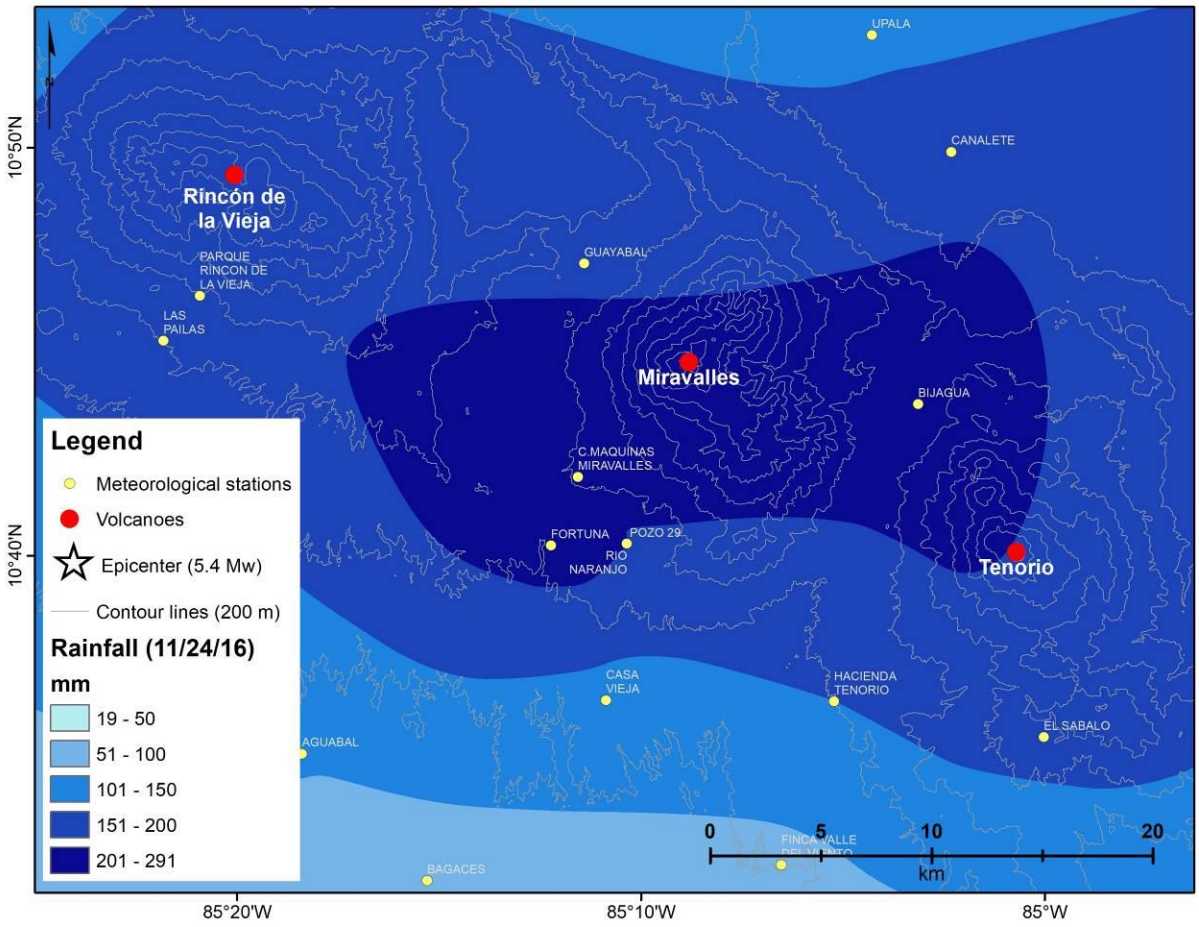

Fig. 13. Rainfall distribution as recorded (yellow dots) and interpolated during the passage of Hurricane Otto on November 24, 2016 in the region around Miravalles volcano.

The spatial distribution of rainfall totals nicely illustrates the interaction of Otto's cyclonic flow with orography, generating an ascent of humid air masses around Miravalles volcano and an important cloud nucleus remaining mostly stationary between 6 and 7 PM (Fig. 14a). This nucleus released 117 mm of rainfall at the Casa de Máquinas Miravalles station in just one hour. Three hour totals from the same station illustrate that this single rainfall event surpassed the monthly rainfall totals of a normal November. November 24, 2016 stands out as the rainiest day ever recorded at the nearby meteorological stations of Canalete, Bijagua, Hacienda Tenorio, Fortuna, C. Máquinas Miravalles, Casa Vieja, and Pozo 29, representing between 60 and 165% of historical mean November rainfall totals (Fig. 14b).

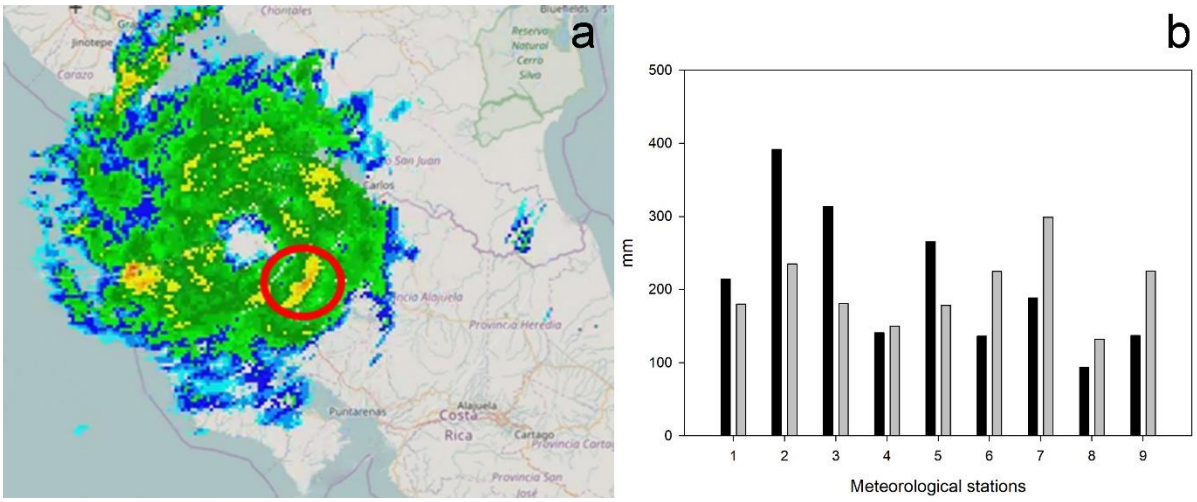

Fig. 14. a. INETER radar image of the spatial distribution of rainfall during Hurricane Otto on November 24, 2016 at 07:15 PM (NOAA 2017), red circle indicates Miravalles volcano location. b. comparison of historical (1975-2017) November rainfall totals of the meteorological stations closest to Miravalles volcano (black bars) and rainfall totals recorded on November 24, 2016 (gray bars): 1. Canalete, 2. Bijagua, 3. Guayabal, 4. Hacienda Tenorio, 5. Rio Naranjo, 6. Fortuna, 7. C.Maquinas Miravalles, 8. Casa Vieja, 9. Pozo 29.

2.4.2. Landslides and debris flows on Miravalles volcano

The surveys made with Sentinel-2A satellite images taken in February 2016 and March 2017 confirmed that Hurricane Otto triggered a substantial number at Miravalles volcano (Fig. 15). Even if the three main volcanoes in the region were affected by more than 250 mm of rainfall during Hurricane Otto, and even if they all have very similar lithologies consisting of Pleistocene lavas, tuffs, debris avalanche and debris-flow deposits as well as comparable hapludands soils, the Rincón de la Vieja and Tenorio volcanoes do not show evident signs of landslide or debris-flow activity.

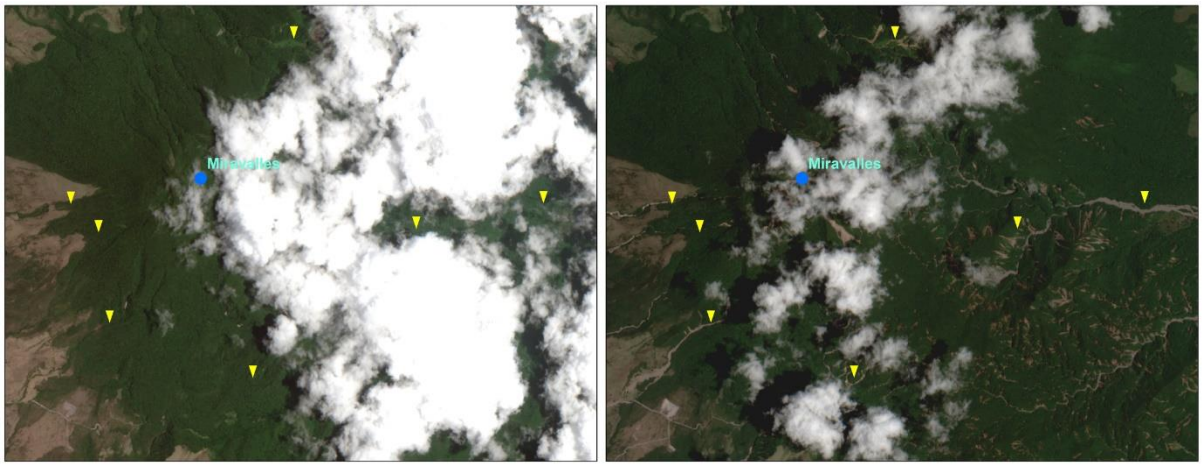

Fig. 15. Sentinel-2A satellite images used to verify landslide occurrence at Miravalles volcano between February 2016 (left) and March 2017 (right). Yellow arrows indicate localities where landslides and debris flows have been triggered by Hurricane Otto.

Some localized landslides occurred after the Bijagua earthquake on July 2, 2016 and were reported by CNE (2016). The vast majority of landslides identified were, however, triggered by Hurricane Otto, and after seismic destabilization of hillslopes of Miravalles volcano. We identified a total of 942 landslides on the volcano of which 497 were located on the Pacific slope, whereas 445 landslides were found on the Caribbean slope. A majority of landslides (62%) was located within 3 to 6 km from the epicenter of the Bijagua earthquake (Fig. 16), and mostly originated from the older volcanic deposits (0.6-0.2 Ma). Landslides and debris flows were triggered predominantly (55%) on eastern, southeastern and southern slopes, presumably as a result of the orientation of regional and local faults (Caño Negro and Río Naranjo-Bijagua faults) and N-S and SW-NE lineaments. With the exception (7%) of a few landslides located on younger Pleistocene igneous rocks (<0.2 Ma), landslide areas were smaller than 2.24 ha. Almost three-quarters (74%) of all landslides were triggered on rather gentle slopes (10.7–30.7 degrees) and 90% of all events were triggered at elevations comprised between 771–1663 m asl (with the summit of the volcano being at 2028 m asl) (Fig. 16).

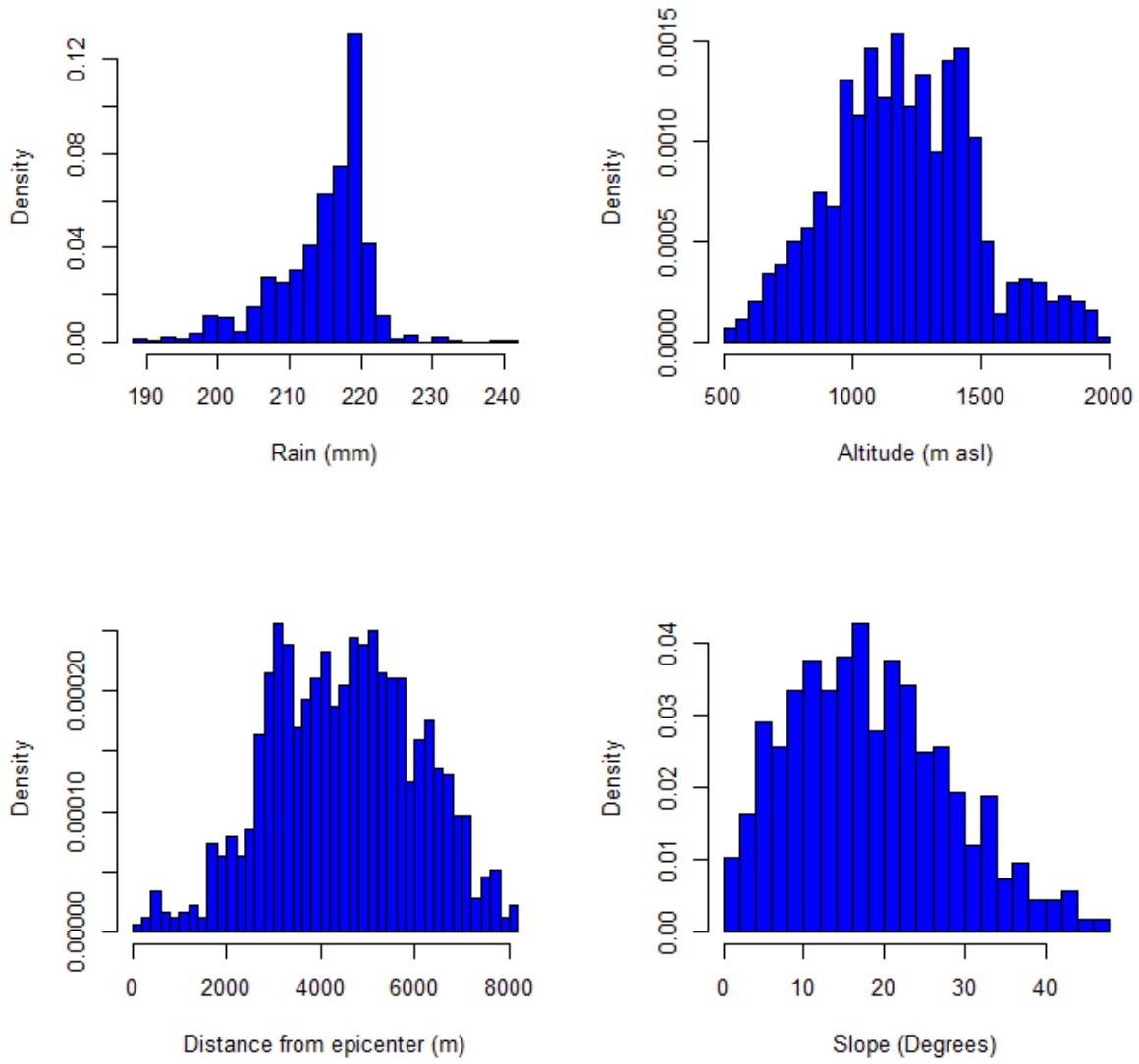

Fig. 16. Landslide density distributions as a function of rainfall totals, altitude, distance from epicenter, and slope.

Statistical analyses of the landslides and debris flows recorded on Miravalles volcano based on the AIC criterion. Results supports the alternative (AIC_{Ha}=6897.5) against the null hypothesis (AIC_{Hn}=7909.0), and suggest that the best generalized linear model supports an interaction between rainfall totals and epicenter distance, but that altitude and slope are relevant additional variables as well (L ~ R×D+A+S). Table 1 provides the model parameters, also indicating that the most significant influence on onset probability of landslides are given by A and R:D, as shown by z-ratio tests of parameter estimates. These findings are consistent with existing, significant influences of altitude and coupled effects of a previous earthquake and subsequent intense rainfalls on landslide occurrence probabilities.

Table 1. Parameters used to model landslide occurrences: Null deviance is 6105.7 on 22021° df, residual deviance is 5084.3 on 22016° df, and the AIC is 6897.5. Pr(>jzj) is the probability of

finding the observed Z-ratio in the normal distribution of Z with a critical point of jzj. ***P = 0.001.

Model terms	Estimate	SE	Z-ratio	Pr(>|z|)
(Intercept)	-3.63509	0.04782	-76.017	< 2e-16***
R	0.44371	0.06391	6.943	3.83e-12***
D	-0.2335	0.04283	-5.452	4.99e-08***
A	0.61512	0.03394	18.126	< 2e-16***
S	0.18596	0.03096	6.007	1.89e-09***
R:D	-0.62565	0.06476	-9.661	< 2e-16***

This coupled effect between epicenter distance and rainfall totals during Hurricane Otto is also very clear in Fig. 17, showing that rainfall has a larger effect on the triggering of landslides close to the epicenter, as shown in panel (D=-2). By contrast, the effect of rainfall is lower with increasing distance from the epicenter (D=0); and almost negligible with greater distances (D=2).

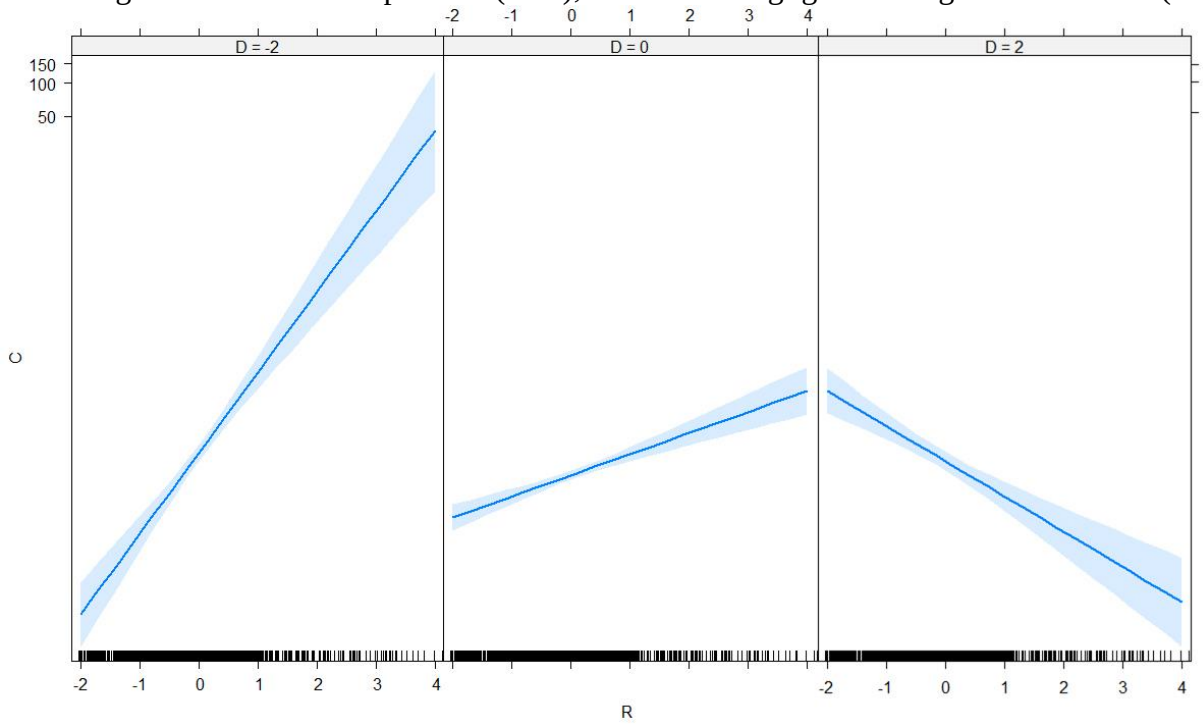

Fig. 17. Influence of rainfall and epicenter distance on landslide triggering. These figures illustrates the relationships between rainfall anomalies (R) and landslides occurrence (C) at (D=-2), near (D=0), and far away (D=2) distances from epicenter.

Landslides were released from shallow, sandy-clayey soils (≤ 50 cm), in the form of translational slides that developed into debris flows once they reached the fluvial network (Fig. 18). The largest debris flows and most severe damage were observed at Aguas Claras, San Isidro, Pata de Gallo, Zapote, Canalete and Bijagua de Upala in the case of the Zapote basin, at Bagaces, Manglar, La Unión, Santa Rosa, Hornillas in the Blanco basin, and at La Giganta, Cuipilapa and Martillete in the Cuipilapa basin. On the Pacific slope, debris flows traveled as far as 40.1 km (close to Bagaces at 90 m asl), and 44.7 km on the Caribbean slope where they reached northern Upala at 34 m asl.

Debris-flow landforms observed after Hurricane Otto varied significantly in width from 6.7 m on the steep slopes to 1064 m in the depositional areas.

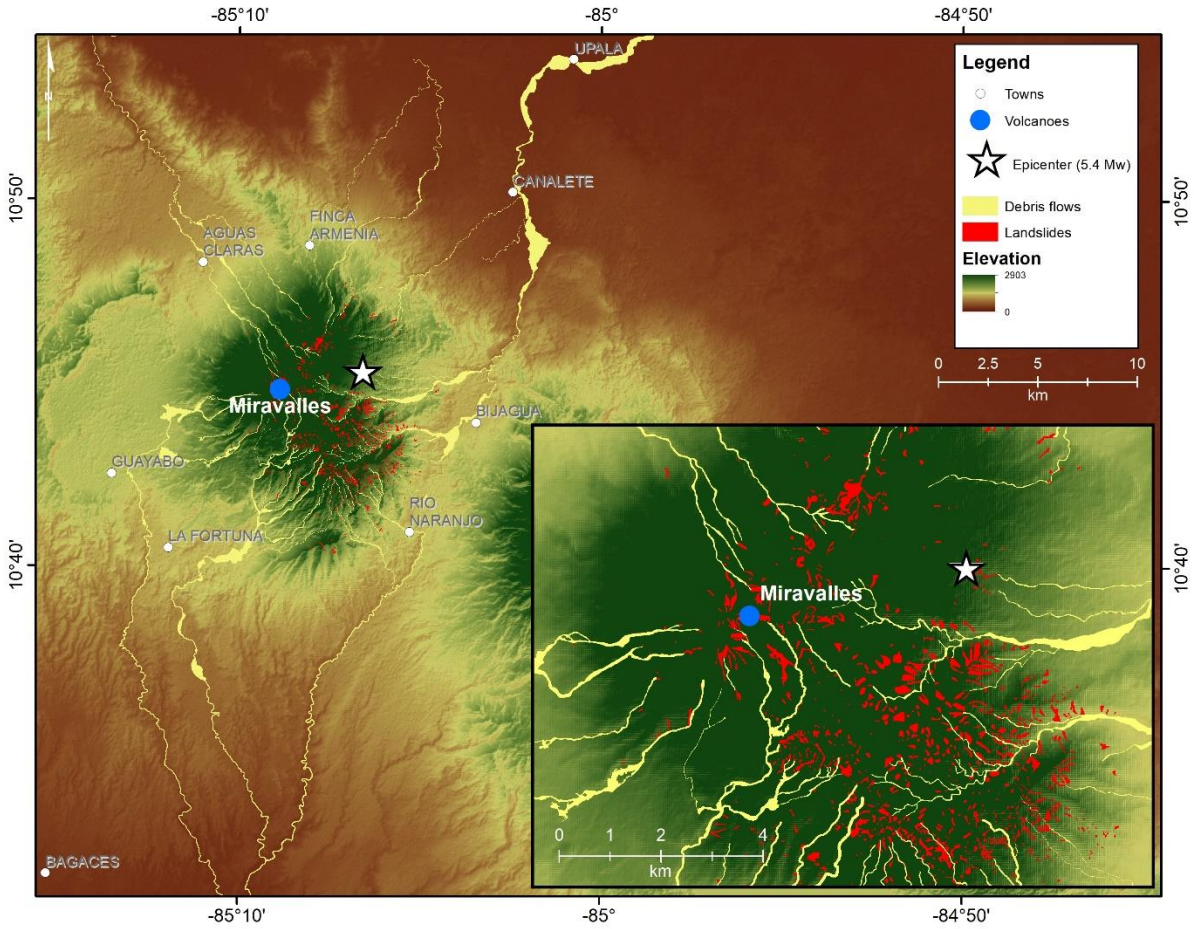

Fig. 18. Landslides (red) and debris flows (yellow) triggered by Hurricane Otto around Miravalles volcano.

Figure 19a illustrates the source areas of landslides on the slopes of Miravalles volcano and the deposits left by debris flows in the fluvial valleys. The debris flow in Bijagua river moved boulders exceeding 2 m in diameter and lateral erosion along its river banks was substantial (Fig. 19b). Along the braided river sections with slopes around 10-15 degrees, the debris flows left ample amounts of boulders and a fine layer of sand (Fig. 19c). In addition, the debris flows eroded substantial amounts of large wood from the river banks and terraces. In the lower areas where slope angles decreased below 10 degrees, huge amounts of large wood and smaller rocks were deposited by the devastating debris flows, with substantial, negative impacts on different types of infrastructure. Damage occurred both on the Pacific and Caribbean slopes of the volcano (Fig. 19d).

Fig. 19. a. Helicopter overflights of the CNE over Miravalles volcano and Bijagua after Hurricane Otto. b. Landslides on Miravalles volcano north-eastern flank. c. Blocks and large wood moved over Bijagua river; in the background it is appreciated a landslide on the massif. d. The debris flows destroyed several houses in Bijagua and caused four casualties.

2.5. Discussion

In this study, we describe one of the most severe hurricanes recorded in Costa Rica and the impacts it has had on shallow landsliding and related debris flows on the slopes and surroundings of Miravalles volcano. Mass movements triggered by severe rainfalls occurred primarily from slopes that have assumedly been weakened by seismic shaking several months prior to the passage of the hurricane. At neighboring volcanoes, farther away from the 2016 Bijagua earthquake, and despite similarities in age, soil, edaphic composition and rainfall totals, landslides have not been recorded.

2.5.1. The hurricane season of 2016

Hurricane Otto did not only occur very late in the hurricane season (which is considered to last until November 30), but it was also the most intense Atlantic basin hurricane recorded since 1851 so late in the year (NOAA, 2017). In addition, Otto also was the first hurricane that passed through Costa Rica to reach the Pacific Ocean while maintaining its name. One of the causes for this hurricane to occur in late November is related to the formation of a La Niña phase at the end of 2016, as well as to warm seas surface temperatures (SST) in the North Atlantic basin. The Atlantic

Multidecadal Oscillation (AMO) – in its warm phase since 1995 – has facilitated the occurrence of anomalously warm SST (1–2 °C above seasonal average) and therefore likely intensified many of the 2016 storms over the Caribbean (Klotzbach and Gray, 2008). Interestingly, several hurricanes reached maximum intensities at unusually high latitudes, not far from 30° N. Consequently, the 2016 hurricane season was more active than average, both in terms of the quantity of tropical storms as well as in terms of numbers and severity, making it the most active year after 2013 (Bell et al., 2017).

The area affected by Hurricane Otto was located primarily in the North Pacific and Northern climate zones of Costa Rica. As a result of the passage of Otto, new absolute November precipitation maxima were recorded at several stations. The passage of Otto was also quite unusual in terms of return periods at some stations. At the meteorological station of Casa de Máquinas Miravalles, the rainfall totals recorded had a return period of 41 years. At Bijagua, a return period of 32 years was obtained, whereas in the case of Fortuna and Canalete, return periods were 83 and even 213 years, respectively (Alvarado et al., 2017a). A 5400 cal yr BP palynological record calibrated with the sedimentary signature of Hurricane Joan (1988), from a very close location where Hurricane Otto landed in Nicaragua, showed an average return period for major hurricanes of ~140–180 yr (McCloskey and Liu, 2012). Increased rainfall is typical on the Pacific slope during the La Niña phase, reflecting the increase in the number of meteorological situations that generate storms, whereas in the case of El Niño, a decrease in precipitation is normally observed throughout the Costa Rican Pacific coast. In terms of annual precipitation in the North Pacific zone, values can go up to almost 50% over the mean during the La Niña phase and are typically one-fourth below average in the case of El Niño events. The influence of ENSO implies that during the La Niña phase, a greater probability exists for hurricane formation in the Atlantic than during an El Niño event (Goldenberg et al., 2001).

In addition, the impact of a tropical cyclone affecting Costa Rica lies in its position and persistence in the Caribbean basin. Hurricane Otto remained offshore Panama and Costa Rica for 6 days as a tropical depression to develop into hurricane (Taylor and Alfaro, 2005; NOAA, 2017). In the specific case of 2016, warm SSTs in the Atlantic Ocean and in the Caribbean Sea created a transverse dipole configuration with respect to the Eastern Tropical Pacific that propitiated a greater amount of rainfall over the Caribbean Basin (Enfield and Alfaro, 1999). Furthermore, the presence of a Warm Water Pool in the Northern Hemisphere waters was quite widespread and conducive to the formation of tropical cyclones (Wang et al., 2006). For these reasons, the 2016 hurricane season was more active than normal with 15 named tropical storms (average: 11.8), of which 7 reached the intensity of a hurricane (6.4) and of which 4 (2.7) developed into major hurricanes (Bell et al., 2017). The 2016 hurricane season was also significantly stronger than what had been recorded between 2013 and 2015, and developed a major number of cyclones affecting mainland (NOAA, 2017).

2.5.2. Seismic and hydrometeorological compound events

The passage of Hurricane Otto over a zone that was affected by seismic activity only months before yielded a very rare opportunity to study the effects of a compound event. The Guanacaste Volcanic Arc are infamous for being covered in clouds almost continuously, such that aerial and/or satellite imagery of Miravalles volcano and the surrounding areas was not easily found. Therefore,

geomorphic impacts of the Bijagua earthquake and the passage of Hurricane Otto was helped greatly by the field surveys of CNE (2017b).

Landslides triggered during Hurricane Otto were mobilized mostly from weathered sandy clayey soils to be transformed into debris flows once fluidized and transported in the fluvial system. Mechanical laboratory tests have shown that typic Hapludands, common for the areas affected by the 2016 landslides, loose their cohesion under intense rainfall inputs (Seguel and Horn, 2005). Alvarado et al. (2017) reported more than 65 landslides out of regolithic materials with velocities of 15 m/s favored by the humic and vegetal cover. Mean velocities for different creeks affected by debris flows were between 4.6 and 22.1 m/s with mainly andesite decimetric to metric blocks deposits. Material was poorly sorted, showed a rough inverse gradation, and large wood amounted to 5-20% of the total flow volumes. At Miravalles volcano, scars of smaller rainfall-triggered landslides occurring after the earthquake stabilized quickly as a result of rapid colonization with tropical vegetation. Larger and deeper landslides remain prone to reactivation even several years after an earthquake with the possibility of new debris flows forming in the form of geologic hazard chains (Fan et al., 2019). The occurrence of landslides and debris flows in tropical environments after intense rainfall events has been described extensively in the literature (e.g. Kanji et al., 2003; Wieczorek and Glade, 2005). Specifically, works on compound events and the influence of a previous, destabilizing earthquake and a subsequent rainfall event triggering landslides and debris flows have been broad studied for Weychuan Mw 7.9 earthquake in 2008 (e.g. Tang et al., 2011; Zhang et al., 2014). Recently, similar studies have been applied to volcanic contexts at Aso volcano in Japan (Saito et al., 2018; Yano et al., 2019). In addition, several studies of the impact of prior earthquakes and subsequent tropical cyclones (typhoons) as landslides coupled trigger have been identified for Taiwan (Lin et al., 2008a; Chen et al., 2011; Lin et al., 2012; Kuo et al., 2018; Chen et al., 2019).

The combined or subsequent occurrence of seismic and hydrometeorological processes can in fact lead to compound events and amplify/intensify disasters (Wallemacq and House, 2018). The high seismicity of Central America and the particular tectonic dynamics of the Cocos-Caribbean subduction margin, Panama microplate, and the Cocos volcanic range subduction make this region particularly susceptible to slope weakening (Alvarado et al., 2017b). The region have presented a vast history of earthquake-induced landslides, especially translational slides in lateritic soils on lengthy slopes and falls and slides in steep slopes in pyroclastic soils (Bommer and Rodríguez, 2002). In combination with the high precipitation totals recorded in the region, Central America and Costa Rica have a high annually incidence of landslides, mostly controlled by regional rainfall patterns linked to the different phases of ENSO. Accordingly, the region also has a very high correlation between mean daily rainfall totals and mean daily landslides worldwide (Froude and Petley, 2018). As such, it would be advisable to monitor regions that have previously been affected by earthquakes, especially during extraordinary rainfall events such as tropical cyclones (Piciullo et al., 2018). Previous examples of earthquake weakening and subsequent landslides and debris flows exist in Costa Rica and have been documented at Sarchí in 1912, San Mateo in 1924 (Alvarado et al., 1988), Los Patillos in 1952 (Alvarado et al., 1995), Limón in 1991 (Quesada-Román, 2016), and Cinchona in 2009 (Alvarado, 2010; Quesada-Román and Barrantes, 2016). The long list of past disasters confirms the recurrent occurrence of compound events in the region and underlines the need for a systematic monitoring and early warning systems on slopes and river networks further.

In addition, the influence of large wood on debris-flow behavior and subsequent impacts they have on infrastructure were critical during the Hurricane Otto disaster. Tropical rivers are known for their significantly different wood loads as a result of extremely high rates of wood decay and high transport capacity for wood associated with very large peak discharge (Cadol et al., 2009; Wohl et al., 2017). As such, large wood is a further amplifier of risk in these environments as it may damage infrastructure, block river channels, and induce flooding (Ruiz-Villanueva et al., 2016). Thousands of large wood pieces were removed from the channel network around Miravalles volcano during post-event channel dredging operations. Field observations also confirm that the dense forest cover on the volcano has been damaged substantially by the strong winds and landslides. In addition, ample amounts of dead logs along the slopes and riverbanks were yet another important input during this particular event.

2.6. Conclusions

In this study, we analysed the compound effects of (i) a seismic weakening of slopes by the Bijagua earthquake in July 2016 and (ii) extraordinary rainfall on November 24, 2016 by Hurricane Otto on subsequent landslide and debris-flow activity on Miravalles volcano. The generalized linear regression model showed a coupled earthquake-hurricane dynamic due that more landslides densities where found closer to the epicenter on greater rainfall sites, also conditioned by higher slopes and altitudes. A total of 942 landslides were mapped around the volcano, of which 62% were located between 3 to 6 km from the Bijagua earthquake epicenter on Pleistocene lavas, tuffs, debris avalanche, and debris-flow deposits. The study demonstrates the importance of monitoring mountain regions previously affected by earthquakes during extraordinary precipitation events. Further research concerning landslides induced by earthquakes and subsequent strong rainfall events is necessary to reduce fatalities and economical losses in tropical countries.

CHAPTER 3

3. Tropical dendroecology: approaches, applications, and future prospects

Adolfo Quesada-Román [a,b,*], Juan Antonio Ballesteros-Cánovas [a,c], Markus Stoffel [a,c,d]

[a] Climatic Change and Climate Impacts, Institute for Environmental Sciences, University of Geneva, Boulevard Carl-Vogt 66, CH-1205 Geneva, Switzerland
[b] Department of Geography, University of Costa Rica, San José, Costa Rica
[c] Dendrolab.ch, Department for Earth Sciences, University of Geneva, 13 rue des Maraîchers, CH-1205 Geneva, Switzerland
[d] Department F.-A. for Aquatic and Environmental Sciences, University of Geneva, Boulevard Carl-Vogt 66, CH-1205 Geneva, Switzerland

Submitted to Earth-Science Reviews

Tropical forests cover only 7% of the Earth's land surface. Yet, they host nearly half of global tree density with a high species number (~40,000 species), store up to 25% of global terrestrial carbon and represent one-third of net primary productivity on Earth. Over the last four decades, the study and interpretation of tree growth in various fields of tropical dendroecology has gained substantial momentum, not least as a result of the increasing application of tree-ring data in tropical climatology, ecology, geomorphology and archaeology. By contrast to exceptions, various tropical species have been shown to form growth rings with a regular, sometimes annual, layering that is driven by the species' sensitivity to climatic, ecological, or geodynamic variations. This paper provides a thorough review of dendroecology in the tropics by (i) highlighting insights into tree growth patterns, (ii) demonstrating the regions that have been studied preferentially and the families and genera of trees that have been employed most frequently, so as to provide an overview on the most suitable species, (iii) summarizing common approaches and techniques used in tropical dendrochronology, (iv) illustrating different applications, and (v) by presenting limitations inherent to tree-ring research in the tropics. The paper concludes with a call for further research in this still understudied environment and provides potential perspectives for future work in the most biodiverse region of the world.

3.1. Introduction

Dendroecology is the science of identifying and quantifying environmental processes through the dating of annual growth layers (or rings) in woody plants including perennial herbs, shrubs and trees (Fritts, 1971; Schweingruber, 1996; Speer, 2010). By doing so, dendroecology represents a powerful tool to yield detailed insights into diverse fields of ecological, climatic and Earth sciences (Schweingruber, 1996). Among various other fields, dendroecology has helped to critically advance our understanding of climatology (Hughes, 2002; Esper et al., 2016), ecology (Fritts, 1989; Amoroso et al., 2017), geomorphology (Stoffel et al., 2010; Stoffel and Corona, 2014; Ballesteros-Cánovas et al., 2015), and archaeology (Kuniholm, 2002; Sass-Klaassen, 2002). For more than a century now, tree-ring research has covered all continents except Antarctica, with chronologies being developed mostly in the mid to high latitudes of the Northern Hemisphere (Zhao et al., 2019). This geographic focus is somehow the result between the availability of trees to record climate and environmental changes (Esper et al., 2016), the extended use of forest regions with long-lived trees (Pearl et al., 2020), and the location of facilities available to perform dendrochronological research, in addition – of course – also to the researchers' interests to address specific research questions (Anchukaitis, 2017).

Tropical forests cover just 7% of the Earth's land surface, but they store an estimated 25% of global terrestrial carbon and account for one-third of global net primary productivity (Amoroso et al., 2017). In addition, tropical and subtropical forests encompass nearly half of the tree density at the global scale (Crowther et al., 2015). In tropical environments, differences between seasons are less marked than in temperate or cold climates, such that the misconception of tropical species exhibiting no growth rings at all persisted over decades (Worbes et al., 2017). Indeed, dendroecology in the tropics is much more complex than in temperate regions because of the larger number of species, variety of habitats, variable cambial activity and phenology over the year, more complex and diverse drivers of growth, predominantly anatomical (rather than macroscopic) markers of tree (or growth) rings and – above all – the absence of well-defined seasons (Silva et al., 2019). Nonetheless, various tropical species still develop growth rings with a certain cyclicity.

First studies in the subtropics were conducted in the 1940s and 1950s by Schulman (1944, 1956) and the publication of the first tree-ring chronologies from northwestern Mexico (*Abies durangensis*, *Pinus* sp., *Pseudotsuga menziesii*) and south of Mexico City (*Abies religiosa*; Schöngart et al., 2017). A large number of multi-centennial chronologies has been published since in the subtropics of North America, a region that is nowadays representing an outstanding network of dendroclimatic chronologies covering the southern United States and Mexico for the past 600 years (Stahle et al., 2016). Since the 1980s, the scope and breadth of tropical dendroecology has increased steadily thanks to the study of growth rings to other regions and the expansion of research to tropical tree species. Likewise, the breadth of fields within the environmental sciences has expanded exponentially (Worbes, 2002). Even if the main focus of tree-ring research today still is on temperate and cold region environments, tropical species have become more frequently studied as they have been shown repeatedly to form growth zones with an annual layering, with the latter being driven by the species' sensitivity to climate, ecological, and/or geodynamic variations (Worbes, 1989; Schöngart et al., 2017).

Over recent decades, tropical dendroecology has become an integral research field in tree-ring research, and now includes research in the fields of ecology, climatology and geomorphology (Worbes, 2002), thereby contributing substantially to the broadening of current knowledge of tropical forest ecosystem functioning (Worbes, 2010). Even if the plethora of studies published on tropical trees and the nature of growth periodicity has provided invaluable insights into growth-climate relations, or the impact of drought and fire histories on tree growth and forest dynamics (e.g., Boninsegna et al. 2009; Rozendaal and Zuidema, 2011; Fichtler, 2017), many research questions yet remain to be addressed and many more species need to be studied to explore the dendroecological potential of tropical species fully. Indeed, the growth rings of various tropical species show greater variations and complexity than those already investigated – and much more so than those growing outside the tropics –, thus underlining the huge diversity of species in the often pristine, tropical environments. At the same time, however, one should also underline the lesser identification accuracy that remains inherent to many of these underexplored tree species (Silva et al., 2019). A clear need thus exists for more detailed investigations of wood-anatomical structures and for a systematic disentangling of variability in the formation of growth zones, so as to (even more) successfully apply dendrochronology in the tropics (Worbes, 1995).

Tropical dendroecology has a vast potential to yield environmental and climatic information for a major ecotone of Earth for which systematic records are generally scarce and short, if not missing completely for times extending back beyond the start of satellite imagery. Therefore, the necessity to fill large geographic gaps with dendrochronological data has propelled the realization of tree-ring analysis in the tropics and the rapid development of a network of previously unstudied species (Pearl et al., 2020). This increase and enhancement of tropical dendrochronology studies currently helps in closing the breach of regions without sufficient tree-ring chronologies and thereby support Earth-system sciences (Babst et al., 2017). Yet, more tree-ring studies are still needed in the lowest latitudes to fill the spatial gap completely (Zuidema et al., 2012).

Here, we review the current state of tree-ring research in the tropics and assess the contribution of tree-ring analyses to an improved understanding of environmental as well as climatic processes and drivers. To this end, we present an overview on the main suitable tree species used today, and describe the main analytical approaches and fields of applications, but also remaining limitations. Based on this review, we provide a series of future prospects of tree-ring analysis in the tropics. The review on tropical dendrochronology was based initially on more than 800 sources but then limited to the 344 reviewed contributions (i.e. peer-reviewed papers published in ISI indexed journals, MSc or PhD theses) available in Scopus and Google Scholar. We filtered only dendroecology papers, with clear location, and the usage of growth rings. The Internet search has been restricted to the keywords “tropical”, “dendrochronology” and “tree rings” (using these keywords in English, French, Spanish, and Portuguese, and to a lesser extent in Chinese, Indonesian and Hindi). The search was realized between November 2019 and January 2020. From the 344 papers (see Supplementary Material), we extracted bibliometric indicators as well as quantitative and qualitative information, including geographic coordinates, elevation, methods used, number of samples, species, genera, and families. In addition, we assessed chronology lengths (years), and information on how individual tree-ring series have been cross-dated (in terms of intercorrelation, mean sensitivity, autocorrelation, and Expressed Population Signals).

On this basis and following a brief appraisal of dendrochronology in the tropics, this paper (i) highlights tree growth patterns at low latitudes, (ii) determines the regions that have attracted most interest in terms of dendrochronological research in the past as well as the most suitable tree families, genera and species, (iii) summarizes the approaches that were most commonly used in tropical dendrochronology so far, (iv) illustrates different applications realized in the tropics over the last decades, (v) present their limitations, and (vi) concludes with a call for future work by presenting possible research perspectives.

3.2. Growth ring formation in the tropics

Growth rings are defined as changes in the structure of the secondary xylem of perennial plants; they are the result of seasonal variations of climatic conditions exerting control on growth conditions of plants, thereby producing areas with contrasting tissues (Schweingruber, 1996). Growth rings can be found in trees, where they are commonly referred to as tree rings, but they can also be found in lianas, shrubs, and perennial herbs, such that the term 'growth ring' will be used here as it has greater generality (Silva et al., 2019). In temperate and warm-temperate environments, where differences between the seasons are distinct, the contrasting tissues that are formed during the growing season (or vegetation period) of plants are commonly called 'earlywood' and 'latewood', with the aim to differentiate the two most prominent, annual growth periods (Fritts, 1971). Wood formed in the first weeks (to months) of the growing season is composed of cells with large diameters and thin cell walls. Later on, cells gradually become smaller with thicker cell walls. The process of earlywood and latewood formation – or the frequency of cambial cell division, enlargement of newly formed xylem cells and cell wall thickening in other words – is controlled by plant hormones (Buttò et al., 2019). Such a differentiation is not equally straightforward in tropical species where clearly defined earlywood and latewood tissues are either lacking or difficult to detect macroscopically (Fichtler and Worbes, 2012). In these cases, anatomical identification of growth rings needs to be based on the presence of analogous tissues resembling early and latewood patterns (Fig. 20). Therefore, one of the major remaining challenges in tropical dendrochronology is inherent to the identification of growth rings, as objective anatomical parameters for the definition of growth ring boundaries is still lacking for many species today (Tarelkin et al., 2016).

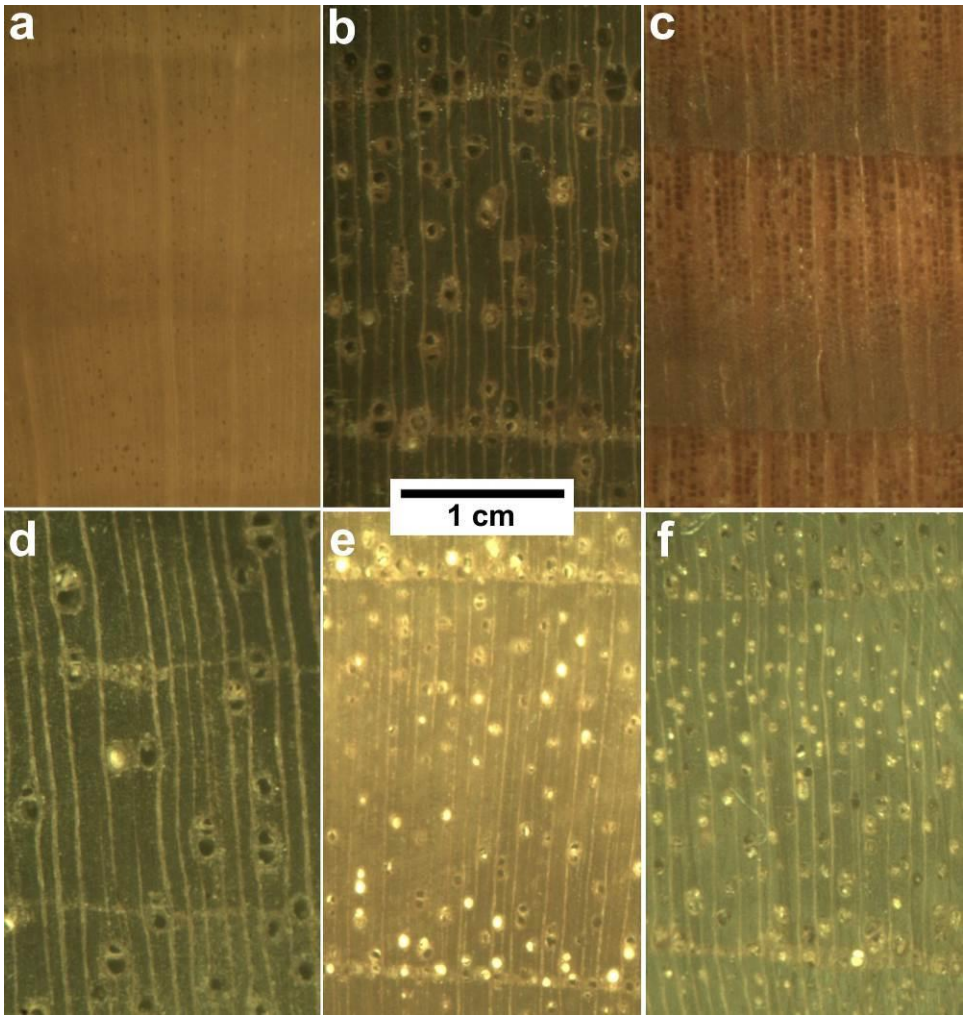

Fig. 20. Macroscopical scans from contrasting tropical ecoregions: a) Highlands neotropical Alnus acuminata. b) Lowlands intertropical Cedrela odorata. c) North American pine Pseudotsuga menziesii. d) Wetlands neotropical Prioria copaifera. e) South Asian Toona ciliata. f) Intertropical Tectona grandis. Samples from the Forest Products Laboratory (FPL), Wisconsin-USA collection (MADw and SJRw) and the Instituto Tecnológico de Costa Rica (ITCR) collection (TECw).

Growth rings in tropical species that have been classified as distinct by tropical wood anatomists would possibly be described as indistinct or absent by anatomists working on temperate species (Silva et al., 2019). In addition, the degree of distinction of individual growth rings may also vary with the magnification at which the wood is observed: In those species for which growth rings are well defined macroscopically, it may become difficult to identify the same rings microscopically – and vice versa (Worbes, 2010). Moreover, tangential discontinuities of growth rings are common in tropical species, thereby inducing the tangential interruption of rings as a consequence of the lack of a complete reactivation of the cambium along the growing stem (Worbes and Fichtler, 2010). This phenomenon – known also in some temperate species – is commonly referred to as false rings (also known as tangential discontinuities). False rings have been ascribed to local differences around a stem in terms of competition for nutrients and/or light (Hallé et al., 2012).

As the clear identification of anatomical markers of ring boundaries renders the recognition of growth rings less arbitrary (Silva et al., 2017), a suite of common anatomical markers has been developed and employed in tropical dendrochronology to identify growth rings and growth ring boundaries (Worbes, 1989, 1995, 2002; Worbes & Fichtler, 2010; Nath et al., 2016). Whereas the wood anatomy of tree rings in conifers is very similar between those formed in (sub-)tropical and those present in boreal and temperate climate trees (Schöngart et al., 2017), tropical broadleaved species present some distinct differences with respect to their extratropical counterparts (Worbes 1989). Luckily and despite the vast diversity of tropical angiosperms, their wood anatomical features can be summarized with four basic types that have first been described by Coster (1927, 1928) for Java. The four basic types have since been adopted for tropical species in more general terms (Worbes, 2002; Schöngart et al., 2017), and the classification has been expanded recently by Silva et al. (2019) to seven anatomical markers that should be taken into consideration when it comes to identifying growth rings in tropical species: (1) thick-walled and/or radially flattened latewood tracheids; (2) thick-walled and/or radially flattened latewood fibers; (3) semi-ring-porous or (4) ring-porous structures in growth rings; as well as the presence of (5) marginal parenchyma; (6) fiber zone; or (7) distended rays. The same authors also propose that growth rings should be classified individually according to the presence of markers, rather than using combinations of markers. It is also widely accepted now that the classification of growth rings into true or false rings (or intra-annual density fluctuation) has no biological basis and serves only to reinforce the concept of growth rings as being annual (De Micco et al., 2016). In general terms, the formation of a new growth ring presupposes an abrupt transition between the end of the latewood of the previous ring and the beginning of the earlywood of the next ring, irrespective of whether rings are annual or not (Fig. 21; Silva et al., 2019).

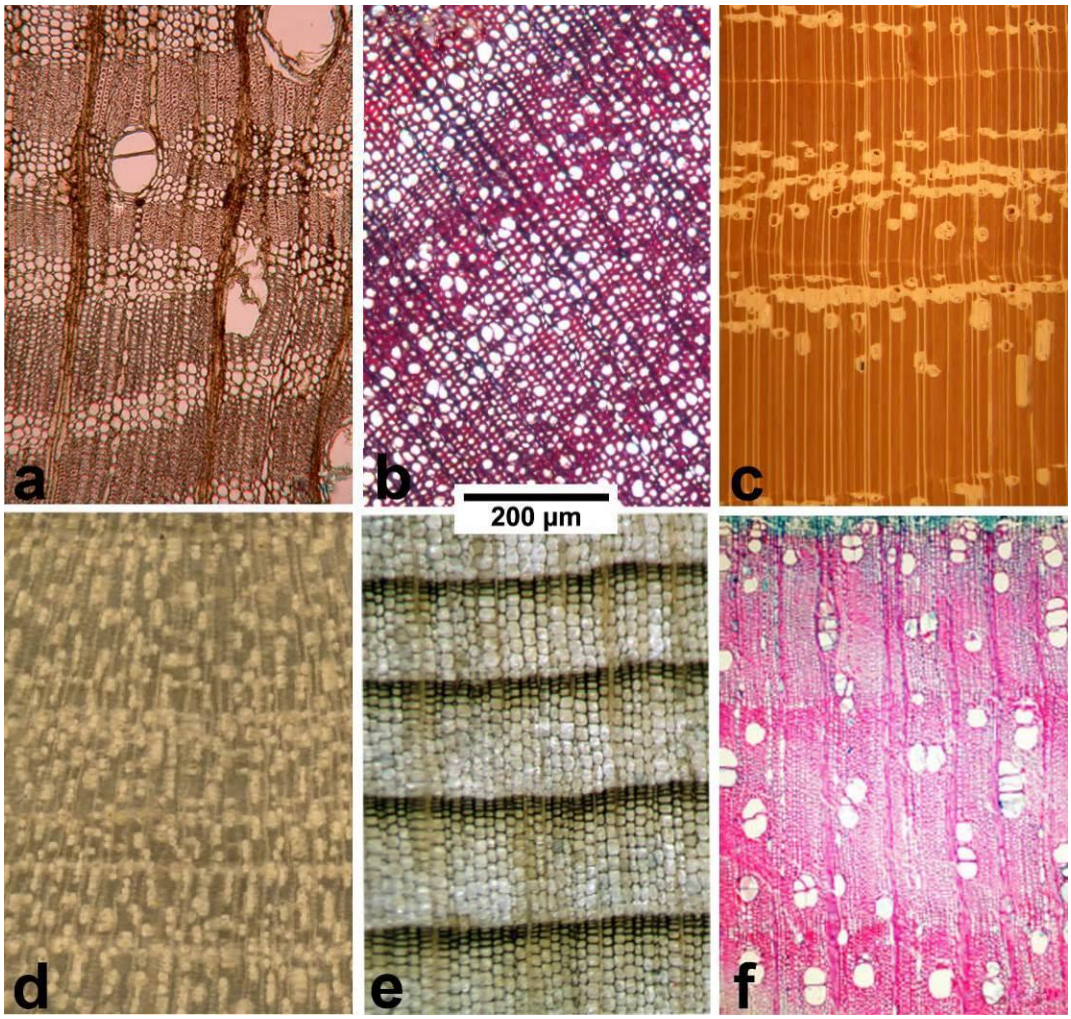

Fig. 21. Microscopical scans from contrasting tropical ecoregions: a) Igapó flooded Amazonian forest, Erisma calcaratum (Worbes and Fichtler, 2010). b) Páramo endemic shrub from highland Costa Rica, Hypericum irazuense (Quesada-Román et al., 2020b). c) Dry forest Acacia tortilis from Ethiopia (Wils et al., 2011). d) Lumnitzera racemosa from mangrove forest in Kenya (Robert et al., 2011). e) Abies guatemalensis from conifer highland forests of Guatemala (Anchukaitis et al., 2013). f) Toona ciliata from tropical rainforests of Thailand (Pumijumnong and Buajan, 2012).

The combination of periods that are favorable and unfavorable to growth may vary over the year depending on locality and species. In the tropics, and even in subtropical regions, species growing in the same habitat may form growth rings asynchronically (Cherubini et al., 2003). This behavior is expected to be the result of the emergence of growth rings due to complex relationships between environmental factors (including ecological relationships among individuals of the same or different species) and specific characteristics that are intrinsic to the species or an individual tree (e.g. genetic factors, ecophysiological, phenological and morphological traits) (De Micco et al., 2016). Primary environmental factors that can directly affect plant growth include light (intensity, quality, duration), water (availability in the soil, humidity), carbon dioxide, oxygen, nutrient content and availability in the soil, as well as temperature and toxins (e.g. heavy metals and salinity). Any alteration in one or more of these environmental factors which affects the levels needed for the normal functioning of plants can have negative consequences on growth (Silva et

al., 2019). Sensitivity to environmental variations will depend on the interaction between the environmental parameter in question and on how susceptible the species/individual is, thus creating a complex relationship (DeMicco et al., 2016). Interestingly, however, correlations between deciduousness of species and the formation of growth rings does not seem to prevail in tropical trees, neither do all deciduous trees form growth rings nor do evergreen tree species systematically lack growth rings (Giraldo et al., 2020).

Tropical trees can form annual growth rings if unfavorable environmental conditions regularly occur in one period of the year, thereby causing cambial dormancy (Worbes 2002; Rozendaal and Zuidema 2011). In tropical regions, where air temperature is more or less constant across the seasons, rainfall may become the main factor modulating the cyclic growth of trees (Jacoby, 1989; Brienen et al., 2016). Small variations in water availability for species adapted to wet habitats can be comparable to the major privations from which species would suffer in arid environments. Over vast regions of the tropics, rainfall seasonality is known to be quite distinct, with an impact on annual growth rhythm and, by consequence, the formation of annual rings (Worbes 1999; Dünisch et al. 2003; Volland-Voigt et al. 2011; Schöngart et al. 2017). Rainfall and its seasonality has repeatedly been demonstrated to have a great impact on annual ring growth (Fichtler, 2017), and to be effective in controlling the layering of growth zones and growth periodicity, even if dry periods were very short (i.e. as short as 10 to 21 days; Silva et al., 2019). It has been shown that an annual dry season with a length of only 2 to 3 months with less than 60 mm monthly precipitation can suffice to induce annual rings to form in tropical trees (Worbes, 1995), thus resulting in a positive relation between precipitation totals and ring widths in many species in different parts of the tropics (Worbes, 2002). Consistently, drier and warmer years will result in reduced tree growth (Brienen et al., 2016). Likewise, the El Niño-Southern Oscillation (ENSO) has been shown to both limit and enhance ring growth in the tropics (Anchukaitis et al., 2013; Alfaro-Sánchez et al., 2017; Quesada-Román et al., 2020b; Rodriguez-Morata et al., 2020). Thus, the seasonality of growth may reflect the effects of predictable, moderately long periods without rain during the ‘‘drier season’’ in tropical forests, thus making these growth layers annual rings (Fichtler et al., 2003). Moreover, numerous species growing at higher elevations have been shown to form annual rings thanks to the existence of a climate with a slightly more marked seasonal contrast (García-Cervigón et al., 2020).

The seasonality of rainfall also has a distinct impact on runoff in catchments of large tropical rivers with monomodal flood pulses in their vast floodplains (Junk et al., 1989). These flood pulses control the annual growth rhythm of trees (Worbes 1986; Schöngart et al., 2005; Herrera and del Valle, 2011; Montanher, 2012) as the anoxic conditions induced by the persisting flooding will prevent the uptake of water by the root system. Affected trees will shed their leaves until the flood waters recede and therefore fall into a phase of cambial dormancy (Schöngart, 2002; Schöngart et al., 2017). In mangrove species, the rainy season seems to reduce soil water salinity as a result of more abundant freshwater input, thereby triggering the formation of annual rings (Robert et al., 2011). As one moves to higher latitudes and altitudes, both photoperiod and air temperature seem to control the onset and cessation of cambial activity (Oliveira et al., 2009; Blagitz et al., 2019; Marcati et al., 2016)

In addition to these field-based studies, a suite of independent approaches has been applied to proof the annual nature of growth-ring formation in tropical plants (Worbes, 1995). One of the

approaches includes the monitoring of stem diameter variations with dendrometers (either through the use of bands or high-resolution, automated measurements) during consecutive years (Détienne, 1989; Schöngart et al. 2002; Spannl et al. 2016). Other approaches included the measurement of cambial activity with electrical resistance (Worbes, 1995) or through wood anatomical analysis of cambium tissues sampled at monthly or seasonal intervals, thereby covering different (dry and wet) periods of a year (Worbes and Raschke, 2012; Morel et al., 2015; Marcati et al., 2016). Alternatively, the wounding of cambial tissues (Mariaux, 1967) was employed to obtain scars that can be dated exactly in the wood and linked to phases of plant growth and/or dormancy (Détienne, 1989; Lisi et al., 2008; Locosselli et al., 2013).

However, not all trees growing in tropical environments form clearly distinctive, annual rings. Based on the systematic analysis of tree species, Alves and Angyalossy-Alfonso (2000) showed that roughly half of the 491 species belonging to 133 genera and 22 families growing in different Brazilian biomes formed distinct growth rings. Whereas a higher ratio was found for the Brazilian Atlantic forests (Silva et al., 2017), only 30% and 35% of the species analyzed in the Peruvian rainforest (Beltrán-Gutiérrez and Valencia-Ramos, 2013) and in the dry forests of Mexico (Roig et al., 2005) showed distinct tree rings. In addition to these regional differences, Worbes (2002) showed that the distinctiveness of annual rings can vary between life stages of a tree: some trees form clear growth rings in the adult phases, but absent or vague ring structures in the juvenile phases, or vice versa. As such, and especially in the case of low-latitude dendroecology, research is still facing long-standing challenges including irregular or indistinct growth patterns, complex morphology and short-ring series (Pearl et al., 2020). Consequently, Silva et al. (2019) recently stressed the importance for more theoretical discussions to develop a clear, robust and universal concept of growth rings, which would ultimately facilitate the study of tropical species further. The overwhelming number of tropical woody species at first sight is a potential benefit to study dendrochronology in tropical species. However, especially in the humid tropics, species do not easily form big species associations (Fedorov, 1966).

Tropical regions are more diverse in terms of the factors driving plant growth to such a degree that in many instances no one factor has a more prominent role than the others. Considering that species have different adaptation and evolutionary strategies to cope with environmental stresses, which in general are less acute in tropical than in temperate regions (Scatena and Lugo, 1995), a variety of distinct patterns can be encountered in the tropics. This is one of the reasons why growth rings of tropical plants are more diverse than their temperate climate counterparts, both in terms of anatomical markers and their degree of distinction, tangential continuity, and periodicity (Silva et al., 2019). Worbes et al. (2017) even considered that the structure of growth rings is genetically fixed, but that the presence or absence of a triggering factor will determine whether they are expressed or not.

3.3. Longevity of tropical trees and drivers of tree mortality

Tropical trees take a minimum of 60 years to reach the canopy, and generally ~200 years for individuals to recruit in shady conditions (Metcalf et al., 2009). As a result, tropical trees show ‘‘bathtub’’ mortality rates, and life expectancy peaks at surprisingly low sizes, often at ~5 cm diameter at breast height (DBH). At the same time, however, life expectancy is high for large trees. Age determination derived through the direct counting of annual rings and/or estimations in the

case of hollow trees (by measuring growth rates and diameters) often result in ages between 400 and 500 years, without, however, exceeding 600 years for larger trunks (Worbes and Junk, 1999). Growth-ring studies indicate that the lifespan of tropical tree species average *c.* 200 years and that only few species live for >500 years (Brienen et al., 2016). These estimates are consistent with tropical tree ages as found through the systematic research of growth-ring data in this review. In fact, our survey of tropical trees yields a mean age across the tropics of 138.4 ± 139.3 years (n_{obs}= 269), with marked differences between regions within the tropics: whereas for the Americas and Africa, trees reach comparable ages with 136.24 ± 127.66 (n_{obs}= 165) and 132.42 ± 143.30 years (n_{obs}= 41), ages are markedly higher in tropical Asia with 153.19 ± 169.53 years (n_{obs}= 59), but substantially lower in tropical Oceania with 71.75 ± 60.51 years. Note that for the latter, the number of observations is, however, extremely small (n_{obs}= 4) and probably not representative. Accordingly, most tropical growth-ring chronologies do not exceed 300 years. Interestingly, however, Figure 22 suggests that chronology lengths tend to increase slightly with increasing distance from the Equator.

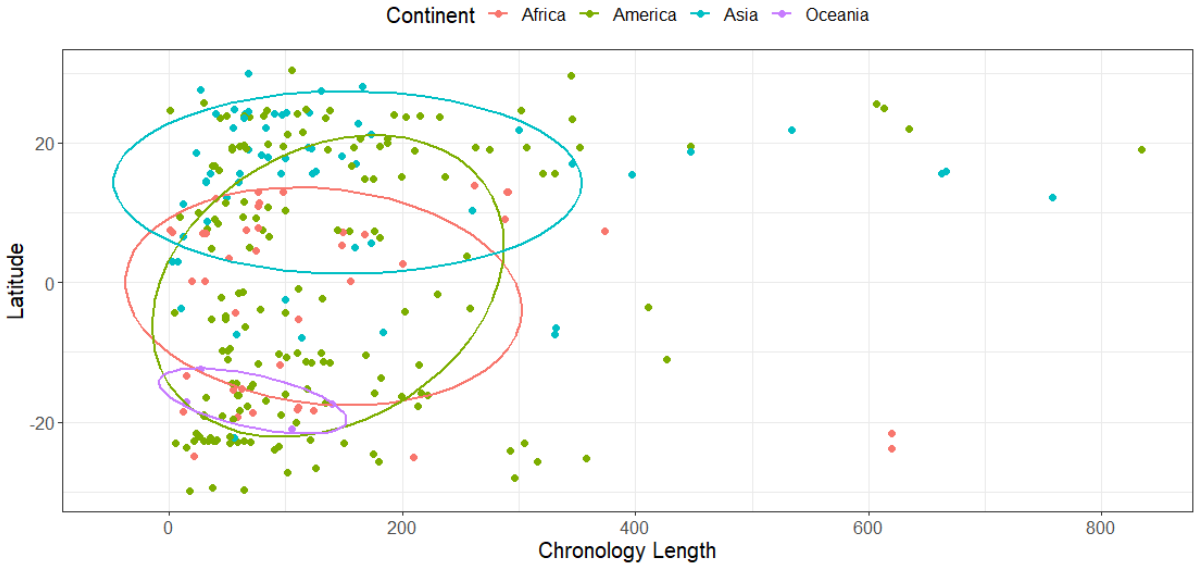

Fig. 22. Scatter plot showing the relation between latitude and chronology length for all continents with (sub-)tropical climates. The ellipses comprise 50 % of the values obtained for each of the continents.

The process of tree mortality has dimensions of intensity, spatial, and temporal scales that reflect the characteristics of endogenic processes (i.e., senescence, embolism) and exogenic disturbances in terms of their severity, frequency, duration, or spatial scale, as well as points of interaction with the ecosystem (Lugo and Scatena, 1996). Little is known about the drivers of tree mortality in tropical forests due to the limited availability of long-term observational data (Brienen et al., 2015). Aleixo et al. (2019) reported that drought (during El Niño years), storms and/or extremely wet years tend to increase tree mortality for at least two years following the disturbance event in the tropics. According to Lugo and Scatena (1996), the presence of old trees in the tropics therefore also means that: (i) not all trees die at once in a catastrophic event, (ii) differential mortality exists among species, (iii) vegetation turnover differs between distinct geomorphic settings as a result of different disturbance regimes (Scatena and Lugo 1995), and that (iv) in the absence of disturbances, different stages of the life cycle can exhibit differential survival rates.

As a consequence, forest turnover is likely to be in the order of at least hundreds of years, with negative implications for rates of carbon absorption (Metcalf et al., 2009). In that context, Groenendijk et al. (2015) not only reported decreasing growth rates over time in wet tropical forests of Bolivia, Cameroon and Thailand, but also concluded that elevated ambient carbon dioxide (CO_2) did not directly lead to higher tree growth. Increasing mortality rates were associated with rising temperature and vapor pressure deficit, liana abundance, drought, wind events, or fires and – possibly – CO_2 fertilization-induced increases in stand thinning or an acceleration of trees reaching larger, more vulnerable heights. A vast majority of these mortality drivers may kill trees in part through carbon starvation and/or hydraulic failure, the relative importance of each driver remains, however, unknown (McDowell et al., 2018). Besides, vessel traits in angiosperms seem to be another key factor in tropical environments mortality (Fonti et al., 2010; Islam et al., 2018) as wider vessels will prioritize water conductivity at the expense of high risk of embolism during droughts (Rahman et al., 2019; Wu et al., 2020). In addition, long-term plasticity in vessel safety and low hydraulic efficiency have been shown to be compromised further by deforestation and climate change (Rodríguez-Ramírez and Luna-Vega, 2020). As a consequence, predicted ongoing and future climate change will likely lead to higher tree mortality rates, especially in short-lived species, sadly common in the tropics (Brienen et al., 2015).

3.4. Tropical regions: diverse, rich in species and understudied

Compared to temperate regions, tropical floras are extremely rich in species, even more so in terms of trees (Hallé et al., 2012), estimated to approximately 40,000 species (Slik et al., 2015). In particular, tropical rainforests have a remarkably complete and uninterrupted series of taxa with many entire plant families with very large genera that are often confined within the limits of the same region (Fedorov, 1966). Despite the immense number of tropical tree species and related families and genera diversity and the limited number of dendroecological studies existing around low latitudes, approximately 230 species have been reported to form annual rings in these regions (Brienen et al., 2016; Schöngart et al., 2017).

A vast majority of dendroecological studies in tropical regions have been realized in the Americas (59%), and much less studies exist today for Asia (22%), Africa (16%), and Oceania (3%). The fact that a clear majority of tropical tree-ring studies are centered in the Americas is presumably the result of the vast tropical forest area existing in these regions (Hansen et al., 2013). This is especially true for the state of Sao Paulo and the Amazon, for forests of the Trans-Mexican Volcanic Belt and Central Mexico, Guatemala, Costa Rica, Panama, Colombia, Ecuador, Peru, Bolivia and northernmost Argentina.

Major gaps in terms of dendroecological research persist today in (sub-)tropical desert environments (Sahara, Namibia, Australian and Mexican deserts) due to the scarcity of vegetation. Similar gaps can, however, also be recognized in the more biodiverse regions of the Caribbean, Southern Mexico, Central America, Africa (in general), South Asia, Southeast Asia and tropical Oceania (Fig. 23). So far, African dendroecology has focused essentially on the dry forests of Ethiopia, with some additional, yet scattered studies undertaken in Kenya, Cameroon, or the Democratic Republic of Congo, and thus in quite different tropical forest types. Dendroecological hotspots in Southeast Asia are clearly centered on India, Thailand, Malaysia and Indonesia, but the potential for more research is still huge as it is for tropical Oceania.

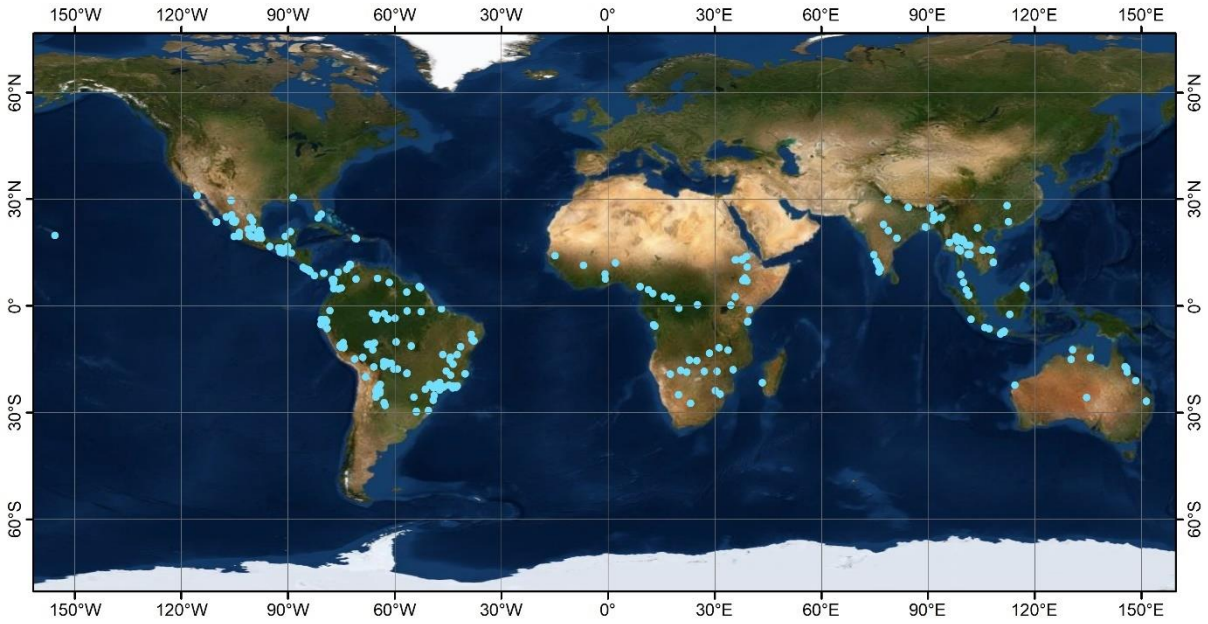

Fig. 23. Distribution of tropical dendroecological studies realized in the past. Blue dots indicate works published for study sites located between 30° N and 30° S. The total number of studies illustrated is 344. For details see Supplementary Material in the published paper.

Table 2 provides a summary of the families and genera that are most commonly used in tropical dendroecology. Members of the *Fabaceae* family are present in America, Africa and Asia, especially in Tropical and Subtropical Moist Broadleaf Forests. This family occurs in very diverse altitudinal and latitudinal tropical settings, with more common occurrences in America and Africa (Table 3; Fig. 24). Members of the *Pinaceae* family have been used widely as well, primarily above 14° N and 14°S, and in environments where Tropical and Subtropical Coniferous Forests are common. Tree-ring studies using *Pinaceae* are particularly widespread in Florida (United States), Mexico, Guatemala, Dominican Republic, India, and Thailand.

More than half of all studies realized on tropical dendroecology focused on species of the *Meliaceae*, *Boraginaceae* and *Anacardiaceae* families, and were realized at latitudes up to 15° N and S, mostly in America and Asia. Studies using *Verbenaceae* are frequent as well, and sites investigated reach latitudes of up to 20° N, majorly in Asia, whereas members of the *Cupressaceae* and *Malvaceae* families have been used in tropical growth-ring research in different ecoregions beyond 14° latitude, mostly in Africa and America.

Table 2. Overview of woody species of the tropics with confirmed annual growth rings (between 30° North and 30° South). A complete list of references can be found in the Supplementary Material of the published paper.

Families	Species	References
Acanthaceae	*Avicennia marina*	Schmitz et al., 2007; Santini et al., 2013

Anacardiaceae	*Schinopsis brasiliensis, Schinopsis lorentzii*	López and Villalba, 2016; de Carvalho Nogueira et al., 2018; Bravo et al., 2008; Ferrero and Villalba, 2009; Ferrero et al., 2013, 2015
Apocynaceae	*Aspidosperma polyneuron, Pentalinon andrieuxii*	Briceño et al., 2018; Godoy-Veiga et al., 2018; Hiebert-Giesbrecht et al., 2018; Blagitz et al., 2019
Araucariaceae	*Agathis robusta, Araucaria angustifolia, Araucaria bidwillii, Araucaria columnaris, Araucaria cunninghamii*	Lisi et al., 2001; Medeiros et al., 2008; Oliveira et al., 2009; Boysen et al., 2014; Santos et al., 2015; Haines et al., 2018;
Asteraceae	*Moquiniastrum polymorphum*	Brandes et al., 2019
Betulaceae	*Alnus acuminata*	Grau et al., 2003; Paolini et al., 2005; Ferrero et al., 2013; Armijos-Montaño et al., 2018
Bignoniaceae	*Tabebuia chrysantha*	Volland-Voigt et al., 2011
Boraginaceae	*Cordia alliodora*	Devall et al., 1995; Enquist and Leffler, 2001; Hayden et al., 2010; Briceño et al., 2016
Burseraceae	*Boswellia papyrifera, Bursera graveolens*	Rodríguez et al., 2005; Rodríguez et al., 2005; Feyissa, 2013; Tolera et al., 2013; Pucha-Cofrep et al., 2015
Capparaceae	*Capparis odoratissima*	Ramírez and del Valle, 2011; del Valle et al., 2012
Clusiaceae	*Chrysochlamys colombiana, Chrysochlamys dependens*	Ayala-Usma et al., 2019
Combretaceae	*Laguncularia racemosa*	Estrada et al., 2008
Cupressaceae	*Callitris columellaris, Callitris endlicheri, Callitris glaucophylla, Callitris intratropica, Cupressus lusitanica, Callitris macleayana, Callitris preissii, Callitris rhomboidea, Fokienia hodginsii, Juniperus monticola, Juniperus procera, Taxodium ascendens, Taxodium distichum, Taxodium mucronatum*	Anderson et al., 2005; Couralet et al., 2005; Sass-Klaassen et al., 2008; Wils et al., 2009; Wils et al., 2010; Bowman et al., 2011; Pearson et al., 2011; Wils et al., 2011; David et al., 2014; Mokria et al., 2015; Villanueva-Díaz et al., 2016; Pompa-García et al., 2017; David et al., 2018; Gebregeorgis et al., 2018; Sano et al., 2009; Buckley et al., 2010; Sano et al., 2012; Buckley et al., 2017; Alcalá-Reygosa et al., 2018; Buckley et al., 2018; Franco-Ramos et al., 2018;Villanueva-Díaz et al., 2020
Dilleniaceae	*Dillenia indica*	Venugopal and Liangkuwang, 2007
Dipterocarpaceae	*Dryobalanops sumatrensis, Hopea odorata, Shorea leprosula, Shorea robusta, Shorea superba*	Sass et al., 1995; Ogata and Fujita, 2005; Azim et al., 2014; Ohashi et al., 2014
Euphorbiaceae	*Alchornea lojaensis*	Spannl et al., 2016

Fabaceae	*Acacia erioloba, Acacia tortilis, Afzelia xylocarpa, Amburana cearensis, Baikiaea plurijuga, Brachystegia floribunda, Brachystegia spiciformis, Burkea africana, Centrolobium microchaete, Centrolobium robustum, Copaifera langsdorffii, Copaifera lucens, Dalbergia cochinchinensis, Dalbergia nigra, Dalbergia frutescens, Daniellia oliveri, Dichrostachys cinerea, Dipteryx magnifica, Enterolobium maximum, Faidherbia albida, Hymenaea courbaril, Hymenaea stigonocarpa, Hymenolobium petraeum, Isoberlinia angolensis, Isoberlinia doka, Julbernardia paniculata, Machaerium scleroxylon, Macrolobium acaciifolium, Millettia stuhlmannii, Mimosa acantholoba, Mimosa tenuiflora, Parkia nitida, Parkia velutina, Parkinsonia praecox, Paubrasilia echinata, Pericopsis elata, Piptadenia adiantoides, Piptadenia micracantha, Poincianella pyramidalis, Prioria copaifera, Prosopis pallida, Pterocarpus angolensis, Pterocarpus macrocarpus, Pterocarpus rohrii, Pterogyne nitens, Schizolobium parahyba, Senegalia mellifera, Senna multijuga, Sindora siamensis, Sophora chrysophylla, Tamarindus indica, Xylia xylocarpa*	Boninsegna et al., 1989; Wyant and Reid, 1992; Enquist and Leffler, 2001; Lisi et al., 2001; Tarhule and Leavitt, 2004; Fichtler et al., 2004; Brienen and Zuidema, 2005; Rodríguez et al., 2005; Schöengart et al., 2005; Brienen and Zuidema, 2006; Brienen et al., 2006; Grundy, 2006; Schöengart et al., 2006; Trouet et al., 2006; Westbrook et al., 2006; Brienen and Zuidema, 2007; Bravo et al., 2008; Steenkamp et al., 2008; Gebrekirstos et al., 2008; Marcati et al., 2008; Ohashi et al., 2009; Brienen et al., 2010; Hayden et al., 2010; Syampungani et al., 2010; Trouet et al., 2010; Brandes et al., 2011; Brienen et al., 2011; Calzón and Giménez, 2011; Giraldo-Jiménez and del Valle-Arango, 2011; Herrera and del Valle, 2011; López et al., 2011; Nicolini et al., 2012; del Valle et al., 2012; López et al., 2012; Ramírez and del Valle, 2012; Locosselli et al., 2013; López et al., 2013; Mbow et al., 2013; Mendivelso et al., 2013; Paredes-Villanueva et al., 2013; Southworth et al., 2013; David et al., 2014; De Ridder et al., 2014; Gebrekirstos et al., 2014; Groenendijk et al., 2014; Kumaran et al., 2014; Mendivelso et al., 2014; Ohashi et al., 2014; Vlam et al., 2014; Vlam, 2014; Alves-Pagotto et al., 2015; Baker et al., 2015; Costa et al., 2015; Francisco et al., 2015; Groenendijk et al., 2015; Hietz et al., 2015; Morel et al., 2015; Paredes-Villanueva et al., 2015; Boakye et al., 2016; de Vasconcellos et al., 2016; Locosselli et al., 2016; Shimamoto et al., 2016; López et al., 2017; Herrera-Ramirez et al., 2017; Köhl et al., 2017; Linares et al., 2017; Ngoma et al., 2017; Barbosa et al., 2018; Batista and Schöngart, 2018; Bovi et al., 2018; David et al., 2018; de Carvalho et al., 2018; de Miranda et al., 2018; Fontana et al., 2018; Mattos et al., 2018; Nakai et al., 2018; Batista and Schöngart, 2018; Zacharias et al., 2018; Granato-Souza et al., 2019; Locosselli et al., 2019; López et al., 2019; Rahman et al., 2019; Macedo et al., 2020; Shikangalah et al., 2020
Fagaceae	*Fagus grandifolia*	Rodríguez-Ramírez et al., 2018
Hypericaceae	*Hypericum irazuense*	Kerr et al., 2018
Juglandaceae	*Juglans neotropica*	Villalba et al., 1985; Villalba et al., 1992; Villalba et al., 1998; Arabe et al., 2011; Ferrero et al., 2013; Ferrero et al., 2015; Inga and del Valle, 2017; Armijos-Montaño et al., 2018
Lamiaceae	*Peronema canescens*	Azim et al., 2014; Harada et al., 2014
Lauraceae	*Cinnamomum amoenum, Nectandra maegapotamica, Nectandra oppositifolia, Ocotea pulchella*	Spathelf et al., 2010; Reis-Avila and Oliviera, 2017; Granato-Souza et al., 2019
Lecythidaceae	*Bertholletia excelsa, Cariniana estrellensis, Cariniana pyriformis*	Brienen and Zuidema, 2005; Brienen and Zuidema, 2006; Baker et al., 2015; Andrade et al., 2019
Malvaceae	*Adansonia grandidieri, Ceiba speciosa, Heritiera fomes, Heritiera littoralis*	Chowdhury et al., 2008; Robert et al., 2011; Patrut et al., 2015; Chowdhury et al., 2016; Barbosa et al., 2018; Maxwell et al., 2018; de Vasconcellos et al., 2019

Meliaceae	*Azadirachta excelsa, Cedrela fissilis, Cedrela lilloi, Cedrela montana, Cedrela nebulosa, Cedrela odorata, Chukrasia tabularis, Lagerstroemia speciosa, Melia azedarach, Neolitsea obtusifolia, Swietenia macrophylla, Toona ciliata, Vitex peduncularis*	Villalba et al., 1985; Boninsegna et al., 1989; Villalba et al., 1992; Villalba et al., 1998; Grau, 2000; Dünisch et al., 2003; Brienen and Zuidema, 2005; Hietz et al., 2005; Brienen and Zuidema, 2006; Brienen et al., 2006; Heinrich and Banks, 2006; Brienen and Zuidema, 2007; Bräuning et al., 2009; Rozendaal et al., 2010; Nock et al., 2011; Ferrero et al., 2013; López et al., 2013; Pumijumnong and Buajan, 2013; Tinco et al., 2013; Wang et al., 2013; Azim et al., 2014; Ohashi et al., 2014; Pereyra-Espinoza et al., 2014; Vlam et al., 2014; Baker et al., 2015; Ferrero et al., 2015; Hietz et al., 2015; Arêdes-dos-Reis et al., 2016; Martínez-Prera, 2016; Paredes-Villanueva et al., 2016; Susatya and Yansen, 2016; Baker et al., 2017; Köhl et al., 2017; Inga and del Valle, 2017; Rahman et al., 2017; Armijos-Montaño et al., 2018; Barbosa et al., 2018; Dünisch and Latorraca, 2018; Islam et al., 2018; Layme-Huaman et al., 2018; Venegas-González et al., 2018; Pereira et al., 2018; Rahman et al., 2018; Rahman et al., 2018; Blagitz et al., 2019; Carlosama-Mejía and Herrera-Carrión, 2019; Granato-Souza et al., 2019; Hammerschlag et al., 2019; Marcelo-Peña et al., 2019; Rahman et al., 2019
Myrtaceae	*Eucalyptus nesophila, Eucalyptus miniata, Eucalyptus tetrodonta, Melaleuca minutifolia, Melaleuca quinquenervia, Melaleuca viridiflora*	Mucha, 1979; Sharp and Bowman, 2004; David et al., 2014; Ohashi et al., 2014; David et al., 2018; Nakai et al., 2018; Adame et al., 2019; Rahman et al., 2019
Pinaceae	*Abies durangensis, Abies guatemalensis, Abies religiosa, Cedrus deodara, Picea chihuahuana, Pinus ayacahuite, Pinus cembroides, Pinus cooperi, Pinus elliottii, Pinus engelmannii, Pinus hartwegii, Pinus jeffreyi, Pinus kesiya, Pinus lagunae, Pinus leiophylla, Pinus lumholtzii, Pinus massoniana, Pinus merkusii, Pinus occidentalis, Pinus oocarpa, Pinus patula, Pinus pseudostrobus, Pinus teocote, Pinus wallichiana, Pseudotsuga menziesii*	Schulman, 1944; Johnson, 1980; Bhattacharyya and Yadav, 1990; Huante et al., 1991; D'Arrigo et al., 1997; Biondi and Fessenden, 1999; Biondi, 2001; Díaz et al., 2001; Díaz et al., 2002; Biondi et al., 2003; Brito-Castillo et al., 2003; Stephens et al., 2003; Hua et al., 2004; Speer et al., 2004; Buckley et al., 2005; González-Elizondo et al., 2005; Martin and Fahey, 2006; Pumijumnong and Wanyaphet, 2006; Ricker et al., 2007; Palakit and Duangsathaporn, 2008; Zimmer and Baker, 2009; Harley et al., 2011; Krepkowski et al., 2011; Szejner, 2011; Harley et al., 2012; Anchukaitis et al., 2013; Franco-Ramos et al., 2013; Cardoza-Martínez et al., 2014; Pompa-García and Jurado, 2014; Anchukaitis et al., 2015; Pompa-García et al., 2015; Venegas-González et al., 2015; Belay, 2016; Carlón-Allende et al., 2016; Díaz-Ramírez et al., 2016; Franco-Ramos et al., 2016; Franco-Ramos et al., 2016; Singh et al., 2016; Trouet et al., 2016; Astudillo-Sánchez et al., 2017; Cabral-Alemán et al., 2017; Franco-Ramos et al., 2017; González-Elizondo et al., 2017; López-Sánchez et al., 2017; Luo et al., 2017; Pompa-García et al., 2017; Venegas-González et al., 2017; Beramendi-Orosco et al., 2018; Carlón-Allende et al., 2018; Carlón-Allende et al., 2018; Anderson et al., 2018; Franco-Ramos et al., 2018; López-Hernández et al., 2018; Rebenack et al., 2018; Tucker et al., 2018; Villanueva-Díaz et al., 2018; Astudillo-Sánchez et al., 2019; Correa-Díaz et al., 2019; Gu et al., 2019; Ho et al., 2019; Alfaro-Sánchez et al., 2020; Brandes et al., 2020; Carlón-Allende et al., 2020; Hua et al., 2000; Pacheco et al., 2020

Podocarpaceae	*Podocarpus falcatus, Podocarpus lambertii*	Poussart et al., 2004; Krepkowski et al., 2011; Krepkowski et al., 2012; Krepkowski et al., 2013; Locosselli et al., 2016
Rhizophoraceae	*Rhizophora mangle, Rhizophora mucronata*	Menezes et al., 2003; Verheyden et al., 2004; Verheyden et al., 2005; Schmitz et al., 2006; Ramírez-Correa et al., 2010; del Valle et al., 2012; Kumaran et al., 2014; Souza et al., 2016
Rosaceae	*Polylepis species, Polylepis pepei, Polylepis subsericans, Polylepis rodolfo-vasquezii, Polylepis rugulosa, Polylepis tarapacana*	Solíz et al., 2009; Jomelli et al., 2012; Roig et al., 2013; Baker et al., 2015; Gunderson, 2019
Rubiaceae	*Breonadia salicina, Cordiera concolor*	Gillespie et al., 1998; Norström et al., 2008; de Lara et al., 2017
Rutaceae	*Esenbeckia cornuta, Esenbeckia leiocarpa*	Bovi et al., 2019; Marcelo-Peña et al., 2019
Sapotaceae	*Pouteria orinocoensis, Pouteria sp., Vitellaria paradoxa*	Dezzeo et al., 2003; Anchukaitis and Evans, 2010; Armijos-Montaño et al., 2018
Verbenaceae	*Tectona grandis*	Pumijumnong et al., 1995; Murphy et al., 1997; Priya and Bhat, 1998; Poussart et al., 2004; Buckley et al., 2005; D'Arrigo et al., 2006; Shah et al., 2007; Wannasri et al., 2007; Ram et al., 2008; Ohashi et al., 2009; Deepak et al., 2010; Managave et al., 2010; D'Arrigo et al., 2011; Palakit et al., 2012; Pumijumnong, 2012; Palakit et al., 2015; Venegas-González et al., 2015; Buajan et al., 2016; Auykim et al., 2017; Managave et al., 2017; Venegas-González et al., 2017; Lumyai and Duangsathaporn, 2018; Gaitan-Alvarez et al., 2019; Khantawan et al., 2019; Pumijumnong et al., 2019; Rahman et al., 2019
Vochysiaceae	*Vochysia divergens*	Fortes et al., 2018

Representatives of the *Pinus* genus are abundantly present in studies realized at latitudes above 12° in both hemispheres, in the Tropical and Subtropical Coniferous, Dry Broadleaf and Moist Broadleaf Forests of Guatemala, Mexico, Brazil, Thailand, India, China and Australia. The most commonly used species of the *Pinus* genus are *Pinus hartwegii* (Carlón-Allende et al., 2020), *P. elliottii* (Tucker et al., 2018), *P. merkusii* (Hua et al., 2004), and *P. kesiya* (Ho et al., 2019). Representatives of the *Cedrela* genus have been studied mostly in the Dry and Moist Broadleaf Forests of Ecuador, Peru, Bolivia, Argentina and Brazil. Here, the species that were most frequently used in dendroecology so far include *Cedrela odorata* and *C. fissilis* (Venegas-González et al., 2018).

Growth-ring studies using species of the *Tectona* genus were performed at latitudes exceeding 10° (mostly N) in the Moist Broadleaf Forests of India, Thailand and Myanmar (Pumijumnong, 2012). Research focused primarily on *Tectona grandis*, a species that has also been introduced for commercial purposes in Latin America, Asia, Africa, and Oceania (Gaitán-Alvarez et al., 2019). The genus *Acacia* is typical for latitudes below 10° in Tropical and Subtropical Grasslands, Savannas and Shrublands of Africa and Southeast Asia, and was employed in growth-ring research through the study of its species *Acacia mearnsii, A. tortilis, A. seyal*, and *A. mangium* (Gebrekirstos et al., 2008). The *Abies* genus is restricted to 14–24° N in the Tropical and Subtropical Coniferous Forests of Guatemala in Mexico and research was so far based mostly on *Abies religiosa* (Franco-Ramos et al., 2016) and *A. guatemalensis* (Anchukaitis et al., 2013).

The genus *Toona* and its most abundant species *Toona ciliata* (Rahman et al., 2017) occur in the Dry Broadleaf Forests at latitudes comprised between 14 and 24° N in Asia and around 21° S in Oceania, whereas the species of the *Hymenaea* genus used in dendroecology was restricted to the Moist Broadleaf Forests of the neotropics, and particularly South America. Its most common representatives are *Hymenaea courbaril* and *H. stigonocarpa* (Locosselli et al., 2013). Growth-ring studies studying species of the *Juniperus* genus have been restricted so far to the Montane Grasslands, Shrublands or Coniferous Forests of Africa (mostly Ethiopia) and high elevation sites of Mexico, with research utilizing primarily *Juniperus procera* (Wils et al., 2011) and *J. monticola* (Villanueva-Díaz et al., 2016). Tree-ring studies realized with *Rhizophora* are common in Mangrove Forests of Africa and America using *Rhizophora mangle* (del Valle et al., 2012) and *R. mucronata* (Verheyden et al., 2005).

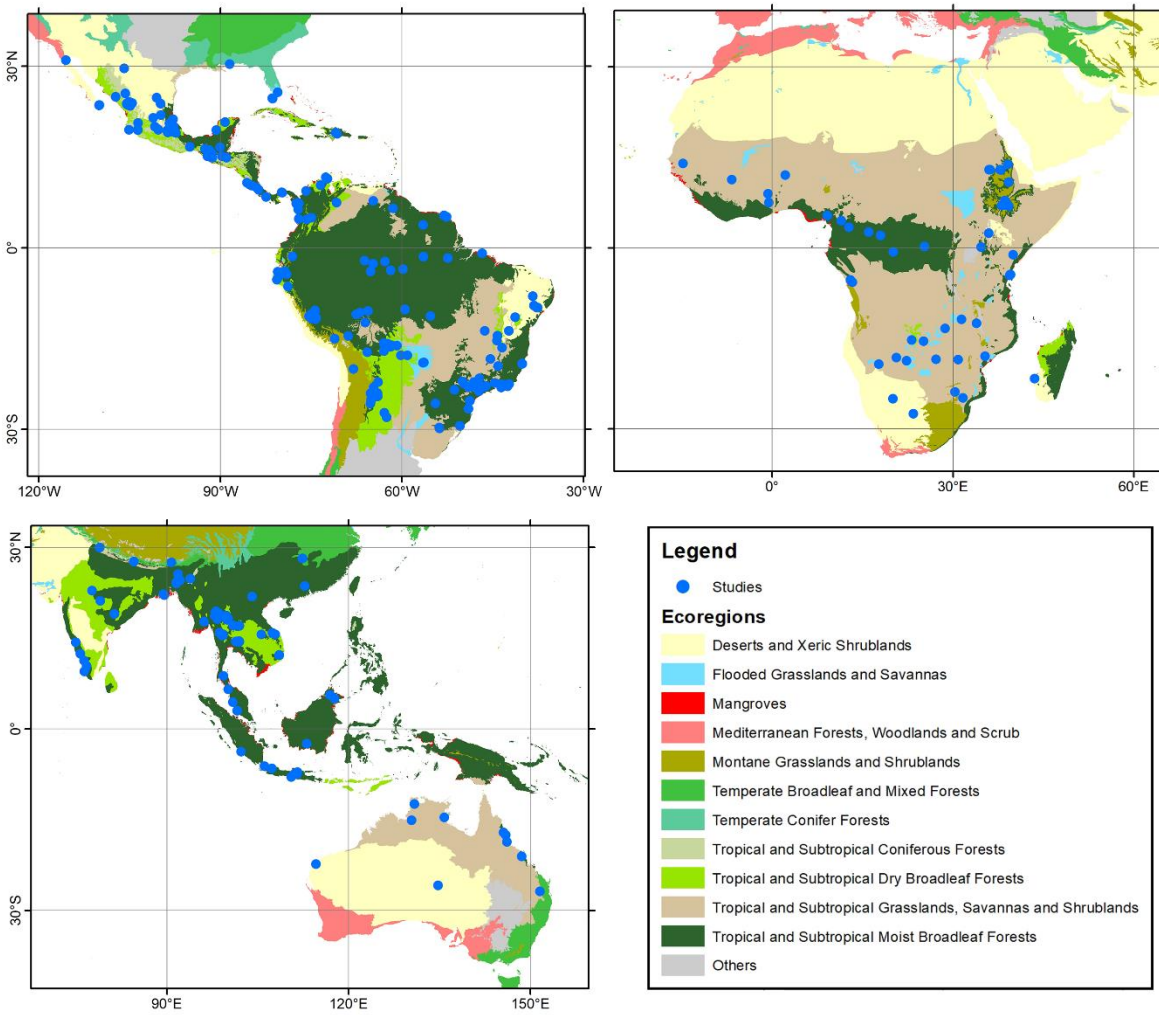

Fig. 24. Spatial representation of dendroecological studies realized in different tropical ecoregions (sensu Olson et al., 2001) comprised between 30° N and 30° S.

Table 3. Absolute and relative numbers of publications on tropical dendroecology by ecoregion (sensu Olson et al., 2001).

Ecoregion	Studies (nb)	Percentage
Tropical and Subtropical Moist Broadleaf Forests	157	45.64
Tropical and Subtropical Dry Broadleaf Forests	60	17.44
Tropical and Subtropical Grasslands, Savannas and Shrublands	45	13.08
Deserts and Xeric Shrublands	27	7.85
Tropical and Subtropical Coniferous Forests	26	7.56
Flooded Grasslands and Savannas	11	3.20
Montane Grasslands and Shrublands	10	2.91
Mangroves	4	1.16
Temperate Conifer Forests	2	0.58
Temperate Broadleaf and Mixed Forests	1	0.29
Mediterranean Forests, Woodlands and Scrub	1	0.29

Figure 25 illustrates that localities of dendroecological studies tend to increase slightly with decreasing latitude. Most research on tropical growth rings and their ecological interpretation has been realized at altitudes (well) below 2,000 m a.s.l. The Americas are somehow the exception to the rule, but the higher numbers can be explained by the fact thatseveral studies have been realized in the Trans-Mexican Volcanic Belt, thereby extending the altitudinal range of tropical study sites in the Americas considerably. In addition, this cluster also contains the Andean tree-ring series, i.e. the highest chronologies collected so far in the tropics. In Africa, the high-elevation Ethiopian chronologies are responsible for the outliers found in the altitudinal range of the African continent.

Interestingly, despite having the highest mountain ranges in the world, maximum altitudes of Asian growth-ring chronologies so far only exhibit a mean elevation of study sites that is slightly exceeding 1500 m a.s.l. The limited number of chronologies reported for Oceania prevents any statistical analysis; in this region, we can only observe that most sites analyzed so far were located below 1000 m a.s.l. Studies realized at altitudes exceeding 2000 m a.s.l. were utilizing most often species from the genera *Podocarpus* (Krepkowski et al., 2013) and *Juniperus* (Mokria et al., 2015) in Africa, and *Pinus* (Pompa-García et al., 2015), *Abies* (Pacheco et al., 2020), *Juniperus* (Alcalá-Reygosa et al., 2018) and *Polylepis* (Gunderson, 2019) in the Americas, whereas research at higher elevations was restricted to *Pinus* in Asia (D'Arrigo et al., 1997).

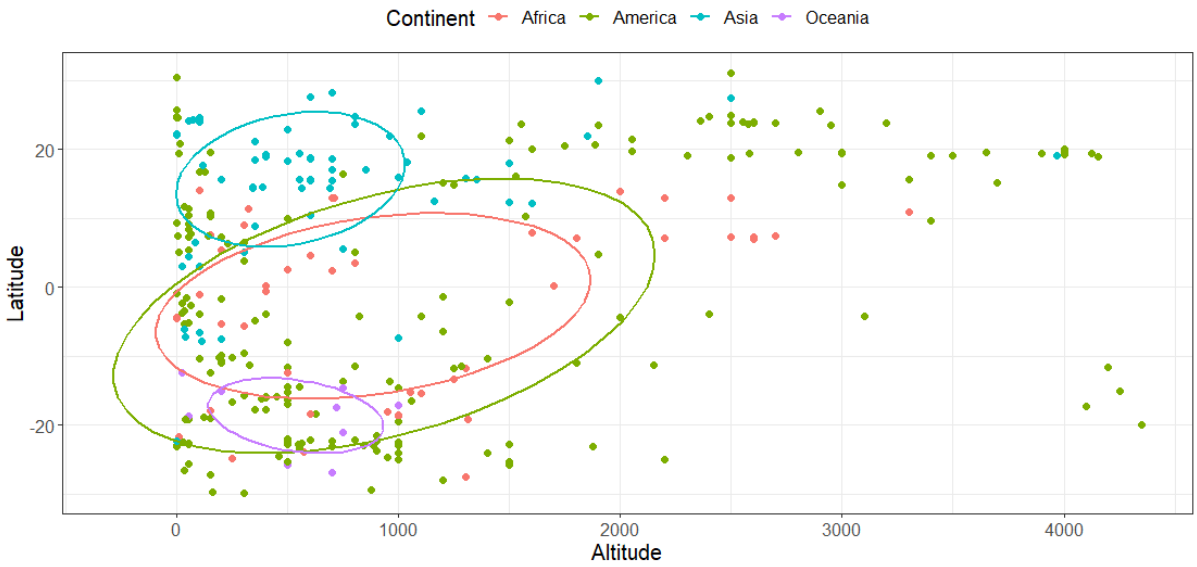

Fig. 25. Scatter plots presenting the altitudinal range of dendroecological studies by latitude and continent. The ellipses comprise 50 % of the altitudinal range observed for each of the continents containing (sub-)tropical environments.

3.5. Dendroecological approaches applied to tropical trees

A dendroecological study typically starts with a field campaign during which samples are acquired from the trunks, stems or roots of woody plants, depending on the goals of the study and the research questions. Sampling can be non-destructive through the extraction of increment cores (Fritts, 1971; usually 5.5 mm in diameter, but thicker borers with inner diameters of up to 12 mm exist and are primarily used in density and isotope analysis) or destructive (Worbes, 1995) in the case that cross sections or wedges are taken with a saw (Fig. 26). Sample depth – i.e. the number of samples selected – will depend primarily on the question to be answered and to the potential of trees to cross-date. According to the literature review, studies have reported between 1 sample using cosmogenic methods (Harada et al., 2014) and 600 samples (Groenendijk et al., 2014). On average, published papers rely on 65.55 ± 91.09 (n_{obs}= 311) samples; fewest samples are used in studies with a focus on geomorphology and climatology, whereas research on ecology and climatology typically relies on the largest sample sizes (Solíz et al., 2009; Bovi et al., 2018; Brandes et al., 2020). Sample depth of tropical tree-ring studies are thus not fundamentally different from what is normally analyzed in extratropical work, with the exception maybe of large dendroclimatological or dendroecological tree-ring networks as they are used primarily in work spanning the northern hemisphere (St George, 2014; Stoffel et al., 2015; Anchukaitis et al., 2017).

Fig. 26. Dendroecology fieldwork sampling with increment borers in trunks (a), cross sections with chainsaw (b), or saws in roots (c).

Most dendroecological studies realized in the tropics so far relied on macroscopic applications (Fig. 27), i.e. on approaches where growth rings are analyzed and ring boundaries distinguished at simple sight or with the aid of a stereomicroscope (Schweingruber, 1996). We found 185 scientific papers (54%) in which analyses were based solely on macroscopic ring analyses. Thirty papers (9%) focused on a microscopic assessment and interpretation of growth rings – especially since the early 2000s – whereas 54 contributions (16%) combined both microscopic and microscopic

analyses (Fig. 28). More recently, ^{14}C, ^{13}C and ^{18}O isotopes have been employed to corroborate results of macroscopic (56 studies; 16%) and microscopic (18 studies; 5%) analyses.

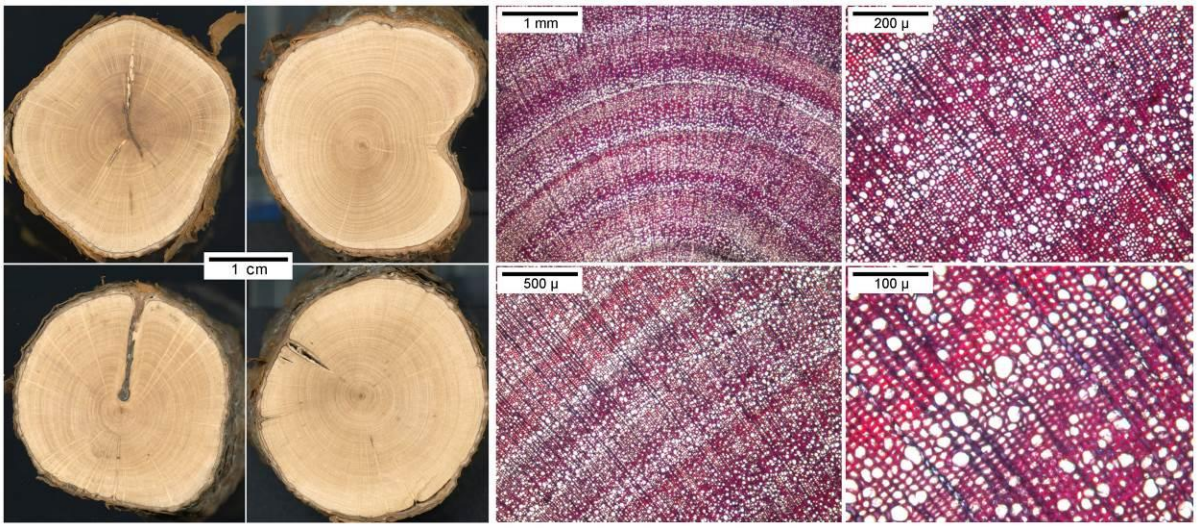

Fig. 27. Macroscopical (left panels) and microscopical (right panels) scans of *Hypericum irazuense*, an endemic neotropical species.

As in temperate and boreal climates, tropical dendroecology also relies on a suite of statistical routines and tools facilitating crossdating, climate reconstructions, as well as ecological and biological response modeling (Speer, 2010). Statistical approaches typically include the assessment of intercorrelation between series, analysis of mean sensitivity of trees, expressed population signal (EPS; Fig. 28) of chronologies, as well as autocorrelation analyses (Fritts, 1976; Cook and Kairiukstis, 1990).

In terms of dendroecological potential and dendroclimatic signal strength, studies generally report more robust cross-dating results – expressed in terms of mean sensivity and/or EPS – at altitudes below 1000 m a.s.l. and across all tropical ecoregions on all continents. Consistently, series with the highest intercorrelation and autocorrelation values are also located below 2500 m a.s.l. Average values of intercorrelation in tropical studies are 0.45 ± 0.16 (n_{obs} = 161), mean sensitivity of records is 0.42 ± 0.15 (n_{obs} = 129), and studies reporting EPS values reach 0.84 ± 0.09 (n_{obs} = 81) on average, whereas autocorrelation values are given at 0.38 ± 0.22 (n_{obs} = 88) on average. The genera with by far the largest amount of intercorrelation series described are *Pinus*, with tree-ring data collected mostly above 1200 m a.s.l. In terms of mean sensitivity, *Chukrasia, Toona, Cedrela* and *Hymenaea* have the highest values (over 0.5); here, all samples were collected below 1000 m a.s.l. Among those studies reporting EPS, *Pinus, Cedrela* and *Tectona* had the highest overall values. *Pinus* and *Cedrela* (usually sampled above 1000 m a.s.l.) as well as *Toona*, *Chukrasia* and *Tectona* (below 1000 m a.s.l) are most frequently published with data on autocorrelation series.

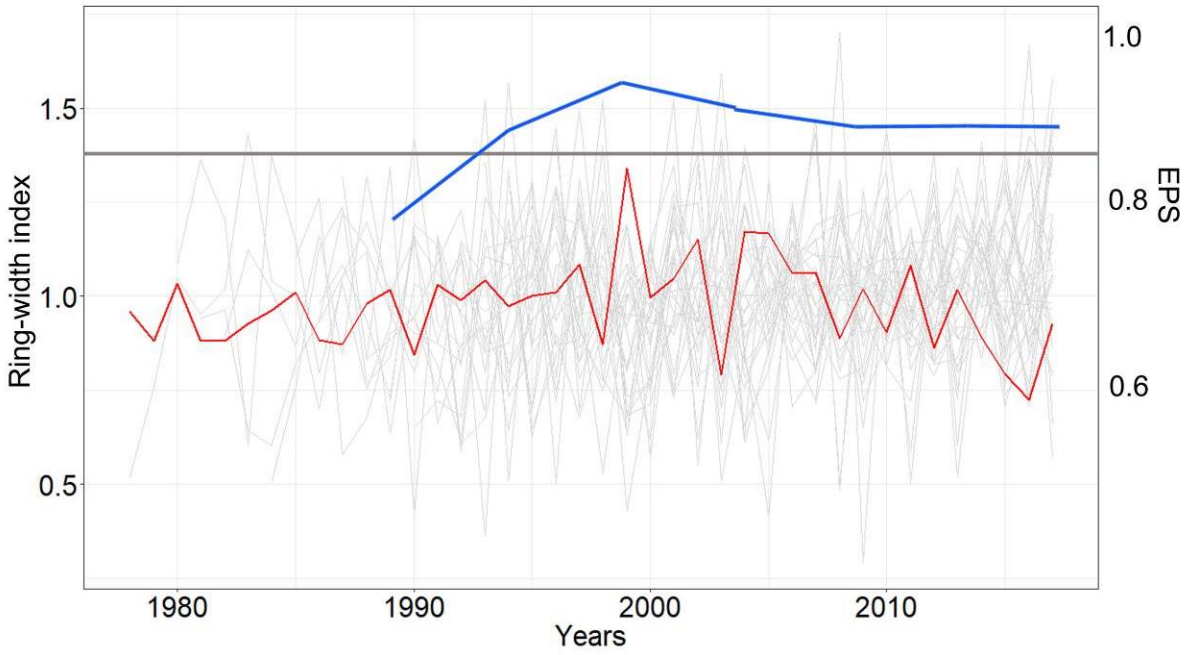

Fig. 28. Statistical analysis example on tropical dendroecology. Ring-width index (RWI; light grey lines), residual chronology (red line) distributed over time. Running EPS are shown above each RWI chronology (thicker blue line). Horizontal thicker grey line indicate the threshold limit of EPS=0.85.

3.6. Applications based on tropical dendroecology

Tropical dendrochronological studies have started to increase almost exponentially at the beginning of the 21st century (Fig. 29), with notable differences, however, between different applications or subdisciplines. Most frequently, research focused on dendroclimatology and dendroecology, encompassing a stunning 96% of all work realized in the tropics, with only scarce and scattered work on dendrogeomorphology in Latin America and dendroarchaeology in Southeast Asia. Dendroclimatological work is most common in America (57%), but less frequently used in Asia (27%), Africa (14%), and Oceania (2%). The focus very often is on climate-growth relationships (Fig. 30), regional or local climatic reconstructions as well as on relations between precipitation and tree growth, especially in the case of species used in the timber industry. Moreover, climatic variability, the response of trees to drought as well as the relationship between tree growth and the state of the El Niño Southern Oscillation (ENSO) are current topics in tropical dendroclimatology as well. Multiple chronologies have been constructed lately to better understand climatic variability and climate-growth response both in mountainous and lowland settings (Fichtler, 2017). As such, and by studying the signals recorded by different species in contrasting biomes along the tropics, dendroclimatology can help to improve our understanding of tree and forest responses to modes of climate variability (e.g., ENSO) and climatic changes (Rozendaal and Zuidema, 2011), as well as to, tropical cyclones or and droughts further (Fig. 31; Boninsegna et al. 2009). Moreover, long-term trends in water use and growth can be obtained from measurements of stable isotopes and growth-ring widths, such that data can be retrieved on physiological changes that would, in turn, most likely be linked to rising CO_2 (Brienen et al., 2016). Woody plants also respond to certain external stressors that can change as a result of climate

change in the tropics. The response of mangrove species to salinity and sea level changes can, for instance, not only improve our understanding of the process itself, but also illustrate how these fragile ecosystems will likely react to further warming and associated changes (Robert et al., 2011). Another topic of increasing relevance is related to wildfires, both in ecological terms but also in terms of ongoing and anticipated future climate change (Lindbladh et al., 2013).

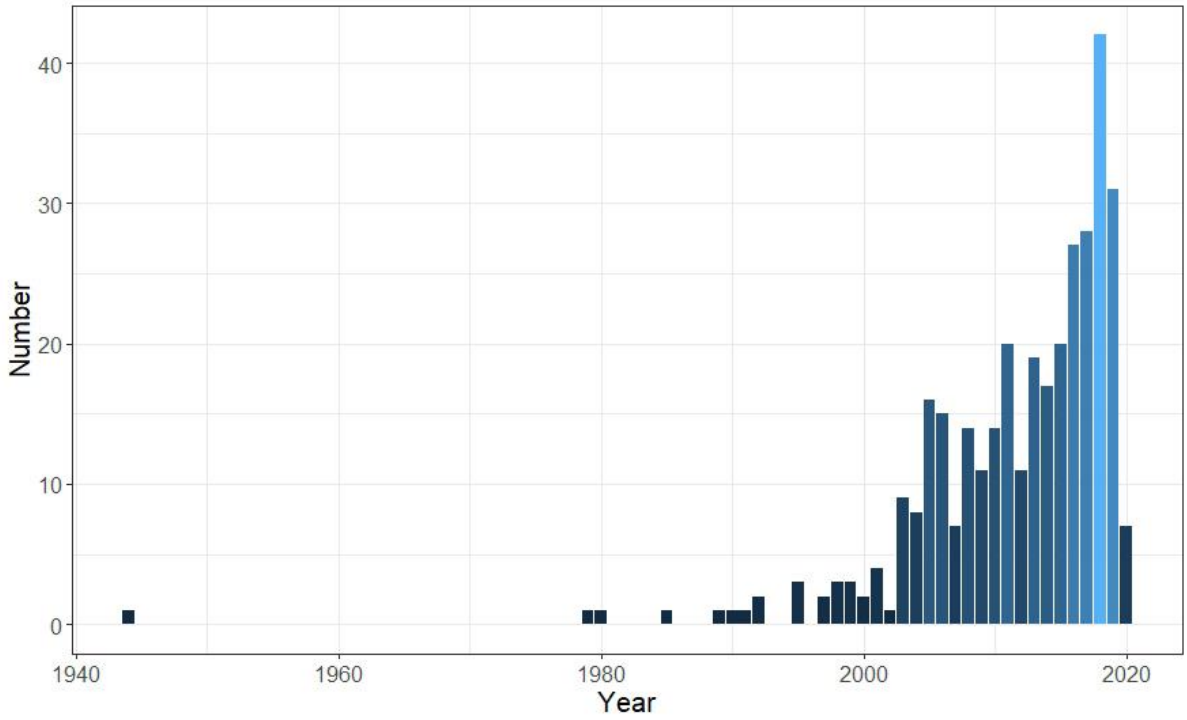

Fig. 29. Annual numbers of articles published in English or Spanish using the keywords “tropical” and “dendrochronology”. Note the almost exponential increase of publications since the early 21st century.

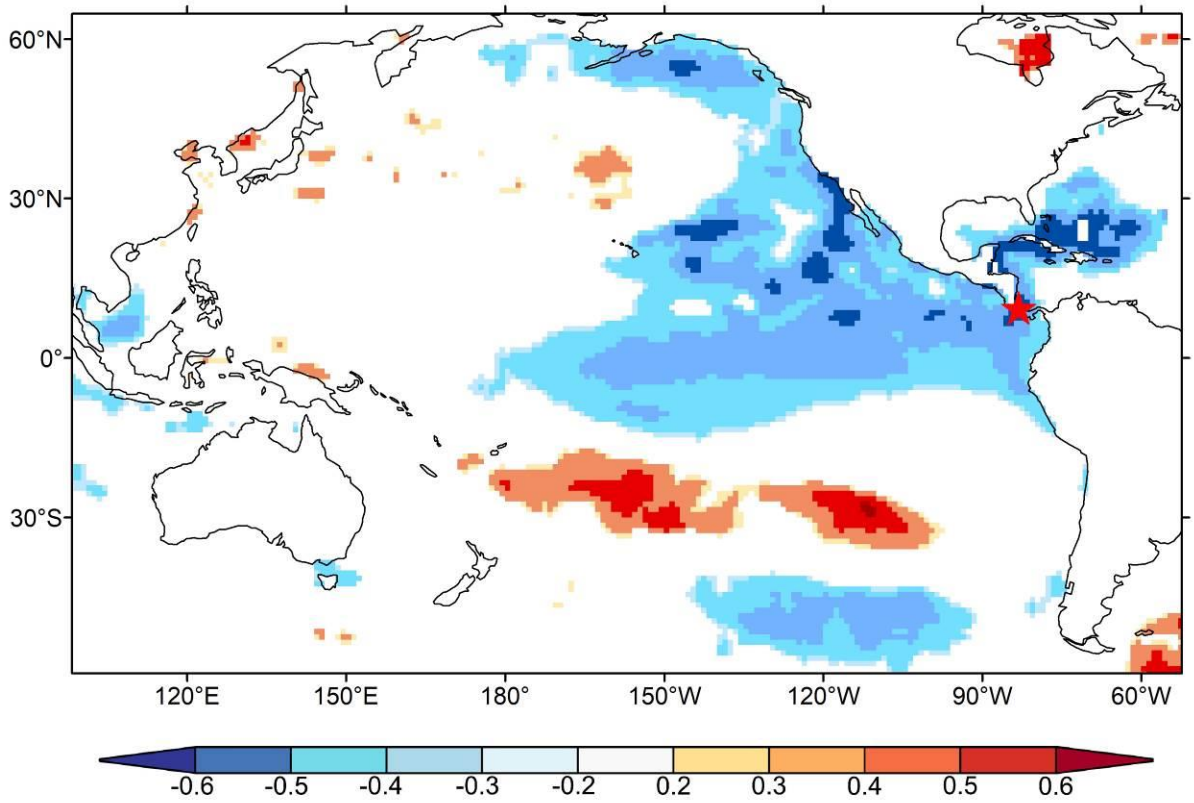

Fig. 30. Spatial correlation between the residual ring width index and December Sea Surface Temperature (SST) linking greater growth-rings with La Niña events. The red star indicates the location of the used chronology.

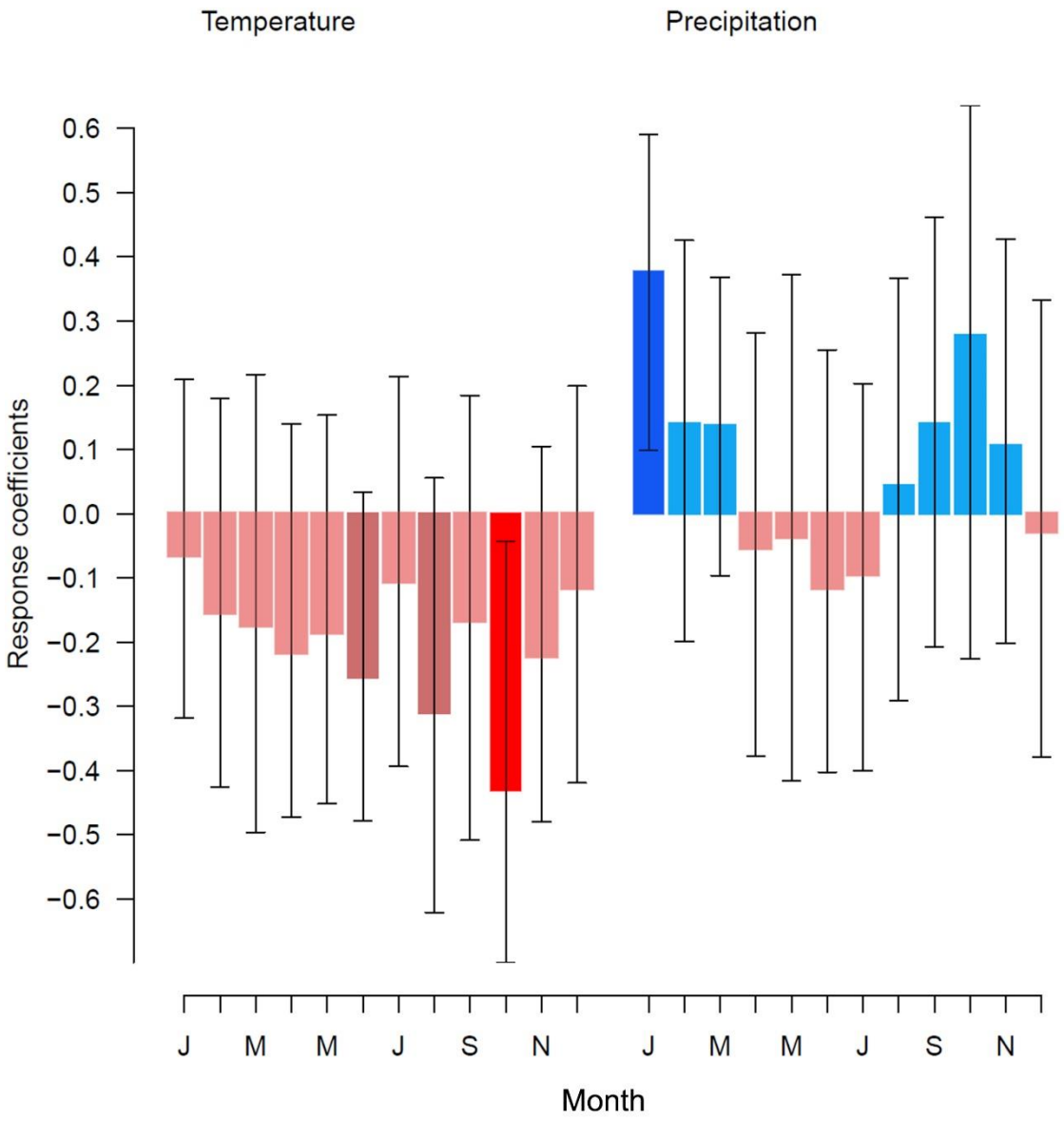

Fig. 31. Residual master chronology correlation temperature-precipitation function of an endemic shrub in Costa Rican highlands (modified from Quesada-Román et al., 2020b).

Dendroecological studies were most frequently realized in the Americas (59%), followed by Africa (20%), Asia (17%) and Oceania (4%). Research here has been devoted primarily to cambial, vessel and xylem anatomy, phenological responses, timber-yield projections for commercial species, potential growth rhythms, wood traits, the impact of lianas on tree growth, water use efficiency as well as forest succession.

This clear focus on dendroclimatology and dendroecology (*sensu stricto*) is also reflected in the selection of journals in which researchers have published their papers (Table 4). Indeed, most of these journals are devoted to ecology and climatology. Regarding the others field comprised within dendroecology (*sensu lato*), dendrogeomorphic research has been restricted largely to the neotropics, with a clear geographic focus on mass-movement processes in volcanic environments

of Mexico, erosional processes in Brazil, floods in Costa Rica and, again, mass-movement processes in northernmost Argentina. With the ongoing climate warming and intensification of rainfall events, weathering rates have been observed to increase across the tropics. The process has been exacerbated further by the fact that tropical regions also are hotspots of tectonic activity, and changing land use, resulting in an intensification of erosional processes and the formation of natural disasters. Growth rings in trees and roots have been applied repeatedly to quantify erosion (and the evolution of erosion rates in extratropical settings) (Ballesteros-Cánovas et al., 2013; Stoffel et al., 2013), and have just lately been applied to tropical species as well (Bovi et al., 2019). Other approaches in the field of dendrogeomorphology have proven their potential in dating past disasters and in providing spatio-temporal records on the frequency and magnitude of past hydro-geomorphic and geological mass-movement events (Stoffel and Bollschweiler, 2008). Interestingly, however, they have only rarely been applied so far in the tropics and mainly to study peak discharges of recent floods (Quesada-Román et al., 2020a) or lahar events (Franco-Ramos et al., 2020) following extreme rainfall episodes. The potential of dendrogeomorphology in the tropics seems huge if one bears in mind that ~40% of the world's population resides in developing, tropical countries facing the increasing impacts of natural disasters, both in terms of economic losses and in death tolls (Alcántara-Ayala, 2002).

Likewise, much more research could still be realized in dendroarchaeology, an approach that has made substantial advances over recent decades and through the inclusion of isotopic and chemical extraction approaches which will ultimately help to remove the historical limitations for dendroprovenance studies. Wood from archeological sites, if preserved, could be combined with growth-ring data from global-scale ecological and climatological studies so as to overcome the environmental restrictions and to elucidate direct anthropogenic disturbances of ancient communities in the tropics (Pearl et al., 2020). As such, and in view of the persisting limitations in growth-ring research in fields other than climatology and ecology, any expansion of innovative multi- and trans-disciplinary approaches to growth-ring studies would definitely enhance our knowledge of these biodiverse regions further. Conformingly, tropical countries could develop their own laboratories and expand international collaboration to explore well-known as well as endemic and non-traditional species, with the ultimate goal to enhance the knowledge and to improve the protection and conservation of the most biodiverse region of the world.

Table 4. Journals with more than 5 articles reporting on research realized using tropical dendroecology.

Journal	N
Trees	47
Dendrochronologia	45
Forest Ecology and Management	17
IAWA Journal	11
Tree-Ring Research	9
PLOS ONE	7
Climate Dynamics	6
Forests	6
Radiocarbon	6
Biotropica	5
Journal of Tropical Ecology	5

Oecologia	5
Revista de Biología Tropical	5

3.7. Limitations and future prospects

Despite of being the most biodiverse, productive, and understudied environments, tropical regions have long been avoided by dendroecologists because of the often inconsistent growth patterns in tropical trees, sampling difficulties, complex wood anatomy, and/or the lack of physiological knowledge of local wood species (Pearl et al., 2020). This review has shown that a multitude of approaches exists and that several hundreds of species have already been shown to be suitable for dendroecological research. Nonetheless, this paper also showed that much remains to be done, and we thus repeat the call for a further development of approaches and techniques aimed at disentangling the climatic and ecological information contained in tropical trees (Worbes, 2002). The recent, yet still emerging fields of chemical and physical wood analyses, substantial progress in improving the sampling design, statistical analyses, and tree-growth modeling are first steps toward the future of tropical dendroecology (Zuidema et al., 2013).

We observe a recently growing number of chronologies from South America and New Zealand, but also recognize that there still is a substantial lack of chronologies from Africa and the tropics in more general terms (Speer, 2010). Zhao et al. (2019) have quantified important limitations and biases as well as the alarming lack of information from Africa and the persistently low representation of tropical habitats, particularly in Asia, Central and South America, and Oceania in publications available in the International Tree-Ring Database (ITRDB; https://www.ncdc.noaa.gov/data-access/paleoclimatology-data/datasets/tree-ring). So far, research on the response of tropical forests to global change focused primarily on the analyses of leaves and forest communities, at the cost of studies addressing individual tree and population level reactions for which important gaps in knowledge still persist (Zuidema et al., 2013). In addition, a vast majority of tropical regions are located primarily in emerging countries, where development and environmental concerns are often synonymous as a result of the constant impact that humans have on agribusiness, wood and mineral extraction; at the same time, the regions are also among those most susceptible to the negative effects of climatic change (Lawrence and Vandecar, 2015). Moreover, old growth stands are becoming increasingly rare in the tropics and, even when left standing, are becoming subject to decomposition, leaving their trunks hollow (Poussart et al., 2004).

Growth-ring studies of tropical trees offer important insights into global change effects in tropical environments and forests. They have the potential to provide much more information on climate-forest interactions and climate reconstructions as new techniques become available and research efforts will hopefully intensify in regions that have been less studied so far and where a huge potential exists to improve local collaboration (Brienen et al., 2016). Many tropical species do not mark simple sight rings and need further anatomical assessments that require extra efforts and expensive lab equipment. This point is key as a vast majority of tree-ring laboratories and dendroecologists are residing and working outside the tropics. Within tropical environments, we are aware of only a limited number of tree-ring laboratories or individual researchers located in

Argentina, Bolivia, Brazil, Colombia, Costa Rica, India, Indonesia, Malaysia, and Thailand. Due to the lack of large labs and high-end infrastructure, the efforts and implementation of cutting edge (and costly) techniques – including quantitative wood anatomy and/or isotopic analyses – have been restricted to labs in the United States and Europe so far.

Over the past three decades, tropical growth-ring research has overcome some of its infancy diseases (e.g., limited number of suitable species, limited spatial coverage, shortness of series) to become an important and increasingly growing branch of dendroecology. Yet, further developments, both methodological and geographic, are still critically needed to bring the science of tropical dendroecology to an adult stage. The lack of ring formation in some tropical species can often be solved by favoring studies focusing on chemical or stable isotopic signals in tropical woods and by examining the wood anatomy of species to unveil annual ring formation (Speer, 2010). Progress can also be expected by simply developing multiproxy approaches relying on the detection and utilization of stable isotopes, radioactive isotopes, genetic information, wood chemistry, and wood anatomical structures in the annual rings (Pearl et al., 2020). In this way, one can expect that dendroecology will likely contribute to solving some of the remaining challenges in tropical forestry, ecological research and the applications of techniques that rely on growth rings as well but would contribute to the understanding of tropical geomorphology, archaeology and chemistry (Worbes, 2002; Schöngart et al., 2017; Pompa-García and Camarero, 2020).

To extend the understanding of annual ring formation in tropical trees further, it will be critical to develop (a) catalogue(s) of species of known dendroecological potential, to better apprehend their wood anatomical features, and to diversify the suite of different analysis and approaches used to study growth rings in tropical trees. Furthermore, we call for a more systematic use of dendrometers and the continuous measurement of diameter growth and tree cambial activity (Worbes, 1995) as these tools could help in the major task of improving the understanding of growth ring formation in tropical trees further, and would allow comparison of dendrometer results with high-resolution climatic data, thereby providing information on growth rhythms in trees. Another way to increase our understanding of growth patterns in growth rings is by realizing experiments in planted trees, by controlling rainfall and drought events so as to simulate dissimilar conditions that would induce anatomical responses under normal conditions along the year (Fig. 32; Van Camp et al., 2017; Hayden et al., 2019). Despite the pernicious effects of non-native species in tropical environments, they can play a non-negligible role in regional species richness, and have a quite direct effect on conservation goals and ecosystem services (Schlaepfer, 2018). In terms of dendroecology, non-native species can be valuable candidates when it comes to enhance our understanding of climatic, ecological, and geomorphic signals contained in growth rings that may not have been easily recognized in the growth rings of tropical chronologies.

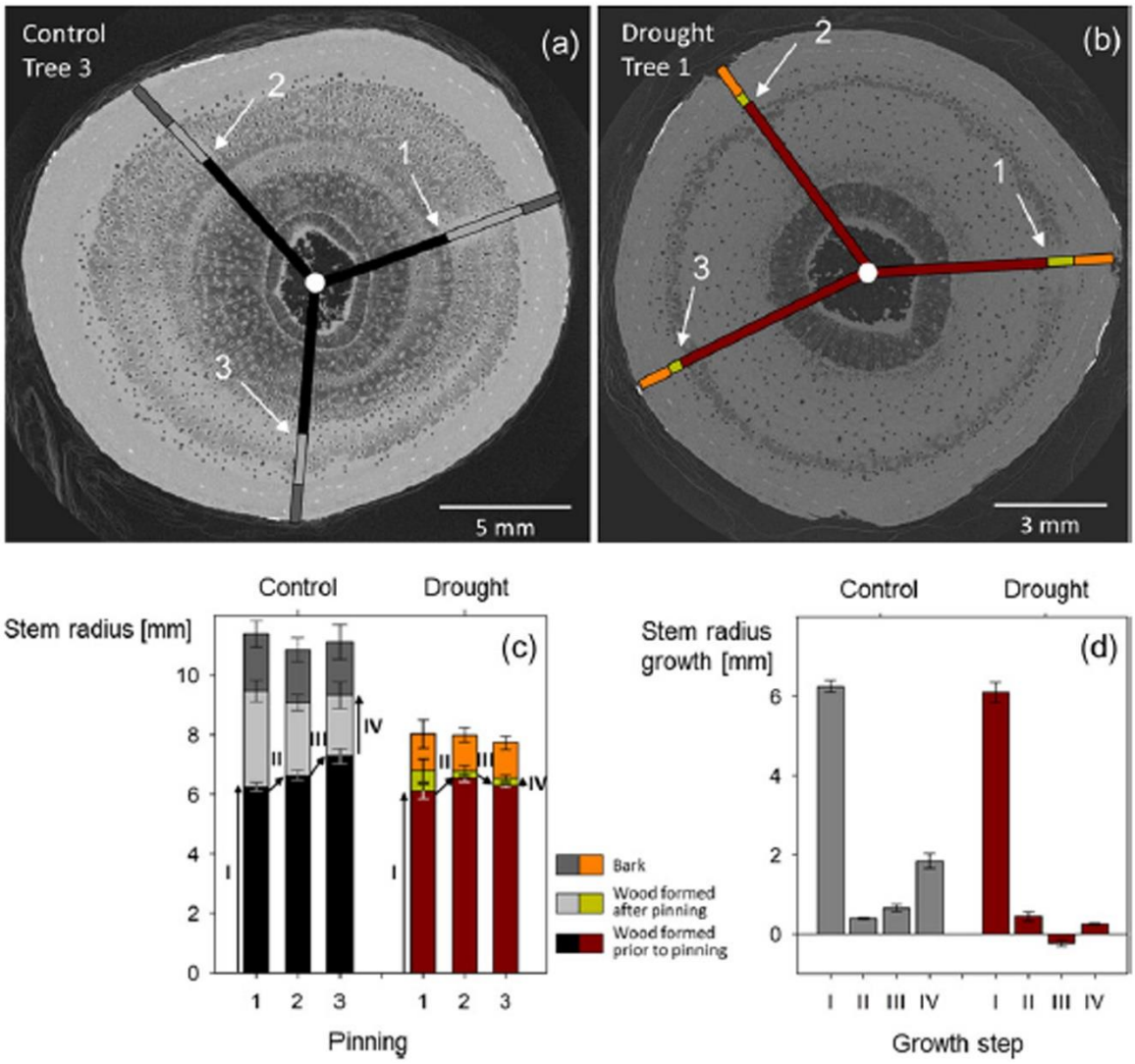

Fig. 32. Wood formation in control and drought-treated Maesopsis eminii trees. X-ray micro-CT transverse section from conditioned samples illustrating pinnings on (a) control Tree 3 (resolution = 11 μm) and (b) drought-treated Tree 1 (resolution = 7 μm). (c) Average stem radius. (d) Stem radius growth according to the growth steps (I, II, III and IV) as defined in (c) to quantify wood formation during a specific time period (Van Camp et al., 2017).

Endemism is higher in the tropics than in any other region of the world, especially in the wet tropics where tropical rainforests are found (Hobohm, 2014). This vast reservoir of wet tropical vegetation still waits to be exploited by dendroecologists. Here, one would need to clearly change the common mentality of using only common or well-known species; instead, we as a community will to challenge the discipline and to go ahead for new endeavors that are likely to yield interesting results from an environment that is increasingly threatened by climate change and human exploitation (Hobohm, 2014). To date, many of these regions with high endemism remain in critically understudied regions (Zhao et al., 2019), both in lowlands but especially also in the mountain systems (such as cordilleras and volcanic areas) of Southern Mexico, Central America, the Caribbean and the South American Andes (Pompa-García and Camarero, 2020), but also in the Himalayas, the Indian Ghats, the Pegu Range of Myanmar or the Central Mountain Range of

Taiwan (Bhattacharyya and Shah, 2009; Pumijumnong, 2013). In Africa, high mountains and volcanic regions remain largely unexplored as well, and research yet has to be realized along the African Rift and Cameroon Volcanic Line (Gebrekirstos et al., 2014). In Oceania, the New Guinean Highlands and the many islands of Hawaii remain white dots in terms of tropical dendroecology. By expanding the geographic scope of tropical dendroecology and by enlarging the thematic fields of research, much more information will become available on how climate has changed at these latitudes, how vegetation has responded (and still is responding) to these changes and how humans have both lived in these pristine regions and changed it through their presence, sometimes even contributing to disasters. Tropical dendroecology can gain in importance further if barriers between disciplines are removed – but even more so also if labs and institutions within the tropics are given the means to develop high-end research locally.

CHAPTER 4

4. Neotropical *Hypericum irazuense* shrubs reveal recent ENSO variability in Costa Rican páramo

Adolfo Quesada-Román [a,b], Juan Antonio Ballesteros-Cánovas [a,c], Sébastien Guillet [a,c], Jaime Madrigal-González [a,d], Markus Stoffel [a,c,e]

[a] Climatic Change and Climate Impacts, Institute for Environmental Sciences, University of Geneva, Boulevard Carl-Vogt 66, CH-1205 Geneva, Switzerland
[b] Escuela de Geografía, Universidad de Costa Rica, 2060 San Pedro, San José, Costa Rica
[c] Dendrolab.ch, Department of Earth Sciences, University of Geneva, Rue des Maraîchers 13, CH-1205 Geneva, Switzerland
[d] Grupo de Ecología y Restauración Forestal, Departamento de Ciencias de la Vida, Universidad de Alcalá, ctra. Madrid-Barcelona, km 33.4, 28805, Alcalá de Henares, Spain
[e] Department F.-A. Forel for Environmental and Aquatic Sciences, University of Geneva, Geneva, Switzerland

Dendrochronologia 61, 125704. https://doi.org/10.1016/j.dendro.2020.125704

Climate-vegetation relations in alpine systems play a pivotal role in regulating hydrology and have thus become a research priority in a context of ongoing climate change. In this paper, we investigate how one of the most dominant shrub species in alpine páramo ecosystems of Central America, *Hypericum irazuense*, responds to changes in precipitation, temperature and El Niño-Southern Oscillation. To this end, we performed dendrochronological and wood-anatomical analyses on *H. irazuense* to determine the limiting climatic factors driving shrub growth, using a bootstrapped correlation and response function analysis. To validate our results further, we also applied Structural Equation Models (SEM), an approach commonly used in ecology, so as to check for climate-growth relations which consider the control of ENSO on growth through its influence on various climatic parameters. Results support a relation between climate and annual growth of *H. irazuense* and demonstrate that the latter is sensitive to precipitation and temperature during boreal winters. In addition, we observe a statistically significant correlation between annual growth and La Niña events. The presence of annual growth rings holds *H. irazuense* as one in only few neotropical species suited for dendrochronological studies. Results of this study could thus contribute to an improved understanding of how changing climatic conditions affect the fragile and threatened páramo ecosystem and the ensuing services it offers in the form of hydrology regulation over the next decades.

4.1. Introduction

Dendrochronological analyses offer potent insights into diverse fields of environmental sciences (Schweingruber, 1996). Trees, shrubs and perennial herbs often represent natural archives as they conserve relevant environmental information in their growth rings as well as in the structures of their stems, branches, and/or roots. Besides various ecological applications (García-Cervigon et al 2013), shrub dendrochronology has also been used to quantify impacts of past and ongoing climate change on shrub growth (Myers-Smith et al., 2015; Francon et al., 2019; Carrer et al., 2019). Whereas the focus of tree and shrub-ring research has been mostly on temperate and cold climates, it could also contribute to our understanding of tropical climate change because a substantial number of tropical species is known to form growth zones with an annual layering driven by the species' sensitivity to climate (i.e. rainfall and temperature), ecological, or geodynamic variations (Schöngart et al., 2017).

In addition to insights on climate-growth relations, analysis of annual rings in tropical trees and shrubs can also contribute substantially to the broadening of our current knowledge of tropical forest ecosystem functioning (Worbes, 2002). Indeed, several studies have addressed the nature of growth periodicity, growth-climate relations, drought and fire histories, flood dynamics, climate variations, and/or ecology by applying dendrochronology to tropical species (e.g., Boninsegna et al. 2009; Rozendaal and Zuidema, 2011; Fichtler and Worbes, 2012). However, growth rings of tropical species typically show greater variations and complexity than those of temperate species, thereby reflecting their huge diversity and weaker identification accuracy (Silva et al., 2019). To warrant the successful application of dendrochronological studies in these regions, detailed knowledge of wood-anatomical structures and the variability of growth zones is thus vital (Worbes, 2010).

Costa Rica concentrates roughly 5% of global biodiversity and is the worldwide leader in terms of species density (Kappelle, 2016). The large altitudinal range, important topographic barriers, and soil diversity explain the presence of several and diverse ecosystems in the region (Antonelli et al., 2018). One of these, the páramo, is a grass and/or shrub dominated ecosystem established in the cool and wet upper slopes of tropical mountains located at latitudes between 11° N and 8° S (Kappelle and Horn, 2016). Páramos typically occur in alpine environments above treeline and below the snow limit. In Costa Rica, this transition from the closed-canopy montane forests to alpine, treeless páramo vegetation occurs above 3100 m asl, and represents 2.3% of the entire neotropical páramo (Kappelle, 2003). In these landscapes located around the highest mountains of Costa Rica, hundreds of palustrine and lacustrine wetlands guarantee paramount hydrological and ecological functions (Esquivel-Hernández et al., 2018). The pristine páramo ecosystems are, however, threatened by increasing temperatures projected for the decades to come (Veas et al., 2018).

Previous work has addressed the dendrochronological potential of Costa Rican páramo shrubs (Horn, 1989; Janzen, 1973; Weberling and Furchheim-Weberling, 2005; Williamson et al., 1986). More recently, Kerr et al. (2017) analyzed *H. irazuense* to determine recruitment dynamics by comparing ring growth with well-known dates of previous wildfires at their study sites. By contrast, little is known about climate–growth relationships of this common páramo species so far. Thus, given that variability of the El Niño Southern Oscillation (ENSO) represents the most important element of natural variations in rainfall pattern over the larger study region (Diaz et al.,

2001), we hypothesize that the growth of *H. irazuense* is sensitive to annual variations in the ENSO. To test this hypothesis, we performed dendrochronological and wood anatomical analyses to measure ring-width series of *H. irazuense* to investigate the species' sensitivity to climate (in terms of precipitation and temperature), including changes in modes of natural climate variability (regarding ENSO).

4.2. Material and methods

4.2.1. Study area

The study area is located in the Chirripó National Park, Cordillera de Talamanca (9.445 to 9.489 °N, and -83.485 to -83.505 °W, Fig. 33a). The highest elevations of Chirripó National Park are at 3820 m asl and are covered by páramo vegetation (Quesada-Román and Zamorano-Orozco, 2019). Local climate is controlled by the latitudinal migration of the Intertropical Convergence Zone, northeastern trade winds, cold continental outbreaks, and the seasonal influence of Caribbean tropical cyclones (Hidalgo et al., 2015). These dynamics cause rainfall to fall during two periods for a total of ~2000 mm (Fig. 34), one in May and another in October, whereas rainfall is discontinued between July and August and during a period known as the *Mid-Summer Drought* (Maldonado et al., 2016). Roughly 89% of the annual rainfall in the study region is recorded between May and November (i.e. during the rainy season), and a clear dry season can usually be observed between December and April (Quesada-Román, 2017). Temperatures are relatively constant throughout the year at around 9.7 °C (Fig. 34; Kappelle and Horn, 2016).

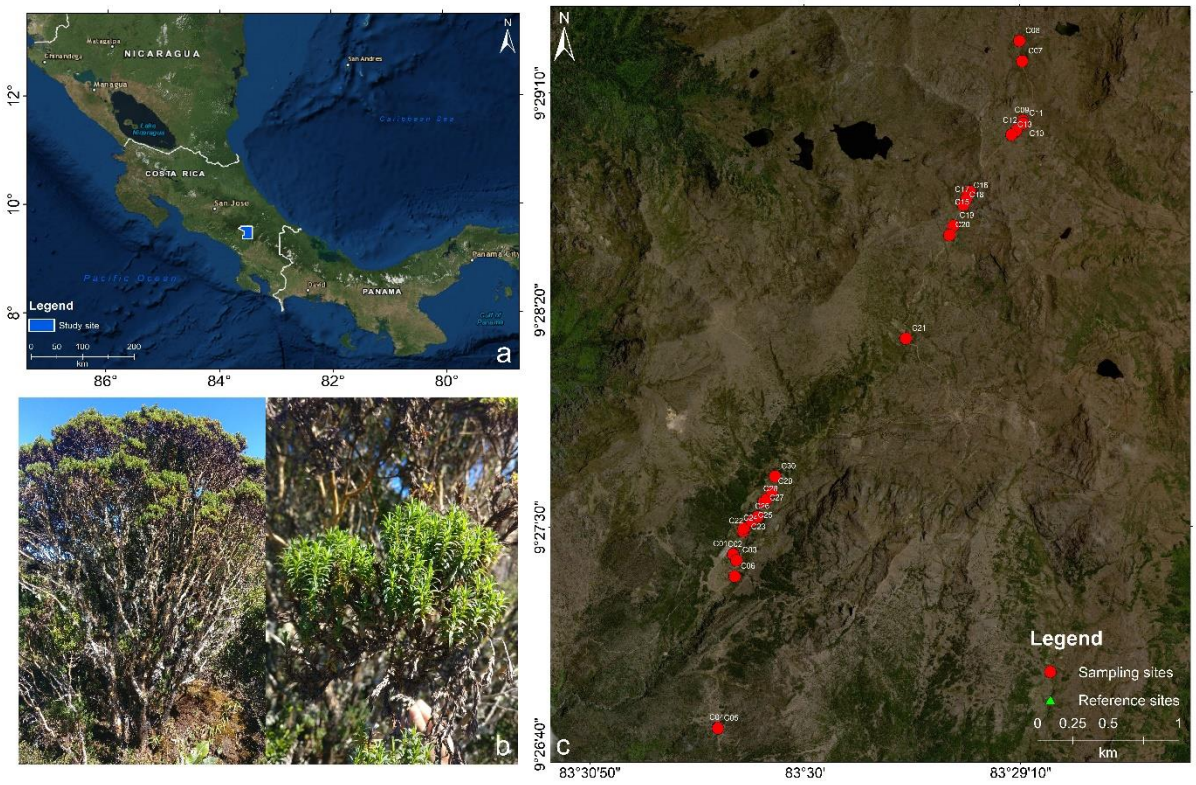

Fig. 33. a) Location of the study area in a Central American and Costa Rican context; b) *Hypericum irazuense* specimen with several stems and a zoom on its leaves; c) *H. irazuense* samples sites in the Chirripó National Park.

The temporal and spatial variability of rainfall in the country is heavily influenced by the ENSO (Méndez et al., 2019). Complex and contrasting responses (i.e. warm or wet) vary in terms of their signs, magnitude, duration and seasonality between catchment areas draining to the Pacific and those flowing into the Caribbean Seas (Waylen and Laporte, 1999). The two slopes behave differently and it seems likely that they will also respond in opposite ways to ENSO conditions (Maldonado et al., 2018). On the Pacific side of Costa Rica, El Niño events generally favor drier conditions along the year and especially during the dry season – as observed in 1997-1998 and 2015, whereas La Niña events favor wetter conditions, as seen in 1998-1999 and 2010-2011 (NOAA, 2019).

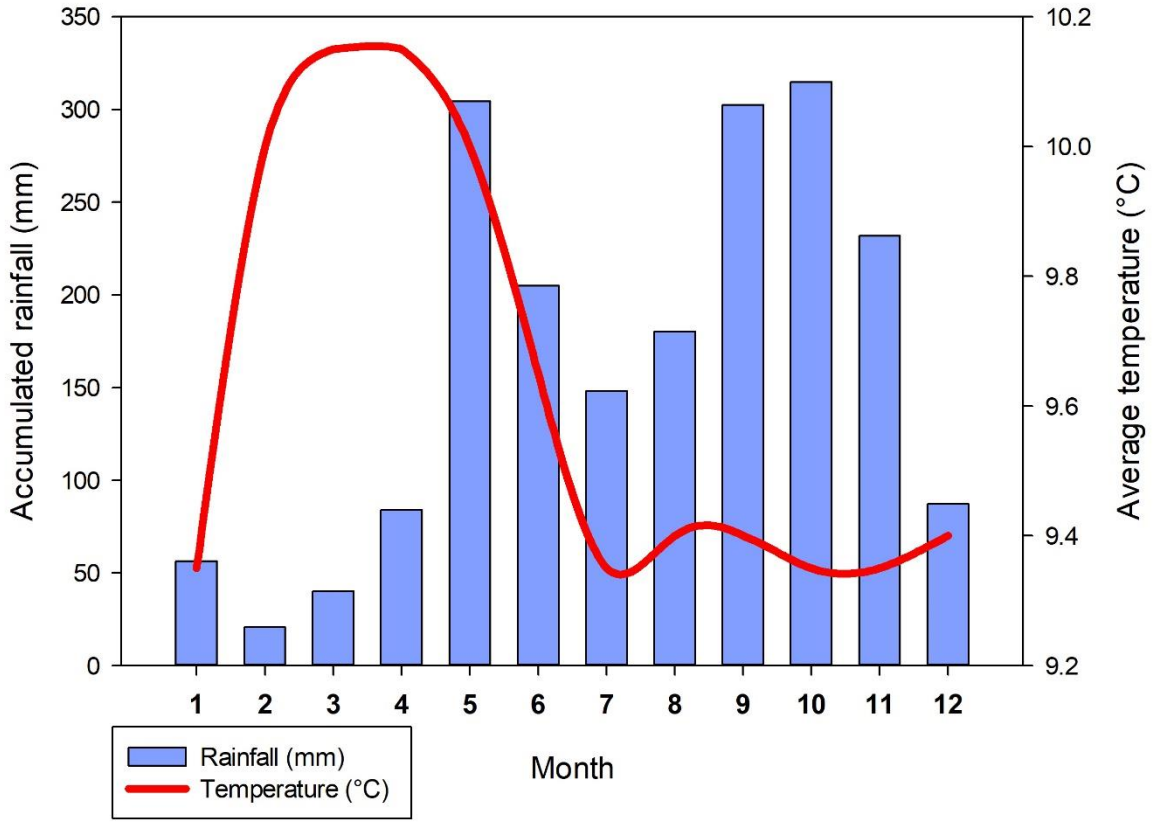

Fig. 34. Ombrothermic diagram of Chirripó National Park for the period 1995–2009.

4.2.2. *Hypericum irazuense* Kuntze ex N. Robson

The *Hypericaceae* family is characterized by opposing leaves containing points or resinous-glandular lines and by their orange and transparent, resinous sap. Members of the *Hypericaceae* family have flowers with petals and separated styles, and are characterized by more or less frequent fasciculated stamens (Crockett et al., 2010). The genus *Hypericum* L. is present on all continents except Antarctica where it occurs in the form of herbs, shrubs, and infrequently also in the form

of trees. The genus is found in a variety of habitats in temperate regions as well as in high tropical mountains, but it avoids zones of extreme aridity, temperature and/or salinity (Crockett and Robson, 2011). In Costa Rica, *Hypericum* spp. includes subwoody grasses or bushes (above 900 m asl). It is densely foliaceous, with sessile or shortly petiolate leaves, a narrow blade (<1 cm), yellow petals (ca. 3-17 mm), as well as glabrous and capsular flowers (Robson, 2003). *Hypericum irazuense* is a subshrub to shrub, 0.15-2.5 (in rare cases also 3) m in height, with internodes of 0.15-0.4 cm, sessile leaves, 0.7-1.2 x 0.2-0.3 cm sheets. It is narrowly elliptical, acute at the base and apex, and with a lateral nerve that is often visible on either side of the base (Fig. 33b). In addition, terminal inflorescences are of one lonely flower of 0.5-0.6 cm, usually shorter than sepals, and widely ovoid (Robson, 1987; Hammel, 2007). Its distribution comprises La Amistad International Park (PILA) between 2100–3700 m, in the cloud forest, low-elevation oak forests, and the páramos of Costa Rica and Panama (Monro et al., 2017; Missouri Botanical Garden, 2019).

4.2.3. Sampling and sample preparation

In the field, we randomly selected shrubs of different size to account for the size structure of the population at elevations comprised between 3295 to 3692 m asl (Fig. 33c). For each shrub, we counted all stems and measured their diameters. Information on the slope angle and geomorphic position were recorded for each site as well. Thirty cross sections were obtained from the biggest stem of each shrub at the ground level. In the lab, samples were analyzed and data processed following the standard procedures described in Myers-Smith et al. (2015). The process involved surface preparation, counting of annual growth rings, as well skeleton plotting (Schweingruber et al., 1990). Due to the difficulties encountered in identifying clear ring boundaries on the cross-sections using classical dendrochronology (Fig. 35), we prepared thin sections with an automated Leica 2245 rotational microtome, with the aim to improve visibility of ring boundaries (Gärtner and Schweingruber, 2013).

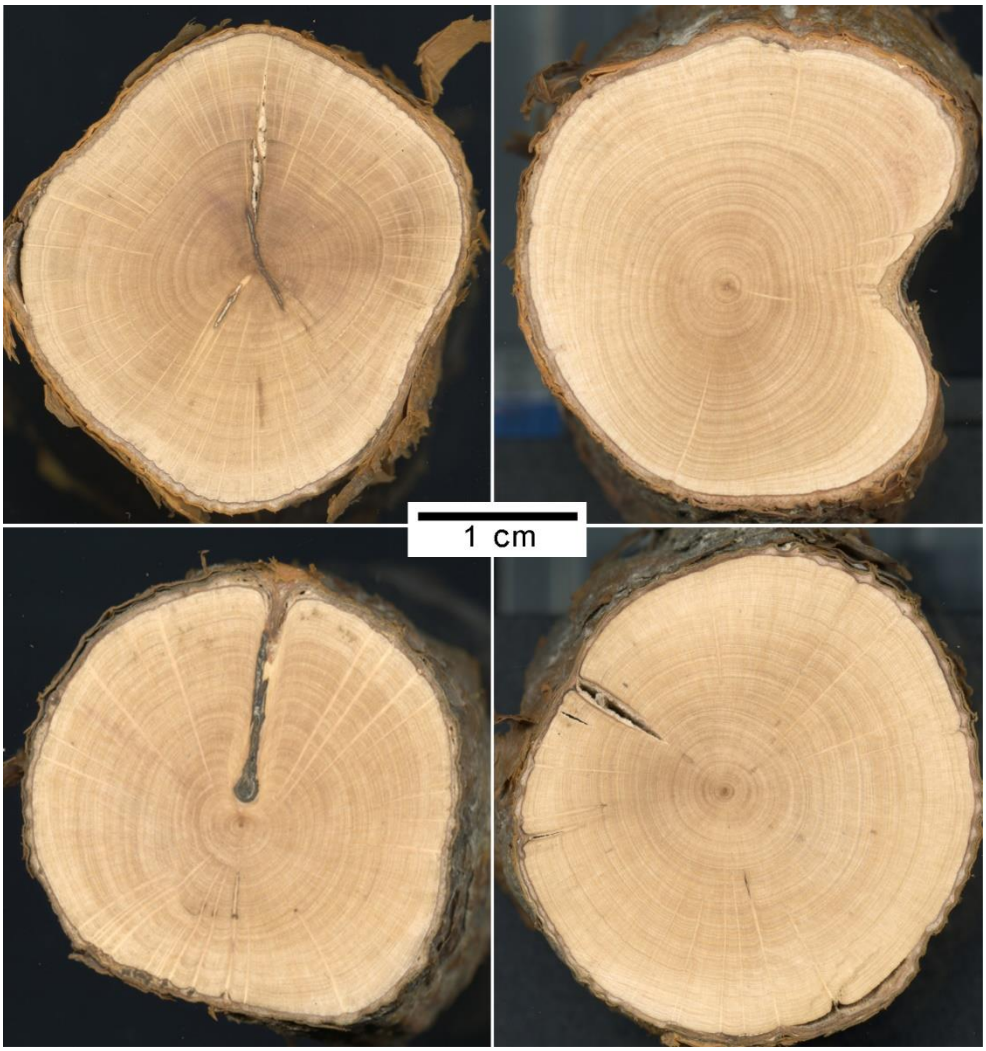

Fig. 35. *Hypericum irazuense* sanded cross sections.

Thirty micro-sections were obtained with a thickness of ~20–30 μm. Individual cuts were stained with a mixture of Safranin and Astra blue and permanently fixed on microslides using Canada balsam (following Ballesteros-Cánovas et al., 2010; Francon et al., 2017). A Leica DM 2000 camera with a 40–100× magnification was then used to capture high-resolution digital pictures. Individual images were merged automatically with Adobe Photoshop to obtain entire cross-sections. Ring widths were measured from scanned images with the help of CooRecorder 7.6 (Larsson, 2003). Radial measurements on individual *H. irazuense* samples were cross-checked through a careful visual inspection of each cross-section so as to reduce the risk of growth underestimation caused by partially missing rings. Statistical methods commonly used in dendrochronology to cross-date tree (shrub) ring series could not be employed in the present study, as most samples obtained from the study site did not exceed 30 years, and thus prevented computation of metrics (rbar or t-test) that are usually used to assess the robustness of cross-dating. For this reason, we instead cross-dated our shrub series with skeleton plots and by using the pointRes R package (van der Maater-Theunissen et al., 2015). We identified eleven pointer years

(six exceptionally narrow and five wide rings) that were then used to synchronize the shrub-growth series.

4.2.4. Standardization

Mean shrub-ring series were detrended using ARSTAN (Cook, 1985; Cook and Krusic, 2005) with the aim to eliminate non-climatic trends (e.g. age-related growth trends) and to maximize climatic information. Each shrub-ring width series was fitted with a cubic *smoothing spline* having a 50 % frequency response cutoff equal to 67 % of the series length. To account for the decreasing number of annual ring series back in time, we used the method developed by Osborn et al. (1997) stabilizing variance of the final shrub-ring chronology. Three shrub-ring chronologies (standard, residual and arstan) were obtained with ARSTAN, each representing a biweight robust mean of the mean shrub-ring series which were individually detrended (Cook, 1985).

Additionally, we also computed basal area increments (BAI) as follows:

$$BAI = \pi (R_n^2 - R_{n1}^2)$$

where R is stem radius (cm) and n is the year of ring formation.

BAI was obtained following van der Maater-Theunissen et al. (2015). BAI increases in mature stages tend to be stable as long as the shrub is not close to the extremes of juvenile stage or biological senescence (Poage and Tappeiner, 2002). The addition of BAI analyses complements classical dendrochronology (ring width index, RWI) and separate tree growth rates as a result of the two-dimensional variable used (Biondi and Qeadan, 2008). If tree-ring series are transformed into basal area increments, the practical use of its units in $cm^2 \cdot year^{-1}$ will allow direct interpretation of tree growth trends; by contrast to BAI, RWI values are relative units and dimensionless (Castruita et al., 2015).

4.2.5. Climatic data and analyses of climate-growth relationships

To analyze climate-growth relationships, monthly air temperature (°C), and monthly precipitation totals (mm) from CRU TS4.01 0.5°gridded dataset were used (Harris et al., 2014). The use of CRU TS4.01 gridded dataset was motivated by the limited number of weather stations nearby Chirripó National Park. The closest functioning weather station in the mountains is inside the study area and was only installed in 1995, preventing the data to be used for climate growth analyses. Analyses were conducted over the time period 1978–2017 for the average of all the grid cells available over the study area (9.3 – 9.5°N, 83.4 – 83.7° W). In addition, we used NCEP Southern Oscillation Index (SOI) due to the lack of better spatial resolution indexes (i.e. ERA 5) covering our chronology, and its successful use in the past (Waylen et al., 1996). Furthermore, we used the gridded sea surface temperature anomalies (SSTA) NOAA (Reynolds et al., 2002) SOI SST V2 dataset in order to further evaluate the potential influence of ENSO on *H. irazuense* (100° E – 60° W, 60° S – 60° N). Two methods were carried out to decipher climate-growth relationships in *H. irazuense*. First, bootstrapped correlation and response functions were computed between the residual chronology – so as to minimize the influence of autocorrelation – and monthly mean

temperature and total precipitation. We used a 12-month window spanning from current January to current December to encompass the full current growing season of the species.

To complement and further validate the bootstrapped response and correlation, we also applied a Structural Equation Model (SEM). Structural equation modeling (SEM) is a series of statistical methods capable of representing a wide array of complex hypotheses about how system components interrelate (Grace, 2006). Growth in tree/shrub-rings can be seen as the sum of several components interacting with each other and the SEM approach is particularly well suited to study the multiple processes that control the behavior of systems. SEMs are increasingly used in the field of Ecology but have so far received limited attention within the tree-ring research community. One advantage of SEM over the more conventional methods used in dendrochronology is that it does not necessarily require tree/shrub-ring series to be detrended. The SEM approach also works at the tree/shrub level and does not require the tree-ring/shrub series of a given population to be averaged together to form a chronology.

This approach also allows to consider other, non-climatic components at the level of individual trees, including parameters that are often neglected in classical tree/shrub-ring studies, such as tree/shrub age, tree/shrub size, and/or its vicinity to other trees/shrubs. Here, we applied SEM to unravel direct and indirect effects of climate variability and global atmospheric-oceanic circulation (i.e. SOI) through local climatic effects having an impact on basal area increments (BAI) at the level of individual shrubs (Madrigal-González et al., 2018). Further variables such as slope, altitude, and vicinity with other shrubs were added to the model as well. We first created a SEM using a potential set of inter-connected regression analyses in which arrows departing from the calendar years (linear temporal trends) represent the above mentioned global-change hypotheses.

Consistently, data from precipitation, temperature and SOI were used to understand the growth patterns (BAI). This initial model included BAI, minimum temperature (MIT), annual total precipitation (AP), and SOI as endogenous variables in five regression analyses, respectively: (i) growth as a function of size, MIT and calendar years; (ii) SOI as a function of MIT and AP; (iii) MIT as a function of SOI and calendar years; (iv) AP as a function of SOI and calendar years. Then, we analyzed the SEM that included each index at a time to test which of the models was most informative in terms of the Akaike Information Criterion (AIC) corrected for small sample sizes (Burnham and Anderson, 2003).

To account for the lack of independence of repeat measurements within individual shrubs in the growth model, we applied linear mixed models to log-transformed BAI, in which individual shrubs were considered as a random factor. Prior to SEM analyses, we sought for potential temporal autocorrelations in the BAI data by using an autoregressive correlation structure. To this end, a set of growth models were built using different orders of temporal autocorrelation (i.e., different numbers of autoregressive parameters), ranging from a non-autocorrelated structure to a fifth-order temporal autocorrelation structure (Camarero et al., 2017). The AIC thereby allowed selection of the best autocorrelation structure to be included in the SEM. Thereafter, we tested the three global change hypotheses by removing each corresponding arrow at a time from the full SEM and compared the resulting models with the full model using AIC in a backward model selection procedure. Once the non-supported global change trends were eliminated from the initial SEM, we tested the goodness of fit using a chi-squared test on Fisher's C statistic (Lefcheck, 2016). This

test evaluates whether potential missing paths should be considered in the initial SEM. In other words, if the associated p-value is higher than 0.05, then a better SEM exists that incorporates paths not accounted for in our full SEM.

Finally, we iteratively removed all non-significant missing paths and each time re-tested the model's adequacy. A pseudo-R2 was calculated following Nakagawa and Schielzeth (2013). SEM analyses were conducted in *R* using the piecewise SEM package (Lefcheck, 2016). We used the function lme (package nlme) (Pinheiro et al., 2018) to fit Linear Mixed Models to BAI. Regarding regressions posing climate as the dependent variable, we applied generalized least squared regressions with an autoregressive structure of variance to account for first order temporal autocorrelation of data. We used the gls function (package nlme) in the R environment (Pinheiro et al., 2018).

4.3. Results

4.3.1. Cross-dating and chronology characteristics of *H. irazuense*

High-resolution digital pictures of *H. irazuense* cross-sections display clearly visible growth rings. These layers can be interpreted the result of the annual cessation of precipitation between December and April in this tropical alpine ecosystem. Growth-ring boundaries are clearly visible and can be differentiated by a radially aligned band, with thick-walled latewood fibers, flattened along the ring boundary. Ring widths range from 0.1 to 0.8 mm and are rather uniform around the circumference, thus revealing that one-sided, mechanical stress has a rather weak influence on radial growth, at least in the stems selected for analysis. Despite this concentricity, wedging rings and micro rings – which often corresponded to missing rings in some other parts of the same plant – were rather common. The structure of annual rings shows a diffuse- to semi-ring-porous pattern with a clear concentration of bigger vessels in earlywood. A transition fiber band marks the start of latewood formation with the presence of small fibers where growth ring boundaries are more or less distinct, depending on the abruptness of pore size transition (Fig. 36).

Analysis of the 30 cross-sections allows the construction of a chronology spanning the period 1978 to 2017 (mean sensitivity: 0.314), with individual shrubs having a mean number of 29 rings. Mean BAI was 83.94 mm^2, ranging from 7.82 mm^2 to 180.31 mm^2. Over the studied period, eleven rings showed marked features among most shrubs that can be considered as pointer years. Six were negative pointer years, of which two, 1998 and 2016, show very narrow rings. On the other hand, five rings are considered positive pointer years, with 2012 showing a very wide ring in most samples.

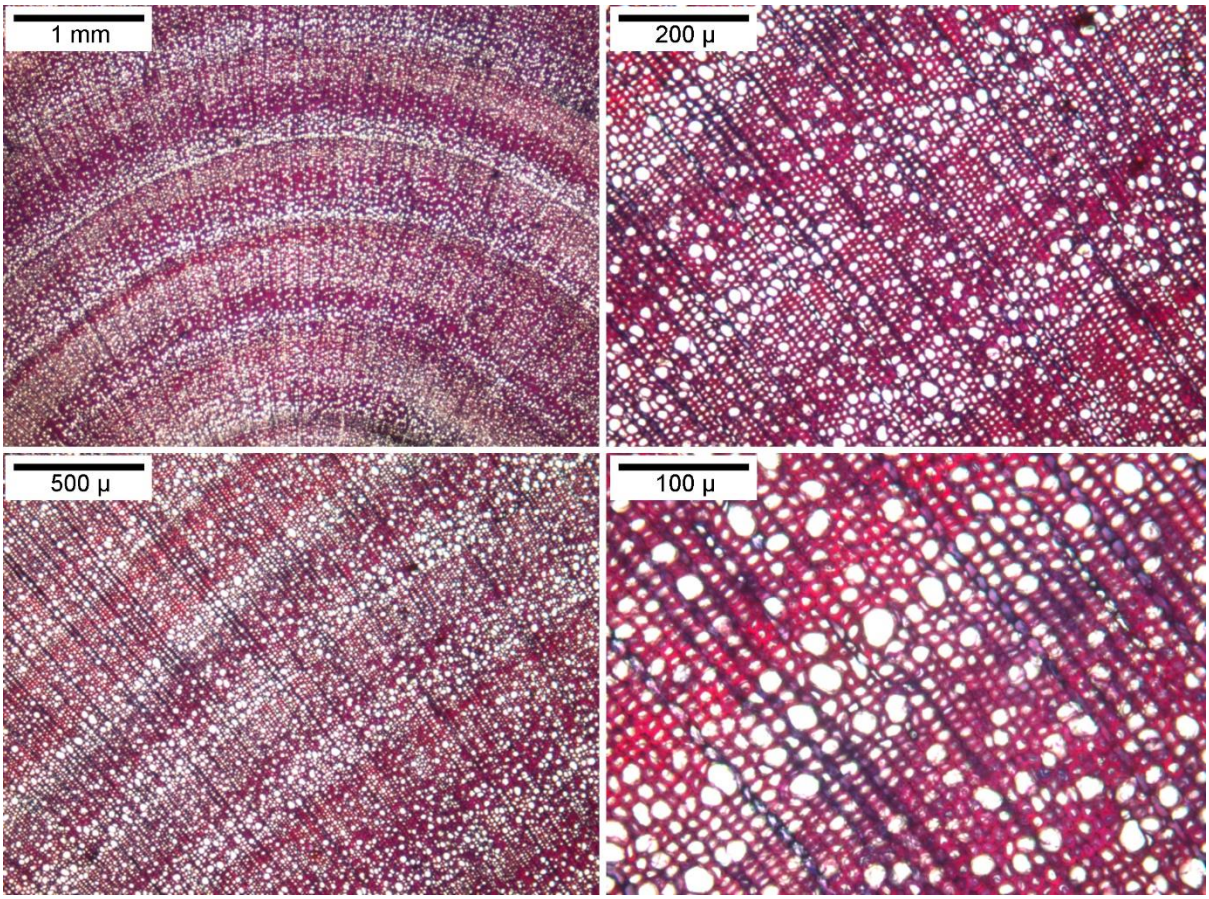

Fig. 36. Examples of wood anatomy of *H. irazuense*: ring boundaries were more or less clear depending on the size of vessels marking the limits of annual rings Presence of annual rings at 1 mm and 500 µ. Differentiation of earlywood and latewood at 200 µ and 100 µ.

4.3.2. Climate-growth relationships

Correlation and response functions are illustrated in Fig. 16, with significant values ($p<0.05$) being indicated with darker colored bars. The period considered for analysis is from 1978 to 2017 for precipitation and temperature. A significant positive correlation is observed between the residual tree-ring chronology and current January (0.39) precipitation (Fig. 37a), whereas a negative correlation exists with October (0.31) temperatures (Fig. 37b). The Chirripó National Park chronology is also negatively correlated with boreal winter (December through February) eastern Pacific SSTs, suggesting wider (narrower) rings during cold (warm) ENSO events (Figure 37c).

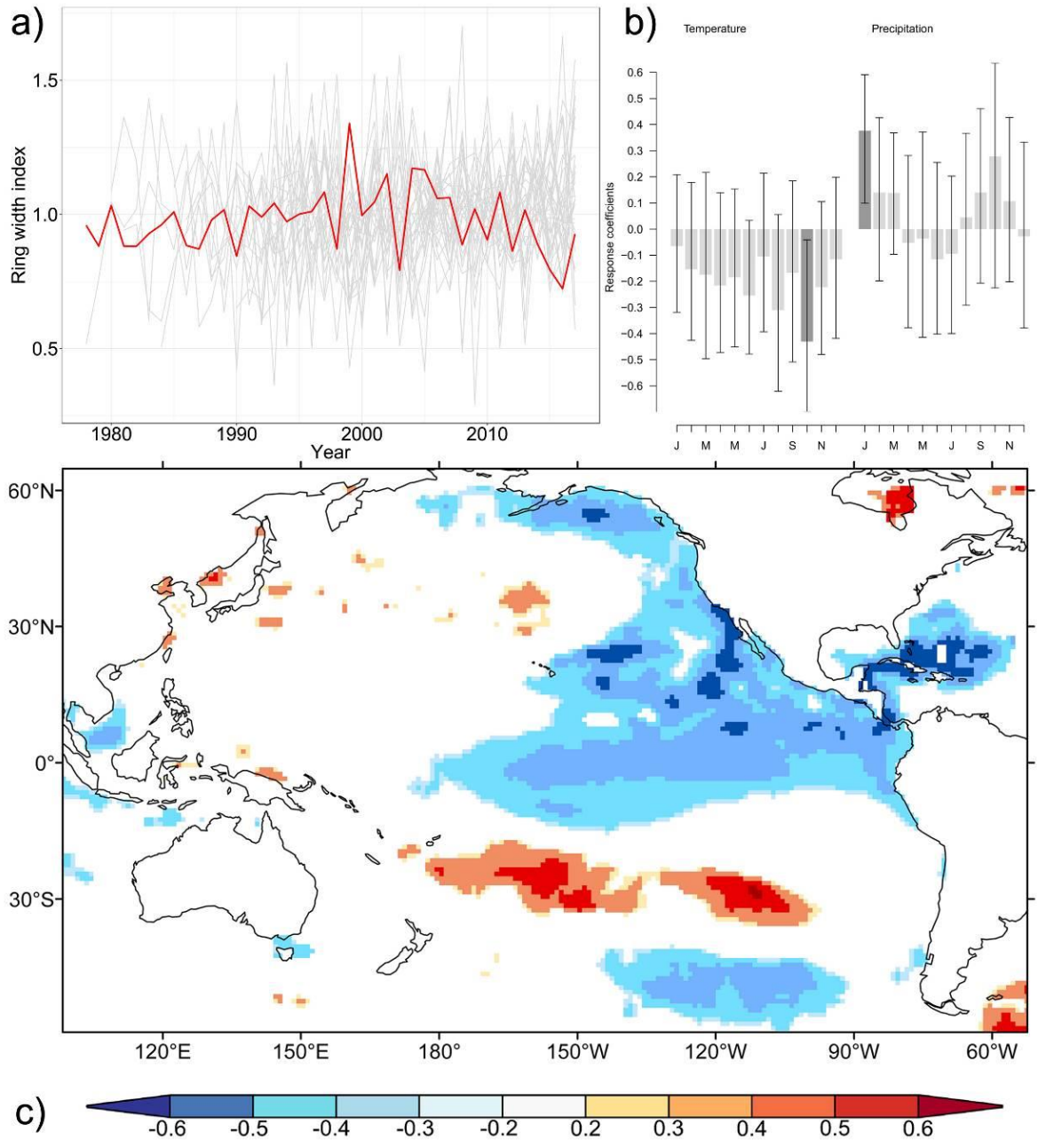

Fig. 37. a) Ring width series (light grey lines) and the residual chronology (red line) distributed over time; b) Residual master chronology correlation temperature-precipitation function; c) Spatial correlation between the residual ring width index and December SSTA.

The Structural Equation Model (SEM) yields results that are comparable with those obtained with the correlation and response functions. The AIC criterion supports the proposed AIC_{Ha}=31.01 against the null hypothesis (AIC_{Hn}=52.89). The best model supports a causal link between growth responses with calendar years, minimum temperature (MIT), annual precipitation (AP), as well as AP and Southern Oscillation Index (SOI) (Table 5). Results of the piecewise SEMs depict possible causalities between the studied variables (Fisher's C statistic = 1.01, p = 0.605) and confirm that

the SOI significantly affects AP and MIT. In turn, accordingly to the model, AP and MIT are significantly related to *H. irazuense* growth (Fig. 38). The effects of aspect (ASPEC), vicinity (VEC), slope (SLOP) and size (SIZE) did not apparently influence shrub growth significantly over the last 40 years; as a result, we do not therefore use them in the final SEM model.

Table 5. SEM coefficients estimates, standard error, and p-value. ***P=0, **P=0.01.

Response	Predictor	Estimate	Std error	p.value
resp	year	-0.9695	0.0084	0.0000 ***
resp	tmin	0.0533	0.0051	0.0000 ***
resp	ap	0.0207	0.0042	0.0000 ***
resp	size	0.0079	0.0078	0.3107
resp	aspec	-0.0040	0.0068	0.5597
resp	slop	0.0001	0.0076	0.9797
resp	vec	-0.0001	0.0079	0.9896
mit	soi	0.1560	0.02589	0.0000 ***
mit	year	0.0003	0.02880	0.9906
ap	soi	0.5398	0.0240	0.0000 ***
ap	year	0.0840	0.0267	0.0017 **

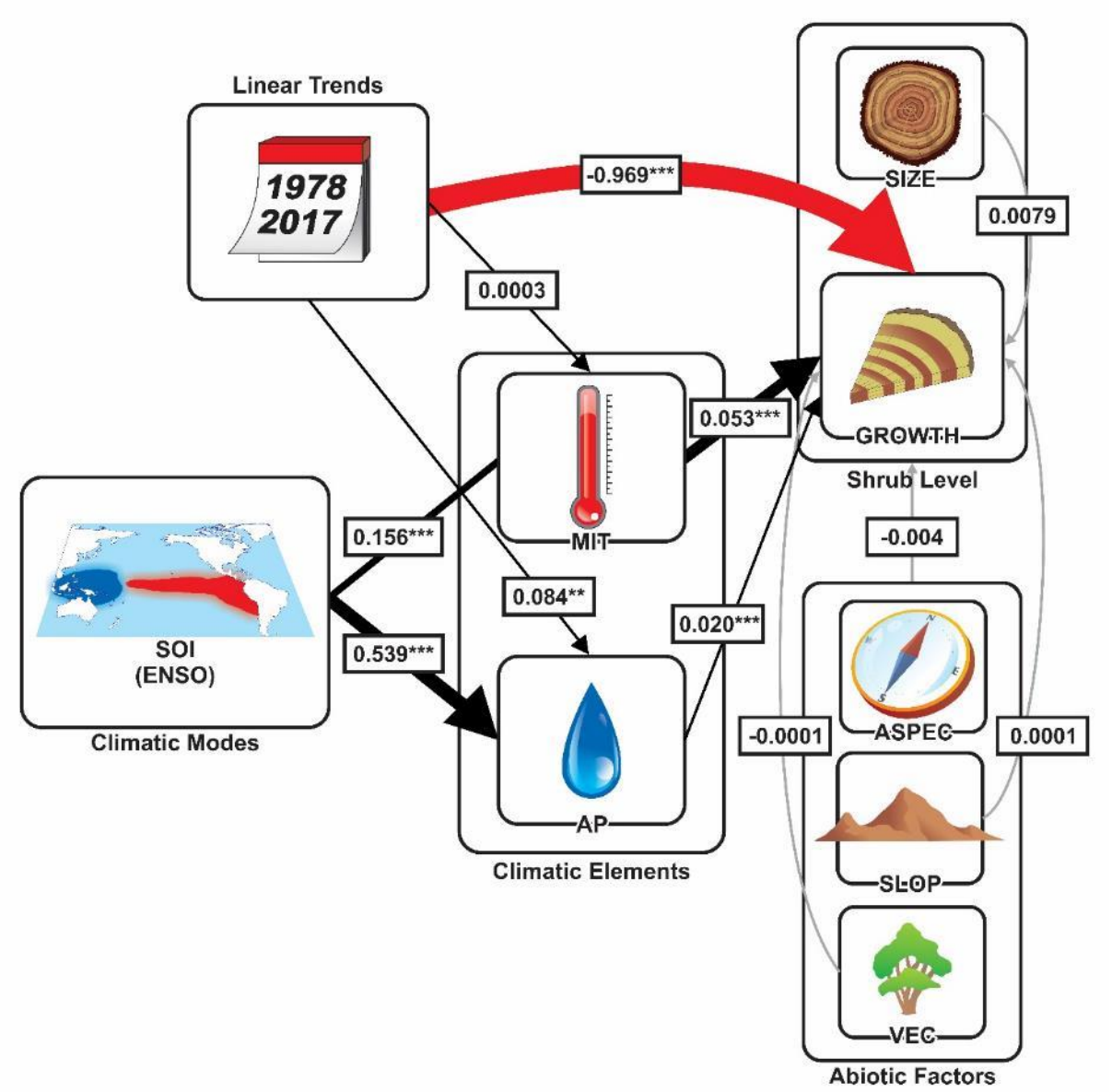

Fig. 38. Best supported Structural Equation Model showing significant paths (***P=0, **P=0.01) with the corresponding standardized parameters. Solid red arrow denote positive causal effects whereas solid black arrows point to weaker effects. Arrow thickness is proportional to the standardized parameters. Conditional R2 under endogenous variables are provided here as a measure of the goodness-of-fit. Legend: Cal_years – calendar years; SOI – Southern Oscillation Index; MIT – minimum temperature; AP – annual total precipitation; GROWTH – yearly basal area increment; VEC – vicinity with other shrubs; SLOP – slope angle; SIZE – size of shrub stems; ASPEC – slope aspect.

We observe significant positive correlations between ring widths and boreal winter as well as local dry season conditions. The full chronology shows distinct wide rings (1996, 2007, 2008, 2011, and 2012) in years during which excessively large rainfall totals were measured, either because of La Niña events and/or tropical storms. On the other hand, small rings – as recorded in 1992, 1995, 1998, 2003, 2010, and 2016 – occur in years that are known for El Niño events and droughts (Fig.

37a). Moreover, comparisons with locally available station data and gridded meteorological datasets suggested that one of the strongest controls of ring width variability in *H. irazuense* in the Chirripó National Park is in fact January precipitation (Figure 37b). Gridded SST data indicates that the Chirripó National Park chronology is also significantly and negatively correlated with boreal winter (December through February) eastern Pacific SSTs, favouring the formation of wider rings during cold ENSO (La Niña) events (Figure 37c).

4.4. Discussion

4.4.1. Factors controlling annual ring formation

The 39-year long shrub chronology of *H. irazuense* may seem short compared to other series built with full-sized trees, but nonetheless represents a significant output for tropical mountain regions and the highest elevations of Costa Rica in Chirripó National Park for which such records, and climatological data in more general terms, is scarce. These summit areas are unique features of Central American environments because they were molded by glacial dynamics during the Last Glacial Maximum (Quesada-Román et al., 2019), and the present páramo ecosystem represents a crucial hydrological and ecological niche of regional importance (Esquivel-Hernández et al., 2018). The mean sensitivity observed in our shrub chronology is consistent with tropical tree-ring studies realized in South East Asia (Rahman et al., 2017), Africa (Wils et al., 2009), and several sites in South America (e.g. Inga and del Valle, 2017; Layme-Huaman et al., 2018). The length of the chronology is of course shorter than what could be obtained with trees, but its length is not unusual at all for shrubs. Schweingruber and Poschlod (2005) reviewed herb and shrub ages of 914 species in Central Europe and conclude that in less than 10% of the cases species were older than 20 years.

SEM models are practical statistical tools to associate the different weights of variables and to understand their ecological relationships with tree or shrub growth (Boscutti et al., 2018; Madrigal-González et al., 2018). In this study, we could not find any significant statistical correlation in the SEM between shrub growth and variables such as slope, aspect, size, and/or vicinity. This can be explained by the fact that most of the slopes in this study are around 20° steep and east facing (150° of aspect). Despite the clear increase/decrease of growth during La Niña and El Niño years, annual ring size does not play a significant role in the SEM model. This same pattern applies for vicinity, a variable with a minor statistical association with shrub growth.

Our results indicate that annual ring formation of *H. irazuense* responds to the dry season which locally persists from December to April. During this time of the year, official meteorological records, although very limited in number (Fig. 34), indicate a very marked reduction in precipitation in the Chirripó National Park. It has been shown in previous work that temperature is not the principal predictor in annual ring formation in the tropics; instead, rainfall has repeatedly been demonstrated to have a great impact on annual ring growth (Fichtler, 2017). It is assumed that short dry periods (even as short as 10 to 21 days) may be effective triggers of growth periodicity in shrubs. Following this concept, the seasonality of growth has thus been suggested to reflect the effects of predictable, moderately long periods without rain during the ‘‘drier season’’ in tropical wet forests (Fichtler et al., 2003) making annual rings out of these growth layers. We argue that the conditions that are obviously favoring growth (and its cessation) in the *H. irazuense*

samples from the Chirripó National Park are comparable to those observed in *Cordia alliodora*, where growth is related to rainfall anomalies which in turn were controlled by ENSO phase (Evans and Schrag, 2004). Likewise, evidence exists that annual growth in moist tropical forest tree species is reduced by drought events such as those associated with strong El Niño events (Alfaro-Sánchez et al., 2017).

According to isotopic analysis, local rainfall in the Chirripó National Park is controlled primarily by the effective contribution of maritime moisture, especially from the Caribbean Sea, and therefore by the influence of northeast trade winds traveling over the central and southeastern Caribbean Sea (Esquivel-Hernández et al., 2019). Despite the great number of wetlands existing inside Chirripó National Park (Veas et al., 2018), precipitation and runoff seem to be the main contributors of groundwater dynamics and soil moisture (Esquivel-Hernández et al., 2018). As a result, any changes in or the absence of rainfall between December and April will likely and very directly determine interannual variations of growth ring formation in *H. irazuense*.

4.4.2. Climate-growth regional climatological insights

The correlation between the *H. irazuense* chronology (1978–2017) and Pacific SSTs is thought to reflect the influence of increased land surface temperatures. This is consistent with enhanced evapotranspiration and drought effects during El Niño events, and an increase of humid and rainy conditions during La Niña events over Central America and Costa Rica. These correlated conditions have been described previously in dendroclimatological studies performed on conifers from Guatemala (Anchukaitis et al., 2013; Anchukaitis et al., 2015), and broadleaved trees in Panama (Devall et al., 1995; Alfaro-Sánchez et al., 2017). Our results from the Chirripó National Park also agree with findings of different studies across the region in indicating that strong ENSO events associated with dryer and sunnier conditions result in reduced annual ring growth in both lowlands (e.g. Alfaro-Sánchez et al., 2017; Clark et al., 2018; Enquist and Leffler, 2001) and in tropical mountain forests/páramos (Anchukaitis et al., 2013; Anchukaitis et al., 2015).

In Costa Rica, Evans and Schrag (2004) used high resolution $\delta^{18}O$ measurements in tropical trees of the Guanacaste dry forest (*Cordia alliodora*) and the wet Caribbean evergreen forest (*Hyeronima alchorneoides*). In their study, they observed small, yet negative rainfall anomalies during ENSO warm-phase events, but could not define clear annual rings. However, high-resolution measurements reveal coherent isotope cycles that provide annual chronological control and paleoclimate information over the last century in mountain cloud forest areas of Costa Rica such as the Monteverde. Climate variability is dominated by the interannual variance in dry season moisture associated with ENSO events (Anchukaitis et al., 2008; Anchukaitis and Evans, 2010). Nevertheless, the authors also report a lack of clear responses in the species used (*Ocotea tenera* and *Pouteria sp*.).

In evergreen forests of La Selva Biological Station in the Costa Rican Caribbean lowlands, annual diameter increments of canopy and emergent tree species were studied between 1982 and 2016 and tree growth was negatively correlated with annual means of daily minimum temperatures and strong reductions were observed during El Niño events (Clark et al., 2018). Similarly, Enquist and Leffler (2001) derived growth records from *Capparis indica* and *Genipa americana* trees growing

in the Guanacaste dry forest and demonstrate that annual growth depends on annual and/or monthly variations in local precipitation and, in the longer term, on ENSO fluctuations.

Findings across the tropical forests of Central America are portraying a picture that is similar to what we observe in the shrubs sampled in the Chirripó National Park, i.e. a dependence of growth-climate relationships with El Niño events and droughts. In our case, small rings in the *H. irazuense* chronology occurred during years (1992, 1995, 1998, 2003, 2010, and 2016). That are known for moderate to very strong El Niño events based on the Oceanic Niño Index (ONI; Huang et al., 2017; NOAA, 2019), and related negative impacts on agricultural production, livestock and economy across Central America (Calvo-Solano et al., 2018). During La Niña years, *H. irazuense* tends to form wider annual rings, as these years tend to be generally wetter in the region in general, and in Costa Rica in particular. Years with wide rings in the *H. irazuense* chronology are 1996, 2007, 2008, 2011, and 2012, when the influence of tropical cyclones (between August and November; such as Hurricane Cesar in 1996, Tropical Storm Alma in 2008, and Tropical Storm Thomas in 2010) favored shrub growth at the study site (Amador et al., 2010).

4.5. Conclusions

Hypericum irazuense growing at high elevations in the Chirripó National Park of Costa Rica forms annual rings that can be successfully identified with microscopic analysis, thereby allowing successful cross-dating of sections taken from different individuals growing at the same site. Interannual (ENSO) variability in ring widths is influenced primarily by the absence of rainfall during the dry season which is locally lasting from December to April. The climate-growth relationship can be detected using both local meteorological observations as well as regional-scale gridded data. Collectively, our findings demonstrate that this species can be used in the future to characterize broadscale hydroclimatic variability and climate reconstructions in a region where climatological records remain scarce. After the successful dating of growth rings in *H. irazuense* and the assessment of climatic drivers of growth, we now call for the collection and dating of older shrub individuals at other sites of Costa Rica so as to extend climate reconstructions farther back in time.

CHAPTER 5

5. Dendrogeomorphic reconstruction of floods in a dynamic tropical river

Adolfo Quesada-Román [a,b,c], Juan Antonio Ballesteros-Cánovas [a,c], Sebastián Granados-Bolaños [b], Christian Birkel [b], Markus Stoffel [a,c,d]

[a] Climatic Change Impacts and Risks in the Anthropocene (C-CIA), Institute for Environmental Sciences, University of Geneva, Boulevard Carl-Vogt 66, CH-1205 Geneva, Switzerland
[b] Department of Geography and Water and Global Change Observatory, University of Costa Rica, 2060 San José, Costa Rica
[c] Dendrolab.ch, Department of Earth Sciences, University of Geneva, 13 rue des Maraîchers, CH-1205 Geneva, Switzerland
[d] Department F.-A. Forel for Environmental and Aquatic Sciences, University of Geneva, Geneva, Switzerland

Geomorphology 359, 107133. https://doi.org/10.1016/j.geomorph.2020.107133

Tropical regions are frequently affected by intense floods causing substantial human and economic losses. A proper management of floods and the prevention of disasters is, however, often hampered by a generalized paucity of systematic discharge measurements, which in turn renders any assessment of the frequency and magnitude of extreme floods challenging or impossible. Here, we analyze the suitability of trees impacted by floods and their growth-ring records to provide insights into past flood activity and to allow estimation of their magnitude. We base this exploratory study on the extreme floods triggered by the passage of tropical storm Nate on October 5, 2017 and investigate whether dendrogeomorphic approaches can be employed to date and quantify floods in the catchment of tropical Río General (Costa Rica). To this end, we sampled 91 trees showing scars in three river reaches and tested their potential to serve as paleostage indicators (PSI). High-resolution (0.5 m) digital surface and elevation models were then obtained with an Unmanned Aerial Vehicle to run a step-backwater hydraulic simulation aimed at defining flood peak discharge for which the mean squared errors between PSI heights and simulated water tables could be minimized. In a last analytical step, we investigated which hydraulic (i.e., Froude number, flow velocity) and fluvial landform characteristics explained deviations between scar heights and modeled water tables best by using a generalized linear model. Our analysis confirms that scarred trees can indeed be used for the reconstruction of past floods in tropical river systems and that the geomorphic position of trees will exert control on deviations between modeled water tables and scar height, with cut banks being most suited for scar-based flood reconstruction.

5.1. Introduction

Tropical mountain zones are densely populated, and land-use changes led to increased vulnerability to extreme weather-related hazards (Lawrence and Vandecar, 2015; Slaymaker and Embleton-Hamann, 2018). Land-use changes enhance stream water and sediment yields, changing sediment dynamics, bed and bank stability, and channel geometry (Wohl, 2006). The seasonally or perennially barotropic conditions that dominate tropical climates are the Intertropical Convergence Zone where the trade winds, cold fronts, cyclonic systems, and orographic uplift converge (Wohl, 2008). In addition, floods in the tropics behave as the combined interaction of land-use change and climatological dynamics associated with intense seasonal and extraordinary rainfall events (Syvitski et al., 2014). As a result of greater inputs and faster rates of change in the tropics compared to e.g., temperate regions, the hydrological processes that cause extreme streamflow events and flash floods are also accelerated (Wohl et al., 2012).

Flood assessments require accurate information on the spatial and temporal distribution of rainfall and on the resulting discharge (Baker, 2008). Such information is often scarce and of poor quality, even more so in tropical countries for which information on hydrological monitoring and measurements are often lacking completely (Wohl et al., 2012). The generalized lack of data availability calls for alternative approaches that allow adequate estimation of peak discharges of past flood events. In the days and weeks after a flood, flood marks left in the field can be used to estimate the extent and magnitude of a flood. Flood marks are, however, highly perishable and often disappear within a few months (Borga et al., 2008; 2014). Botanical indicators typically cover much longer time windows and can therefore serve as a relevant source of evidence to date floods and to quantify their magnitude in rivers with insufficient or nonexistent gauge records (Sigafoos, 1964; Ballesteros-Cánovas et al., 2015b). Thereby, woody plants are used as palaeoflood indicators on the basis of the "process–event–response" concept, in which a specific flood represents the "process" and the resulting tree disturbance is considered an "event" in the tree-ring series (Shroder, 1978; Wilhelm et al., 2019). Botanical evidence of past floods includes exposed roots, tilted trunks and mutilated branches of trees growing along river corridors (Gottesfeld and Gottesfeld, 1990, Stoffel and Wilford, 2012; Díez-Herrero et al., 2013). Scars in trees constitute the most reliable indicator of past floods as they allow precise dating of the event as well as a determination of water stages during floods (Gottesfeld, 1996; Ballesteros et al., 2011a, b).

The use of tree-ring records in river corridors has allowed the extension of flood records back in time in various rivers, but past research has focused mostly on temperate mountain environments (Sigafoos, 1964; McCoord, 1990; Ballesteros-Cánovas et al., 2015b; Wilhelm et al., 2019). In addition to "conventional" floods, tree-ring records have also been used to date ice jam (Smith and Reynolds, 1983; Lagadec et al., 2015) or lahar events (Franco-Ramos et al., 2020). After its initial application in North America, the approach has since been employed in various catchments of the Iberian Peninsula (Ruiz-Villanueva et al., 2013; Rodriguez-Morata et al., 2016), Central Europe (Zielonka et al., 2008; Ballesteros- Cánovas et al., 2015a; 2016), and the Himalayas (Ballesteros-Cánovas et al., 2017; Speer et al., 2019).

Some uncertainties, however, remain in the dendrogeomorphic assessment and interpretation of past floods. For instance, uncertainties still persist regarding the most suitable locations for the

sampling of scars that would allow the minimization of deviations between real and reconstructed flood heights (Ballesteros-Canovas et al., 2015a; Victoriano et al., 2018). In addition, despite substantial advances realized in the field of palaeoflood reconstructions, to our best knowledge, scars in trees have not been used so far to reconstruct floods in the tropics, probably because of inherent difficulties in correctly analyzing growth ring records from tropical trees (Silva et al., 2019).

In this paper, we therefore aim to test the suitability of tropical trees for the reconstruction of the magnitude of a recent extreme flood in Costa Rica that was caused by the passage of tropical storm Nate. The focus of this study is on channel segments of Río General, Costa Rica. We apply dendrogeomorphic approaches to study (i) the potential for tropical trees to record evidence of past floods, (ii) the effects of tree position on peak discharge reconstructions, so as to (iii) identify relations among as well as dependencies between hydrological and dendrogeomorphic variables in reconstructions, with the aim to inform future studies on how to improve sampling of trees for flood peak discharge reconstructions.

5.2. Study area

5.2.1. Geographic setting

Río General (or General River) has a length of 23 km for a catchment size of 316 km^2, with a channel slope of 8.22°, and a mean annual bankfull discharge (1970-2019) of 222 m^3/s. Río General is one of the main tributaries of the Térraba River, the largest catchment of Costa Rica (Quesada-Román and Zamorano-Orozco, 2019a; Camacho et al., 2020). The river drains the Pacific slopes of the Cordillera de Talamanca and has its source at the highest peak of the country (Quesada-Román et al., 2019b), Cerro Chirripó (3,810 m asl), and flows into the Térraba River at 800 m asl, thus covering an altitudinal range of >3 km. The three reaches of the Río General investigated in this study have mainly braided channel morphologies that consist primarily of cobbles and boulders and are located around the central coordinates 9.432 °N and -83.638 °W (Fig. 39). The tree sites are representative of the larger study region and show a high density of scarred trees suitable for dendrogeomorphic analyses: whereas site A is located in the Buenavista tributary of Río General, sites B and C are found in the Chirripó Pacífico tributary.

Vegetation is composed mostly of tropical premontane rainforests with evidence of deforestation (slash-burning) and landscape fragmentation dating back to the 1950s. Even if anthropogenic changes continued into mid-1980s, deforestation locally reached its peak during the 1960s and 1970s. In 1996, a deforestation ban was put into force. Together with the rise of ecotourism and the development of more sustainable production alternatives, this ban has contributed to the recovery of the ecosystem (Kappelle, 2016; Krishnaswamy et al., 2018).
According to the National Forestry Inventory, the average square hectare in this region contains 16 species with a mean diameter at breast height (DBH) of 20.8 cm, as well as at least 40 individuals with a DBH >10 cm. According to the same data, mean Stand Basal Area (SBA) corresponds to 1.64 m^2 (REDD/CCAD-GIZ - SINAC, 2015).

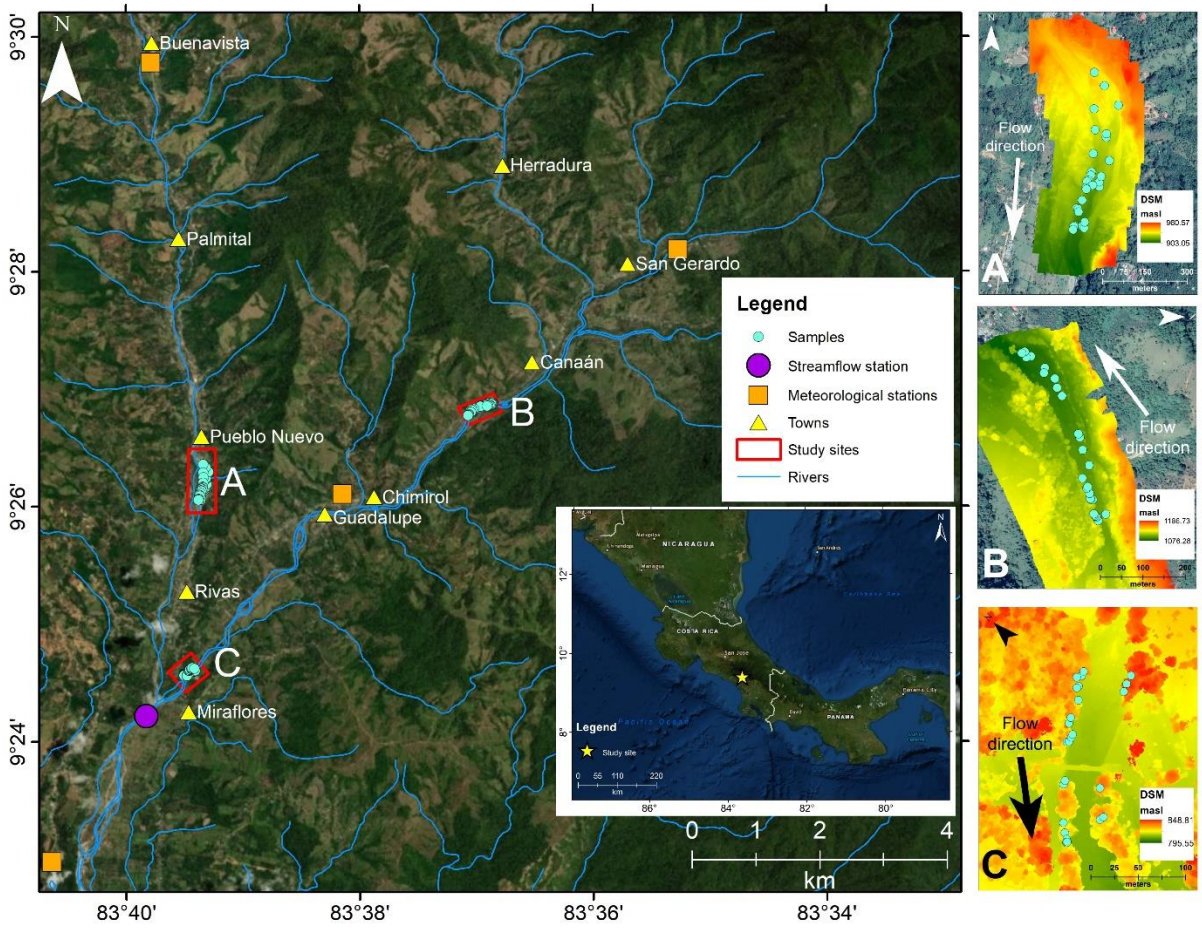

Fig. 39. Location of the three study reaches (A, B, and C) within the Río General catchment, streamflow station, meteorological stations, towns and drainage network. The right panels present the Digital Surface Models derived from Unmanned Aerial Vehicle photogrammetry as well as the location of trees sampled.

5.2.2. Climate characteristics and tropical cyclone activity

The latitudinal migration of the Intertropical Convergence Zone (ITCZ), the El Niño Southern Oscillation (ENSO), northeast trade winds, cold fronts, and tropical cyclones influence the local climate and precipitation patterns (Alfaro et al., 2010; Campos-Durán and Quesada-Román, 2017). Annual rainfall totals typically reach 3000–5000 mm in the region with two distinct rainfall maxima, one in May and a second, more distinct rainfall peak in October. In July and August, rainfall decreases during two to four weeks, known as the Mid-Summer Drought (Maldonado et al., 2016; Quesada-Román, 2017). About 85% of the annual rainfall occurs between May and November (rainy season) with a distinct dry season from December to April. Annual average temperatures range between 18 and 22°C at the study site (Quesada-Román and Zamorano-Orozco, 2018; 2019b).

Floods can be favored by intense local convection, but historically the most severe floods were triggered by tropical cyclones. The 2017 North Atlantic hurricane season was very active, with

anomalously warm sea surface temperatures in the tropical Atlantic and neutral-to-colder La Niña conditions in the tropical Pacific (NOAA, 2019). Normally, these conditions are favorable to the formation of hurricanes in the Atlantic basin (Goldenberg et al., 2001). The focus of this study is on tropical storm "Nate" because it caused an extreme discharge event in the General River catchment. Nate originated from a large area of low pressure in the eastern Pacific ITCZ and over Central America that gradually developed in early October (Papin et al., 2017; Beven and Berg, 2018).

Tropical cyclones are one of the main triggers of floods in General River and produce events every nine years on average. Historical discharges have increased gradually between Hurricane Joan in 1988 (597 m^3/s), Hurricane Cesar in 1996 (~650-700 m^3/s), and Tropical Storm Alma in 2008 (756 m^3/s; Cervantes-Cordero, 1999; ICE, 2018). Prior to the passage of Nate, Costa Rica already experienced intense rainfall for over two weeks under the influence of the ITCZ. These conditions of antecedent soil wetness in combination with intense and prolonged rainfall during the passage of Nate (200–500 mm) triggered floods and landslides across the country (CNE, 2018). At the study site, between 300–400 mm of rainfall had been recorded between October 4–8, 2017 (Beven and Berg, 2018), resulting in an observed discharge peak of 947 m^3/s. The 2017 Río General flood lasted from October 4–10 and had a total flow volume of 124 Hm^3 (ICE, 2018). Nate impacted 85% of the Costa Rican territory with widespread landsliding and flooding, causing 11 fatalities and economic losses of US$ 578 million (CNE, 2018), or 1.3% of the Gross Domestic Product (Brenes and Girot, 2018).

5.3. Materials and methods

5.3.1. Experimental work and dendrogeomorphic techniques

We surveyed a total of 91 scarred trees at three different study reaches of the Río General in January 2018, i.e., only two months after the passage of Nate and the flood event (Fig. 40). In the field, we only sampled scars that could be attributed clearly to past flooding to avoid any biases for the subsequent peak discharge reconstruction (Ballesteros-Cánovas et al., 2015a). Criteria used for the selection of scars were defined as follows: scars (i) were inflicted by the flood triggered by Nate, (ii) had to face the direction of flow, and (iii) had to exhibit a shape typical of flood impacts (Sigafoos, 1964; Hupp, 1988; Ballesteros-Cánovas et al., 2011a).

All scars fulfilling these criteria were considered as paleostage indicators (PSI), their position recorded with a Global Positioning System (GPS; precision of <1 m) and scar height with respect to the channel measured as the central height of the injury from tree base (Ballesteros-Cánovas et al., 2011b). In addition, a preliminary geomorphic map was derived from images obtained with Unmanned Aerial Vehicle (UAV) High Resolution Photogrammetry, with the aim to identify different fluvial landforms at the study sites (Smith et al., 2011). In a further step, we classified trees according to their geomorphic position (Leopold et al., 1995; Wheaton et al., 2015) within the floodplain. To this end, we classified tree positions according to their location on cut bank (CB), point bar (PB), and straight channel (SC) segments within the study reaches (Fig. 40).

Fig. 40. Representative scarred tree individuals affected by the flood triggered by Tropical Storm Nate on point bars of Site A (a) as well as on cut banks of Sites A and C, respectively (b, d). Example (c) characterizes scarred trees growing in a straight channel of Site B.

5.3.2. Hydraulic modelling, peak discharge estimation and regression analysis

The two-dimensional (2D) hydrodynamic model IBER (www.iberaula.es) was used to model water depth, Froude number, and flow velocities of the flood event of 2017. IBER simulates turbulent-free, unsteady surface flows and environmental processes in rivers by solving depth-averaged 2D shallow water equations (2D Saint-Venant) using a finite volume method with a second-order roe scheme (Cea et al., 2019). This approach is particularly suitable for flows in mountain streams where shocks and discontinuities can occur, and where flow hydrographs tend to be flashy. The method is conservative, even in cases where wetting and drying processes occur. The model works in a non-structured mesh consisting of triangles or quadrilateral elements. In our study, we used high resolution UAV elevational data obtained from digital imagery. A Structure from Motion (SfM) approach was applied to obtain georectified orthomosaics and digital elevation models (Turner et al., 2012). Digital images were obtained with a DJI Phantom 4 Pro V2 drone. The photogrammetric reconstruction of the fluvial environments for hydraulic modelling and point cloud classification was realized using Agisoft Photoscan 1.4.0 so as to generate precise elevation models for environmental analysis (Langhammer and Vackova, 2018).

Bed friction was evaluated in the field with Manning's *n* roughness coefficient considering homogenous roughness units (Chow, 1959). We used a Manning's *n*=0.075 for the main channel, 0.16 for the forest, and 0.08 for those sectors with sparse vegetation (Barnes, 1967; Arcement and Schneider, 1989). To compute the inlet water discharge (i.e., steady flow regime), velocity and Froude number (Fr) into each study reach, we thereafter modeled successive inlet discharges based on historical extremes (using steps of 100 m^3/s up to 1500 m^3/s). Peak discharge of the 2017 flood was simulated with an iterative step-backwater procedure and consisted of a (i) calculation of water stages from modeled peak discharges and (ii) a fitting of resulting modeled water surfaces with PSI heights identified in the field (Webb and Jarrett, 2002). For more robust flood discharge estimations, we then calculated the mean squared error (MSE) of each modeled discharge output against every scar height. The magnitude of the flood event in each river reach was then defined as the peak discharge for which the MSE between the model and scar heights was smallest (Fig. 41).

Thereafter, we analyzed combinations of hydraulic and geomorphic characteristics for which the MSE between modeled flow heights and scar heights was smallest at the level of individual trees. We therefore applied a least squares regression analysis to calculate peak discharges at each of the three study reaches. With the help of a generalized linear models (GLM), we then described the MSE of each tree statistically by adding the Froude number (as an indicator of flow regime) and the geomorphic position (or landform) of trees at each site (A, B, and C). To this end, all variables were transformed into z-scores. The Akaike Information Criterion (AIC; Anderson and Burnham, 2004) was used in a backward selection to contrast the full hypothesis
MSE ~ Froude × (Landform + Site), for which an interaction between the hydraulic and landform variables is defined, against the alternative hypothesis, where only landform is considered: *MSE ~ Landform + Site.* Model parameters were then used to evaluate the weight of each co-variable to define the most suitable landform for tree sampling in (tropical) mountain rivers.

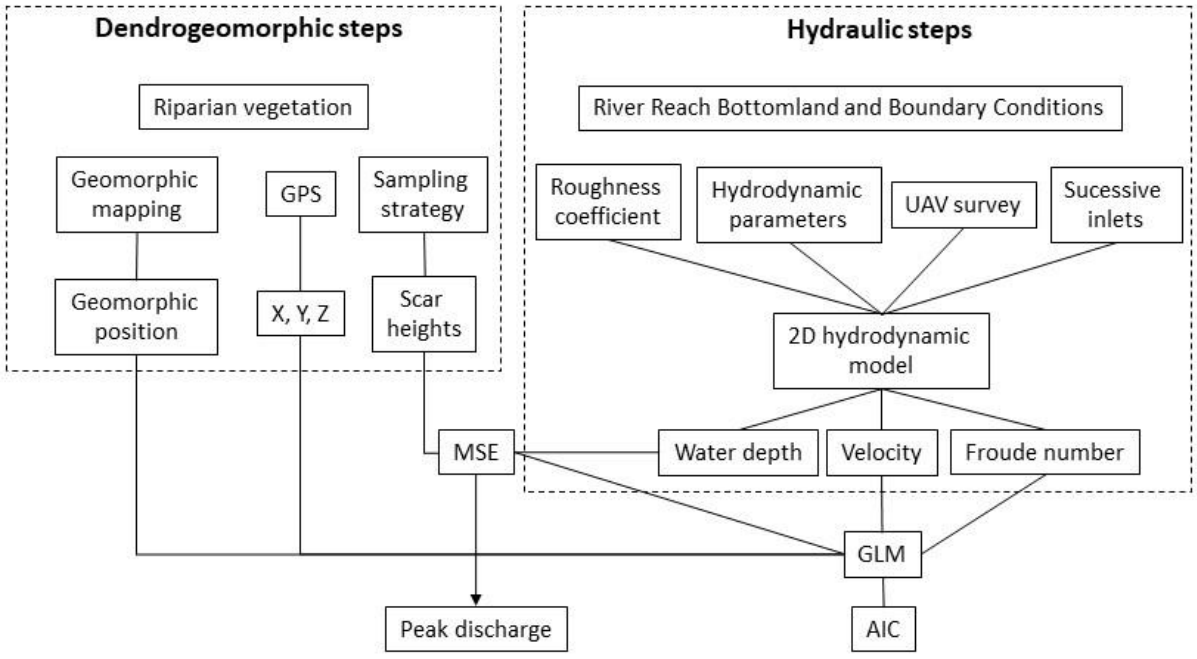

Fig. 41. Methodological diagram used for the assessment of locations that are best suited for palaeoflood discharge reconstruction.

5.4. Results

5.4.1. Peak discharge reconstruction based on scars in tropical trees

A total of 91 trees showed visible scars that were inflicted by sediment and wood transported during the flood triggered by tropical storm Nate; 29 scars were identified in sector A, 31 in B, and 31 in C. Mean scar heights were similar for all trees that were considered for peak discharge reconstruction with 2.32 m ($\sigma = 0.76$, Table 6). On average, the highest scar heights were recorded in reach B (2.57 ± 0.731 m above the channel bed), whereas the lowest scar heights were found in reach C (2.15 ± 0.784 m). The positions of scarred trees with respect to cut banks (CB), point bars (PB) and straight channels (SC) are presented in Table 6.

Table 6. Characteristics of the scars used as paleostage indicators (PSI) for each of the study reaches. Abbreviations: MSE — mean squared error; SC — straight channel; PB — point bar; CB — cut bank.

Study reach	Scars in trees	Scar heights (m)	MSE	Tree positions (%)
A	29	2.25 ± 0.70	1.46	SC = 41, PB = 21, CB = 38
B	31	2.57 ± 0.73	1.64	SC = 29, PB = 19, CB = 52
C	31	2.15 ± 0.78	2.10	SC = 38, PB = 21, CB = 41

The hydraulic model points to differing hydraulic conditions prevailing at the three sites during the 2017 flood induced by tropical storm Nate (Fig. 42). Site A presents a peak discharge of 636 m^3/s ($\sigma = 0.16$) with a mean water depth of 1.87 m, an average velocity of 2.37 m/s, a mean Froude number of 0.54, and absolute deviations between modeled flow heights and scar heights ranging from -2.27 to 2.79 m. Site B shows a peak discharge of 455 m^3/s ($\sigma = 0.24$) with a mean water depth of 2.33 m, an average flow velocity of 2.35 m/s, a mean Froude number of 0.70, and absolute deviations between modeled flow heights and scar heights of -3.01 to 3.30 m. Site C has a peak discharge of 1249 m^3/s ($\sigma = 0.43$) with a mean water depth of 3.18 m, an average flow velocity of 2.23 m/s, a mean Froude number of 0.43, and absolute deviations between modeled flow heights and scar heights between -2.86 and 2.57 m. The reconstructed high flows correspond with observations at the gauging station at which a discharge of 947 m^3/s was measured.

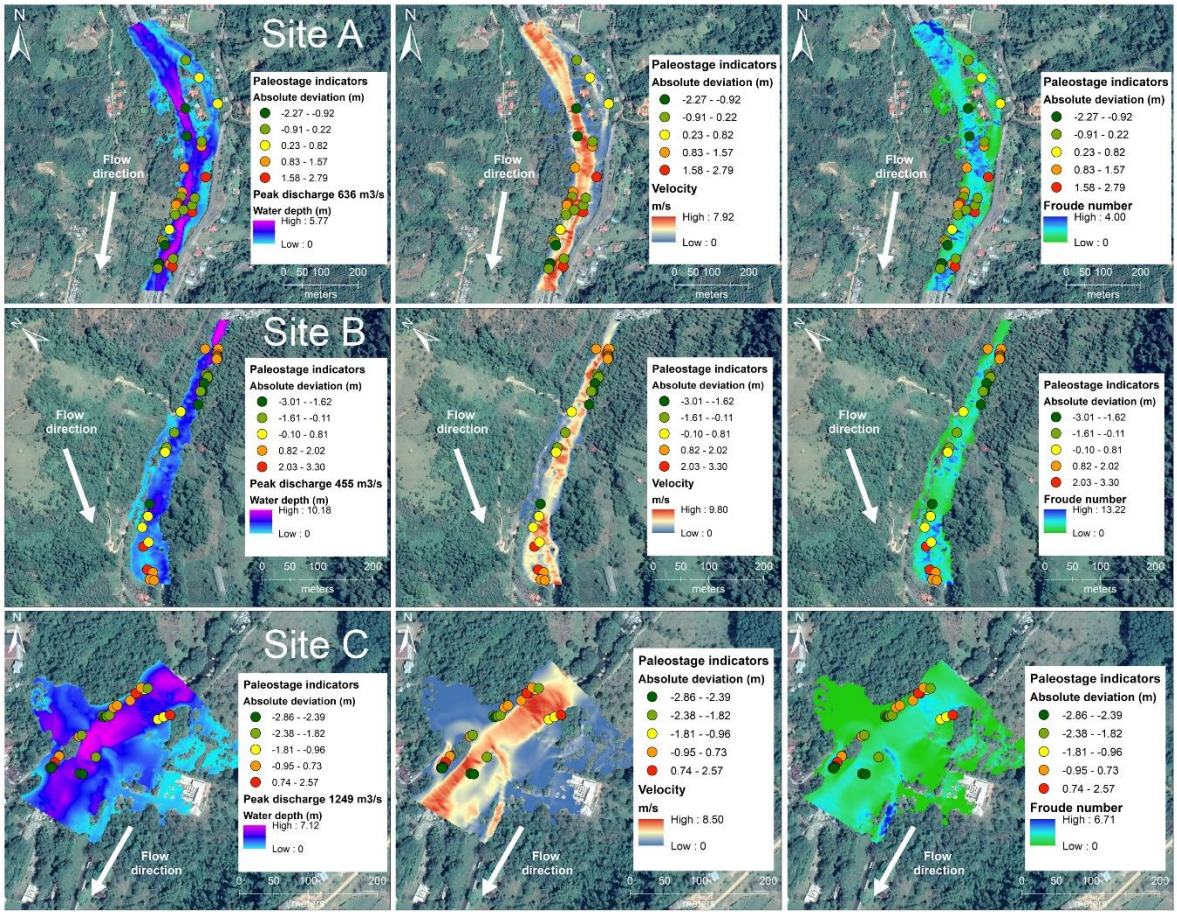

Fig. 42. Absolute deviations (in m) of PSI as observed on tree trunks and modeled with Iber, as well as their relationship with water depth, flow velocity, and Froude number at study reaches A, B, and C of the Río General.

5.4.2. Fluvial and dendrogeomorphic factors controlling deviations between field and model data

Statistical analyses of the average mean squared error between the reconstructed and modeled flood peak discharge were analyzed with the AIC criterion. Our results support the alternative model with AIC_{Ha}=31.65 against the null hypothesis (*MSE ~ Froude × (Landform + Froude) × Site*; AIC_{Hf}= 32.16) and suggest that the best generalized linear model supports an interaction between the geomorphic position of sampled trees and study reach (*MSE ~ Landform + Site*). Table 7 provides the model parameters, but also indicates that the most significant influence on flood peak discharge probability is given by the straight channel as well as Site B and C, as shown by the z-ratio tests of parameter estimates.

Table 7. Parameters used to model peak discharge of the 2017 flood. The residual standard error is 0.15 on 77° df, the multiple R-squared is 0.62, and the AIC is 34.86. Pr(>jzj) is the probability of finding the observed Z-ratio in the normal distribution of Z with a critical point of jzj. ***P=0.001 and *P=0.05.

Model terms	Estimate	Std. Error	t value	Pr(>|t|)	
(Intercept)	1.30	0.03	35.38	<0.001	***
Landform PB	0.06	0.05	1.34	0.18	
Landform SC	0.09	0.04	2.24	0.02	*
Site B	0.45	0.05	10.63	<0.001	***
Site C	0.35	0.04	8.21	<0.001	***

Results also show that trees scarred at cut banks have the smallest MSE (~1.52) and best fit with peak discharge reconstructions, whereas for scars in trees located at point bars (~1.78) generally exhibited larger MSE and can thus be considered less reliable for peak discharge reconstructions based on dendrogeomorphic evidence (Fig. 43).

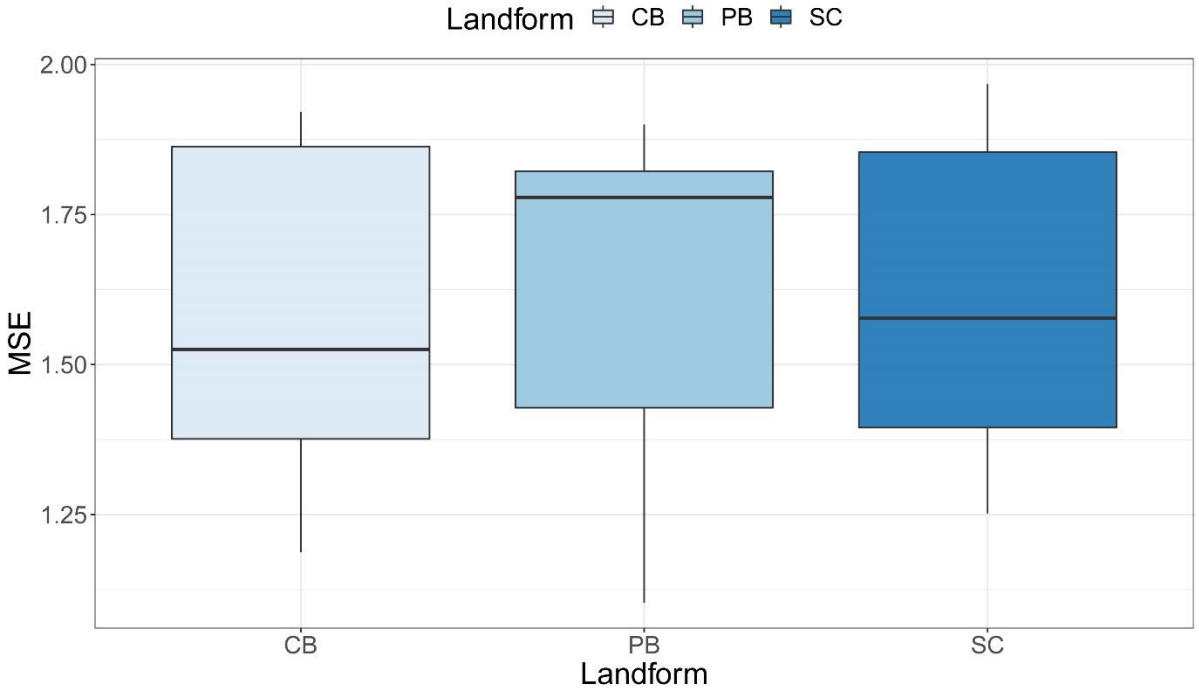

Fig. 43. Boxplots with calculated mean squared error between observed (scars) and modeled peak discharge as a function of geomorphic position of trees. CB–cut bank; PB–point bar; SC–straight channel.

In line with the GLM, the relation of the Froude number with the MSE varied with geomorphic position (Fig. 44). Point bars showed an increase of MSE as the Froude number increases, whereas in the case of straight channels, no such tendency could be found. At cut banks, MSE decreased with increasing Froude numbers. The geomorphic position also influences modeled flow velocity and shear stress. As such, point bars often show the smallest flow velocities and shear stress but are also more easily transformed or destroyed during the flood. In the case of straight channels, morphology constantly changes during floods as well. In addition, the highest velocity and shear stresses are found within the main channel where trees are not commonly present. Cut banks are

characterized by strong flow velocities and shear stress as well, but the intermittent, progressive erosion still favors tree growth on river banks, rendering these ideal sites to sample flood scars in trees.

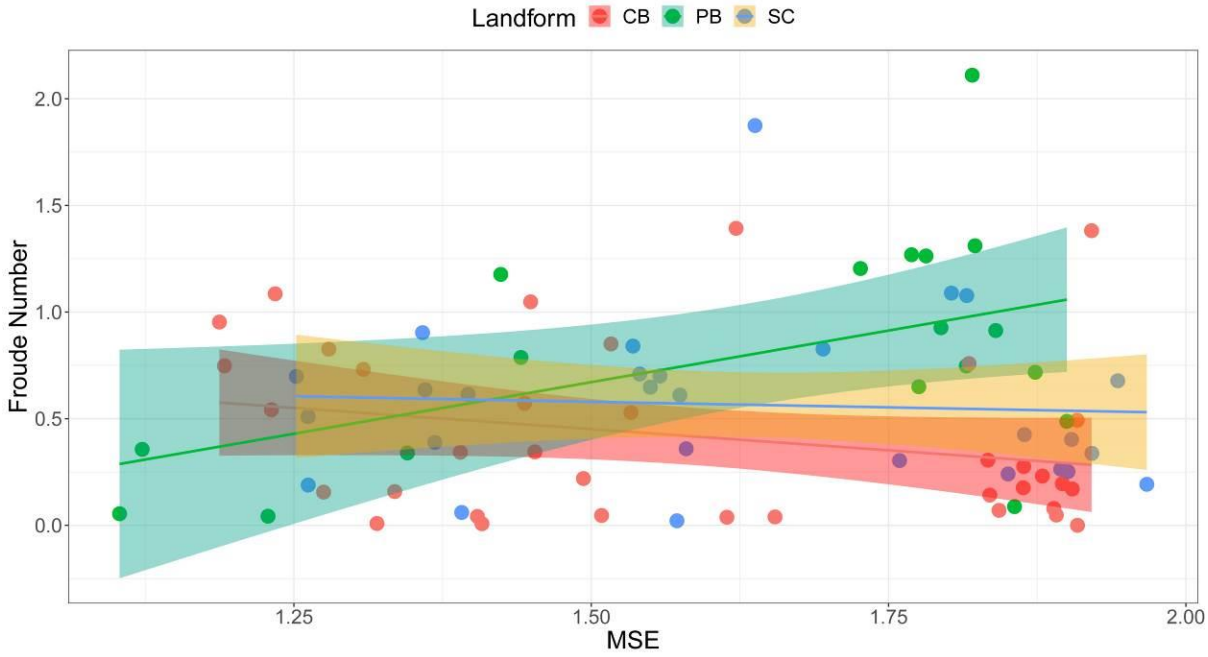

Fig. 44. Relation between Froude number and calculated average mean squared error depending on the geomorphic position (cut bank, straight channel, point bar) of trees with scars.

5.5. Discussion

In this contribution, we provide a scar-based flow discharge reconstruction for three floodplain sections of the General River, southeastern Costa Rica. In particular, we analyzed 91 trees with clear flood-induced scars and used a 2D hydraulic model run on a highly-resolved topography to estimate peak discharge of the extraordinary 2017 flood triggered by the passage of Tropical Storm Nate in October 2017. Moreover, we investigated the role of relative tree positions on the quality of flow discharge reconstructions and searched for ways to reduce deviations between modeled and reconstructed peak discharges.

5.5.1. Methodological uncertainties

In regions where baseline data on floods are lacking, one must limit all other sources of possible uncertainties to obtain the best results. One such possible source of uncertainties is related to topography on which hydraulic models are run. In this study, good precision of hydraulic models could be achieved thanks to the use of high-resolution orthoimages obtained from UAV photogrammetry (Perks et al., 2016). Based on the highly resolved topography, the MSE between modeled water stages and the height of scars could be limited to 1.25 m on average between the three reaches analyzed. These results are comparable to those obtained at sites in Poland based on the same 2D-hydraulic model (~0.8 m; Ballesteros-Cánovas et al., 2016). Yanosky and Jarrett (2002) observed deviations ranging from -0.6 to 1.5 m in a high-gradient stream, whereas

Gottesfeld (1996) obtained 0.196 ± 0.03 m error variations in low gradient rivers of British Columbia. Similarly, Victoriano et al. (2018) determined a MSE of 0.35 m using a total station and a 1D hydraulic model in a single mountain stream in Spain. Other studies have reported deviations similar to those obtained in our study, despite the fact that differential GPS (Ballesteros-Cánovas et al., 2011a) or terrestrial laser scans (Ballesteros-Cánovas et al., 2011b) were used in these cases. On the other hand, a MSE exceeding >1.5 m was obtained for a stream in Bhutan for which high-resolution topographic data was missing (Speer et al., 2019). Interestingly, Garrote et al. (2018) reported MSE exceeding 2 m at a site of the Canary Islands, Spain, and with flow magnitudes (1235 m^3 s^{-1}) comparable to those at our study sites. According to Webb and Jarret (2002) and Ballesteros-Canovas et al. (2011b), the creation of impact scars by large wood transported that is partially submerged in the flood flow could explain these deviations in peak discharge. Such dynamics have indeed been observed and documented in tropical channel reaches with high stream power (Cadol et al., 2009), also in relation with tropical cyclones (Wohl et al., 2019). During tropical (flash) floods, wooden logs are easily fragmented into pieces and may crash against standing trees (Cadol and Wohl, 2010).

5.5.2. Reliable geomorphic locations of trees

One of the main weaknesses of dendrogeomorphic approaches is the substantial time required for an exhaustive sampling of a site and geomorphic process (Mainieri et al., 2019). Therefore, it seems essential to identify the landforms for which scar heights in trees deviate least from modeled flow heights. As previously speculated by Ballesteros-Cánovas (2011a), we confirm that the geomorphic position of trees is the main factor explaining deviations between models and field observations. It is also known that mean heights of scars in trees located in overbank positions are smaller than scar heights in trees standing within the main channel (Gottesfeld, 1996; Yanosky and Jarret, 2002). More recently, Victoriano et al. (2018) found that landforms characterized by intermediate energy, such as alluvial terraces, are more reliable for a sampling of scars to estimate peak discharge, as riparian vegetation growing in such a context would have a better biogeomorphic resilience against streambank erosion (Abernethy and Rutherfurd, 2001; Stallins and Corenblit, 2018). Field observations confirm that smaller floods modify or erode point bars and straight channels morphologies and their vegetation more easily (Simon and Collison, 2002; Polvi et al., 2015). Our results indicate that trees standing on point bars and in straight channels are affected by higher flow velocities and Froude numbers in the model. A systematic sampling of scars in trees located in more stable landforms, such as cut banks, could reduce significantly the time needed in dendrogeomorphic studies and also improve results.

5.5.3. Implications for flood risk reduction on tropics

Despite the inherent uncertainties of the method, our assessment provided a peak discharge reconstruction for a flood of the Río General that was triggered by the passage of Tropical Storm Nate in October 2017. The reconstructed peak discharge is in the same order of magnitude as the values obtained by the Electricity Institute of Costa Rica on October 4, 2017 (947 m^3/s), and therefore confirms the suitability of dendrogeomorphic techniques to reconstruct past floods and their magnitude with trees in the tropics. However, the study could have benefitted further from additional post-event surveys that would have helped to reduce the remaining uncertainties that are inherent to flood reconstructions (Wilhelm et al., 2019). The approach used in this study should

be replicated in other tropical catchments as an improved understanding of peak discharge in catchments without or with very limited meteorological and/or flow discharge data will always be of paramount importance to increase resilience of local inhabitants and/or to improve infrastructure crossing rivers (i.e., bridges) and flood zoning. Even if tropical areas count for only 19% of the global land surface (Peel et al., 2007), they host between 40-50% of the global population (Tatem, 2017). This is even more relevant as emerging countries and smaller economies located in the tropics also often face more difficult economic situations after a disaster and during recovery (Noy, 2009). The practical dendrogeomorphic approach presented here can be a means to improve flood area zonation and thereby assist in the development of more detailed flood hazard and risk maps.

5.6. Conclusions

In this study we have shown that peak discharge of a recent flood in a poorly gauged tropical mountain catchment can be estimated with dendrogeomorphic techniques if coupled to a 2D hydraulic model and channel topography derived from UAV photogrammetry. As the first study of its kind in the humid tropics, this publication thus expands the geographic scope of tree-ring based hazard analysis. The approach presented here did not only provide results on past peak discharge with limited uncertainly, but also yielded valuable data on flood dynamics that will help to improve our understanding of flood processes in tropical regions. We also find that future research should focus on trees on cut banks or on terraces where deviations between modeled and observed flow heights are minimal. At the same time, we recommend that impacted trees growing on alluvial bars or within straight channel reaches should not be sampled in the future. By limiting differences between reconstructions, direct observations and model outputs, we conclude that dendrogeomorphic approaches are becoming an increasingly important tool for disaster risk reduction and territorial management decisions in (tropical) regions where data on past events are scarce or rather unreliable.

CHAPTER 6

6. Improving regional flood risk assessment in mountain catchments impacted by tropical cyclones

Adolfo Quesada-Román [a,b], Juan Antonio Ballesteros-Cánovas [a,c], Sebastián Granados-Bolaños [b], Christian Birkel [b], Markus Stoffel [a,c,d]

[a] Climatic Change and Climate Impacts, Institute for Environmental Sciences, University of Geneva, Boulevard Carl-Vogt 66, CH-1205 Geneva, Switzerland
[b] Department of Geography and Water and Global Change Observatory, University of Costa Rica, 2060 San José, Costa Rica
[c] Dendrolab.ch, Institute for Environmental Sciences, University of Geneva, Boulevard Carl-Vogt 66, CH-1205 Geneva, Switzerland
[d] Department F.-A. Forel for Environmental and Aquatic Sciences, University of Geneva, Geneva, Switzerland

Submitted to Journal of Hydrology: Regional Studies

Floods are a frequent hazard causing disasters in the tropics mainly due to extraordinary precipitation events such as tropical cyclones. Coping with future flood disasters requires a better understanding of the frequency and magnitude of past flood events. However, many tropical countries are characterized by scarce systematic and long-term discharge data to derive peak discharges. Here, we aim to develop a regional flood-frequency analysis to determine flood risk for Térraba catchment (4765 km^2) in southern Costa Rica. We firstly performed a regional dendrogeomorphic analysis to estimate historical peak discharges during tropical cyclones in seven ungauged sections of the catchment. Such estimates were then incorporated into a regional flood-frequency analysis (RFFA) using eight hydrological stations with discharge data from 1962 to 2019 deriving flood quartiles. We used the 10-year return period because it is a reliable recurring order associate with the impact of tropical cyclones in this region. Moreover, we combined this flood quartile with the Topographic Wetness Index (TWI) to determine flood hazard at the catchment scale along the hydrogeomorphic floodplains. The flood risk assessment was then based on high-resolution infrastructure mapping, population density information (i.e. exposure), and a social development index (i.e. vulnerability). Tropical cyclones peak discharges through flood-frequency and dendrogeomorphic records are useful outputs to determine the frequency and magnitude of flood events in poorly gauged catchments. We demonstrate that regional flood risk assessments in large scale catchments are feasible using coarse and detailed inputs. About 5585 inhabitants are located in the flood-prone areas of the Térraba catchment within different risk conditions. Furthermore, our results agree with impacted regions in the past by tropical cyclones floods. Our results will be useful for the design of future flood risk strategies promoting resilience of the local population in the Térraba catchment and also provide potential to be used in other tropical catchments.

6.1. Introduction

Tropical regions have faced land-use changes, especially in the last century, that promote an increased vulnerability to extreme weather-related hazards (Lawrence and Vandecar, 2015; Carabella et al., 2020). Land-use changes dynamize sediment yields and riverscapes variations in different time scales and intensities (Wohl, 2006; Piacentini et al., 2020). Tropical climates are controlled, among others, by the Intertropical Convergence Zone, trade winds, cold fronts, cyclonic systems, and orographic effects (Wohl, 2008). In addition, the interaction of land-use changes and climatological dynamics associated with extraordinary rainfall events (e.g. tropical cyclones) trigger intense and recurrent floods with large socio-economic impacts to the population (Syvitski et al., 2014; Rodríguez-Morata et al., 2018). Tropical cyclones have provoked intense devastation during the last decades mainly interconnected with societal drivers such as urbanization and lack of flood risk assessments (Raymond et al., 2020). Flood assessments need precise information on the spatial and temporal distribution of rainfall and discharge (Baker, 2008; IPCC, 2014; UNDRR, 2019). Tropical countries commonly offer scarce and poor-quality data, this condition is even more complex for hydrological measurements (Wohl et al., 2012). The limited data availability motivates different methods/techniques that permit adequate estimation of peak discharges and their return periods of past flood events (Baker, 2008; Bodoque et al., 2015; Wilhelm et al., 2019).

Flood marks left in the field, even months after the event, can be used to calculate the distribution and magnitude of a flood (Borga et al., 2008). Botanical indicators serve as a relevant source of evidence to date floods and to quantify their magnitude in rivers with limited or nonexistent gauge records (Ballesteros-Cánovas et al., 2015a). Botanical evidence of past floods comprises exposed roots, tilted trunks and injured branches of trees growing along river reaches (Wilhelm et al., 2019). Scars in trees constitute the most reliable paleostage indicator (PSI) of past floods as they allow precise dating of the event as well as a determination of water stages during floods (Ballesteros et al., 2011a, b). The use of tree-ring records in river corridors has allowed the extension of flood records back in time in several rivers (Ballesteros-Cánovas et al., 2015b). Therefore, dendrochronology assessments can provide information to analyze not only the peak discharge and the flood recurrence of a river reach, but also to develop flood hazard zonation (Ballesteros-Cánovas et al., 2013; Brooks and St George, 2015; Garrote et al., 2019).

Determination of flood quantiles probability is required for many engineering works and flood risk management projects (Nguyen et al., 2014; Díez-Herrero and Garrote, 2020). Based on statistics, flood-frequency analysis acquire the relationship amid flood quantiles and their nonexceedance probability to quantify the risk that a flood with a given discharge will be reached in the future (Wilhelm et al., 2019). Two main families of approaches can be distinguished to reduce the uncertainties of at-site flood frequency analyses and produce more robust flood quantile estimates based on larger sample sizes (Gaál et al., 2010). First, the ones that preserve the spatial extension (e.g. Hosking and Wallis, 1997), and second the ones which look to extend the temporal extension of information by historical floods or paleofloods (e.g. Reis and Stedinger, 2005). Bayesian Markov Chain Monte Carlo (MCMC) approach provides a precise statistical tool in order to perform flood frequency analyses (Gaume, 2018). Moreover, regional and historical information can be incorporated into flood frequency analyses to increase the precision of the estimators. The use of historical information can be of great value in the reduction of the uncertainty in flood

quantiles estimators, though many have raised concerns with measurement and recording errors (Baker, 2008; Benito et al., 2015).

Risk management strategies principal aims are to reduce risk and losses (UNDRR, 2019). A flood risk assessment can be achieved implementing integrated economic, structural, cultural, legal, social, health, environmental, technological, political, institutional and educational actions in order to prevent and reduce hazard, exposure, and vulnerability (IPCC, 2014; UNISDR, 2015). This requires a comprehensive and holistic disaster-related knowledge at a local level including the flood risk (Pinto Santos et al., 2020). Tropical climatic conditions favor that over 90% of the disasters in Costa Rica are hydrometeorological in nature (LA RED, 2020). The study of flood processes has been extensive in Costa Rica, nonetheless, hazard cartography resolution and its integration with vulnerability, exposure, and risk analysis has been scarce (Quesada-Román and Mata-Cambronero, 2020).

The intense deforestation and land-use change to extensive croplands have intensified the erosion and sediment yield rates increase in Térraba catchment (Krishnaswamy et al., 2001b). Intense flood events often occur at Térraba catchment linked to the passage of tropical cyclones approximately every 10 years (Quesada-Román and Zamorano-Orozco, 2019a). These processes affect different sections of the catchment provoking casualties, economic impacts in agriculture as well as in the road infrastructure, especially roads and bridges. Renowned events were Hurricanes Joan (1988) and Cesar (1996) and Tropical Storms Alma (2008) and Nate (2017) (Quesada-Román et al., 2020b). These tropical cyclones produced hundreds of affected population, dozens of casualties and huge economic losses in Térraba catchment during the last decades (Table 1). We hypothesize that the tropical cyclones are the most intense phenomena triggering floods in the region. There is a clear need to adapt to tropical extraordinary rainfall events such as tropical cyclones which are becoming more frequent and affect the population. Therefore, it become a necessity to create planning measures to mitigate their impacts. A regional flood frequency analysis coupled with a risk assessment associated with tropical cyclones for Térraba catchment can be a helpful input for land-use planning and reduce their disasters risk conditions. Besides, this approach can be a useful methodology that can be applied in other tropical contexts. Therefore, we aim to (i) develop a regional flood frequency analysis coupled with a dendrogeomorphic approach, and (ii) determine a risk assessment related to tropical cyclones for the Térraba catchment in Costa Rica as a novel and practical tool to be implemented along the tropics.

6.2. Study area

6.2.1. Geographic setting

The Térraba catchment is located in the southeast of Costa Rica from 8.7 to 9.5 N and -82.7 to -83.8 W (Fig. 45). Its landscape is result of the subduction processes between Cocos and Caribbean plates (Alvarado et al. 2017). The collision of the Cocos Ridge approximately 2 Ma ago stopped volcanism in the Cordillera de Talamanca and provoke high uplift rates oscillating from 1.7 to 8.5 m kyr^{-1} (Gardner et al., 2013). Térraba catchment drains from the Pacific slopes of the Cordillera de Talamanca to the Pacific Ocean (Quesada-Román and Zamorano-Orozco, 2019b). The highest peak of the country, Cerro Chirripó (3820 m asl), marks the origin of the headwaters and the Térraba flows across an alluvial fan sequence (Camacho et al., 2020) entering in the General-Coto

Brus Valley. Afterwards, it cuts through the Fila Brunqueña as antecedent fluvial system summing 4765 km^2 until the Térraba-Sierpe deltaic wetlands begin (Acuña-Piedra and Quesada-Román, 2016). During the Last Glacial Maximum, glacial or periglacial action modeled the highest elevations over 3000 m of Térraba catchment (Quesada-Román et al., 2019; 2020c). The subsequent LGM deglaciation favored the formation of an extensive alluvial fans sequence (Camacho et al., 2020). These hillslopes, alluvial fans, and floodplains along the General-Coto Brus Valley concentrated intense agricultural colonization and explosive land-use changes that provoked strong erosion rates especially after 1950s (Krishnaswamy et al., 2001a). Population projections indicate that in 2020 around 256,000 inhabitants (inh) live in the Térraba catchment. The most populated municipality Pérez Zeledón has 143,000 inh, followed by Buenos Aires (53,000 inh), Coto Brus (44,000 inh), and Osa (16,000 inh). Additionally, the municipalities of Buenos Aires and Coto Brus house a 30% and 10% of indigenous population, respectively (INEC, 2020).

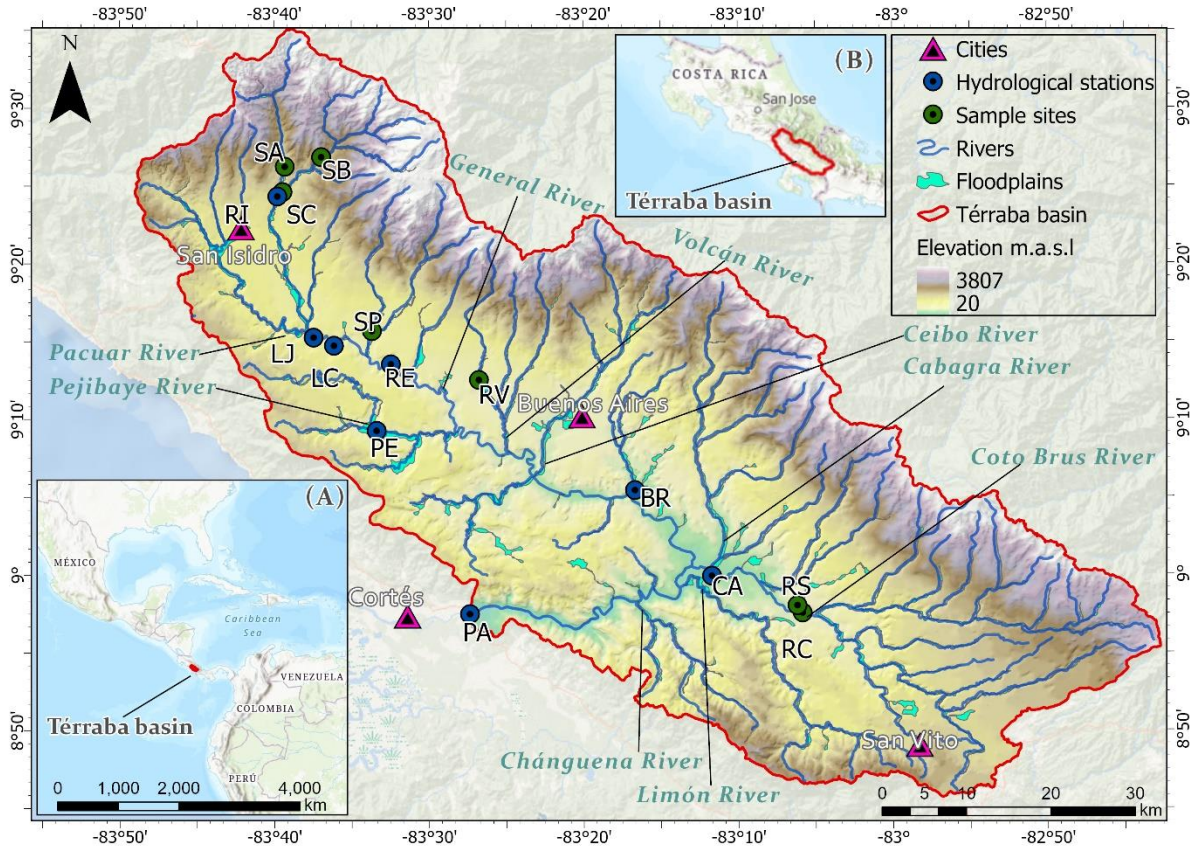

Fig. 45. Location of Térraba catchment in the Americas (A), in Costa Rica (B), and sampling sites and hydrological stations located in the Térraba catchment in Costa Rica.

6.2.2. Climate characteristics and tropical cyclones

The local climate is conditioned by the migration of the Intertropical Convergence Zone, northeast trade winds, cold fronts, El Niño-Southern Oscillation (ENSO), and the seasonal influence of Caribbean tropical cyclones (Hidalgo et al., 2015; Durán-Quesada et al., 2020; Quesada-Román et

al., 2020a). These conditions produce two rainfall maxima that sum between 1500 and 6000 mm annually, the first one in May and another in October, discontinued by the Midsummer Drought during July and August (Maldonado et al., 2016). Most of the rainfall occur between May and November during the rainy season, while the dry season is from December to April with annual mean temperatures from 8 to 28 °C depending on altitude (IMN, 2008).

Floods can be triggered by intense local convection, but severe floods are normally generated by tropical cyclones in Térraba River with an average of nine years over the last 50 years (Table 8). According to the Costa Rican Electricity Institute, during tropical cyclones, the upper catchment have reported peak flows of 947 m^3/s (Tropical Storm Nate in 2017), while the downstream Palmar hydrological station reported a record peak flow of 13,500 m^3/s during Hurricane Cesar in 1996 (Table 9; ICE, 2019) causing socio-economic losses (MIDEPLAN, 2017).

Table 8. Tropical cyclones that affected Térraba catchment between 1970 and 2018 (LA RED, 2018).

Date	Municipalities affected	Tropical cyclone	Impacts
9/19/1971	Pérez Zeledón, Osa	Tropical Storm Irene	1 death, 18 victims, 1 home destroyed and 8 affected
10/22/1988	Osa	Hurricane Joan	1200 victims
7/25/1996	Pérez Zeledón, Buenos Aires, Osa	Hurricane Cesar	13 deaths, thousands of victims, 449 houses destroyed
10/22/1998	Pérez Zeledón, Buenos Aires, Coto Brus, Osa	Hurricane Mitch	954 victims, 18 houses destroyed, 592 houses affected
5/29/2008	Pérez Zeledón, Buenos Aires, Osa	Tropical Storm Alma	900 affected
10/5/2017	Pérez Zeledón, Buenos Aires, Coto Brus, Osa	Tropical Storm Nate	640 victims, 160 houses affected, 15 US million in economic losses

6.3. Materials and methods

The Fig. 46 describes the applied approach. The methodological steps are (i) the study site selection based on historical and flow gauge records related with tropical cyclones, (ii) acquisition of topographic and geomorphic information, (iii) tree-ring based flood reconstruction, (iv) hydraulic and statistical modelling and (v) flood risk assessment based on exposure and socio-economic indicators.

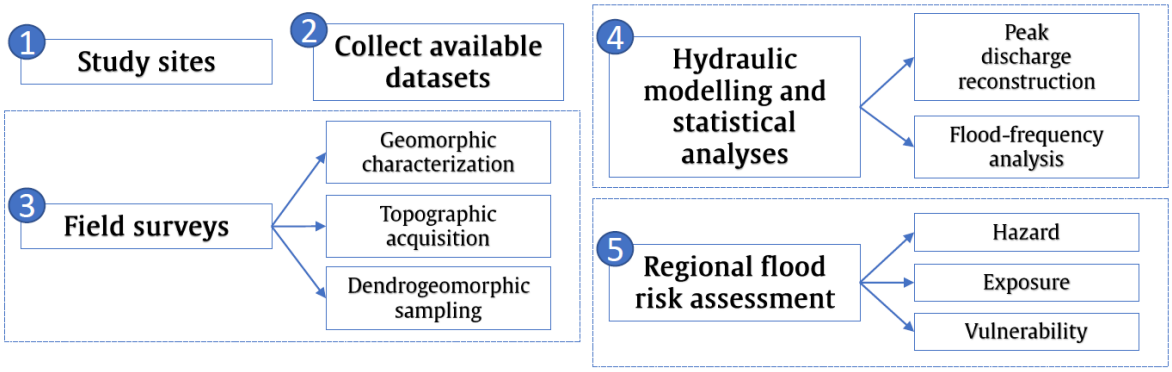

Fig. 46. Conceptual diagram summarizing the step-by-step work plan.

6.3.1. Field surveys, hydraulic modelling and peak discharge reconstruction

During the field surveys, we sampled trees with scars that could be clearly attributed to past flooding triggered by Tropical Storm Nate in 2017 (Sigafoos, 1964; Ballesteros-Cánovas et al., 2011a). The trees position was recorded with a Global Positioning System (GPS; precision of <1 m) and scar height was measured with respect to the channel as the central height of the injury from tree base (Ballesteros-Cánovas et al., 2011b). The two-dimensional (2D) hydrodynamic model IBER (www.iberaula.es) was used to model water depth of the flood event of 2017 produced by Tropical Storm Nate in seven stream reaches (Fig. 1). IBER simulates turbulent-free, unsteady surface flows and environmental processes in rivers by solving depth-averaged 2D shallow water equations (2D Saint-Venant) using a finite volume method with a second-order roe scheme (Cea et al., 2019). This approach is particularly suitable for turbulent mountain streams where shocks and discontinuities can occur. The method is conservative, even in cases where wetting and drying processes occur. The model works in a non-structured mesh consisting of triangles or quadrilateral elements. We used high resolution UAV elevation data obtained from digital imagery. A Structure from Motion (SfM) approach was applied to obtain georectified orthomosaics and digital elevation models (Turner et al., 2012). Digital images were obtained with a DJI Phantom 4 Pro V2 drone. The photogrammetric reconstruction of the fluvial environments for hydraulic modelling and point cloud classification was realized using Agisoft Photoscan 1.4.0 generating 0.5 m elevation models (Langhammer and Vackova, 2018).

Bed friction was evaluated in the field with Manning's *n* roughness coefficient considering homogenous roughness units (Chow, 1959). We used a Manning's n=0.075 for the main channel, 0.16 for the forest, and 0.08 for those sectors with sparse vegetation (Barnes, 1967; Arcement and Schneider, 1989). To compute the inlet water discharge (i.e., steady flow regime) of each study reach, we thereafter modeled successive inlet discharges based on historical extremes (using steps of 100 m^3/s up to 1500 m^3/s). Peak discharge of the 2017 flood was simulated with an iterative step-backwater procedure and consisted of a (i) calculation of water stages from modeled peak discharges and (ii) a fitting of resulting modeled water surfaces with PSI heights identified in the field (Webb and Jarrett, 2002). For more robust flood discharge estimations, we then calculated the mean squared error (MSE) of each modeled discharge output against every scar height. The magnitude of the flood event in each river reach was then defined as the peak discharge for which the MSE between the model and scar heights was smaller (Fig. S1; Quesada-Román et al., 2020b).

6.3.2. Regional flood-frequency analysis

Reconstructed peak discharge values and associated uncertainty were included as a range of values into the systematic records of annual maximum discharge from eight hydrological stations for the period 1962-2019 (Table 2; ICE, 2019). We implemented a regional flood frequency analysis method based on Bayesian Markov Monte Carlo Chain (MCMC) algorithms (Gaál et al., 2010; Gaume, 2018). Moreover, a Generalized Extreme Value distribution (GEV) was applied to calculate flood quantiles. Homogeneity of the existing systematic flow series were verified using the Hosking and Wallis (1987) algorithm (Table S1), which compares the variation between-site in samples Lcv (coefficient of L-variation) for the analyzed sites (Fig. S2). The regional flood frequency analysis therefore permits inclusion of flood quantile estimations at different catchment locations by flow-index regionalization (Fig. S3, S4). This approach is based on the distribution of a flow discharge from different catchments of a homogenous region (Fig. S5). This analysis was completed using the R package nsRFA (Viglione, 2013). The robustness of this method has been tested previously in other hydrological contexts (Reis and Stedinger, 2005; Gaume et al., 2010; Ballesteros-Cánovas et al., 2015b, 2016). Finally, we compared the impact which the addition of the seven modeled historical peak discharges (Tropical Storm Nate 2017) from the dendrogeomorphic method previously indicated to systematic series has on flood quantiles and uncertainties at each of the study catchments (Fig. 47; Bodoque et al., 2020). The occurrence of floods with different exceedance probability per catchment surface unit (1 km^2) were then calculated (Table S3).

Table 9. Hydraulic model estimated peak discharge sites (1-7) and observed peak flows at hydrological stations (8-15) used for the regional flood-frequency analysis of Térraba catchment.

Number	Code	Name	Area (km^2)	Maximum peak discharge (m^3/s)	Year
1	SA	Site A (Pueblo Nuevo)	101.5	636	2017
2	SB	Site B (Canaán)	164.4	455	2017
3	SC	Site C (Miraflores)	205.8	1249	2017
4	SP	San Pedro	67.6	146	2017
5	RV	Río Volcán	65.8	143	2017
6	RC	Río Coto Brus	851.5	336	2017
7	RS	Río Sábalo	53.88	212	2017
8	RI	Rivas	316.7	947	2017
9	LJ	Las Juntas	822.9	2007	2005
10	LC	La Cuesta	842.9	2776	2017
11	RE	Remolino	1071	5250	1996
12	PE	Pejibaye	129.3	1373	1993
13	BR	El Brujo	2399	8809	1996
14	CA	Caracucho	1135	3366	1996
15	PA	Palmar	4766	13500	1996

6.3.3. Regional flood risk assessment

In order to identify the flood-prone areas in Térraba catchment and subsequently identify the flood hazard, first we determined the hydrogeomorphic floodplain mapping (GFPLAIN) using the algorithm developed by Nardi et al. (2006, 2019) and the parameters of a 10-meter DEM by Annis et al. (2019). To separate the different flood hazard inside the determined floodplains we used the Topographic Wetness Index (TWI), which combines local upslope contributing area and slope, and is commonly used to quantify topographic control on hydrological processes (Sörensen et al., 2006). TWI was multiplied by the calculated 10-year return period associated with tropical cyclones impacts (Table S3). We used the 10-year return period because it is mean reported frequency of the intense tropical cyclones impacts in the region during the last five decades (Table 1). Otherwise, flood exposition was calculated using the best resolution infrastructure and population density by WorldPop (Tatem, 2017) which uses machine learning approaches to produce estimates of numbers of people residing in 100 × 100 m grid cells. Moreover, for flood vulnerability we used the social development index (IDS 2017) made by the Ministry of National Planning and Economic Policy of Costa Rica (MIDEPLAN). The index gathers and evaluates economic, educational, public health, civic participation, and security variables of the districts of Térraba catchment (MIDEPLAN, 2017). All variables were normalized from 0 to 1 (Fig. S5). Flood risk is the probability of the occurrence of a flood that can cause direct and indirect impacts on people, property, and the infrastructure (Pinto Santos et al., 2020). Expressing the risk of flooding at the catchment level implies a direct probabilistic relation between the physical processes of flooding in a given exposed element with a given vulnerability (Pinto Santos et al., 2019). Flood risk (FR) is therefore a dimensionless and comparable measure calculated at catchment level and is the product of hazard (H), exposure (E), and vulnerability (V):

$$FR = H^{\frac{1}{3}} * E^{\frac{1}{3}} * V^{\frac{1}{3}} \quad (1)$$

This enunciation of flood risk considering the due differences with regards to the scale, risk components, and input data is based on the INFORM risk index (De Groeve et al., 2014). When compared to the simple product of H, E, and V, used without the exponentiation, the dispersal and increase in the range of the final flood risk scores is observed. Finally, we produced a point map with the flood risk categorized into high, medium, and low risk using Jenks natural breaks classification method for practical applications (Jiang, 2013; Allen et al., 2018).

6.4. Results

6.4.1. Tropical cyclones flood discharge reconstruction

A total of 148 trees showed visible scars made by sediment and wood transported during the flood triggered by Tropical Storm Nate (Table 10). Mean scar heights for all trees that were considered for peak discharge reconstruction had a mean of 1.74 m and a standard deviation average of 0.63 m. On average, the highest scar heights were recorded in Site B (2.57 ± 0.731 m above the channel bed), whereas the lowest scar heights were found in San Pedro (1.03 ± 0.66 m). The average mean square error (MSE) between the observed scar height and the simulated water depth for all the reaches was 1.39 m. The hydraulic model points to differing hydraulic conditions prevailing at the

seven sites during the 2017 flood induced by Tropical Storm Nate varying from 143 to 1249 m^3/s (Table 2).

Table 10. Dendrogeomorphic characteristics of the trees used as paleostage indicators (PSI) for each of the study reaches. MSE — mean squared error.

Study reach	Scars in trees	Scar heights (m)	MSE	Area (km^2)	Calculated peak discharge (m^3/s)
Site A (Pueblo Nuevo)	29	2.25 ± 0.70	1.46	101.45	636
Site B (Canaán)	31	2.57 ± 0.73	1.64	164.41	455
Site C (Miraflores)	31	2.15 ± 0.78	2.1	205.79	1249
San Pedro	15	1.03 ± 0.66	1.05	67.6	146
Río Volcán	9	1.63 ± 0.38	0.88	65.8	143
Río Coto Brus	17	1.10 ± 0.47	1.13	851.47	336
Río Sábalo	16	1.46 ± 0.70	1.49	53.88	212

6.4.2. Ungauged floods and regional flood frequency analysis

The Hosking and Wallis test was applied on eight flow gauge records covering the period 1962–2019 and contributing catchment areas ranging from 129.28 and 4765.51 km^2; it generated a H1 value of -0.40, therefore indicating that the dataset used in this study can be assumed homogeneous for as long as $H1 \leq 1$ (see Supplementary Information; Table S1). Based on the eight available flow gauge records and the seven modeled (historical) peak discharges, we identified the resulting flood frequency for a runoff surface of 1 km^2 during which flow exceeded the 90th percentile for the length of the record (Table S3). Fig. 47 shows example of the fit of the distribution function including uncertainties at the 90% interval confidence level, between the obtained regional flood frequencies and extrapolated estimates based on the flow gauge data from Pejibaye and Palmar stations. All measurements at each of the hydrological stations are provided in Supplementary Information (Table S2). The inclusion of the reconstructed flood events suggest that flood hazards in Térraba catchment can be underestimated up to 10.7% if systematic records is only considered in the analyses with uncertainties ranging between 5^{th} and 95^{th} percentile (Table 11). Uncertainties variability is probably related with the different catchment areas summing Térraba totality (129.28 to 4764.51 km^2), their orientation (RI, CA, and PA have a NE-SW direction, and LJ, LC, RE, PE, and BR have a NW – SE bearing), are tectonically controlled by faults, and lithology (RI and CA have mostly volcanic substrates, PE is a sedimentary catchment, while the rest are a compose both of volcanic and sedimentary bedrocks). Bigger (BR and PA) and smaller (RI, PE, and LJ) catchment areas presented middle and higher observed changes values. While midsize catchment areas had the slower uncertainties among systematic and nonsystematic analyses (RE, LC, and CA).

Table 11. Comparison of flood return period (T) estimates Térraba catchment before and after including the reconstructed peak discharges. ML – mean values, X5, X95 – 5% and 95% uncertainties, respectively.

Code	Area (km^2)	ONLY SYST T=10 years	SYST + NONSYST T=10 years	OBSERVED CHANGES (%)

		ML	X5	X95	ML	X5	X95	ML	X5	X95
RI	316.67	393.89	340.30	537.80	710.31	709.28	886.96	80.33	-98.93	-31.93
LJ	822.88	970.54	837.43	1252.95	1516.39	1450.63	1750.88	56.24	-68.38	-46.86
LC	842.94	1534.05	1285.62	2057.28	1566.49	1457.24	1751.34	2.11	-56.94	-65.40
RE	1070.56	1915.90	1501.34	2715.43	1899.18	1731.47	2099.61	-0.87	-59.19	-74.71
PE	129.28	714.46	535.77	1372.29	358.81	341.14	446.21	-49.78	-80.31	-73.54
BR	2399.3	3899.15	3417.58	4141.13	3527.82	3177.39	3885.21	-9.52	-19.57	63.24
CA	1134.53	2109.92	1759.00	2681.04	1993.36	1808.87	2189.87	-5.52	-44.35	-63.58
PA	4765.51	5491.15	4617.96	6121.71	6184.95	5266.29	6896.07	12.63	-6.59	0.13

6.4.3. Flood risk assessment related to tropical cyclones

To represent the flood hazard (H), we determined the hydrogeomorphic floodplain of the entire Térraba catchment, and combined the 10-year return period with the TWI. The spatial distribution of the hazard using a Jenks natural breaks classification method shows a graded differentiation between the northern and western catchments such as General, Pacuar, Unión, Volcán, and Ceibo with low and medium flood hazard. Otherwise, high and moderate flood hazard is observed at the south and southeast in the medium-sized catchments s, such as the Pejibaye, Cabagra, Coto Brus, Limón, and Chánguena (Fig. 48). The exposure (E) behavior is likely the opposite than the flood hazard. General, Pacuar, and Ceibo catchments present important urban centers such as San Isidro del General and its surrounding urbanized areas at the northwest and Buenos Aires at the center of the catchment (Fig. 49). These areas comprise the medium to high exposure values of the Térraba catchment due to their higher population and infrastructure density based on satellite and census assessments. The rest of the catchment are mainly rural with very low population and infrastructure densities that strongly influence the lowest exposure values.

Vulnerability (V) distribution presents a similar distribution than exposure a graded differentiation between the northern-western to the south-southeast medium-sized catchments (Fig. 50). The major cities of San Isidro del General and San Vito, were found to have lower vulnerability. Higher vulnerability values are strongly linked to rural areas with a majority of extensive or subsistence agricultural activities and indigenous territories in Buenos Aires and Coto Brus municipalities. Risk values responded to the hazard, exposure, and vulnerability interaction (Fig. 51). The highest risk values are distributed along the catchment in isolated spots but mainly located in General, Unión, Pejibaye, Ceibo, and Limón catchments, which are very populated, low-income, and/or indigenous territories. Medium and low risk values responded to less inhabited catchments, mainly agricultural landscapes such as Pacuar, some parts of General, Volcán, and Coto Brus. Approximately 5585 inhabitants are located in the flood-prone areas of Térraba catchment.

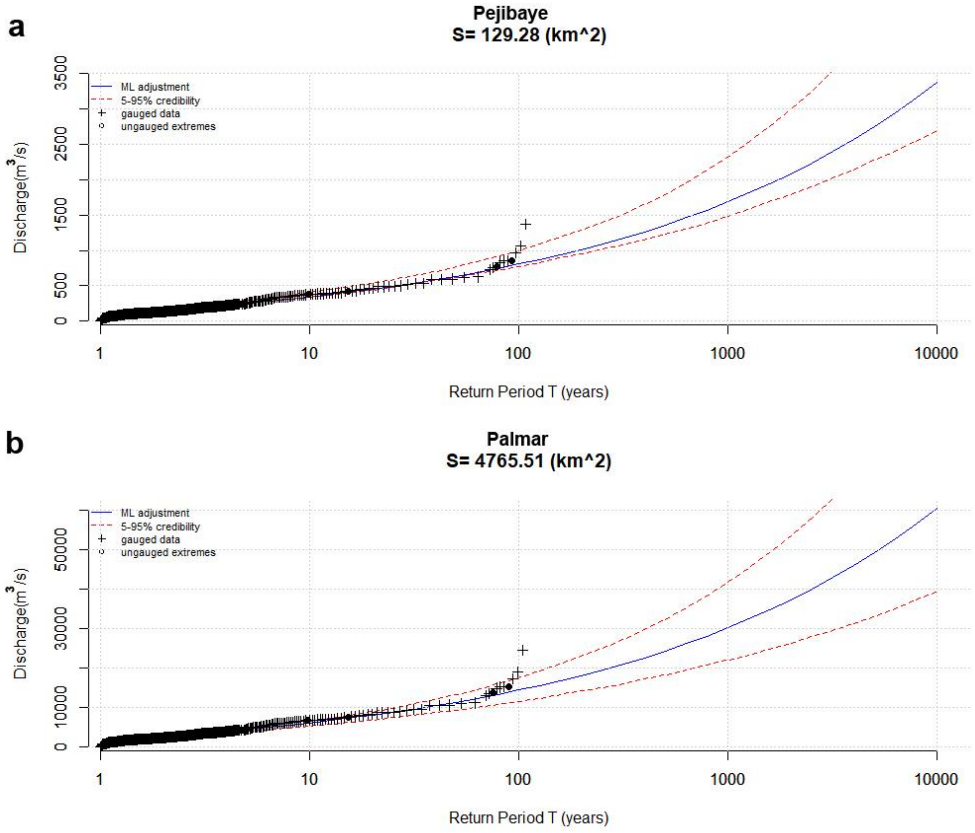

Fig. 47. Flood frequency distribution based on systematic flow-gauge series and the reconstructed paleodischarges of the smallest (a) and the biggest (b) gauged stations.

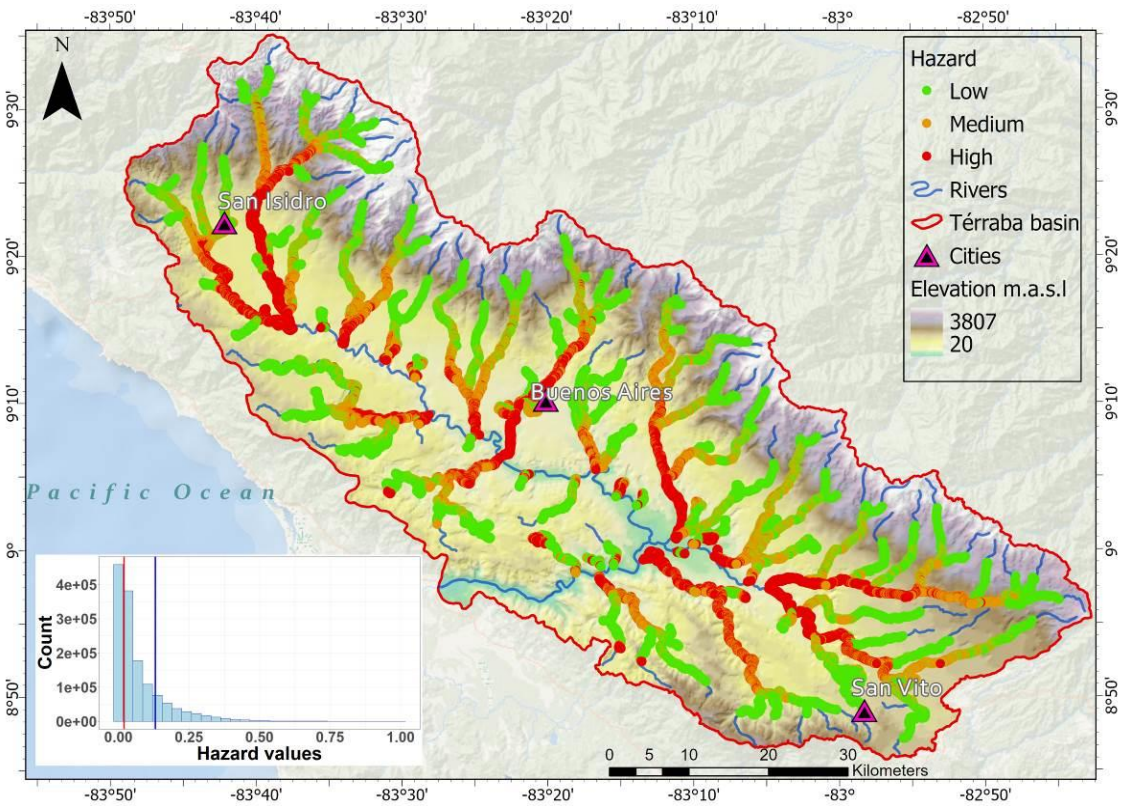

Fig. 48. Flood hazard map of the Térraba catchment, Costa Rica. Histogram show the low (red line) and high (blue line) values threshold.

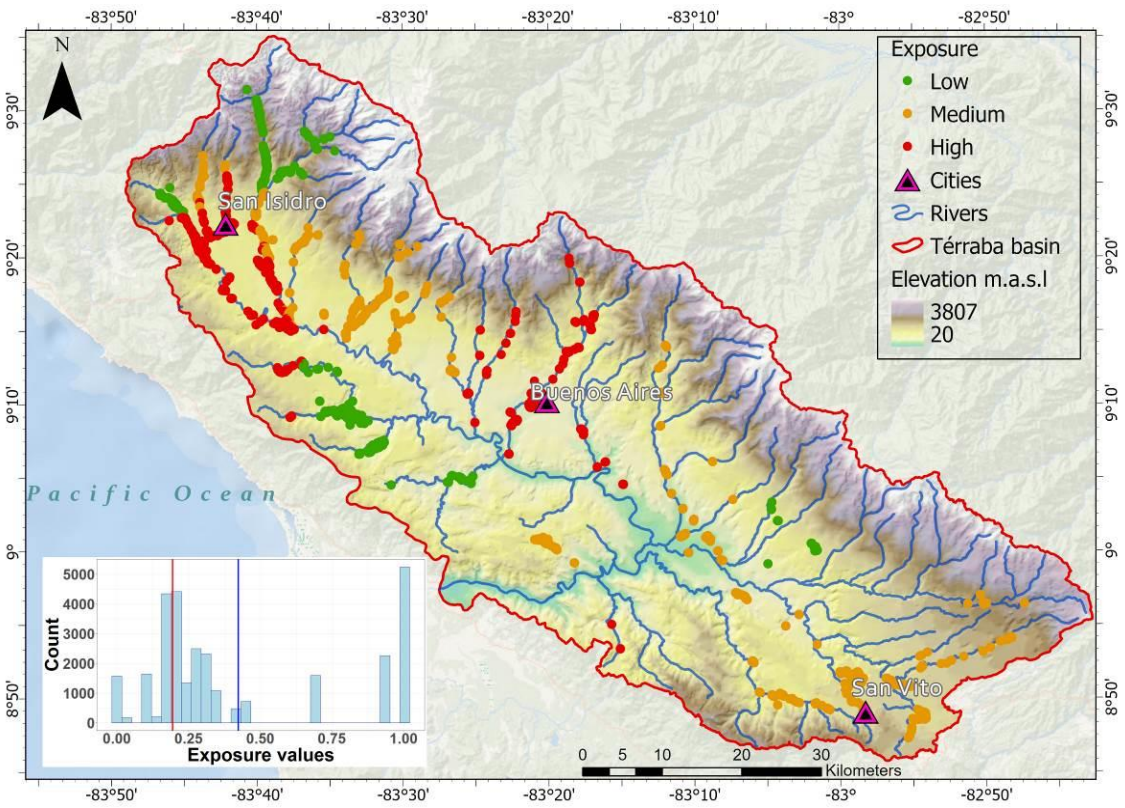

Fig. 49. Exposure map of the Térraba catchment, Costa Rica. Histogram show the low (red line) and high (blue line) values threshold.

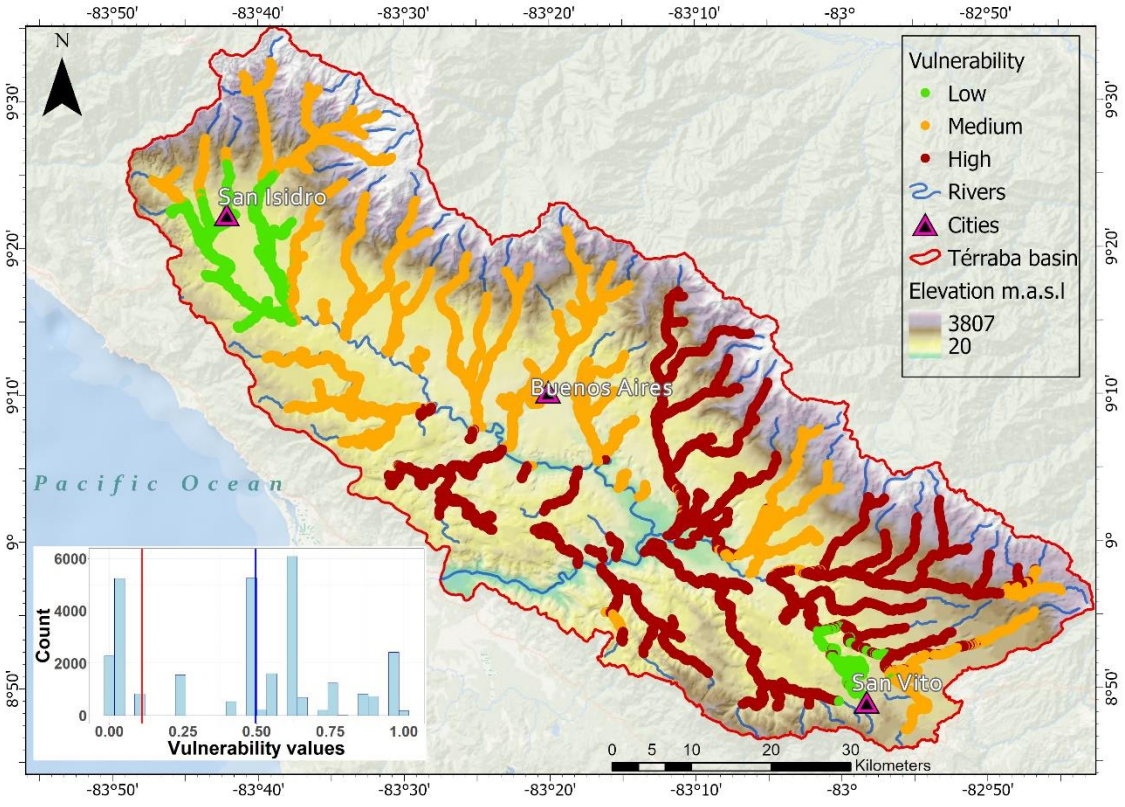

Fig. 50. Vulnerability map of the Térraba catchment, Costa Rica. Histogram show the low (red line) and high (blue line) values threshold.

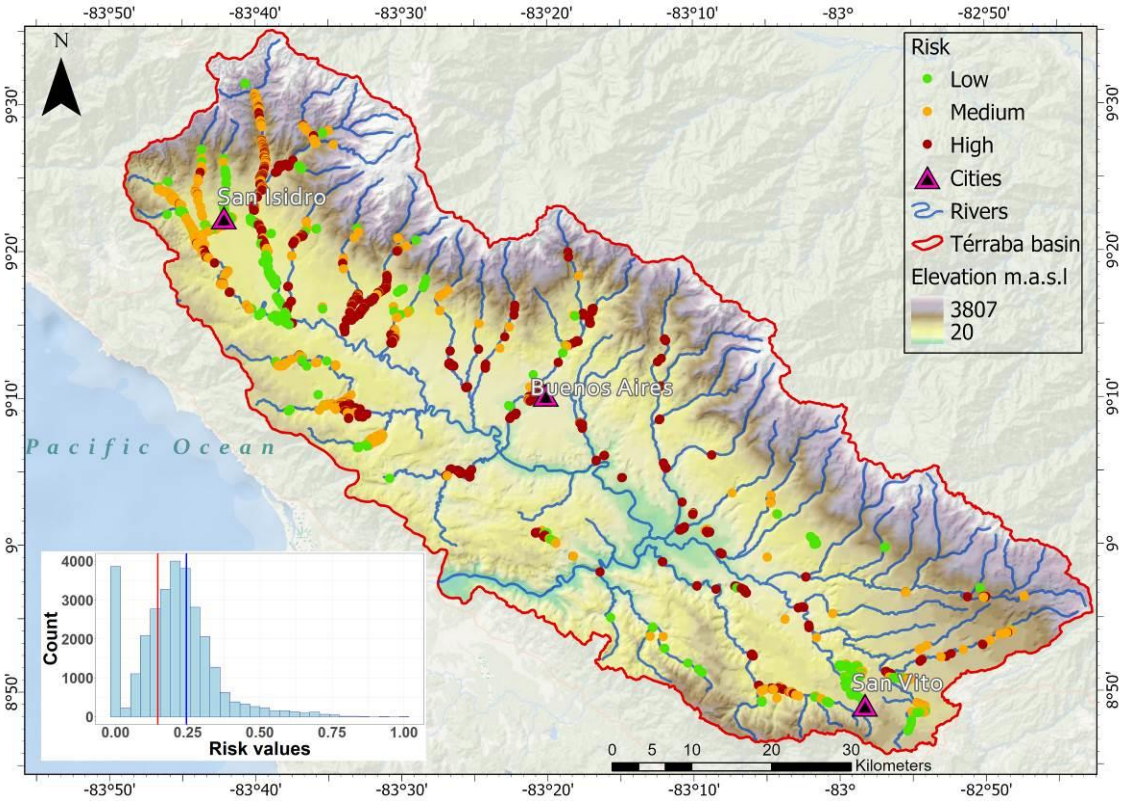

Fig. 51. Flood risk map of the Térraba catchment, Costa Rica. Histogram show the low (red line) and high (blue line) values threshold.

6.5. Discussion

6.5.1. Flood-frequency analysis supported by dendrogeomorphic measurements and hydraulic modelling

We have shown how tropical cyclones peak discharges through flood-frequency and dendrogeomorphic records can be used to inform authorities and the population about the frequency and magnitude of flood events in a selection of poorly gauged catchments of Térraba catchment. Flood frequency analysis, as a classical method in hydrology, have been widely used for flood hazard mapping (Stephens and Bledsoe, 2020). Historical and paleoflood data can increase the information length and include the information of extreme events often missed in gauge records (Baker, 2008). Regional flood-frequency assessments have been also applied to merge nonsystematic and systematic records by flow-index regionalization (Gáal et al., 2010; Gaume et al., 2010; Nguyen et al., 2014). Dendrochronology have proven its efficiency coupled as nonsystematic records with flood-frequency analysis to reconstruct stream flows in temperate regions (Meko et al., 2012; Ballesteros-Cánovas et al., 2019). As far as we know, our results are one of the first flood-frequency analysis combined with dendrogeomorphology on the tropics.

The reconstructed high flows correspond with observations at the gauging stations closely linked with tropical cyclones as the main triggers of extraordinary floods in the whole catchment (Table 8 and 9; ICE, 2019). There is a particular regionalization of the rainfall distribution during the tropical cyclones, due that the main peak discharges do not affect homogenously. This point is consistent with the complexity of a hydrologic regime of Térraba catchment which is mainly a tropical mountainous catchment characterized by the abundance of energy and moisture, high inter and intra-annual variability (ENSO) and high-magnitude infrequent events such as tropical cyclones (Krishnaswamy et al., 2001a). High rainfall erosivity is associated with land uses that provide inadequate soil protection and consequently the sediment delivery ratio increases downstream with increasing catchment area (Krishnaswamy et al., 2001b). Actually, recent decades reforestation in Térraba catchment due to environmental policies strengthen have favoured a sponge soil infiltration effect on dry-season flows (Krishnaswamy et al., 2018).

Our coupled results from the dendrogeomorphic assessment with the regional flood-frequency analysis are consistent with previous studies. In this line, Ruiz-Villanueva et al. (2013) demonstrated that uncertainty decreases if historical data is included in small ungauged or poorly gauged mountain catchments of Central Spain. Otherwise, another study in Tatra Mountains in Poland demonstrated that the inclusion of nonsystematic paleohydrological data from tree-ring analysis can have an important impact on the results of flood frequency analysis (Ballesteros-Cánovas et al., 2016). In addition, Ballesteros-Cánovas et al. (2017) found in Kullu district in India that these methods can be comparable once dendrochronology sampling is taken close to the existing gauging stations as we performed in Rivas, San Pedro, Sábalo, and Coto Brus rivers. Flood hazard assessments at regional or large scales along the main river valleys have proven to be useful as a first approximation to detect high susceptible areas to be considered in future more detailed studies (Allen et al., 2018).

Limitations of regional flood-frequency assessments merging nonsystematic and systematic records are related with the increased uncertainties in large catchments, where flow gauge data is less representative (Ruiz-Villanueva et al., 2013; Ballesteros-Cánovas et al., 2017). Our results had similar uncertainties in the lower sections of the Térraba catchment. Bigger catchments (BR and PA) had middle observed changes, while small catchments (RI, LJ and PE) showed the higher uncertainties. Midsize catchments (LC, RE and CA) had lower uncertainties between systematic and the inclusion of nonsystematic records using dendrogeomorphic measurements. In addition, these lower uncertainties sites are highly controlled by regional faults associated with the General-Coto Brus Valley and predominant sedimentary-fluvial substrates what make them geomorphically more stable. Therefore, we concentrated our analysis in the mountain sections where the systematic, nonsystematic, and modeled outputs were consistent with reported peak discharges.

Our approach can be implemented in other catchments commonly affected by tropical cyclones, phenomena which seems to become more intense in future decades (Bhatia et al., 2019). From the total number of tropical cyclones formed in the Atlantic basin, 14% produced indirect effects in Costa Rica, but the chances of a direct impact to the country were less than 6% during the 20th century (Alvarado and Alfaro, 2003). Consistently, since the 1970s a positive and statistically significant linear trend has been observed in the annual number of intense hurricanes in the

Caribbean Sea (Saunders and Lea, 2008). In addition, documented global increases in the proportion of very intense cyclones and also of trends in the latitude of maximum tropical cyclones intensity are consistent with modeled projections for future climate along the tropics (Walsh et al., 2016). Besides, recent studies indicate that tropical and extratropical cyclones have an increased trend on their lifetime maximum intensity (Tennille and Ellis, 2017).

6.5.2. Improved regional flood risk assessment and potential applications

We demonstrated that regional flood risk assessments in large scale geomorphic units $10^3 – 10^4$ km^2 (Dramis et al., 2011) are feasible using an assemblage of coarse (hydrological stations data, social indexes) and detailed inputs (UAV data, hydraulic modeling, high-resolution population density spatio-temporal information). The hydrogeomorphic floodplains were very useful to delineate flood-prone areas along the catchment as reported in previous studies (Annis et al., 2019; Nardi et al., 2019). In addition, TWI have been used to detect flood-prone areas in the past (Pourali et al., 2016). Likewise, the combination of the hydrogeomorphic floodplains, the TWI, and the 10-year return periods associated with tropical cyclones showed a very detailed flood hazard zonation. Previous local studies have identified distinct flood hazard levels using geomorphological mapping techniques (Quesada-Román, 2016, 2017). Most of these studies have associated tropical cyclones every 10 years as their main extraordinary triggers that coincide with our results, especially in Upper General River catchment where high hazard and risk values were determined (Quesada-Román and Zamorano-Orozco, 2018, 2019).

At large scales (state to district level), human exposure is difficult to directly quantify, and studies must rely on proxy indicators such as population or housing density to provide an approximate indicator of the level of human exposure (Allen et al., 2018). We had very realistic results for exposure determination using WorldPop (https://www.worldpop.org/) in Térraba catchment compared with available census non-updated data from 2011. As an open access high-resolution, these spatial demographic datasets were widely used in the past to support development and disaster response applications. Phongsapan et al. (2019) used this database to determine a flood risk index at national scale in Myanmar. In addition, certain methods to assess flood risk mapping worldwide proposed the use of WorldPop for vulnerability determination (Glas et al., 2019). For instance, WorldPop (Tatem, 2017) is a very good resolution dataset of infrastructure and population density for practical exposure calculation, and it can be implemented worldwide. The use of social indexes such as the IDS 2017 (MIDEPLAN, 2017) to determine the vulnerability is a practical way to show the economic, social participation, health, educative, and security conditions of political-administrative units. In addition, our social development index application for the vulnerability calculation demonstrated that other social constructed or established indexes (i.e. human development index at municipal scales) can be useful for risk assessments. Numerous studies have assessed the social vulnerability in a specific area, with examples in the United States (Cutter et al., 2013), China (Zhou et al., 2014), the United Kingdom (Tapsell et al., 2002; Fielding and Burningham, 2005), Israel (Felsenstein and Lichter, 2014), Germany (Fekete, 2009), Netherlands (Koks et al., 2015), and Spain (Aroca-Jiménez et al., 2020). It is important to consider the uncertainties, resilience and sensitivity of the social vulnerability indices depending on the outputs scale (Tate, 2012; Rufat et al., 2015; Spielman et al., 2020).

Térraba catchment nearly 60% of its inhabitants are considered to live in rural settings where 40% of the workforce is associated with agriculture (INEC, 2020). Resilience in rural areas is driven primarily by community capital and a considerable spatial variability in the components of disaster resilience (Cutter et al., 2016). Settlements closer to cities have a better capacity to deal with floods (Jamshed et al., 2020). Moreover, rural areas in developing countries are disproportionately vulnerable to disasters. Furthermore, its vulnerability responds with high migration rates, diffused benefit from social protection schemes, and scarcer or no savings to smooth the impacts (Deria et al., 2020). Furthermore, Térraba catchment comprise several indigenous territories that should be assessed using their knowledge and cultural appropriation of the risk management strategies (Kelman et al., 2012). Consequently, rural and indigenous incomes depend on fewer livelihood assets, and they are more likely to live in vulnerable ecosystems (UNDRR, 2019). Therefore, the impact of disasters affects more, and in a disproportionate manner, lower income households in rural developing countries (Jakobsen, 2012; Arouri et al., 2015). In this sense, public policy instruments such as poverty reduction, land use planning, and environmental management would become primary instruments for managing disaster risks (Lavell and Maskrey, 2014).

Despite of the good scientific and technical production of flood studies in Costa Rica (mainly in Spanish), regional high-resolution flood risk assessments in large-scale catchments , such as Térraba, have not been done previously in Costa Rica and perhaps many scarce-data availability countries (Quesada-Román et al. 2020d). This approach become critical for mountain tropical regions due that low-latitude regions present high values for expected economical-social loss scenarios by next decades for tropical cyclones and floods (Shi and Karsperson, 2015). In addition, many urban centers in mountain tropical regions have presented an unplanned growth or urban sprawl that favor disasters occurrence (Zhou et al. 2019). Therefore, it is necessary to integrate risk management and climate change scenarios within the urban planning processes (Park and Lee, 2019; Pinos et al., 2020). Without clear land use planning regulatory plans disaster risk will continue increasing, hence further research concerning flood risk mapping is necessary to reduce fatalities and economic losses due to tropical cyclones in low-latitude and developing countries. Hence, when baseline information lack, innovative and practical approaches must be applied as disaster risk assessment tools (Quesada-Román and Villalobos-Chacón, 2020).

6.6. Conclusions

We performed a regional flood-frequency analysis along with a risk assessment that includes hazard, exposure, and vulnerability mapping associated with tropical cyclones impacts in the Térraba catchment in Costa Rica. We used a 10-year return period because it is a reliable recurring order associate with the impact of tropical cyclones to determine with observed and not extrapolated data the flood risk in a large scale catchment. Tropical cyclones peak discharges determination using flood-frequency and dendrogeomorphic records proved its suitability in limited gauged catchments. We validated that regional flood risk assessments in large scale catchments are feasible using coarse and detailed inputs. Approximately 5585 inhabitants are located in the flood-prone areas of the Térraba catchment within different risk conditions and these results should be taken in account by stakeholders in order to take actions. Furthermore, our results agreed with affected regions in the past by tropical cyclones floods. This approach can be a useful input for land use planning and disaster risk reduction, increasing population resilience of Térraba

catchment in Costa Rica. Furthermore, this innovative and practical method may be successfully applied in developing and tropical countries with hydrological data scarcity.

CHAPTER 7

7. Overall conclusions

7.1. Principal results synthesis

The principal purpose of this thesis was to create baseline data that can improve the understanding of hydrogeomorphic process activity in the tropics of Costa Rica. To this end, we also tested the prospective use of tropical tree species for the reconstruction of natural hazard processes in Costa Rica. Despite the great efforts made over the last few decades to improve the understanding, studying and monitoring of hydrogeomorphic processes, a marked gap of knowledge remains due to the short time series on natural disasters of Costa Rica. In addition, significant ongoing land use changes, both in rural and urban areas, the increase in population, and the occupation of floodplains over the last centuries have provoked an increase in the exposure and vulnerability of local populations, a process that has been rendered even more severe due to limited territorial planning and risk assessment response. In addition, climate change scenarios predict more intense and frequent hydrometeorological hazards, which normally sum most of the events and fatalities worldwide. Tropical countries are often underdeveloped, present higher exposure and vulnerability to natural hazards impacts take longer to overcome as has been indicated in Costa Rica.

Chapter 2 presented an interesting and peculiar case on the interaction between a volcano, an earthquake, a hurricane passage and the subsequent mass movements. The research hypothesis here tested was that a tropical cyclone rainfall on volcanic slopes previously weakened by earthquakes triggered debris flows, landslides and flash floods in a limited-data region. The results found the existence of coupled earthquake-hurricane dynamics with higher landslide densities close to the epicenter and at sites receiving larger rainfall totals. The combined or subsequent occurrence of seismic and hydrometeorological processes can in fact lead to compound events and amplify/intensify disasters. Our results agree with findings presented in other studies where the destabilizing effect of an earthquake and a subsequent extreme rainfall was shown to trigger landslides and debris flows in China (Tang et al. 2011; Zhang et al. 2014). Similar studies have been applied to volcanic contexts in Japan (Saito et al. 2018; Yano et al. 2019). In addition, several studies on the impact of prior earthquakes and subsequent tropical cyclones as a coupled trigger of landslides have been identified for Taiwan (Lin et al. 2008a; Chen et al. 2011; Lin et al. 2012; Kuo et al. 2018; Chen et al. 2019). Nonetheless, our study is the first of this kind in the Americas. Besides, the effects of large wood found in debris flows also demonstrated the importance of monitoring densely forested mountain regions that have been hit by earthquakes during subsequent extraordinary precipitation events. These outputs are useful for the assessment and understanding of geological and hydrometeorological hazards coupling in tropical countries such as Costa Rica.

Tropical woody species have the potential to provide insights into past climatic, ecological and geomorphic conditions using dendrochronology. This hypothesis was positively tested in Chapter 3 where tropical dendroecology was evaluated contemplating its tree growth patterns, most studied regions, families, genera and most suitable species, as well as its common approaches and techniques, different applications, limitations, and further research prospects. Tropical trees chronologies length are normally less than 300 years due to catastrophic events, differential mortality between species, vegetation turnover disparity, as well as physiological breakdowns, and

human impacts. These results are in agreement with several previous works (Worbes and Junk, 1999; Brienen et al., 2016). Dendrochronological studies in tropical regions primarily exist for America (59%), Asia (22%), Africa (16%), and Oceania (3%). Major gaps in dendroecological research persist today in (sub-)tropical desert environments (Sahara, Namibia, Australian and Mexican deserts) as well as the Caribbean, Southern Mexico, Central America, Africa (in general), South Asia, Southeast Asia and tropical Oceania. The most studied families are *Fabaceae*, *Pinaceae* and *Meliaceae*. Consequently, the most common genera and species are *Pinus*, *Cedrela*, *Tectona*, *Acacia*, and *Abies* mainly present in tropical and subtropical moist broadleaf, dry broadleaf, as well as grasslands, savannas and shrublands forests. Our results improve prior extensive inventory studies along the tropics (e.g. Brienen et al., 2016; Schöngart et al., 2017). Furthermore, most research on tropical growth rings and their ecological interpretation has been realized at altitudes below 2,000 m a.s.l. Normally, geomorphic and archaeological studies need least samples while ecology and climatology research typically relies on the biggest sample sizes. Most dendroecological studies gathered in the tropics so far trusted on macroscopic applications. Most frequently, research focused on dendroclimatology and dendroecology, encompassing a stunning 96% of all work made in the tropics, with only occasional and dispersed work on dendrogeomorphology. These findings are key for countries or regions such as Costa Rica that holds a huge biodiversity and potential to discover new woody species that mark growth rings and the possible applications in ecology, climatology and geomorphology.

Short-lived and endemic species could produce growth rings controlled by climatic variability and rainfall seasonal oscillations in the tropics. Dendrochronological techniques in Chapter 4 confirmed the hypothesis of the potential of an endemic shrub from the Costa Rican highlands to be used in dendrochronology. The Chirripó National Park in Costa Rica comprises one understudied tropical ecosystem, the páramo. This ecosystem is located from Central America to the Andes and mostly occurs at the base of high mountains (over 3000 m a.s.l.) with perennial glaciers or landforms that have been modeled during the Last Glacial Maximum. In this study, *Hypericum irazuense* was used to define the climatic factors limiting shrub growth, using a bootstrapped correlation and response function analysis. This research reported a relation between climate and annual growth of *H. irazuense,* and demonstrated the latter is sensitive to precipitation and temperature during boreal winters influenced primarily by the absence of rainfall during the dry season that is locally lasting from December to April. In addition, a statistically significant correlation between annual growth and La Niña events is present. Our results agree with different studies across Central America indicating that strong ENSO events associated with dryer and sunnier conditions result in reduced annual ring growth in lowlands (e.g. Alfaro-Sánchez et al., 2017; Clark et al., 2018; Enquist and Leffler, 2001) and in tropical mountain forests/páramos (Anchukaitis et al., 2013; Anchukaitis et al., 2015). The existence of annual growth rings makes *H. irazuense* as one in only few neotropical species appropriate (so far) for dendrochronological studies. The study thereby also demonstrated the suitability of dendrochronology in Costa Rica, especially in uncommon and endemic species, opening an immense window of dendrochronological opportunities in the Central American region and throughout the tropics.

The potential of dendrochronology was also tested positively in Chapter 5 where the hypothesis was that flood peak discharges related to tropical cyclones (or other extraordinary rainfalls) can be reconstructed using a dendrogeomorphic approach in ungauged catchments. The research outputs showed that trees scarred at cut banks have the smallest uncertainties, best fit and are more reliable

for peak discharge reconstructions using dendrogeomorphic evidence. The geomorphic position also influences modeled flow velocity and shear stress. A systematic sampling of scars in trees located in more stable landforms, such as cut banks or alluvial terraces, can reduce significantly the time needed in dendrogeomorphic studies. Our results confirmed that the geomorphic position of trees is the main factor explaining deviations between models and field observations, as previously reported in other studies realized in temperate environments (Gottesfeld, 1996; Yanosky and Jarret, 2002; Ballesteros-Cánovas et al., 2011a; Victoriano et al., 2018). It is the first study of its kind in the humid tropics and expands the geographic scope of tree-ring based hazard analysis. By limiting differences between reconstructions, direct observations, and model outputs, the dendrogeomorphic approach is becoming an increasingly important tool for disaster risk reduction and territorial management decisions in (tropical) regions where data on past events are scarce or rather unreliable. This study demonstrated the suitability of dendrogeomorphology methods applied for highly dynamic catchments recurrently affected by tropical storms and hurricanes in Costa Rica and other extraordinary rainfall environments.

Chapter 6 tested the hypothesis that regional flood risk assessments associated with the return periods of floods triggered by tropical cyclones can provide useful inputs for land use planning and disaster risk reduction in data-scarce catchments. In this study, the use of dendrogeomorphic approaches went further integrating a regional flood-frequency analysis to determine a regional flood risk for the entire Térraba basin, the largest watershed of Costa Rica affected approximately every 10 years by tropical cyclones (tropical storms or hurricanes). The principal reason of this study relies in the scarce systematic and long-term data on past floods and peak discharge estimations. Here, the use of dendrochronology has proven its efficiency through the coupling of nonsystematic records with flood-frequency analyses to reconstruct stream flows in temperate regions (Meko et al., 2012; Ruiz-Villanueva et al., 2013; Ballesteros-Cánovas et al., 2016, 2017, 2019; Allen et al., 2018). This application is one of the first flood-frequency analysis combined with dendrogeomorphology in the tropics. The study also demonstrated that a regional flood frequency approach can be realized with dendrogeomorphic techniques. In addition, flood frequency analyses for larger regions identifying the different flood hazard, exposure, vulnerability, and risk in a detailed resolution for a regional scale output are critical for stakeholders in territorial and disaster risk management. These analyses support the feasibility of regional flood risk assessments induced by tropical cyclones in Costa Rica. In that sense, these findings will be useful for the design and implementation of future strategies dealing with flood risks in other mountainous watersheds of Costa Rica providing potential applications in other tropical catchments with scarce hydrological data.

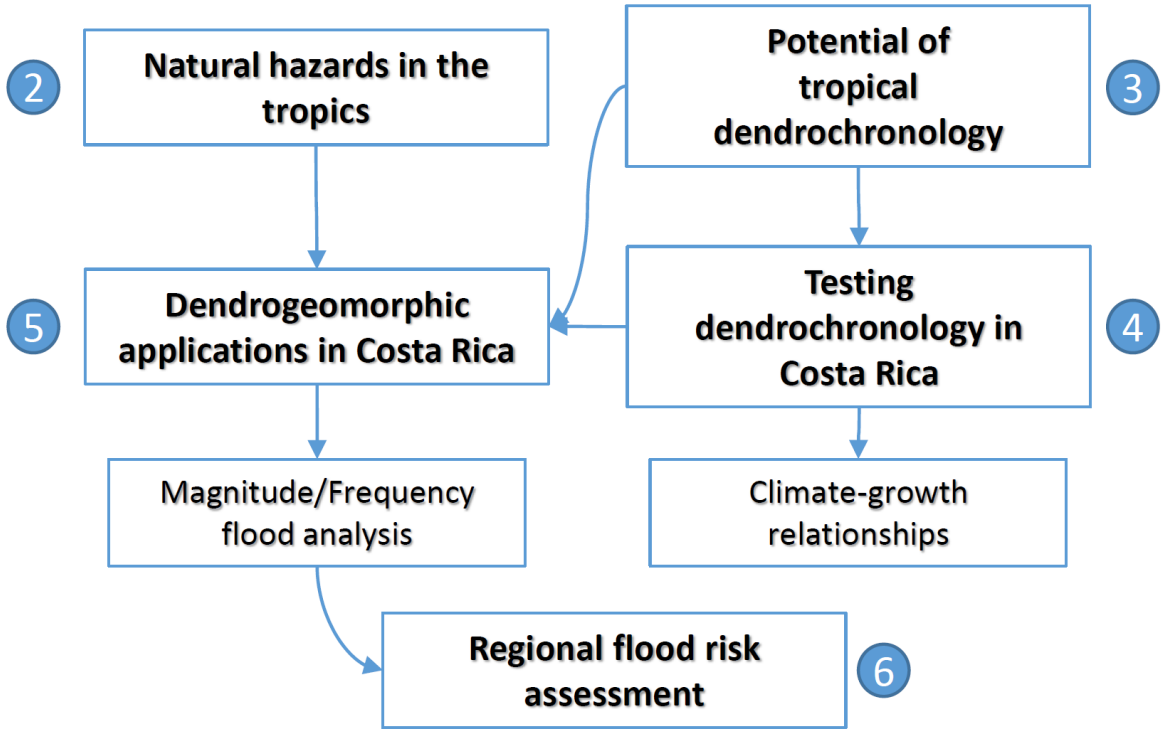

Fig. 52. Conceptual scheme with the corresponding chapter numbers presented in this thesis.

7.2. Research limitations

Natural hazards cause dozens of thousands of casualties and huge economic losses in the tropics every year. Baseline information on topography, climatology and hydrology are often limited or lacking completely in tropical or developing countries. When available, reference data is rough in resolution, not necessarily updated to the present date, with significant gaps and its access often requires heavy bureaucratic procedures. In Costa Rica, limitations of those described above clear exist. The main limitations for hydrogeomorphic process research the country are multiple: High-resolution topography data is limited, in many instances cloudiness controls the quality of spaceborne imagery, whereas existing airborne imagery at scales of either 1:50.000 or 1:25.000 is not frequently updated. Better products such as specific satellite or airborne imagery are expensive or generated with UAVs, but with a limited spatial range and larger efforts that are required for acquisition and post-processing. Only in few catchments do important records of systematic hydrological and climatological data exist. Nonetheless, its access requires a set of justifications and permissions that normally slow down research. Furthermore, many public institutions generate very good data through private contracts but will then need approval and sharing protocol designs before it can be made accessible for the public, provoking its quick obsolescence. Historical data of natural hazards is available but not necessarily systematic, which again limits its precision. During the last years, disaster databases (i.e. DesInventar, EM-DAT) have partially filled this gap by compiling records of recent decades.

Despite the immense potential of dendrochronology in low latitudes, a series of limitations deserve consideration for future successful assessments. Tropical woody species do not normally mark

growth rings at simple sight. Microscopic methods require much more time than macroscopic methods, what limits the research time advances. Therefore, one of the major remaining challenges in tropical dendrochronology is inherent to the identification of growth rings, as objective anatomical parameters for the definition of growth ring boundaries is still lacking for many species today. Hence, growth ring classifications in tropical woody species need to consider different anatomical markers to expand the knowledge of tropical ecosystems. Microscopic and isotopic methods are expensive, requires specific equipment, trained scientists and technicians to develop precise anatomical or chemical methods. This limitation is a big challenge and requires innovative methods and solutions.

Tropical regions are most diverse in terms of the factors driving plant growth to such a degree that in many instances no one factor has a more prominent role than the others in controlling growth (e.g. rainfall, humidity, dry season, and/or salinity). Experimental research is limited in tropical dendrochronology which in turn leads to a huge lack in knowledge regarding the conditions that favor annual layering. High biodiversity also brings a limitation to identify properly all the species found during fieldwork. Sometimes a single species does not present enough number of specimens in a small spatial range and random sampling is necessary. As an alternative, proper statistical sampling method can still be achieved by covering wider areas. Due to these limitations, protected areas (both public and private) are the best zones to perform dendrochronology in the tropics but need permissions that require time in advance.

7.3. Future research lines

This research found a set of future research lines for natural hazards and dendrochronology in Costa Rica and the tropics. The study of hydrogeomorphic processes can be improved through the creation of higher-resolution baseline data, especially also in terms of better imagery (e.g. satellite, airborne, drones, LiDAR) and more intensive fieldwork so as to generate better geomorphic maps and statistical modelling to develop suitable natural hazard assessments and zonation. Densely forested mountain regions that have been affected previously by earthquakes and subsequent precipitation events shall be monitored with early warning systems integrating national, regional, and local participants in order to succeed and reduce disaster risk in highly dynamic tropical catchments. Therefore, further research concerning landslides induced by earthquakes and subsequent strong rainfalls is necessary to reduce fatalities and economical losses in tropical countries.

The implementation of dendrogeomorphic approaches has shown its efficiency in recent peak discharge reconstructions at local and regional scales. It is possible to extrapolate these results to other regions affected by extraordinary rainfall events (not necessarily tropical cyclones). Future research focusing on trees affected by floods should focus on specimens on cut banks or alluvial terraces where uncertainties between modeled and observed flow heights are minimal. Therefore, recent extreme events are good proxies for flood zonation, and can thus contribute to risk reduction. Consistently, the use of dendrogeomorphic techniques can serve as a strong tool to determine not only flood dynamics but also to measure the magnitude and chronology of mass movements and erosion processes in tropical environments. A main goal of this research is to expand the geographic scope of dendrochronology hazard analyses in a region that concentrates one-third of global rainfall in a warming context with an increasing population, rapid land-use

changes and more people living in floodplains. Hence, exposition and vulnerability studies should improve their scales, periodicity and information quality to perform precise and continuous risk assessments.

The vast geo- and biodiversity of low latitudes as well as the intense tectonic and hydrometeorological dynamics can serve as a large open-air laboratory to apply tropical dendrochronology. Nonetheless, there is a need for additional development of approaches and techniques aimed at unravelling the climatic, ecological, archaeological, and geomorphic information contained in tropical woody plants. Tropical countries could develop their own laboratories and expand international collaboration to explore well-known, endemic and non-traditional species, with the ultimate goal to enhance the knowledge, as well as to improve the protection and conservation of the most biodiverse region of the world. Additionally, the extent of tropical dendrochronology requires the implementation of cutting-edge methods in wood anatomy, species prospection, and intense alliance among developed and developing countries research groups. The often-inconsistent growth patterns in tropical trees, sampling difficulty, complex wood anatomy, or the lack of physiological knowledge of local woody species can only be improved increasing the number of studies and used species along low latitudes. The combination of macroscopic, microscopic and isotopic methods are compulsory to improve the growth ring dynamics knowledge in contrasting tropical environments.

The persisting limitations in growth-ring research in fields other than climatology and ecology, any expansion of innovative multi- and trans-disciplinary approaches to growth-ring studies would enhance our knowledge of these biodiverse regions further. Along these lines of thoughts, dendrogeomorphic approaches can be useful to assess debris-flow, landslide, floods and erosional processes, common dynamic events causing great number of casualties and economical losses around the tropics. Similarly, much more research in dendroarchaeology can produce substantial advances including isotopic and chemical extraction approaches helping to remove the historical limitations for dendroprovenance studies. Finally, there is a clear need for more instrumentation, monitoring through experimental research to improve our knowledge of the different tropical ecosystems.

REFERENCES

Abernethy, B., Rutherfurd, I.D., 2001. The distribution and strength of riparian tree roots in relation to riverbank reinforcement. Hydrol. Process. 15, 63–79.

Acuña-Piedra, J.F., Quesada-Román, A., 2016. Evolución geomorfológica entre 1948 y 2012 del delta Térraba–Sierpe, Costa Rica. Cuat. Geom. 30 (3-4), 49-73.

Aerts, J.C., Botzen, W.J., Clarke, K.C., Cutter, S.L., Hall, J.W., Merz, B., Michel-Kerjan, E., Mysiak, J., Surminski, S., Kunreuther, H., 2018. Integrating human behaviour dynamics into flood disaster risk assessment. Nature Climate Change 8 (3), 193-199.

Alcántara-Ayala, I., 2002. Geomorphology, natural hazards, vulnerability and prevention of natural disasters in developing countries. Geomorphology 47 (2-4), 107-124.

Alfaro, A., Denyer, P., Alvarado, G.E., Gazel, E., Chamorro, C., 2018. Estratigrafía y petrografía de las rocas ígneas en la Cordillera de Talamanca, Costa Rica. Rev. Geol. Amér. Cent 58, 7–36.

Alfaro-Sánchez, R., Muller-Landau, H.C., Wright, S.J., Camarero, J.J., 2017, Growth and reproduction respond differently to climate in three Neotropical tree species. Oecologia 184 (2), 531-541.

Alfaro, E., Quesada-Román, A., Solano, F.J., 2010 Análisis del impacto en Costa Rica de los ciclones tropicales ocurridos en el Mar Caribe desde 1968 al 2007. Rev. Diálogos 11 (2), 25-38.

Alfaro, E., Quesada-Román, A., 2010. Ocurrencia de ciclones tropicales en el Mar Caribe y sus impactos sobre Centroamérica. Rev. InterSedes 11 (22), 136-153.

Alfaro, E., Pérez-Briceño, P.M., 2014. Análisis del impacto de fenómenos meteorológicos en Costa Rica, América Central, originados en los mares circundantes. Rev. Clim. 14, 1-11.

Allen, S.K., Ballesteros-Canovas, J.A., Randhawa, S.S., Singha, A.K., Huggel, C., Stoffel, M., 2018. Translating the concept of climate risk into an assessment framework to inform adaptation planning: Insights from a pilot study of flood risk in Himachal Pradesh, Northern India. Environ. Sci. Policy 87, 1-10.

Alvarado, G.E., 2010. Aspectos geohidrológicos y sedimentológicos de los flujos de lodo asociados al terremoto de Cinchona (M_w 6.2) del 8 de enero del 2009, Costa Rica. Rev. Geol. Amér. Cent. 43, 67-96.

Alvarado, G.E., 2011. Los volcanes de Costa Rica: geología, historia, riqueza natural y su gente. EUNED, San José, Costa Rica.

Alvarado L.F., Alfaro, E., 2003. Frecuencia de los ciclones tropicales que afectaron a Costa Rica durante el siglo XX. Tóp. Meteo. Ocean. 10 (1), 1-11.

Alvarado, G.E., Benito, B., Staller, A., Climent, A., Camacho, E., Rojas, W., Marroquín, G., Molina, E., Talavera, J.E., Martínez-Cuevas, S., Lindholm, C., 2017b. The new Central American seismic hazard zonation: mutual consensus based on up to day seismotectonic framework. Tectonophysics 721, 462-476.

Alvarado, G.E., Fallas, B., Vargas, V., Vega, E., Bakkar, H., Barrantes, G., 2017a. Los lahares del Volcán Miravalles disparados por el huracán Otto (24 de noviembre del 2016), Costa Rica: Meteorología, sedimentología, periodos de recurrencia, alerta temprana y recomendaciones. - vi + 85 p. Instituto Costarricense de Electricidad [Informe interno].

Alvarado, G.E., Morales, L.D., Montero, W., Climent, A., Rojas, W., 1988. Aspectos sismológicos y morfotectónicos en el extremo occidental de la Cordillera Volcánica Central de Costa Rica. Rev. Geol. Amér. Cent. 9, 75-98.

Alves, E.S., Angyalossy-Alfonso, V. 2000. Ecological trends in the wood anatomy of some Brazilian species. 1. Growth rings and vessels. IAWA J, 21, 3-30.

Amador, J.A., Alfaro, E.J., Rivera, E.R., Calderón, B., 2010. Climatic features and their relationship with tropical cyclones over the Intra-Americas seas. In Hurricanes and climate change (p. 149-173). Springer, Dordrecht.

Amoroso, M.M., Daniels, L.D., Baker, P.J., Camarero, J.J. (Eds.)., 2017. Dendroecology: tree-ring analyses applied to ecological studies (Vol. 231). Springer.

Anchukaitis, K.J., 2017. Tree Rings Reveal Climate Change Past, Present, and Future. Proc. Amer. Philos. Soc. 161 (3), 244-263.

Anchukaitis, K.J., Evans, M.N., Wheelwright, N.T., Schrag, D.P., 2008. Stable isotope chronology and climate signal calibration in neotropical montane cloud forest trees. J. Geophys. Res-Biogeo. 113 (G030030), 1-17.

Anchukaitis, K.J., Evans, M.N., 2010. Tropical cloud forest climate variability and the demise of the Monteverde golden toad. P. Natl Acad Sci. USA 107 (11), 5036-5040.

Anchukaitis, K.J., Taylor, M.J., Martin-Fernández, J., Pons, D., Dell, M., Chopp, C., Castellanos, E.J., 2013. Annual chronology and climate response in Abies guatemalensis Rehder (Pinaceae) in Central America. Holocene 23 (2), 270-277.

Anchukaitis, K.J., Taylor, M.J., Leland, C., Pons, D., Martin-Fernández, J., Castellanos, E.J., 2015. Tree-ring reconstructed dry season rainfall in Guatemala. Clim. Dynam. 45 (5–6), 1537–1546.

Anchukaitis, K. J., Wilson, R., Briffa, K. R., Büntgen, U., Cook, E. R., D'Arrigo, R., Davi, N., Esper, J., Frank, D., Gunnarson, B.E., Hegerl, G., Helama, S., Klesse, S., Krusic, P.J., Linderholm, H.W., Myglan, V., Osborn, T.J., Zhang, P., Rydval, M., Schneider, L., Schurer, A., Wiles, G., Zorita, E., 2017. Last millennium Northern Hemisphere summer temperatures from tree rings: Part II, spatially resolved reconstructions. Quat. Scie. Rev. 163, 1-22.

Anderson, D.R., Burnham, K., 2004. Model selection and multi-model inference. Second Edition. New York, Springer-Verlag. p. 488.

Annis, A., Nardi, F., Morrison, R.R., Castelli, F., 2019. Investigating hydrogeomorphic floodplain mapping performance with varying DTM resolution and stream order. Hydrolog. Sci. J. 64 (5), 525-538.

Antonelli, A., Kissling, W.D., Flantua, S.G.A., Bermúdez, M.A., Mulch, A., Muellner- Riehl, A.N., Kreft, H., Linder, P., Badgley, C., Fjeldså, J., Fritz, S.A., Rahbek, C., Herman, F., Hooghiemstra, H., Hoorn, C., 2018. Geological and climatic influences on mountain biodiversity. Nat. Geosci. 11, 718-725.

Araya, C., Linkimer, L., Taylor, W., 2016. Modelo mínimo unidimensional de velocidades de la onda P para la Cordillera Volcánica de Guanacaste. Rev. Geol. Amér. Cent. 54, 179-191.

Arcement, G.J., Schneider, V.R., 1989. Guide for selecting Manning's roughness coefficients for natural channels and flood plains. United States Geological Survey. Water-Supply Paper 2339.

Aristizábal, E., Vélez, J.I., Martínez, H.E., Jaboyedoff, M., 2016. SHIA_Landslide: a distributed conceptual and physically based model to forecast the temporal and spatial occurrence of shallow landslides triggered by rainfall in tropical and mountainous basins. Landslides 13 (3), 497-517.

Aroca-Jiménez, E., Bodoque, J.M., García, J.A., 2020. How to construct and validate an Integrated Socio-Economic Vulnerability Index: Implementation at regional scale in urban areas prone to flash flooding. Sci. Total Environ. 140905. https://doi.org/10.1016/j.scitotenv.2020.140905

Arouri, M., Nguyen, C., Youssef, A.B., 2015. Natural disasters, household welfare, and resilience: evidence from rural Vietnam. World Dev. 70, 59-77. https://doi.org/10.1016/j.worlddev.2014.12.017

Babst, F., Poulter, B., Bodesheim, P., Mahecha, M.D., Frank, D.C., 2017. Improved tree-ring archives will support earth-system science. Nat. Ecol. Evol. 1 (2), 1-2.

Baker, V.R., 2008. Paleoflood hydrology: Origin, progress, prospects. Geomorphology 101 (1-2), 1-13.

Ballesteros-Cánovas, J.A., Allen, S., Stoffel, M., 2019. The importance of robust baseline data on past flood events for regional risk assessment: a study case from Indian Himalayas. UNISDR Global Assessment Report.

Ballesteros-Cánovas, J.A., Bodoque, J.M., Díez-Herrero, A., Sanchez-Silva, M., Stoffel, M., 2011a. Calibration of floodplain roughness and estimation of flood discharge based on tree-ring evidence and hydraulic modelling. J. Hydrol. 403, 103-115.

Ballesteros-Cánovas, J.A., Eguibar, M., Bodoque, J.M., Díez-Herrero, A., Stoffel, M., Gutiérrez-Pérez, I., 2011b. Estimating flash flood discharge in an ungauged mountain catchment with 2D hydraulic models and dendrogeomorphic palaeostage indicators. Hydrol. Process. 25, 970-979.

Ballesteros-Cánovas, J.A., Bodoque, J.M., Lucía, A., Martín-Duque, J.F., Díez-Herrero, A., Ruiz-Villanueva, V., Rubiales, J.M., Genova, M., 2013. Dendrogeomorphology in badlands: methods, case studies and prospects. Catena 106, 113-122.

Ballesteros-Cánovas, J.A., Czajka, B., Janecka, K., Lempa, M., Kaczka, R.J., Stoffel, M., 2015a. Flash floods in the Tatra Mountain streams: Frequency and triggers. Scie. Total Environ. 511, 639-648.

Ballesteros-Cánovas, J.A., Sanchez-Silva, M., Bodoque, J.M., Díez-Herrero, A., 2013. An integrated approach to flood risk management: a case study of Navaluenga (Central Spain). Water Resour. Manag. 27 (8), 3051-3069.

Ballesteros-Cánovas, J.A., Stoffel, M., Bollschweiler, M., Bodoque, J.M., Díez-Herrero, A., 2010. Flash-flood impacts cause changes in wood anatomy of Alnus glutinosa, Fraxinus angustifolia and Quercus pyrenaica. Tree Physiol. 30 (6), 773-781.

Ballesteros-Cánovas, J.A., Stoffel, M., Spyt, B., Janecka, K., Kaczka, R.J., Lempa, M., 2016. Paleoflood discharge reconstruction in Tatra Mountain streams. Geomorphology 272, 92-101.

Ballesteros-Cánovas, J.A., Stoffel, M., St George, S., Hirschboeck, K., 2015b. A review of flood records from tree rings. Prog. Phys. Geog. 39 (6), 794-816.

Ballesteros-Cánovas, J.A, Trappmann, D., Shekhar, M., Bhattacharyya, A., Stoffel, M., 2017. Regional flood-frequency reconstruction for Kullu district, Western Indian Himalayas. J. of Hydrology 546, 140-149.

Barnes, H.H., 1967. Roughness characteristics of natural channels. United States Geological Survey. Water-Supply Paper 1849.

Barquero, J., Ellenberg, L., 1983. Geomorfología del piso alpino del Chirripó en la Cordillera de Talamanca, Costa Rica. Rev. Geog. Amér. Cent. 17-18, 293-299.

Bell, G.D., Blake, E.S., Landsea, C.W., Wang, C., Schemm, J., Kimberlain, T.B., Pasch, R.J., Goldenberg, S.B., 2017. Tropical Cyclones - Atlantic Basin, State of the Climate in 2016. Bull. Amer. Meteor. Soc. 98, S108-S112.

Beltrán-Gutiérrez, B., Valencia-Ramos, G.M., 2013. Anatomía de anillos de crecimiento de 80 especies arbóreas potenciales para estudios dendrocronológicos en la Selva Central, Perú. Rev. Biol. Trop. 61 (3), 1025-1037.

Bender, M.A., Knutson, T.R., Tuleya, R.E., Sirutis, J.J., Vecchi, G.A., Garner, S.T., Held, I.M., 2010. Modeled impact of anthropogenic warming on the frequency of intense Atlantic hurricanes. Science 327, 454-458.

Benito, G., Brázdil, R., Herget, J., Machado, M.J., 2015. Quantitative historical hydrology in Europe. Hydrol. Earth Syst. Sci. 19, 3517–3539

Benn, D.I., Owen, L.A., Osmaston, H.A., Seltzer, G.O., Porter, S.C., Mark, B., 2005. Reconstruction of equilibrium-line altitudes for tropical and sub-tropical glaciers. Quat. Int. 138–139, 8–21.

Bergoeing, J.P., 1977. Modelado glaciar en la Cordillera de Talamanca, Costa Rica. Instituto Geográfico Nacional. Informe Semestral. Julio-Diciembre: 33-44.

Bergoeing, J.P., 2017. Geomorphology and volcanology of Costa Rica. Elsevier. p. 280.

Beven, J.L., Berg, R., 2018. National Hurricane Center tropical cyclone report: Hurricane Nate. NOAA/NWS Rep.AL162017. p. 45. https://www.nhc.noaa.gov/data/tcr/AL162017_Nate.pdf.

Bhatia, K.T., Vecchi, G.A., Knutson, T.R., Murakami, H., Kossin, J., Dixon, K.W., Whitlock, C.E., 2019. Recent increases in tropical cyclone intensification rates. Nat. Commun. 10 (1), 1-9.

Bhattacharyya, A., Shah, S.K., 2009. Tree-ring studies in India past appraisal, present status and future prospects. IAWA J. 30 (4), 361-370.

Biondi, F., Qeadan, F., 2008. A theory-driven approach to tree-ring standardization: defining the biological trend from expected basal area increment. Tree-Ring Res. 64 (2), 81–96.

Bishop, M.P., James, L.A., Shroder, J.F., Walsh, S.J., 2012. Geospatial technologies and digital geomorphological mapping: Concepts, issues and research. Geomorphology 137 (1), 5–26.

Blagitz, M., Botosso, P.C., Longhi-Santos, T., Bianchini, E., 2019. Tree rings in tree species of a seasonal semi-deciduous forest in southern Brazil: wood anatomical markers, annual formation and radial growth dynamic. Dendrochronologia 55, 93-104.

Bodoque, J.M., Díez-Herrero, A., Eguibar, M.A., Benito, G., Ruiz-Villanueva, V., Ballesteros-Cánovas, J.A., 2015. Challenges in paleoflood hydrology applied to risk analysis in mountainous watersheds–A review. J. Hydrol. 529, 449-467.

Bodoque, J.M., Ballesteros-Cánovas, J.A., Stoffel, M., 2020. An application-oriented protocol for flood frequency analysis based on botanical evidence. J. Hydrol. 125242. https://doi.org/10.1016/j.jhydrol.2020.125242

Bommer, J.J., Rodríguez, C.E., 2002. Earthquake-induced landslides in Central America. Eng. Geol. 63 (3-4), 189-220.

Bonan, G.B., 2008. Forests and climate change: forcings, feedbacks, and the climate benefits of forests. Science 320, 1444–1449

Boninsegna, J.A., Argollo, J., Aravena, J.C., Barichivich, J., Christie, D., Ferrero, M.E., Lara, A., Le Quesne, C., Luckman, B.H., Masiokas, M., Morales, M., Oliviera, J.M., Roig, F., Srur, A., Villalba, R., 2009. Dendroclimatological reconstructions in South America: a review. Palaeogeog. Palaeoecol. 281 (3-4), 210-228.

Borga, M., Gaume, E., Creutin, J. D., Marchi, L., 2008. Surveying flash floods: gauging the ungauged extremes. Hydrol. Process. 22 (18), 3883-3885.

Borga, M., Stoffel, M., Marchi, L., Marra, F., Jakob, M. 2014. Hydrogeomorphic response to extreme rainfall in headwater systems: flash floods and debris flows. J. of Hydrology 518, 194-205.

Boscutti, F., Casolo, V., Beraldo, P., Braidot, E., Zancani, M., Rixen, C., 2018. Shrub growth and plant diversity along an elevation gradient: Evidence of indirect effects of climate on alpine ecosystems. PLOS ONE 13 (4), e0196653.

Bovi, R.C., Chartier, M.P., Domínguez-Castillo, V., Chagas, M.P., Tomazello Filho, M., Cooper, M., 2018. Application of growth rings and scars in exposed roots of Schizolobium parahyba as a tool for dating geomorphic processes in the State of São Paulo, Brazil. Dendrochronologia 50, 1-9.

Bovi, R.C., Chartier, M.P., Roig, F.A., Filho, M.T., Castillo, V.D., Cooper, M., 2019. Dynamics of erosion processes in the tropics : a dendrogeomorphological approach in an Ultisol of southeastern Brazil Dynamics of erosion processes in the tropics : a dendrogeomorphological approach in an Ultisol of southeastern Brazil. Plant Soil 443, 369–386.

Brenes, A., Girot, P., 2018. Gestión del riesgo y cambio climático. Informe Estado de la Nación en Desarrollo Humano Sostenible. Pavas, Costa Rica: CONARE, Programa Estado de la Nación, p. 1-52.

Brienen, R.J., Phillips, O.L., Feldpausch, T.R., Gloor, E., Baker, T.R., Lloyd, J., et al., 2015. Long-term decline of the Amazon carbon sink. Nature 519 (7543), 344-348.

Brienen, R.J.W., Schöngart, J., Zuidema, P.A., 2016. Tree rings in the tropics: insights into the ecology and climate sensitivity of tropical trees. In Tropical Tree Physiology (Goldstein, G., Santiago, L. Eds.), Springer, Berlin. pp. 439–461.

Brooks, G., St George., 2015. Flooding, Structural Flood Control Measures, and Recent Geomorphic Research along the Red River, Manitoba, Canada. In: Springer, (Ed.), Geomorphic Approaches to Integrated Floodplain Management of Lowland Fluvial Systems in North America and Europe. New York, pp. 87–117.

Buttò, V., Deslauriers, A., Rossi, S., Rozenberg, P., Shishov, V., Morin, H., 2020. The role of plant hormones in tree-ring formation. Trees 34, 315–335.

Cadol, D., Wohl, E., Goode, J.R., Jaeger, K.L., 2009 Wood distribution in neotropical forested headwater streams of La Selva, Costa Rica. Earth Surf. Process. Land. 34, 1198–1215.

Cadol, D., Wohl, E., 2010. Wood retention and transport in tropical, headwater streams, La Selva Biological Station, Costa Rica. Geomorphology 123 (1-2), 61-73.

Calvo-Solano, O.D., Quesada-Hernández, L., Hidalgo, H., Gotlieb, Y., 2018. Impactos de las sequías en el sector agropecuario del Corredor Seco Centroamericano. Agron. Mesoam. 29 (3), 695-709.

Camacho, M.E., Quesada-Román, A., Mata, R., Alvarado, A. 2020. Soil-geomorphology relationships of alluvial fans in Costa Rica. Geoderma Regional 21, 1-12, e00258.

Camarero, J.J., Linares, J.C., García-Cervigón, A.I., Batllori, E., Martínez, I., Gutiérrez, E., 2017. Back to the future: the responses of alpine treelines to climate warming are constrained by the current ecotone structure. Ecosystems 20 (4), 683–700.

Campos-Durán, D., Quesada-Román, A., 2017. Impacto de los eventos hidrometeorológicos en Costa Rica, periodo 2000-2015. Rev. Geo UERJ 30, 440-465.

Carabella, C., Buccolini, M., Galli, L., Miccadei, E., Paglia, G., Piacentini, T., 2020. Geomorphological analysis of drainage changes in the NE Apennines piedmont area: the case of the middle Tavo River bend (Abruzzo, Central Italy). Journal of Maps 16 (2), 222-235.

Carrer, M., Pellizzari, E., Prendin, A.L., Pividori, M., Brunetti, M., 2019. Winter precipitation-not summer temperature-is still the main driver for Alpine shrub growth. Sci. Total Environ. 682, 171-179.

CARTA - Costa Rica Airborne Research and Technology Applications., 2005. Aerial photographs scale 1:25,000 of Costa Rica. NASA (USA) and Costa Rica Government.

Castillo-Muñoz, R., 2010. Glaciaciones e Interglaciaciones en Costa Rica: Realidades y enigmas geológicos. San José, Costa Rica: Litografía e Imprenta LIL, S.A. p. 197.

Castruita-Esparza, L.U., Correa-Díaz, A., Gómez-Guerrero, A., Villanueva-Díaz, J., Ramírez-Guzmán, M.E., Velázquez-Martínez, A., Ángeles-Pérez, G., 2016. Basal area increment series of dominant trees of Pseudotsuga menziesii (Mirb.) Franco show periodicity according to global climate patterns. Rev. Chapingo. Ser. Cie. 22 (3), 379-397.

Cea, L., Bladé, E., Sanz-Ramos, M., Bermúdez Pita, M., Mateos-Alonso, Á., 2019. Iber applications basic guide.

Cervantes-Cordero, R., 1999. Disminución de la escorrentía superficial debido a variaciones en el uso del suelo. Informe de Trabajo de Graduación. Licenciatura en Ingeniería Civil. Escuela de Ingeniería Civil. Universidad de Costa Rica. p. 61.

Chandler, B.M., Lovell, H., Boston, C.M., Lukas, S., Barr, I.D., Benediktsson, Í.Ö., ... & Stroeven, A. P. (2018). Glacial geomorphological mapping: A review of approaches and frameworks for best practice. Earth-Scie. Rev. 185, 806-846.

Cherubini, P., Gartner, B.L., Tognetti, R., Bräker, O.U., Schoch, W., Innes, J.L., 2003. Identification, measurement and interpretation of tree rings in woody species from mediterranean climates. Biol. Rev. 78, 119–148.

Cervantes, C., 1977. Caracterización de la fracción mineral y determinación del ZPC en cuatro Andepts de la Provincia de Guanacaste. Tesis Ing. Agrón. Escuela Fitotecnia, Facultad de Agronomía, Universidad de Costa Rica. San José, Costa Rica.

Chen, H., Hawkins, A.B., 2009. Relationship between earthquake disturbance, tropical rainstorms and debris movement: an overview from Taiwan. Bull. Eng. Geol. Environ. 68 (2), 161-186.

Chen, H., Lin, G.W., Lu, M.H., Shih, T.Y., Horng, M.J., Wu, S.J., Chuang, B., 2011. Effects of topography, lithology, rainfall and earthquake on landslide and sediment discharge in mountain catchments of southeastern Taiwan. Geomorphology 133 (3-4), 132-142.

Chen, Y.C., Chang, K.T., Wang, S.F., Huang, J.C., Yu, C.K., Tu, J.Y., Hone-Jay, C., Liu, C.C., 2019. Controls of preferential orientation of earthquake-and rainfall-triggered landslides in Taiwan's orogenic mountain belt. Earth Surf. Process. Land. 44 (9), 1661-1674.

Chow, V., 1959. Open-channel Hydraulics. McGraw-Hill, New York. p. 680.

Cigolini, C., Taticchi, T., Alvarado, G.E., Laiolo, M., Coppola, D., 2018. Geological, petrological and geochemical framework of Miravalles-Guayabo caldera and related lavas, NW Costa Rica. J. Volc. Geoth. Res. 358, 207-227.

Clark, D.A., Clark, D.B., Letcher, S.G., 2018. Three decades of annual growth, mortality, physical condition, and microsite for ten tropical rainforest tree species. Ecology 99 (8), 1901-1901.

CNE - Comisión Nacional de Prevención de Riesgos y Atención de Emergencias, 2016. Valoración de riesgo y estabilidad de laderas en varios puntos de Upala, por afectaciones del sismo ocurrido el 02 de julio, 5.4 M.w. Unidad de Investigación y Análisis de Riesgo. IAR-INF-0595-2016. San José, Costa Rica.

CNE - Comisión Nacional de Prevención de Riesgos y Atención de Emergencias, 2017ª. Plan general de la emergencia ante la situación provocada por el paso del huracán Otto por territorio costarricense. San José, Costa Rica. pp 25. From: https://www.cne.go.cr/Documentos/planes-emergencia/plan_emergencia_40027.pdf

CNE - Comisión Nacional de Prevención de Riesgos y Atención de Emergencias, 2017b. Geospatial information of the geomorphic impacts of Hurricane Otto. Unidad de Investigación y Análisis de Riesgo. San José, Costa Rica.

CNE - Comisión Nacional de Prevención de Riesgos y Atención de Emergencias, 2018. Plan general de la emergencia ante la situación provocada por la Tormenta Tropical Nate. San José, Costa Rica. p. 23. Accessed in: https://www.cne.go.cr/Documentos/Plan_de_Emergencia_40677.pdf

Cook, E.R., 1985. A Time Series Analysis Approach to Tree Ring Standardization. PhD thesis. University of Arizona. 171 pp.

Cook, E.R., Kairiukstis, L.A., 1990. Methods of Dendrochronology: Applications in the environmental sciences. Kluwer Academic Publishers, Dordrecht, The Netherlands.

Cook, E.R., Krusic, P.J., 2005. Program ARSTAN. A Tree-ring Standardization Program Based on Detrending and Autoregressive Time Series Modeling, With Interactive Graphics. Tree-Ring Laboratory Lamont Doherty Earth Observatory of Columbia University, Palisades, NY.

Coster, C. 1927. Zur Anatomie und Physiologie der Zuwachszonenund Jahresringbildung in den Tropen. Ann Jard Bot Buitenzorg 37, 49–161.

Coster, C. 1928. Einiges u¨ber das Dickenwachstum und die Inhaltsstoffe des Djatistammes, Tectona grandis L.f. Tectona 17, 1056–1057.

Cotecchia, F., Santaloia, P., Lollino, C., Vitone, G., Pedone G., Bottiglieri, O., 2016. From a Phenomenological to a Geomechanical Approach to Landslide Hazard Analysis. European Journal of Environmental and Civil Engineering 20 (9), 1004-1031.

Crockett, S.L., Eberhardt, M., Kunert, O., Schuhly, W., 2010. Hypericum species in the Paramos of Central and South America: a special focus upon H. irazuense Kuntze ex N. Robson. Phytochem. Rev. 9, 255–269.

Crockett, S.L., Robson, N.K. 2011. Taxonomy and chemotaxonomy of the genus Hypericum. WAG UR FRON. 5, 1-13.

Crowther, T.W., Glick, H.B., Covey, K.R., Bettigole, C., Maynard, D.S., Thomas, S.M., et al., 2015. Mapping tree density at a global scale. Nature 525 (7568), 201-205.

Cunningham, M., Stark, C.P., Kaplan, M., Schaefer, J., 2019. Glacial limitation of tropical mountain height. Earth Surface Dynamics, 7, 147–169.

Cutter, S.L., Ash, K.D., Emrich, C.T., 2016. Urban–rural differences in disaster resilience. Ann. Am. Assoc. Geogr. 106 (6), 1236-1252. https://doi.org/10.1080/24694452.2016.1194740

Cutter, S.L., Emrich, C.T., Morath, D.P., Dunning, C.M., 2013. Integrating social vulnerability into federal flood riskmanagement planning. J. Flood Risk Manag. 6, 332–344

De Groeve, T., Vernaccini, L., Polansek, K., 2014. Index for risk management - InfoRM. Report EUR 26528 EN. https://doi.org/10.2788/78658.

DeMets, C., Gordon, R.G., Argus, D.F., 2010. Geologically current plate motions. Geoph. J. Intl. 181, 1–80.

De Micco, V., Campelo, F., De Luis, M., Bräuning, A., Grabner, M., Battipaglia, G., Cherubibi, P., 2016. Intra-annual density fluctuation in tree rings: how, when, where, and why? IAWA J. 37, 232–259.

Denyer, P., Alvarado, G.E., 2007. Mapa geológico de Costa Rica. Escala 1:400 000. Librería Francesa. San José, Costa Rica.

Deria, A., Ghannad, P., Lee, Y.C., 2020. Evaluating implications of flood vulnerability factors with respect to income levels for building long-term disaster resilience of low-income communities. Int. J. Disast. Risk Re. 101608.

Destro, E., Marra, F., Nikolopoulos, E.I., Zoccatelli, D., Creutin, J.D., Borga, M., 2017. Spatial estimation of debris flows-triggering rainfall and its dependence on rainfall return period. Geomorphology 278, 269–279.

Détienne, P., 1989. Appearence and periodicity of growth rings in some tropical woods. IAWA Bull 10, 123–132.

Devall, M.S., Parresol, B.R., Wright, S.J., 1995. Dendroecological analysis of Cordia alliodora, Pseudobombax septenatum and Annona spraguei in central Panama. IAWA J. 16 (4), 411-424.

Diaz, H.F., Hoerling, M.P., Eischeid, J.K., 2001. ENSO variability, teleconnections and climate change. Int. J. Climatol. 21 (15), 1845-1862.

Díez-Herrero, A., Ballesteros, J.A., Ruiz-Villanueva, V., Bodoque, J.M., 2013. A review of dendrogeomorphological research applied to flood risk analysis in Spain. Geomorphology 196, 211–220.

Díez-Herrero, A., Garrote, J., 2020. Flood Risk Analysis and Assessment, Applications and Uncertainties: A Bibliometric Review. Water 12, 2050. https://doi.org/1 0.3390/w12072050

Dünisch, O., Montóia, V.R., Bauch, J., 2003. Dendroecological investigations on Swietenia macrophylla King and Cedrela odorata L.(Meliaceae) in the central Amazon. Trees 17 (3), 244-250.

Dramis, F., Guida, D., Cestari, A., 2011. Nature and aims of geomorphological mapping. In Smith, M, Paron, P., Griffiths, J.M. (Eds.) Geomorphological mapping. Developments in Earth Surface Processes (pp. 39-73). Elsevier.

Durán-Quesada, A.M., Sorí, R., Ordoñez, P., Gimeno, L., 2020. Climate Perspectives in the Intra–Americas Seas. Atmosphere 11 (9), 959.

Dzierma, Y., Rabbel, W., Thorwart, M., Flueh, M., Mora, M., Alvarado, G.E., 2011. The steeply subducting edge of the Cocos Ridge: Evidence from receiver functions beneath the northern Talamanca Range, south-central Costa Rica. Geoch. Geoph. Geosyst. 12, 4-25.

EEL-UCR (Earthquake Engineering Laboratory - University of Costa Rica), 2016. Peak ground acceleration for Mw 5.7 Bijagua earthquake of 2nd of July, 2016. http://www.lis.ucr.ac.cr/mapas/2016-07-02-19:58:30/

Enfield, D., Alfaro, E., 1999. The dependence of Caribbean rainfall on the interaction of the tropical Atlantic and Pacific Oceans. J. Climate 12, 2093-2103.

England Jr, J.F., Cohn, T.A., Faber, B.A., Stedinger, J.R., Thomas Jr, W.O., Veilleux, A.G., Kiang, J.E., Mason Jr, R.R., 2019. Guidelines for determining flood flow frequency—Bulletin 17C (No. 4-B5). US Geological Survey.

Enquist, B.J., Leffler, A.J., 2001. Long-term tree ring chronologies from sympatric tropical dry-forest trees: individualistic responses to climatic variation. J. Trop. Ecol. 17 (1), 41-60. https://doi.org/10.1017/S0266467401001031

Esper, J., Krusic, P.J., Ljungqvist, F.C., Luterbacher, J., Carrer, M., Cook, E., Davi, N.K., Hartl-Meier, C., Kirdyanov, A., Konter, O., Myglan, V., Timonen, M., Tryde, K., Trouet, V., Villalba, R., Yang, B., Büntgen, U., 2016. Ranking of tree-ring based temperature reconstructions of the past millennium. Quat. Sci. Rev. 145, 134-151.

Esquivel-Hernández, G., Sánchez-Murillo, R., Quesada-Román, A., Mosquera, G. M., Birkel, C., Boll, J., 2018. Insight into the stable isotopic composition of glacial lakes in a tropical alpine ecosystem: Chirripó, Costa Rica. Hydrol. Proc. 32 (24), 3588-3603.

Esquivel-Hernández, G., Mosquera, G.M., Sánchez-Murillo, R., Quesada-Román, A., Birkel, C., Crespo, P., Célleri, R., Windhorst, D., Breuer, L., Boll, J., 2019. Moisture transport and seasonal variations in the stable isotopic composition of rainfall in Central American and Andean Páramo during El Niño conditions (2015-2016). Hydrol. Process. 33 (13), 1802-1817.

Evans, M.N., Schrag, D.P., 2004. A stable isotope-based approach to tropical dendroclimatology. Geochim. Cosmochim. Ac. 68 (16), 3295-3305.

Fan, X., Juang, C.H., Wasowski, J., Huang, R., Xu, Q., Scaringi, G., van Westen, C.J., Havenith, H.B., 2018. What we have learned from the 2008 Wenchuan Earthquake and its aftermath: A decade of research and challenges. Eng. Geol. 241, 25-32.

Fan, X., Scaringi, G., Korup, O., West, A.J., van Westen, C.J., Tanyas, H., Hovius, N., Hales, T.C., Jibson, R.W., Allsdadt, K.E., Zhang, L., Evans, S.G., Xu, C., Li, G., Pei, X., Xu, Q., Huang, R., 2019. Earthquake-induced chains of geologic hazards: patterns, mechanisms, and impacts. Rev. Geoph. 57 (2), 421-503.

Fedorov, A.A., 1966. The structure of the tropical rain forest and speciation in the humid tropics. J. Ecol. 54 (1), 1-11.

Fekete, A., 2009. Validation of a social vulnerability index in context to river-floods in Germany. Nat. Hazards Earth Syst.Sci. 9, 393–403, http://dx.doi.org/10.5194/nhess-9-393-2009

Felsenstein, D., Lichter, M., 2014. Social and economic vulnerability of coastal communities to sea-level rise and extreme flooding. Nat. Hazards 71 (1) 463–491.

Fichtler, E., Clark, D.A., Worbes, M., 2003. Age and long-term growth of trees in an old-growth tropical rain forest, based on analyses of tree rings and 14C1. Biotropica 35 (3), 306-317.

Fichtler, E., Worbes, M., 2012. Wood anatomical variables in tropical trees and their relation to site conditions and individual tree morphology. IAWA J. 33 (2), 119-140.

Fichtler, E., 2017. Dendroclimatology using tropical broad-leaved tree species–a review. Erdkunde 71 (1), 5-22.

Fielding, J., Burningham, K., 2005. Environmental inequality andflood hazard. Local Environ. 10, 379–395, http://dx.doi.org/10.1080/13549830500160875

Fonti, P., von Arx, G., García-González, I., Eilmann, B., Sass-Klaassen, U., Gärtner, H., Eckstein, D., 2010. Studying global change through investigation of the plastic responses of xylem anatomy in tree rings. New Phytol. 185, 42–53.

Franco-Ramos, O., Ballesteros-Cánovas, J.A., Figueroa-García, J.E., Vázquez-Selem, L., Stoffel, M., Caballero, L., 2020. Modelling the 2012 Lahar in a Sector of Jamapa Gorge (Pico de Orizaba Volcano, Mexico) Using RAMMS and Tree-Ring Evidence. Water 12, 333.

Francon, L., Corona, C., Roussel, E., Lopez-Saez, J., Stoffel, M., 2017. Warm summers and moderate winter precipitation boost Rhododendron ferrugineum L. growth in the Taillefer massif (French Alps). Sci. Total Environ. 586, 1020-1031.

Fritts, H.C., 1971. Dendroclimatology and dendroecology. Quat. Res. 1 (4), 419-449.

Fritts, H.C., 1976. Tree rings and climate. Academic Press. New York. 567 pp.

Fritts, H.C., Swetnam, T.W., 1989. Dendroecology: a tool for evaluating variations in past and present forest environments. In Advances in ecological research (Vol. 19, pp. 111-188). Academic Press.

Froude, M.J., Petley, D.N., 2018. Global fatal landslide occurrence from 2004 to 2016. Nat. Haz. Earth Syst. Sci. 18, 2161-2181.

Gaitan-Alvarez, J., Moya, R., Berrocal, A., 2019. The use of X-ray densitometry to evaluate the wood density profile of Tectona grandis trees growing in fast-growth plantations. Dendrochronologia 55, 71–79.

Gaál, L., Szolgay, J., Kohnová, S., Hlavčová, K., Viglione, A., 2010. Inclusion of historical information in flood frequency analysis using a Bayesian MCMC technique: a case study for the power dam Orlík, Czech Republic. Contributions to Geophysics and Geodesy 40 (2), 121-147.

García-Cervigón, A.I., Camarero, J.J., Cueva, E., Espinosa, C.I., Escudero, A., 2020. Climate seasonality and tree growth strategies in a tropical dry forest. J. Veg. Sci. 31 (2), 266-280.

García-Cervigón, A.I., Gazol, A., Sanz, V., Camarero, J.J., Olano, J.M., 2013. Intraspecific competition replaces interspecific facilitation as abiotic stress decreases: The shifting nature of plant–plant interactions. Perspect. Plant Ecol. 15 (4), 226-236.

Gardner, T.W., Fisher, D.M., Morell, K.D., Cupper, M.L., 2013. Upper-plate deformation in response to flat slab subduction inboard of the aseismic Cocos Ridge, Osa Peninsula, Costa Rica. Lithosphere 5 (3), 247–264.

Garrote, J., Díez-Herrero, A., Génova, M., Bodoque, J., Perucha, M., Mayer, P., 2018. Improving Flood Maps in Ungauged Fluvial Basins with Dendrogeomorphological Data. An Example from the Caldera de Taburiente National Park (Canary Islands, Spain). Geosciences 8 (8), 1-18.

Garrote, J., Gutiérrez-Pérez, I., Díez-Herrero, A., 2019. Can the quality of the potential flood risk maps be evaluated? A case study of the social risks of floods in Central Spain. Water *11* (6), 1284.

Gärtner, H., Schweingruber, F.H., 2013. Microscopic Preparation Techniques for Plant Stem Analysis. Kessel Publishing House, Remagen, Germany. pp. 20.

Gaume, E., 2018. Flood frequency analysis: The Bayesian choice. WIREs Water 5 (4), e1290.

Gebrekirstos, A., Bräuning, A., Sass-Klassen, U., Mbow, C., 2014. Opportunities and applications of dendrochronology in Africa. Curr. Opin. Een. Sust. 6, 48-53.

Giraldo, J.A., del Valle, J.I., Sierra, C.A., Melo, O., 2020. Dendrochronological Potential of Trees from America's Rainiest Region. In Latin American Dendroecology (pp. 79-119). Springer, Cham.

Glas, H., Rocabado, I., Huysentruyt, S., Maroy, E., Salazar Cortez, D., Coorevits, K., De Maeyer, P., Deruyter, G., 2019. Flood Risk Mapping Worldwide: A Flexible Methodology and Toolbox. Water 11 (11), 2371.

Godínez-Rodríguez, K., Arroyo-Solórzano, M., Linkimer-Abarca, L., 2018. Distribución geográfica de los sismos contenidos en el catálogo de la Red Sismológica Nacional de Costa Rica. Rev. Geol. Amér. Cent. 60, 161-188.

Goldenberg, S.B., Landsea, C.W., Mestas-Nuñez, A.M., Gray, W.M., 2001. The recent increase in Atlantic hurricane activity: Causes and implications. Science 293 (5529), 474-479.

Gottesfeld, A.S., Gottesfeld, L.M.J., 1990. Floodplain dynamics of a wandering river: Dendrochronology of the Morice River, British Columbia, Canada. Geomorphology 3, 159–179.

Gottesfeld, A.S., 1996. British Columbia flood scars: Maximum flood-stage indicator. Geomorphology 14, 319–325.

Grace, J.B., 2006. Structural Equation Modeling and Natural Systems. Cambridge University Press, UK.

Groenendijk, P., van der Sleen, P., Vlam, M., Bunyavejchewin, S., Bongers, F., Zuidema, P. A., 2015. No evidence for consistent long-term growth stimulation of 13 tropical tree species: results from tree-ring analysis. Glob. Change Biol. 21 (10), 3762-3776.

Gustavsson, M., Kolstrup, E., Seijmonsbergen, A.C., 2006. A new symbol-and-GIS based detailed geomorphological mapping system: Renewal of a scientific discipline for understanding landscape development. Geomorphology 77 (1–2), 90–111.

Guzzetti, F., Peruccacci, S., Rossi, M., Stark, C.P., 2008. The rainfall intensity–duration control of shallow landslides and debris flows: an update. Landslides 5 (1), 3-17.

Hallé, F., Oldeman, R.A., Tomlinson, P.B., 2012. Tropical trees and forests: an architectural analysis. Springer Science & Business Media.

Hammel, B.E., 2007. Hypericaceae. In: Manual of Plants of Costa Rica. Vol. VI. B.E. Hammel, B.E., Grayum, M.H., Herrera, C., Zamora, N., Troyo, S. (Eds.). Manual de Plantas de Costa Rica Volume VI Dicotyledons (Haloragaceae-Phytolaccaceae). Monogr. Syst. Bot. Missouri Bot. Gard. 111: 26–31.

Hansen, M.C., Potapov, P.V., Moore, R., Hancher, M., Turubanova, S.A., Tyukavina, A., et al., 2013. High-resolution global maps of 21st-century forest cover change. Science 342 (6160), 850-853.

Harris, I., Jones, P.D., Osborn, T.J., Lister, D.H., 2014. Updated high-resolution grids of monthly climatic observations–the CRU TS3. 10 Dataset. Int. J. Climatol. 34 (3), 623-642.

Hastenrath, S., 1973. On the Pleistocene glaciation of the Cordillera de Talamanca, Costa Rica. Zeitschrift für Gletscherkunde und Glazialgeologie 9(1-2), 105-121.

Hastenrath, S., 2009. Past glaciation in the tropics. Quat. Scie. Rev. 28 (9–10), 790–798.

Hettig, E., Lay, J., Sipangule, K., 2016. Drivers of households' land-use decisions: A critical review of micro-level studies in tropical regions. Land 5(4), 32.

Hidalgo, H.G., Durán-Quesada, A.M., Amador, J.A., Alfaro, E.J., 2015. The Caribbean low-level jet, the inter-tropical convergence zone and precipitation patterns in the intra-americas sea: a proposed dynamical mechanism. Geogr. Ann. A. 97, 41–59.

Hobohm, C., 2014. Endemism in vascular plants. Dordrecht: Springer.

Horn, S.P., 1989. Postfire vegetation development in the Costa Rican paramos. Madroño 36, 93–114.

Horn, S.P., 1990. Timing of deglaciation in the Cordillera de Talamanca, Costa Rica. Clim. Res. 1, 81-83.

Horn, S.P., Orvis, K., Haberyan, K., 2005. Limnología de las lagunas glaciales en el páramo del Chirripó, Costa Rica. In: Kappelle, M., Horn, S. P. (Eds.). Páramos de Costa Rica. Santo Domingo de Heredia, Costa Rica: Instituto Nacional de Biodiversidad (INBio). p. 767.

Horn, S.P. 2007. Late Quaternary Lake and Swamp Sediments: Recorders of Climate and Environment. Pp. 423–441. In Bundschuh, J. and Alvarado I., G.E. (Eds.), *Central America: Geology, Resources, Hazards*. Volume 1. Leiden, The Netherlands: Taylor & Francis/Balkema.

Horn, S.P., Haberyan, K.A., 2016. Lakes of Costa Rica. In: Kappelle, M. (Ed.). Costa Rican Ecosystems. p. 744.

Hosking J.R.M., Wallis, J.R., 1997. Regional frequency analysis: an approach based on L-moments. Cambridge University Press, Cambridge, 224 pp.

Hu, P., Zhang, Q., Shi, P., Chen, B., Fang, J., 2018. Flood-induced mortality across the globe: Spatiotemporal pattern and influencing factors. Scie. Total Environ. 643, 171-182.

Huang, B., Thorne, P.W., Banzon, V.F., Boyer, T., Chepurin, G., Lawrimore, J.H., Menne, M.J., Smith, T.M., Vose, R.S., Zhang, H.M., 2017. Extended reconstructed sea surface temperature, version 5 (ERSSTv5): upgrades, validations, and intercomparisons. J. Climate 30 (20), 8179-8205.

Hughes, M.K., 2002. Dendrochronology in climatology–the state of the art. Dendrochronologia 20 (1-2), 95-116.

Hungr, O., Leroueil, S., Picarelli, L., 2014. The Varnes classification of landslide types, an update. Landslides 11 (2), 167-194.

Hupp, C.R., 1988. Plant ecological aspects of flood geomorphology and paleoflood history. Flood Geomorphology. John Wiley & Sons, New York. 1988. p. 335-356.

ICE – Instituto Costarricense de Electricidad, 2018. Flow discharge information of Rivas Station. Centro de Servicios Estudios Básicos de Ingeniería – Hidrología. San José, Costa Rica.

ICE - Instituto Costarricense de Electricidad, 2019. Registro de Caudales. Medios Anuales. Centro de Servicio Estudios Básicos de Ingeniería, Ingeniería & Construcción. San José, Costa Rica.

IMN - Instituto Meteorológico Nacional, 2008. Atlas Climatológico Interactivo. Available on https://www. imn.ac.cr/atlas-climatologico

INEC - Instituto Nacional de Estadística y Censos, 2020. National Population Projections for 2020 based on 2011 National Census. San José, Costa Rica. Available on https://www.inec.cr/poblacion/estimaciones-y-proyecciones-de-poblacion

Inga, J.G., del Valle, J.I., 2017. Log-relative growth: A new dendrochronological approach to study diameter growth in Cedrela odorata and Juglans neotropica, Central Forest, Peru. Dendrochronologia 44, 117-129.

IPCC, 2014. In: Field, C.B., Baros, V., Dokken, D.J., Mach, K.J., Mastrandrea, M.D., Bilir, T.E., Chatterjee, M., Ebi, K.L., Estrada, Y.O., Genova, R.C. (Eds.), Climate Change 2014: Impacts, Adaptation, and Vulnerability. Part A: Global and Sectoral Aspects. Contribution of Working Group II to the Fifth Assessment Report of the Intergovernmental Panel on Climate Change. Cambridge University Press, Cambridge, UK and New York, USA, pp. 1132.

Islam, M., Rahman, M., Bräuning, A., 2018. Long-term hydraulic adjustment of tree tropical moist forest tree species to changing climate. Front. Plant Sci. 4 (9).

Jacoby, G.C., 1989. Overview of tree-ring analysis in tropical regions. IAWA J. 10, 99–108.

Jacquin, P., Longuetaud, F., Leban, J.M., Mothe, F., 2017. X-ray microdensitometry of wood: A review of existing principles and devices. Dendrochronologia 42, 42-50.

Jakobsen, K.T., 2012. In the eye of the storm—The welfare impacts of a hurricane. World Dev. 40 (12), 2578-2589. https://doi.org/10.1016/j.worlddev.2012.05.013

Jamshed, A., Birkmann, J., Rana, I.A., Feldmeyer, D., 2020. The effect of spatial proximity to cities on rural vulnerability against flooding: An indicator based approach. Ecol. Indic. 118, 106704.

Janzen, D.H., 1973. Rate of regeneration after a tropical high elevation fire. Biotropica 5, 117–122.

Jiang, B., 2013. Head/tail breaks: A new classification scheme for data with a heavy-tailed distribution. Prof. Geogr 65 (3), 482-494.

Kanji, M.A., Massad, F., Cruz, P.T., 2003. Debris flows in areas of residual soils: occurrence and characteristics. Int. Workshop on Occurrence and Mechanisms of Flows in Natural Slopes and Earthfills. Iw-Flows2003, Sorrento: Associacione Geotecnica Italiana 2. pp 1–11

Kappelle, M., 2003. Costa Rica. In: R. Hofstede, P. Segarra, and P. Mena (eds). Los Páramos del Mundo: Proyecto Atlas Mundial de los Páramos. Quito, Ecuador: Global Peatland Initiative / NC / IUCN / EcoCiencia, 87–90.

Kappelle, M., 2016. The Montane Cloud Forests of the Cordillera de Talamanca. In: M. Kappelle (Ed.), Costa Rican Ecosystems. University of Chicago Press, Chicago. p. 774.

Kappelle, M., Horn, S.P., 2016. The Páramo Ecosystem of Costa Rica's Highlands. In: Kappelle, M. (Ed.). Costa Rican Ecosystems. p. 744.

Kayano, M.T., Capistrano, V.B., 2014. How the Atlantic multidecadal oscillation (AMO) modifies the ENSO influence on the South American rainfall. Int. J. Climatol. 34(1), 162-178.

Kelman, I., Mercer, J., Gaillard, J.C., 2012. Indigenous knowledge and disaster risk reduction. Geography 97 (1), 12-21.

Kerr, M.T., Horn, S.P., Grissino-Mayer, H.D., Stachowiak, L.A., 2017. Annual growth zones in stems of Hypericum irazuense (Guttiferae) in the Costa Rican páramos. Phys. Geogr. 39 (1), 39-50.

Kirschbaum, D., Stanley, T., Zhou, Y., 2015. Spatial and temporal analysis of a global landslide catalog. Geomorphology 249, 4-15.

Klotzbach, P.J., Gray, W.M., 2008. Multidecadal variability in North Atlantic tropical cyclone activity. J Climate 21 (15), 3929-3935.

Knight, J.R., Folland, C.K., Scaife, A.A., 2006. Climate impacts of the Atlantic multidecadal oscillation. Geophys. Res. Lett. 33(17), 1-4.

Koks, E.E., Jongman, B., Husby, T.G., Botzen, W.J., 2015. Combining hazard, exposure and social vulnerability to provide lessons for flood risk management. Environ. Sci. Policy 47, 42-52.

Korup, O., Densmore, A.L., Schlunegger, F., 2010. The role of landslides in mountain range evolution. Geomorphology 120 (1–2), 77–90.

Krishnaswamy, J., Halpin, P.N., Richter, D.D., 2001a. Dynamics of sediment discharge in relation to land-use and hydro-climatology in a humid tropical watershed in Costa Rica. J. Hydrol. 253, 91-109.

Krishnaswamy, J., Richter, D.D., Halpin, P.N., Hofmockel, M.S., 2001b. Spatial patterns of suspended sediment yields in a humid tropical watershed in Costa Rica. Hydrol. Proc. 15 (12), 2237-2257.

Krishnaswamy, J., Kelkar, N., Birkel, C., 2018. Positive and neutral effects of forest cover on dry-season stream flow in Costa Rica identified from Bayesian regression models with informative prior distributions. Hydrol. Process. 32 (24), 3604-3614.

Kundzewicz, Z.W., Krysanova, V., Benestad, R.E., Hov, Ø., Piniewski, M., Otto, I.M., 2018. Uncertainty in climate change impacts on water resources. Environmental Science & Policy 79, 1-8.

Kuniholm, P.I., 2002. Archaeological dendrochronology. Dendrochronologia 20 (1-2), 63-68.

Kuo, H.L., Lin, G.W., Chen, C.W., Saito, H., Lin, C.W., Chen, H., Chao, W.A., 2018. Evaluating critical rainfall conditions for large-scale landslides by detecting event times from seismic records. Nat. Hazards Earth Syst. Sci. 18, 2877-2891.

Lachniet, M.S., Seltzer, G.O., 2002. Late Quaternary glaciation of Costa Rica. Geol. Soc. Am. Bull. 114 (5), 547-558.

Lachniet, M.S., Seltzer, G.O., Solís, L., 2005. Geología, geomorfología y depósitos glaciares en los páramos de Costa Rica. In: Kappelle, M., Horn, S. P. (Eds). Páramos de Costa Rica. Santo Domingo de Heredia, Costa Rica: Instituto Nacional de Biodiversidad (INBio). p. 767.

Lachniet, M.S., Vázquez-Selem, L., 2005. Last Glacial Maximum equilibrium line altitudes in the circum-Caribbean (Mexico, Guatemala, Costa Rica, Colombia, and Venezuela). Quat. Intl 138–139, 129–144.

Lachniet, M.S., Asmerom, Y., Polyak, V., Bernal, J. P., 2017. Two millennia of Mesoamerican monsoon variability driven by Pacific and Atlantic synergistic forcing. Quat, Scie. Rev. 155, 100-113.

Lacroix, P., Perfettini, H., Taipe, E., Guillier, B., 2014. Coseismic and postseismic motion of a landslide: Observations, modeling, and analogy with tectonic faults. Geoph. Res. Lett. 41 (19), 6676-6680.

Lagadec, A., Boucher, É., Germain, D., 2015. Tree ring analysis of hydro-climatic thresholds that trigger ice jams on the Mistassini River, Quebec. Hydrol. Process. 29 (23), 4880-4890.

Langhammer, J., Vacková, T., 2018. Detection and mapping of the geomorphic effects of flooding using UAV photogrammetry. Pure Appl. Geoph. 175 (9), 3223-3245.

LA RED, 2018. DesInventar – Inventory system of the effects of disasters. Corporación OSSA, Cali, Colombia. Available at: http://desinventar.org, Accessed 15 july 2020.

Larsson, L., 2013. CooRecorder and Cdendro programs of the CooRecorder/Cdendro package version 7.6.

Latte, N., Beeckman, H., Bauwens, S., Bonnet, S., Lejeune, P., 2015. A novel procedure to measure shrinkage-free tree-rings from very large wood samples combining photogrammetry, high-resolution image processing, and GIS tools. Dendrochronologia 34, 24-28.

Lavender, S.L., Walsh, K.J., Caron, L.P., King, M., Monkiewicz, S., Guishard, M., Zhang, Q., Hunt, B., 2018. Estimation of the maximum annual number of North Atlantic tropical cyclones using climate models. Scie. Adv. 4 (8), 1-7.

Lawton, R.O., Lawton, M.F., Lawton, R.M., Daniels, J.D., 2016. The Montane Cloud Forests of the Volcanic Cordilleras. In: M. Kappelle (Ed.), Costa Rican Ecosystems. University of Chicago Press, Chicago. pp 538-588

Lawrence, D., Vandecar, K., 2015. Effects of tropical deforestation on climate and agriculture. Nature Climate Change 5 (1), 27-36.

Lavell, A., Maskrey, A., 2014. The future of disaster risk management. Environ. Hazards 13 (4), 267-280.

Layme-Huaman, E.T., Ferrero, M.E., Palacios-Lazaro, K.S., Requena-Rojas, E.J., 2018. Cedrela nebulosa: A novel species for dendroclimatological studies in the montane tropics of South America. Dendrochronologia 50, 105-112.

Lefcheck, J.S., 2016. piecewiseSEM: piecewise structural equation modelling in R for ecology, evolution, and systematics. Methods Ecol. Evol. 7 (5), 573–579.

Leonard, M., Westra, S., Phatak, A., Lambert, M., van den Hurk, B., McInnes, K., ... Stafford-Smith, M., 2014. A compound event framework for understanding extreme impacts. Wiley Interd. Rev. Clim. Chang. 5 (1), 113-128.

Leopold, L.B., Wolman, M.G., Miller, J.P., 1995. Fluvial processes in geomorphology. Courier Corporation.

Li, Y., Tieche, T., Horn, S.P., Li, Y., Chen, R., Orvis, K.H., 2019. Mapping glacial landforms on the Chirripó massif, Costa Rica, based on Google Earth, a digital elevation model, and field observations. Rev. Geol. Amér. Cent. 60, 109-121.

Lin, G.W., Chen, H., Chen, Y.H., Horng, M.J., 2008a. Influence of typhoons and earthquakes on rainfall-induced landslides and suspended sediments discharge. Eng. Geol. 97 (1-2), 32-41.

Lin, G.W., Chen, H., Hovius, N., Horng, M.J., Dadson, S., Meunier, P., Lines, M., 2008b. Effects of earthquake and cyclone sequencing on landsliding and fluvial sediment transfer in a mountain catchment. Earth Surf. Process. Land. 33, 1354-1373.

Lin, G.W., Chen, H., Shih, T.Y., Lin, S., 2012. Various links between landslide debris and sediment flux during earthquake and rainstorm events. J. Asian Earth Sci. 54, 41-48.

Lin, L., Lin, Q., Wang, Y., 2017. Landslide susceptibility mapping on a global scale using the method of logistic regression. Nat. Haz. Earth System Scie. 17 (8), 1411-1424.

Lindbladh, M., Fraver, S., Edvardsson, J., Felton, A., 2013. Past forest composition, structures and processes - How paleoecology can contribute to forest conservation. Biol. Conserv. 168, 116–127.

Linkimer, L., Arroyo, M., Mora, M., Vargas, A., Soto, G.J., Barquero, R., Rojas, W., Taylor, W., Taylor, M., 2013. El terremoto de Sámara (Costa Rica) del 5 de setiembre del 2012 (Mw 7,6). Rev. Geol. Amér. Cent. 49, 73–82.

Linkimer, L., Arroyo, I.G., Alvarado, G.E., Arroyo, M., Bakkar, H., 2018. The National Seismological Network of Costa Rica (RSN): An Overview and Recent Developments. Seism. Res. Lett. 89 (2A), 392-398.

Lisi, C.S., Fo, M.T., Botosso, P.C., Roig, F.A., Maria, V.R., Ferreira-Fedele, L., Voigt, A.R., 2008. Tree-ring formation, radial increment periodicity, and phenology of tree species from a seasonal semi-deciduous forest in southeast Brazil. IAWA J. 29 (2), 189-207.

Locosselli, G.M., Buckeridge, M.S., Moreira, M.Z., Ceccantini, G., 2013. A multi-proxy dendroecological analysis of two tropical species (Hymenaea spp., Leguminosae) growing in a vegetation mosaic. Trees 27 (1), 25-36.

Madrigal-González, J., Andivia, E., Zavala, M.A., Stoffel, M., Calatayud, J., Sánchez-Salguero, R., Ballesteros-Cánovas, J., 2018. Disentangling the relative role of climate change on tree growth in an extreme Mediterranean environment. Sci. Total Environ. 642, 619-628.

Mainieri, R., Lopez-Saez, J., Corona, C., Stoffel, M., Bourrier, F., Eckert, N., 2019. Assessment of the recurrence intervals of rockfall through dendrogeomorphology and counting scar approach: A comparative study in a mixed forest stand from the Vercors massif (French Alps). Geomorphology 340, 160-171.

Maldonado, T., Rutgersson, A., Alfaro, E., Amador, J., Claremar, B., 2016. Interannual variability of the midsummer drought in Central America and the connection with sea surface temperatures. Adv. in Geoscie. 42, 35-50.

Maldonado, T., Alfaro, E., Hidalgo, H.G., 2018. A review of the main drivers and variability of Central America's Climate and seasonal forecast systems. Rev. Biol. Trop. 66 (1-1), S153-S175.

Marcati, C.R., Machado, S.R., Podadera, D.S., de Lara, N.O.T., Bosio, F., Wiedenhoeft, A.C., 2016. Cambial activity in dry and rainy season on branches from woody species growing in Brazilian Cerrado. Flora 223, 1-10.

Mark, B.G., Harrison, S.P., Spessa, A., New, M., Evans, D.J., Helmens K.F., 2005. Tropical snowline changes at the last glacial maximum: A global assessment. Quat. Intl 138–139, 168–201.

Marshall, J., Fisher, D., Gardner, T., 2000. Central Costa Rica deformed belt: Kinematics of diffuse faulting across the western Panama block. Tectonics 19, 468–492.

Marshall, J., 2007. The Geomorphology and Physiographic Provinces of Central America. In: Bundschuh, J., Alvarado, G E. (Eds.). Central America: Geology, Resources and Hazards. Taylor & Francis. p. 1436.

McCloskey, T.A., Liu, K.B., 2012. A sedimentary-based history of hurricane strikes on the southern Caribbean coast of Nicaragua. Quat. Res. 78 (3), 454-464.

McCord, V.A., 1990. Augmenting flood frequency estimates using flood-scarred trees. PhD Thesis, University of Arizona, Tucson.

McDowell, N., Allen, C.D., Anderson-Teixeira, K., Brando, P., Brienen, R., Chambers, J., et al., 2018. Drivers and mechanisms of tree mortality in moist tropical forests. New Phytol. 219 (3), 851-869.

Medeiros, J.G.S., Tomazello, F.M., Krug, F.J., Vives, A.E.S., 2008. Tree-ring characterization of Araucaria columnaris Hook and its applicability as a lead indicator in environmental monitoring. Dendrochronologia 26 (3), 165–171.

Meko, D.M., Woodhouse, C.A., Morino, K., 2012. Dendrochronology and links to streamflow. J. Hydrol. 412, 200-209.

Méndez, L.F., 1977. Clasificación y caracterización de cinco Andepts de la Cordillera Volcánica de Guanacaste. Tesis Ing. Agrón. Escuela Fitotecnia, Facultad de Agronomía, Universidad de Costa Rica. San José, Costa Rica, 55 p.

Méndez, M., Calvo-Valverde, L.A., Maathuis, B., Alvarado-Gamboa, L.F., 2019. Generation of Monthly Precipitation Climatologies for Costa Rica Using Irregular Rain-Gauge Observational Networks. Water 11 (1), 70.

Metcalf, C.J.E., Horvitz, C.C., Tuljapurkar, S., Clark, D.A., 2009. A time to grow and a time to die: a new way to analyze the dynamics of size, light, age, and death of tropical trees. Ecology 90 (10), 2766-2778.

MIDEPLAN - Ministerio de Planificación Nacional y Política Económica, 2017. Índice de Desarrollo Social 2017. San José, Costa Rica. MIDEPLAN. pp. 126.

Missouri Botanical Garden., 2019. Tropicos Database; www.tropicos.org.

Mitchell, D., Enemark, S., Van der Molen, P., 2015. Climate resilient urban development:
481 Why responsible land governance is important. *Land Use Policy* 48, 190-198.

Monro, A.K., Santamaría-Aguilar, D., González, F., Chacón, O., Solano, D., Rodríguez, A., Zamora, N., Fedele, E., Correa, M., 2017. A first checklist to the vascular plants of La Amistad International Park (PILA), Costa Rica-Panama. Phytotaxa 322 (1), 1–283.

Montero, W., Lewis, J.C., Araya, M.C., 2017. The Guanacaste Volcanic Arc Silver of Northwestern Costa Rica. Sci. Rep. 7:1-9.

Morel, H., Mangenet, T., Beauchêne, J., Ruelle, J., Nicolini, E., Heuret, P., Thibaut, B., 2015. Seasonal variations in phenological traits: leaf shedding and cambial activity in Parkia nitida Miq. and Parkia velutina Benoist (Fabaceae) in tropical rainforest. Trees 29 (4), 973-984.

Morell, K.D., Kirby, E., Fisher, D.M., Soest, M., 2012. Geomorphic and exhumational response of the Central American Volcanic Arc to Cocos Ridge subduction. J Geoph. Res.: Solid Earth 117, 1-23.

Munich RE., 2020. NatCatSERVICE. Natural catastrophe know-how for risk management and research.

Muñoz-Jiménez, R., Giraldo-Osorio, J.D., Brenes-Torres, A., Avendaño-Flores, I., Nauditt, A., Hidalgo-León, H. G., Birkel, C., 2019. Spatial and temporal patterns, trends and teleconnection of cumulative rainfall deficits across Central America. Int. J. Climat. 39 (4), 1940-1953.

Myers-Smith, I.H., Hallinger, M., Blok, D., Sass-Klaassen, U., Rayback, S.A., Weijers, S., Trant, A.J., Tape, K.D., Naito, A.T., Wipf, S., Rixen, C., Dawes, M.A., Wheler, J.A., Buchwal, A., Baittinger, C., Macias-Fauria, M., Forbes, B.C., Lévesque, E., Boulanger-Lapointe, N., Beil, I., Ravolainen, V., Wilmking, M., 2015. Methods for measuring arctic and alpine shrub growth: A review. Earth-Sci. Rev. 140, 1–13.

Nakagawa, S., Schielzeth, H., 2013. A general and simple method for obtaining R2 from generalized linear mixed-effects models. Methods Ecol. Evol. 4 (2), 133–142.

Nardi, F., Grimaldi, S., Santini, M., Petroselli, A., Ubertini, L., 2008. Hydrogeomorphic properties of simulated drainage patterns using digital elevation models: the flat area issue. Hydrolog. Sci. J. 53 (6), 1176–1193. https://doi.org/10.1623/hysj.53.6.1176

Nardi, F., Annis, A., Di Baldassarre, G., Vivoni, E.R., Grimaldi, S., 2019. GFPLAIN250m a global high-resolution dataset of earth's floodplains. Sci. Data 6, 180309.

Nguyen, C.C., Gaume, E., Payrastre, O., 2014. Regional flood frequency analyses involving extraordinary flood events at ungauged sites: further developments and validations. J. Hydrol. 508, 385-396.

Nikolopoulos, E.I., Borga, M., Marra, F., Creutin, J.D., 2015 Estimation of debris flow triggering rainfall: influence of rain gauge density and interpolation methods. Geomorphology 243, 40–50.

NOAA (National Oceanic and Atmospheric Administration), 2017. 2016 Atlantic Hurricane Season, National Hurricane Center, Annual Summary. National Weather Service. URL: http://www.nhc.noaa.gov/data/tcr/summary_atlc_2016.pdf

NOAA – National Oceanic and Atmospheric Administration, 2019. El Niño and La Niña years and intensities based on Oceanic Niño Index (ONI). https://origin.cpc.ncep.noaa.gov/products/analysis_monitoring/ensostuff/ONI_v5.php (accessed 15 April 2019).

NOAA - National Oceanic and Atmospheric Administration, 2019. Cold and Warm Episodes by Season. National Weather Service. Climate Prediction Center. URL: http://www.cpc.ncep.noaa.gov/products/analysis_monitoring/ensostuff/ensoyears.shtml

Noy, I., 2009. The macroeconomic consequences of disasters. J. Develop. Econ. 88 (2), 221-231.

Oliveira, J.M., Santarosa, E., Pillar, V.D., Roig, F.A., 2009. Seasonal cambium activity in the subtropical rain forest tree Araucaria angustifolia. Trees 23 (1), 107-115.

Olson, D.M., Dinerstein, E., Wikramanayake, E.D., Burgess, N.D., Powell, G.V.N., Underwood, E.C., D'Amico, J.A., Itoua, I., Strand, H.E., Morrison, J.C., Loucks, C.J., Allnutt, T.F., Ricketts, T.H., Kura, Y., Lamoreux, J.F., Wettengel, W.W., Hedao, P., Kassem, K.R., 2001. Terrestrial ecoregions of the world: a new map of life on Earth. Bioscience 51 (11),933-938.

Osborn, T.J., Briffa, K.R., Jones, P.D., 1997. Adjusting variance for sample-size in tree-ring chronologies and other regional mean timeseries. Dendrochronologia 15, 89–99.

Orvis, K.H., Horn, S.P., 2000. Quaternary Glaciers and Climate on Cerro Chirripó, Costa Rica. Quat. Res. 54(1), 24–37.

Orvis, K.H., Horn, S.P., 2005. Los glaciares cuaternarios y el clima del cerro Chirripó, Costa Rica. In: Kappelle, M., Horn, S.P. (Eds.). Páramos de Costa Rica. Santo Domingo de Heredia, Costa Rica: Instituto Nacional de Biodiversidad (INBio). p. 767.

Paolini, L., Villalba, R., Grau, H.R., 2005. Precipitation variability and landslide occurrence in a subtropical mountain ecosystem of NW Argentina. Dendrochronologia 22 (3), 175-180.

Papin, P.P., Bosart, L.F., Torn, R.D., 2017. A climatology of Central American gyres. Monthly Weather Review 145 (5), 1983-2000.

Park, K., Lee, M.H., 2019. The development and application of the urban flood risk assessment model for reflecting upon urban planning elements. Water 11 (5), 920.

Pearl, J.K., Keck, J.R., Tintor, W., Siekacz, L., Herrick, H.M., Meko, M.D., Pearson, C.L., 2020. New frontiers in tree-ring research. Holocene 30 (6), 923-941.

Peel, M.C., Finlayson, B.L., McMahon, T.A., 2007. Updated world map of the Köppen– Geiger climate classification. Hydrol. Earth Syst. Sci. 11, 1633–1644.

Perks, M.T., Russell, A.J., Large, A.R., 2016. Advances in flash flood monitoring using unmanned aerial vehicles (UAVs). Hydrol. Earth Syst. Scie. 20 (10), 4005-4015.

Phongsapan, K., Chishtie, F., Poortinga, A., Bhandari, B., Meechaiya, C., Kunlamai, T., San Aung, K., Saah, D., Anderson, E., Markert, K., Markert, A., Towashiraporn, P., 2019. Operational flood risk index mapping for disaster risk reduction using Earth Observations and cloud computing technologies: a case study on Myanmar. Front. Environ. Sci. 7, 191.

Piacentini, T., Carabella, C., Boccabella, F., Ferrante, S., Gregori, C., Mancinelli, V., Pacione, A., Pagliani, T., Miccadei, E., 2020. Geomorphology-Based Analysis of Flood Critical Areas in Small Hilly Catchments for Civil Protection Purposes and Early Warning Systems: The Case of the Feltrino Stream and the Lanciano Urban Area (Abruzzo, Central Italy). Water 12 (8), 2228.

Piciullo, L., Calvello, M., Cepeda, J., 2018. Territorial early warning systems for rainfall-induced landslides. Earth-Sci. Rev. 179, 228-247.

Pinheiro, J., Bates, D., Debroy, S., Sarkar, D., Core Team, R., 2018. nlme: linear and nonlinear mixed effects models. R package version 3.1-131.1. https://CRAN.R-project.org/ package=nlme.

Pinos, J., Orellana, D., Timbe, L., 2020. Assessment of microscale economic flood losses in urban and agricultural areas: case study of the Santa Bárbara River, Ecuador. Natural Hazards 103, 2323-2337.

Pinto Santos, P., Reis, E., Pereira, S., Santos, M., 2019. A flood susceptibility model at the national scale based on multicriteria analysis. Sci. Total Environ. 667, 325-337.

Pinto Santos, P., Pereira, S., Zêzere, J.L., Tavares, A.O., Reis, E., Garcia, R.A., Oliveira, S.C., 2020. A comprehensive approach to understanding flood risk drivers at the municipal level. J. Environ. Manage. 260, 110127.

Poage, N.J., Tappeiner, II, J.C., 2002. Long-term patterns of diameter and basal area growth of old-growth Douglas-fir trees in western Oregon. Can. J. Forest Res. 32 (7), 1232-1243.

Polvi, L.E., Wohl, E., Merritt, D.M., 2014. Modeling the functional influence of vegetation type on streambank cohesion. Earth Surf. Proc. Landf. 39 (9), 1245-1258.

Pompa-García, M., Camarero, J., 2020. Latin American Dendroecology. Springer. pp. 381.

Porras, J.L., Linkimer, L., Araya, M.C., Arroyo, M., Taylor, M., Rojas, W., 2017. Sismicidad registrada por la RSN en el 2016. Rev. Geol. Amér. Cent. 56, 117-128.

Porter, S.C., 2001. Snowline depression in the tropics during the last glaciation. Quat. Scie. Rev. 20 (10), 1067–1091.

Potter, R.S., Li, Y., Horn, S.P., Orvis, K.H., 2019. Cosmogenic Cl-36 surface exposure dating of late Quaternary glacial events in the Cordillera de Talamanca, Costa Rica. Quat. Res., 92 (1), 216-231.

Pourali, S.H., Arrowsmith, C., Chrisman, N., Matkan, A.A., Mitchell, D., 2016. Topography wetness index application in flood-risk-based land use planning. Appl. Spat. Anal. Policy 9 (1), 39-54.

Pumijumnong, N., 2013. Dendrochronology in Southeast Asia. Trees 27 (2), 343-358.

Pumijumnong, N., Buajan, S., 2013. Seasonal cambial activity of five tropical tree species in central Thailand. Trees 27 (2), 409-417.

Quesada-Hernández, L.E., Calvo-Solano, O.D., Hidalgo, H.G., Perez-Briceno, P.M., Alfaro, E.J., 2019. Dynamical delimitation of the Central American Dry Corridor (CADC) using drought indices and aridity values. Prog. Phys. Geogr. 43 (5), 627-642.

Quesada-Román, A., 2016. Peligros geomorfológicos: inundaciones y procesos de ladera en la cuenca alta del río General (Pérez Zeledón), Costa Rica. Maestría en Geografía con énfasis en Geografía Ambiental. Posgrado en Geografía. Universidad Nacional Autónoma de México. 157 p.

Quesada-Román, A., Barrantes, G., 2016. Procesos de ladera cosísmicos del terremoto de Cinchona (Costa Rica) del 8 de enero de 2009 (Ms= 6,2). Cuad. Geog.: Rev. Colom. Geog. 25 (1), 217-232.

Quesada-Román, A., 2016. Impactos geomorfológicos del Terremoto de Limón (1991; ms=7.5) y consideraciones para la prevención de riesgos asociados en Costa Rica. Rev. Geog. Amér. Cent. 56, 93-111.

Quesada-Román, A., 2017. Geomorfología Fluvial e Inundaciones en la Cuenca Alta del Río General, Costa Rica. Anuá. Inst. Geociê. 40(2), 278-288.

Quesada-Román, A., Zamorano-Orozco, J.J., 2018a. Geomorphology of the Upper General River Basin, Costa Rica. J. Maps 15 (2), 95-101.

Quesada-Román, A., Zamorano-Orozco, J.J., 2018b. Peligros Geomorfológicos en Costa Rica: Cuenca Alta del Río General. Anuá. Inst. Geociê. 41 (3), 239-251.

Quesada-Román, A., Fallas-López, B., Hernández-Espinoza, K., Stoffel, M., Ballesteros-Cánovas, J.A., 2019a. Relationships between earthquakes, hurricanes, and landslides in Costa Rica. Landslides 16 (8), 1539-1550.

Quesada-Román, A., Stoffel, M., Ballesteros-Cánovas, J.A., Zamorano-Orozco, J.J., 2019b. Glacial geomorphology of the Chirripó National Park, Costa Rica. J. Maps 15 (2), 538–545.

Quesada-Román, A., Zamorano-Orozco, J.J., 2019a. Geomorphology of the Upper General River Basin, Costa Rica. J. Maps 15 (2), 95-101.

Quesada-Román, A., Zamorano-Orozco, J.J., 2019b. Zonificación de procesos de ladera e inundaciones a partir de un análisis morfométrico en la cuenca alta del río General, Costa Rica. Inv. Geog. 99, 1-19.

Quesada-Román, A., Ballesteros-Cánovas, J.A., Granados-Bolaños, S., Birkel, C., Stoffel, M., 2020a. Dendrogeomorphic reconstruction of floods in a dynamic tropical river. Geomorphology 359, 107133.

Quesada-Román, A., Ballesteros-Cánovas, J.A., Guillet, S., Madrigal-González, J., Stoffel, M., 2020b. Neotropical Hypericum irazuense shrubs reveal recent ENSO variability in Costa Rican páramo. Dendrochronologia 61, 125704.

Quesada-Román, A., Campos, N., Alcalá-Reygosa, J., Granados-Bolaños, S., 2020c. Equilibrium-line altitude and temperature reconstructions during the Last Glacial Maximum in Chirripó National Park, Costa Rica. J. S. Am. Earth Sci. 100, 102576.

Quesada-Román, A., Villalobos-Portilla, E., Campos-Durán, D., 2020d. Hydrometeorological disasters in urban areas of Costa Rica, Central America. Environ. Hazards. https://doi.org/10.1080/17477891.2020.1791034

Quesada-Román, A., Mata-Cambronero, E., 2020. The geomorphic landscape of the Barva volcano, Costa Rica. Phys. Geogr. https://doi.org/10.1080/02723646.2020.1759762

Quesada-Román, A., Pérez-Umaña, D., 2020. State of the Art of Geodiversity, Geoconservation, and Geotourism in Costa Rica. *Geosciences* 10 (6), 211. https://doi.org/10.3390/geosciences10060211

Quesada-Román, A., Villalobos-Chacón, A., 2020. Flash flood impacts of Hurricane Otto and hydrometeorological risk mapping in Costa Rica. Geogr. Tidsskr. https://doi.org/10.1080/00167223.2020.1822195

Rahman, M., Islam, M., Bräuning, A., 2017. Local and regional climatic signals recorded in tree-rings of Chukrasia tabularis in Bangladesh. Dendrochronologia 45, 1-11.

Rahman, M., Islam, M., Bräuning, A., 2019. Species-specific growth resilience to drought in a mixed semi-deciduous tropical moist forest in South Asia. For. Ecol. Manag. 433, 487–496.

Raymond, C., Horton, R. M., Zscheischler, J., Martius, O., AghaKouchak, A., Balch, J., Bowen, S.G., Camargo, S.J., Hess, J., Kornhuber, K., Oppenheimer, M., Ruane, A.C., Wahl, T., White, K., 2020. Understanding and managing connected extreme events. Nat. Clim. Chang. 10, 611-621.

REDD/CCAD-GIZ - SINAC., 2015. Inventario Nacional Forestal de Costa Rica 2014-2015 [National Forestry Inventory of Costa Rica 2014-2015]. Programa Reducción de Emisiones por Deforestación y Degradación Forestal en Centroamérica y la República Dominicana (REDD/CCAD/GIZ) y Sistema Nacional de Áreas de Conservación (SINAC) Costa Rica. San José, Costa Rica. p. 380.

Reichenbach, P., Rossi, M., Malamud, B., Mihir, M., Guzzetti, F., 2018. A review of statistically-based landslide susceptibility models. Earth-Sci. Rev. 180, 60-91.

Reis Jr, D.S., Stedinger, J.R., 2005. Bayesian MCMC flood frequency analysis with historical information. J. Hydrology 313 (1-2), 97-116.

Reynolds, R.W., Rayner, N.A., Smith, T.M., Stokes, D.C., Wang, W., 2002. An improved in situ and satellite SST analysis for climate. J. Climate 15, 1609-1625.

Ripple, W. J., Wolf, C., Newsome, T. M., Barnard, P., & Moomaw, W. R. (2019). World Scientists ' Warning of a Climate Emergency. BioScience 70 (1), 8–12.

Robert, E.M.R., Schmitz, N., Okello, J.A., Boeren, I., Beeckman, H., Koedam, N., 2011. Mangrove growth rings: Fact or fiction? Trees, 25(1), 49–58.

Robson, N.K.B., 1987. Studies in the genus Hypericum L. (Guttiferae). 7. Section 29. Brathys (part 1). Bull. Brit. Mus. 16, 1–106.

Robson, N.K.B., 2003. Hypericum botany. In E. Ernst (Ed). Hypericum: the genus Hypericum. CRC Press.

Rodriguez-Morata, C., Ballesteros-Cánovas J.A., Trappmann, D., Beniston, M., Stoffel, M., 2016. Regional reconstruction of flash flood history in the Guadarrama range (Central System, Spain). Scie. Total Environ. 550, 406–417.

Rodríguez-Morata, C., Ballesteros-Cánovas, J. A., Rohrer, M., Espinoza, J. C., Beniston, M., Stoffel, M., 2018. Linking atmospheric circulation patterns with hydro-geomorphic disasters in Peru. Int. J. Climatol. 38 (8), 3388-3404.

Rodriguez-Morata, C., Ballesteros-Cánovas, J.A., Madrigal, J., Stoffel, M., 2020. Global warming impairs tree growth in a Neotropical high mountain forest in the Peruvian Andes. iForest 13 (3), 194-201.

Rodríguez-Ramírez, E.C., Luna-Vega, I., 2020. Dendroecology as a Research Tool to Investigate Climate Change Resilience on Magnolia vovidesii, a Threatened Mexican Cloud Forest Tree Species of Eastern Mexico. In Latin American Dendroecology (pp. 3-20). Springer, Cham.

Roig, F.A., Osornio, J.J.J., Diaz, J.V., Luckman, B., Tiessen, H., Medina, A., Noellemeyer, E.J., 2005. Anatomy of growth rings at the Yucatán Peninsula. Dendrochronologia 22 (3), 187-193.

Rozendaal, D.M., Zuidema, P.A., 2011. Dendroecology in the tropics: a review. Trees 25 (1), 3-16.

Rufat, S., Tate, E., Burton, C.G., Maroof, A.S., 2015. Social vulnerability to floods: Review of case studies and implications for measurement. Int. J. Disaster Risk Reduc. 14, 470-486.

Ruiz-Villanueva, V., Díez-Herrero, A., Bodoque, J.M., Ballesteros, J.A., Stoffel, M., 2013. Characterization of flash floods in small ungauged mountain basins of central Spain using an integrated approach. Catena 110, 32–43.

Ruiz-Villanueva, V., Piégay, H., Gurnell, A.M., Marston, R.A., Stoffel, M., 2016. Recent advances quantifying the large wood dynamics in river basins: New methods and remaining challenges. Rev. Geoph. 54 (3), 611–652.

Sáenz, M., Alvarado, A., Ureña, H., 1993. Suelos del Área de Conservación Arenal, Guanacaste, Costa Rica. Proyecto de Conservación y Desarrollo de Arenal. Convenio MIRENEM/ACDI/WWF/CANADA. 68 p.

Saito, H., Uchiyama, S., Hayakawa, Y.S., Obanawa, H., 2018. Landslides triggered by an earthquake and heavy rainfalls at Aso volcano, Japan, detected by UAS and SfM-MVS photogrammetry. Prog. Earth and Plan. Sci. 5 (1), 5-15.

Samia, J., Temme, A., Bregt, A.K., Wallinga, J., Stuiver, J., Guzzetti, F., Ardizzone, F., Rossi, M., 2018. Implementing landslide path dependency in landslide susceptibility modelling. Landslides 15 (11), 2129-2144.

Sánchez-Asunción, W., Cerano-Paredes, J., Franco-Ramos, O., Cornejo-Oviedo, E., Villanueva-Díaz, J., Flores-López, C., Garza-Martínez, M., 2020. Dendrogeomorphological potential of Pinus ponderosa Douglas ex C. Lawson for the reconstruction of flash floods in Los Picos de Davis, Coahuila. Rev. Chapingo, Ser. Cienc. For. y del Ambient. 26(3), 451–467.

Sass-Klaassen, U., 2002. Dendroarchaeology: Successes in the past - challenges for the future. Dendrochronologia 20 (1-2), 87-95.

Sassa, K., Fukuoka, H., Wang, F., Wang, G., 2007. Landslides induced by a combined effect of earthquake and rainfall. In: Progress in Landslide Science (pp. 193-207). Springer, Berlin, Heidelberg.

Saunders, M.A., Lea, A.S., 2008. Large contribution of sea surface warming to recent increase in Atlantic hurricane activity. Nature 451, 557-560.

Savi, S., Schneuwly-Bollschweiler, M., Bommer-Denns, B., Stoffel, M., Schlunegger, F., 2013. Geomorphic coupling between hillslopes and channels in the Swiss Alps. Earth Surf. Process. Land. 38, 959–969.

Scatena, F.N., Lugo, A.E., 1995. Geomorphology, disturbance, and the soil and vegetation of two subtropical wet steepland watersheds of Puerto Rico. Geomorphology 13 (1-4), 199-213.

Schauwecker, S., Gascón, E., Park, S., Ruiz-Villanueva, V., Schwarb, M., Sempere-Torres, D., Stoffel, M., Vitolo, C., Rohrer, M., 2019 Anticipating cascading effects of extreme precipitation with pathway schemes – Three case studies from Europe. Env. Int. 127, 291–304.

Shi, P., Karsperson, R. (eds.). 2015. World atlas of natural disaster risk. Heidelberg: Springer.

Schlaepfer, M.A., 2018. Do non-native species contribute to biodiversity? PLoS Biol. 16 (4), e2005568.

Schöngart, J., Bräuning, A., Campos-Barbosa, A.C.M., Lisi, C.S., Morales de Oliveira, J., 2017. Dendroecological studies in the neotropics: history, status and future challenges. In M.M. Amoroso, L.D. Daniels, P.J. Baker, J.J. Camarero (Eds), Dendroecology: Tree-Ring Analyses Applied to Ecological Studies, Springer, Switzerland. 35-73 pp.

Schöngart, J., Piedade, M. T. F., Ludwigshausen, S., Horna, V., Worbes, M., 2002. Phenology and stem-growth periodicity of tree species in Amazonian floodplain forests. J. Trop. Ecology 18, 581-597.

Schulman, E., 1944. Dendrochronology in Mexico, I. Tree-Ring Bulletin 10 (3), 18-24.

Schulman, E., 1956. Dendroclimatic changes in semiarid America. University of Arizona Press.

Schweingruber, F., Eckstein, D., Serre-Bachet, F., Bräker, O.U., 1990. Identification, presentation and interpretation of event years and pointer years in dendrochronology. Dendrochronologia 8, 9–39.

Schweingruber, F.H., 1996. Tree rings and environment: dendroecology. Paul Haupt AG Bern.

Schweingruber F., Poschlod P., 2005. Growth rings in herbs and shrubs: life span, age determination and stem anatomy. For. Snow Lands. Res. 79 (3), 195–415.

Segoni, S., Piciullo, L., Gariano, S.L., 2018. A review of the recent literature on rainfall thresholds for landslide occurrence. Landslides 15, 1483–1501.

Seguel, O., Horn, R., 2005. Mechanical behavior of a volcanic ash soil (Typic Hapludand) under static and dynamic loading. Soil & Till Res. 82, 109-116.

Shi, P., Karsperson, R. (eds.). 2015. World atlas of natural disaster risk. Heidelberg: Springer.

Shi, P., Yang, X., Xu, W., 2016. Mapping global mortality and affected population risks for multiple natural hazards. Int. J. Disaster Risk Scie. 7 (1), 54-62.

Shimizu, C., 1992. Glacial landforms around Cerro Chirripó in Cordillera de Talamanka, Costa Rica. J. Geography [Japan] 101, 615–621.

Shroder, J.F., 1978. Dendrogeomorphological analysis of mass movement on Table Cliffs Plateau, Utah. Quat. Res. 9, 168–185.

Shroder, J.F., 1980. Dendrogeomorphology: review and new techniques of tree-ring dating. Prog Phys Geogr. 4 (2), 161-188.

Sidle, R.C., Bogaard, T.A., 2016. Dynamic earth system and ecological controls of rainfall-initiated landslides. Earth-Sci. Rev. 159, 275–291.

Sidle, R.C., Gomi, T., Usuga, J.C.L., Jarihani, B., 2017. Hydrogeomorphic processes and scaling issues in the continuum from soil pedons to catchments. Earth-Sci. Rev. 175, 75-96.

Sidle, R.C., Onda, Y., 2004. Hydrogeomorphology: overview of an emerging science. Hydrol. Process. 18(4), 597-602.

Sigafoos, R.S., 1964. Botanical evidence of floods and flood-plain deposition. Professional Paper, 485A. United States Geological Survey. p. 35.

Šilhán, K., 2020. Dendrogeomorphology of landslides: principles, results and perspectives. Landslides, 1-21. https://doi.org/10.1007/s10346-020-01397-4

Silva, M.S., Santos, F.A.R., Callado, C.H., Barros, C.F., Silva, L.B., 2017. Growth rings in woody species of Ombrophilous Dense Forest: occurrence, anatomical features and ecological considerations. Brazilian Journal of Botany 40, 281–290.

Silva, M.D.S., Funch, L.S., da Silva, L.B., 2019. The growth ring concept: seeking a broader and unambiguous approach covering tropical species. Biol. Rev. 94 (3), 1161-1178.

Simon, A., Collison, A.J.C., 2002. Quantifying the mechanical and hydrologic effects of riparian vegetation on streambank stability. Earth Surf. Proc. Landf. 27, 527–546.

Slaymaker, O., Embleton-Hamann, C., 2018. Advances in global mountain geomorphology. Geomorphology 308, 230–264.

Slik, J.F., Arroyo-Rodríguez, V., Aiba, S.I., Alvarez-Loayza, P., Alves, L.F., Ashton, P., et al., 2015. An estimate of the number of tropical tree species. Proc. Natl. Acad. Sci. U.S.A. 112 (24), 7472-7477.

Smith, M.J., Paron, P., Griffiths, J.S., 2011. Geomorphological mapping: Methods and Applications. (Vol. 15). Elsevier.

Smith, D.G., Reynolds, D.M., 1983. Trees scars to determine the frequency and stage of high magnitude river ice drives and jams, Red Deer, Alberta. Canad. Water Res. J. 8 (3), 77-94.

Sörensen, R., Zinko, U., Seibert, J., 2006. On the calculation of the topographic wetness index: evaluation of different methods based on field observations. Hydrol. Earth Syst. Sci. 10, 101–112.

Spannl, S., Homeier, J., Bräuning, A., 2016. Nutrient-induced modifications of wood anatomical traits of Alchornea lojaensis (Euphorbiaceae). Front. Earth Scie. 4, 50.

Speer, J.H., 2010. Fundamentals of Tree-Ring Research. University of Arizona Press, Tucson, pp. 333.

Speer, J.H., Shah, S.K., Truettner, C., Pacheco, A., Bekker, M.F., Dukpa, D., Cook, E.J., Tenzin, K., 2019. Flood History and River Flow Variability Recorded in Tree Rings on the Dhur River, Bhutan. Dendrochronologia 56, 125605.

Spielman, S.E., Tuccillo, J., Folch, D.C., Schweikert, A., Davies, R., Wood, N., Tate, E., 2020. Evaluating social vulnerability indicators: criteria and their application to the Social Vulnerability Index. Nat. Hazards 100 (1), 417-436.

Stahle, D.W., Cook, E.R., Burnette, D.J., Villanueva, J., Cerano, J., Burns, J.N., Griffin, R.D. Cook, B.I., Acuna, R., Torbenson, M.C.A., Szejner, P. 2016. The Mexican Drought Atlas: Tree-ring reconstructions of the soil moisture balance during the late Pre-Hispanic, Colonial, and Modern Eras. Quat. Sci. Rev. 149, 34-60.

Stallins, J.A., Corenblit, D., 2018. Interdependence of geomorphic and ecologic resilience properties in a geographic context. Geomorphology 305, 76-93.

Stephens, T.A., Bledsoe, B.P., 2020. Probabilistic mapping of flood hazards: Depicting uncertainty in streamflow, land use, and geomorphic adjustment. Anthropocene 29, 100231.

St. George, S., 2010. Tree Rings as Paleoflood and Paleostage Indicators. In: Tree rings and natural hazards (pp. 233-239). Springer, Dordrecht.

St George, S., 2014. An overview of tree-ring width records across the Northern Hemisphere. Quat. Sci. Rev. 95, 132-150.

Stoffel, M., Bollschweiler, M., 2008. Tree-ring analysis in natural hazards research–an overview. Nat. Hazards Earth Syst. Sci. 8 (2), 187-202.

Stoffel, M., Butler, D.R., Corona, C., 2013. Mass movements and tree rings: A guide to dendrogeomorphic field sampling and dating. Geomorphology 200, 106-120.

Stoffel, M., Corona, C., 2014. Dendroecological dating of geomorphic disturbance in trees. Tree-ring Res. 70 (1), 3-20.

Stoffel, M., Corona, C., Ballesteros-Cánovas, J.A., Bodoque, J.M., 2013. Dating and quantification of erosion processes based on exposed roots. Earth-Sci. Rev. 123, 18-34.

Stoffel, M., Huggel, C., 2012. Effects of climate change on mass movements in mountain environments. Prog. Phys. Geog. 36 (3), 421-439.

Stoffel, M., Wilford, D.J., 2012. Hydrogeomorphic processes and vegetation: disturbance, process histories, dependencies and interactions. Earth Surf. Proc. Landf. 37, 9-22.

Sun, C., Kucharski, F., Li, J., Jin, F.F., Kang, I.S., Ding, R., 2017. Western tropical Pacific multidecadal variability forced by the Atlantic multidecadal oscillation. Nature Commun 8(1), 1-10.

Syvitski, J.P.M., Cohen, S., Kettner, A.J., Brakenridge, G.R., 2014. How important and different are tropical rivers? - An overview. Geomorphology 227, 5–17.

Tang, C., Zhu, J., Qi, X., Ding, J., 2011. Landslides induced by the Wenchuan earthquake and the subsequent strong rainfall event: A case study in the Beichuan area of China. Eng. Geol. 122 (1-2), 22-33.

Tapsell, S.M., Penning-Rowsell, E.C., Tunstall, S.M., Wilson, T.L., 2002. Vulnerability to flooding: health and socialdimensions. Philos. Trans. R. Soc. Lond. Ser. A: Math. Phys.Eng. Sci. 360, 1511–1525.

Tarelkin, Y., Delvaux, C., De Ridder, M., El Berkani, T., De Cannière, C., Beeckman, H., 2016. Growth-ring distinctness and boundary anatomy variability in tropical trees. IAWA J. 37 (2), 275-S7.

Tate, E., 2012. Social vulnerability indices: a comparative assessment using uncertainty and sensitivity analysis. Nat. Hazards 63 (2), 325-347.

Tatem, A.J., 2017. WorldPop, open data for spatial demography. Scientific Data 4, 1-4.

Taylor, M., Alfaro, E., 2005. Climate of Central America and the Caribbean. In: J Oliver (Ed) Encyclopedia of World Climatology. Springer, Netherlands: pp 183-189

Taylor, W., Chaves, J.E., Bakkar, H.H., 2016. Informe preliminar sobre el sismo de Bijagua de Upala 2016 (5,4 Mw), Costa Rica. San José: Instituto Costarricense de Electricidad. Informe interno.

Tennille, S.A., Ellis, K.N., 2017. Spatial and temporal trends in the location of the lifetime maximum intensity of tropical cyclones. Atmosphere 8 (10), 198.

Trauth, M.H., Sillmann, E., 2018. Collecting, Processing and Presenting Geoscientific Information. Springer-Verlag GmbH Germany.

Turner, D., Lucieer, A., Watson, C., 2012. An Automated Technique for Generating Georectified Mosaics from Ultra-High Resolution Unmanned Aerial Vehicle (UAV) Imagery, Based on Structure from Motion (SfM) Point Clouds. Remote Sensing, 4 (5), 1292-1410.

UNDRR – United Nations Disaster Risk Reduction, 2019. Global Assessment Report on Disaster Risk Reduction. United Nations Office for Disaster Risk Reduction (UNDRR). Geneva, Switzerland.

UNISDR – United Nations Disaster Risk Reduction, 2009. Global Assessment Report on Disaster Risk Reduction. United Nations Office for Disaster Risk Reduction (UNDRR). Geneva, Switzerland.

UNISDR, 2015. Sendai Framework for Disaster Risk Reduction 2015 - 2030. In: Third World Conference on Disaster Risk Reduction, Sendai, Japan, 14-18 March 2015.

Van Camp, J., Hubeau, M., Van den Bulcke, J., Van Acker, J., Steppe, K., 2018. Cambial pinning relates wood anatomy to ecophysiology in the African tropical tree *Maesopsis eminii*. Tree Physiology *38* (2), 232-242.

van der Maaten-Theunissen, M., van der Maaten, E., Bouriaud, O., 2015. pointRes: An R package to analyze pointer years and components of resilience. Dendrochronologia 35, 34-38.

Van Lidth de Jeude, M., Schütte, O., Quesada, F., 2016. The vicious circle of social segregation and spatial fragmentation in Costa Rica's greater metropolitan area. Habitat Int. 54, 65-73.

Vargas-Zeppetello, L., Parsons, L., Spector, J., Naylor, R., Battisti, D., Masuda, Y., Wolff, N.H., 2020. Large scale tropical deforestation drives extreme warming. Environmental Research Letters 15(8), 84012.

Vázquez-Selem, L., Lachniet, M.S., 2017. The deglaciation of the mountains of Mexico and Central America. Cuad. Inv. Geog. 43 (2), 553–570.

Veas-Ayala, N., Quesada-Román, A., Hidalgo, H., Alfaro, E.J., 2018. Humedales del Parque Nacional Chirripó, Costa Rica: características, relaciones geomorfológicas y escenarios de cambio climático. Rev. Biol. Trop. 66 (4), 1436–1448.

Verstappen, H.T., Zuidam, R.V., Meijerink, A.M.J., Nossin, J.J., 1991. The ITC System of Geomorphologic Survey: A Basis for the Evaluation of Natural Resources and Hazards. ITC: Enschede, The Netherlands. p. 89.

Victoriano, A., Díez-Herrero, A., Génova, M., Guinau, M., Furdada, G., Khazaradze, G., Calvet, J., 2018. Four-topic correlation between flood dendrogeomorphological evidence and hydraulic parameters (the Portainé stream, Iberian Peninsula). Catena 162, 216-229.

Viglione, A., 2013. Non-supervised regional frequency analysis R library, http://cran.r-project.org/web/packages/nsRFA/.

Volland-Voigt, F., Bräuning, A., Ganzhi, O., Peters, T., Maza, H., 2011. Radial stem variations of Tabebuia chrysantha (Bignoniaceae) in different tropical forest ecosystems of southern Ecuador. Trees 25 (1), 39-48.

Wallemacq, P., House, R., 2018. Economic losses, poverty & disasters. Centre for Research on the Epidemiology of Disasters and United Nations Office for Disaster Risk Reduction. Geneva, Switzerland. pp 1-30

Walsh, K.J., McBride, J.L., Klotzbach, P.J., Balachandran, S., Camargo, S.J., Holland, G., Knutson, T.R., Kossin, J.P., Tz.cheung, L., Sobel, A., Sugi, M., 2016. Tropical cyclones and climate change. Wiley Interdiscip. Rev. Clim. Change 7 (1), 65-89.

Wang, C., Enfield, D.B., Lee, S.K., Landsea, C.W., 2006. Influences of Atlantic Warm Pool on western hemisphere summer rainfall and Atlantic Hurricanes. J of Clim 19:3011-3028.

Wang, B., Liu, J., Kim, H.J., Webster, P.J., Yim, S.Y., Xiang, B., 2013. Northern Hemisphere summer monsoon intensified by mega-El Niño/southern oscillation and Atlantic multidecadal oscillation. Proc. Natl. Acad. Sci. U.S.A. 110(14), 5347-5352.

Waylen, P.R., Caviedes, C.N., Quesada, M.E., 1996. Interannual variability of monthly precipitation in Costa Rica. J. Climate 9 (10), 2606-2613.

Waylen, P., Laporte, S., 1999. Flooding and the El Niño-Southern Oscillation phenomenon along the Pacific coast of Costa Rica. Hydrol. Process. 13 (16), 2623-2638.

Webb, R.H., Jarrett, R.D., 2002. One-dimensional estimation techniques for discharges of paleofloods and historical floods. In: House P.K., Webb, R.H., Baker, V.R., Levish, D.R. (eds). Ancient Floods, Modern Hazards: Principles and Applications of Paleoflood Hydrology: Water Science and Application. Vol. 5. American Geophysical Union, Washington, D.C. pp. 111–126.

Weberling, F., Furchheim-Weberling, B., 2005. El mosaico de formas de crecimiento en los páramos de Costa Rica. In: M. Kappelle and S.P. Horn (Eds.)., Páramos de Costa Rica. Santo Domingo de Heredia, INBio Press. pp. 437–473.

Weyl, R., 1955. Contribución a la geología de la Cordillera de Talamanca. Instituto Geográfico Nacional: San José, Costa Rica. p. 77.

Wheaton, J.M., Fryirs, K.A., Brierley, G., Bangen, S.G., Bouwes, N., O'Brien, G., 2015. Geomorphic mapping and taxonomy of fluvial landforms. Geomorphology 248, 273–295.

Wieczorek, G.F., Glade, T., 2005. Climatic factors influencing occurrence of debris flows. In: M. Jakob and O. Hungr. Debris-flow Hazards and Related Phenomena. Springer Berlin Heidelberg. pp 325-362

Wilhelm, B., Ballesteros Cánovas, J.A., Macdonald, N., Toonen, W.H., Baker, V., Barriendos, M., Benito, G., Brauer, A., Corella, J.P., Denniston, R., Glaser, R., Ionita, M., Kahle, M., Liu, T., Luetscher, M., Macklin, M., Mudelsee, M., Munoz, S., Schulte, L., St. George, S., Stoffel, M., Wetter, O., 2019. Interpreting historical, botanical, and geological evidence to aid preparations for future floods. Wiley Interd. Rev.: Water 6 (1), e1318.

Williamson, G.B., Schatz, G.E., Alvarado, A., Redhead, C.S., Stam, A.C., Sterner, R.W., 1986. Effects of repeated fires on tropical paramo vegetation. Trop. Ecol. 27, 62–69.

Wils, T.H., Robertson, I., Eshetu, Z., Sass-Klaassen, U.G., Koprowski, M., 2009. Periodicity of growth rings in Juniperus procera from Ethiopia inferred from crossdating and radiocarbon dating. Dendrochronologia 27 (1), 45-58.

Wils, T.H., Robertson, I., Eshetu, Z., Touchan, R., Sass-Klaassen, U., Koprowski, M., 2011. Crossdating Juniperus procera from North Gondar, Ethiopia. Trees 25 (1), 71-82.

Wistuba, M., Malik, I., Badura, J., 2019. Tree rings as an early warning against catastrophic landslides: Assessing the potential of dendrochronology for determining slope stability. Dendrochronologia 53, 82-94.

Wohl, E., 2006. Human impacts to mountain streams. Geomorphology 79 (3–4), 217–248.

Wohl, E., 2008. Hydrology and discharge. In: A. Gupta, (Ed.). Large rivers: Geomorphology and management. John Wiley & Sons, pp. 29-44.

Wohl, E., Barros, A., Brunsell, N., Chappell, N.A., Coe, M., Giambelluca, T., Goldsmith, S., Harmon, R., Hendrickx, J.M.H., Juvik, J., McDonnell, J., Ogden, F., 2012. The hydrology of the humid tropics. Nature Climate Change 2 (9), 655-662.

Wohl, E., Lininger, K.B., Fox, M., Baillie, B.R., Wayne, D., Erskine, D., 2017. Instream large wood loads across bioclimatic regions. For. Ecol. Man. 404, 370-380.

Wohl, E., Hinshaw, S.K., Scamardo, J.E., Gutiérrez-Fonseca, P.E., 2019. Transient organic jams in Puerto Rican mountain streams after hurricanes. River Res. Appl. 35 (3), 280-289.

Worbes, M., 1989. Growth rings, increment and age of trees in inundation forests, savannas and a mountain forest in the Neotropics. IAWA J. 10 (2), 109-122.

Worbes, M., 1995. How to measure growth dynamics in tropical trees a review. IAWA J. 16 (4), 337-351.

Worbes, M., Junk, W.J., 1999. How old are tropical trees? The persistence of a myth. IAWA J. 20 (3), 255-260.

Worbes, M., 2002. One hundred years of tree-ring research in the tropics–a brief history and an outlook to future challenges. Dendrochronologia 20 (1-2), 217-231.

Worbes, M., 2010. Wood anatomy and tree-ring structure and their importance for tropical dendrochronology. In: Junk, W.J., Piedade, M., Wittman, F., Schöngart, J., Parolin, P. (Eds) Amazonian Floodplain Forests. Springer, Dordrecht. 329-346 pp.

Worbes, M., Fichtler, E., 2010. Wood anatomy and tree–ring structure and their importance for tropical dendrochronology. In: Junk, W.J., Piedade, M., Wittman, F., Schöngart, J., Parolin, P. (Eds) Amazonian Floodplain Forests. Springer.

Worbes, M., Herawati, H., Martius, C., 2017. Tree growth rings in tropical peat swamp forests of Kalimantan, Indonesia. Forests 8, 1–15.

Worbes, M., Raschke, N., 2012. Carbon allocation in a Costa Rican dry forest derived from tree ring analysis. Dendrochronologia 30 (3), 231-238.

Wu, M., Zhang, Y., Oya, T., Marcati, C. R., Pereira, L., Jansen, S., 2020. Root xylem in three woody angiosperm species is not more vulnerable to embolism than stem xylem.
Plant Soil 450, 479–495.

Wunsh, O., Calvo, G., Willsher, B., Seyfried H., 1999. Geologie der Alpinen Zone des Chirripó-Massives (Cordillera de Talamanca, Costa Rica, Mittlelamerika). Profil, 16, 193-210.

Yano, A., Shinohara, Y., Tsunetaka, H., Mizuno, H., Kubota, T., 2019. Distribution of landslides caused by heavy rainfall events and an earthquake in northern Aso Volcano, Japan from 1955 to 2016. Geomorphology 327, 533-541.

Yanosky, T.M., Jarrett, R.D., 2002. Dendrochronologic evidence for the frequency and magnitude of paleofloods. In: House PK, Webb RH, Baker VR, et al. (eds) Ancient Floods, Modern Hazards: Principles and applications of paleoflood hydrology, Water Science and Application vol. 5. Washington, DC: American Geophysical Union, pp. 77–89.

Zhang, S., Zhang, L.M., Glade, T., 2014. Characteristics of earthquake-and rain-induced landslides near the epicenter of Wenchuan earthquake. Eng. Geol. 175, 58-73.

Zhang, S., Zhang, L., Lacasse, S., Nadim, F., 2016. Evolution of mass movements near epicentre of Wenchuan Earthquake, the first eight years. Sci. Rep. 6, 1-9.

Zhao, Z., Oliver, E.C.J., Ballestero, D., Vargas-Hernández, J.M., Holbrook, N.J., 2019. Influence of the Madden–Julian oscillation on Costa Rican mid-summer drought timing. Int. J. Clim. 39 (1), 292–301.

Zhao, S., Pederson, N., D'Orangeville, L., HilleRisLambers, J., Boose, E., Penone, C., Bauer, B., Jiang, Y., Manzanedo, R.D., 2019. The International Tree-Ring Data Bank (ITRDB) revisited: Data availability and global ecological representativity. J. Biogeogr. 46 (2), 355-368.

Zhou, Y., Li, N., Wu, W., et al., 2014. Local spatial and temporal factors influencing population and societal vulnerability to natural disasters. Risk Anal. 34, 614–639.

Zhou, W., Jiao, M., Yu, W., Wang, J., 2019. Urban sprawl in a megaregion: A multiple spatial and temporal perspective. Ecol. Indic. 96, 54-66. https://doi.org/10.1016/j.ecolind.2017.10.035

Zielonka, T., Holeksa, J., Ciapała, S., 2008. A reconstruction of flood events using scarred trees in the Tatra Mountains, Poland. Dendrochronologia 26 (3), 173-183.

Zscheischler, J., Westra, S., Hurk, B.J., Seneviratne, S.I., Ward, P.J., Pitman, A., AghaKouchak, A., Bresh, D.N., Leonard, M., Wahl, T., Zhang, X., 2018. Future climate risk from compound events. Nat. Clim. Chan. 8, 469–477.

Zuidema, P.A., Brienen, R.J.W., Schöngart, J., 2012. Tropical forest warming: looking backwards for more insights. Trends Ecol. Evol. 27, 193–194.

ANNEX

Glacial geomorphology of the Chirripó National Park, Costa Rica

Adolfo Quesada-Román [a,b,] Juan Antonio Ballesteros-Cánovas [a,] Markus Stoffel [a,c,] José Juan Zamorano-Orozco [d]

[a] Climatic Change Impacts and Risks in the Anthropocene (C-CIA), Institute for Environmental Sciences, University of Geneva, Geneva, Switzerland
[b] Escuela de Geografía, Universidad de Costa Rica, San José, Costa Rica
[c] Department F.-A. Forel for Environmental and Aquatic Sciences, University of Geneva, Geneva, Switzerland
[d] Instituto de Geografía, Universidad Nacional Autónoma de México, Mexico City, Mexico

Journal of Maps 15 (2), 538–545. https://doi.org/10.1080/17445647.2019.1625822

Several regions of tropical America show imprints of past glacial activity. These relict landforms can support the understanding of past climate conditions, such as during the Last Glacial Maximum (LGM), and the implications that these paleoclimatic conditions could have had on landscape change. Here, we present and analyze glacial morphologies for the Chirripó National Park in Costa Rica based on aerial imagery (1:25,000), detailed Digital Elevation Models, geomorphic mapping, as well as geomorphic assessments in the field to determine and validate landforms. This study adds valuable insights into the reconstruction of the maximum expansion of tropical glaciation during the LGM in Costa Rica and into tropical America glacial landscapes in general.

1. Introduction

Past fluctuations of tropical glaciers provide important paleoclimate proxies for regions where other forms of evidence are generally scarce (Benn et al., 2005). During the Last Glacial Maximum (LGM), numerous valley glaciers advanced above 3000 m asl in the tropics of America, and more particularly in mountain regions of Mexico, Guatemala, Costa Rica, the Dominican Republic, and along the Andes (Mark et al., 2005; Vázquez-Selem and Lachniet, 2017) (Fig. 53).

Several past studies have focused on the description of Pleistocene and Quaternary glaciers in Costa Rica since the late 19th century when Henri Pittier described the presence of past glacial activity on the high peaks of the Cordillera de Talamanca (Castillo-Muñoz, 2010). More than half of a century later, Weyl (1955) used aerial photographs and field observations to document and explain the glacially molded landscape of Cerro Chirripó. Hastenrath (1973) mapped numerous glacier lakes and cirques at the top of Cordillera de Talamanca. Other studies such as those of Bergoeing (1977), Barquero and Ellenberg (1983), Shimizu (1992), and Wunsh et al. (1999) presented large-scale maps derived from aerial photographs to illustrate the glacial morphology of Cerro Chirripó. Lachniet and Seltzer (2002) and Lachniet et al. (2005) mapped large glacial extensions of late Pleistocene glaciers as well as some erosive and depositional morphologies of the glacial valleys in the surroundings of the Cerro Chirripó. These authors mapped 35 km^2 of the Cerro Chirripó area and mention that the local ELA (equilibrium line altitudes) was located at 3500 m asl. Nevertheless, they also suggested that in surrounding areas, the ELA may have descended to 3200 m asl. More recently, Quesada-Román and Zamorano-Orozco (2018a) described the glacial geomorphology of the Upper General River Basin, whereas, Li et al. (2019) mapped 22.1 km^2 of the surfaces with glacial remnants around Cerro Chirripó.

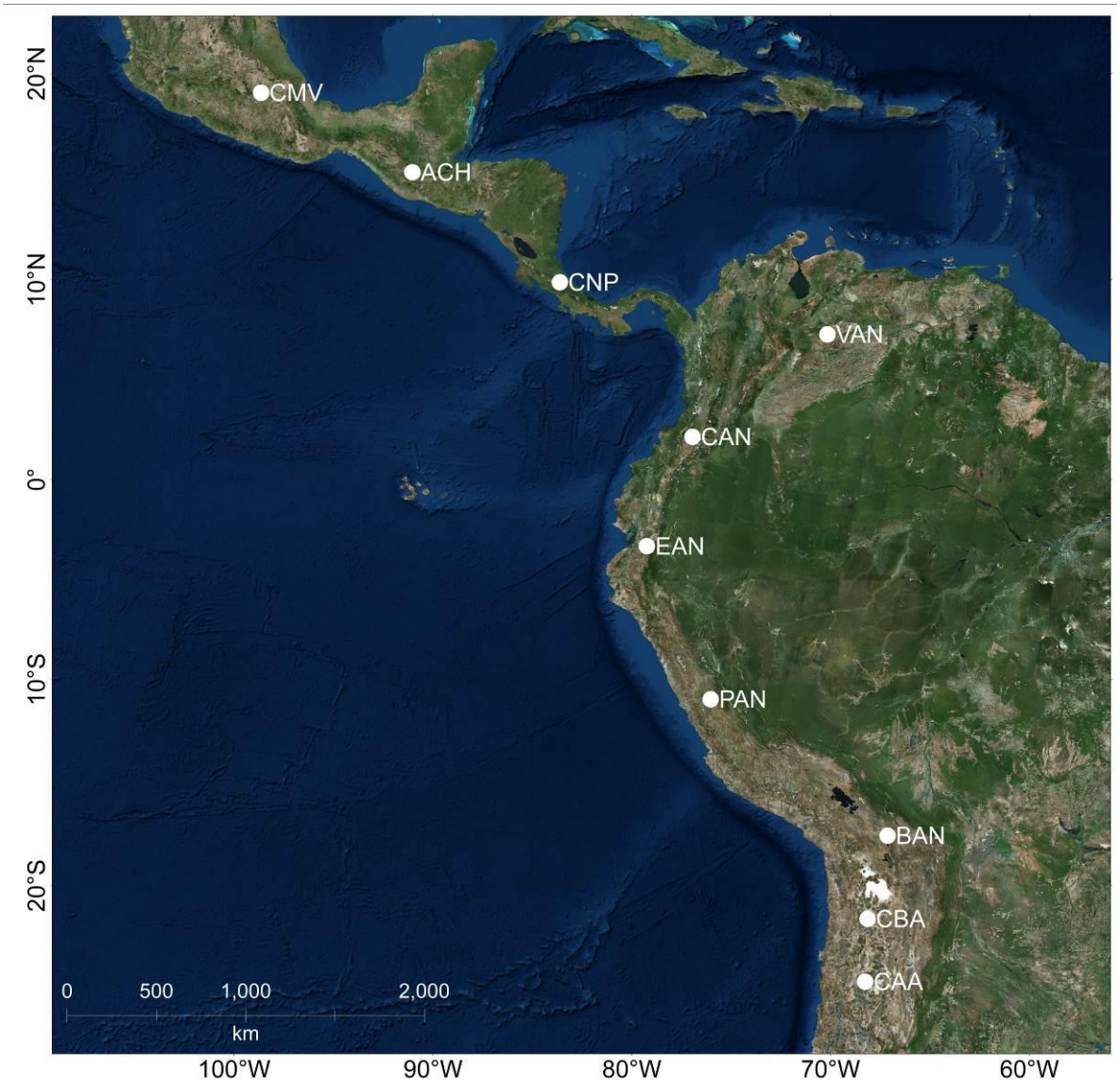

Fig. 53. Localization of glacial landscapes that have been determined in tropical America. CMV: Central Mexican Volcanoes; ACH: Altos de Cuchumatanes, Guatemala; CNP: Chirripó National Park (this study); CAN: Colombian Andes; VAN: Venezuelan Andes; EAN: Ecuadorian Andes; PAN: Peruvian Andes; BAN: Bolivian Andes; CBA: Chilean-Bolivian Andes, CAA: Chilean-Argentinian Andes (Modified from Porter, 2001; Mark et al., 2005; Hastenrath, 2009).

In recent decades, most studies focused on the dating of these glacial-like geomorphic features. For instance, Horn (1990) used charcoal and pollen analysis to determine the end of glacial dynamics in the largest lake of Valle de las Morrenas at ca. ~10 ka. Orvis and Horn (2000) concluded that deglaciation occurred between 12.36 ka and before 9.7 ka, which then ultimately ended at ca. 8,580 ± 70 BP. More recently, Potter et al. (2019) used ^{36}Cl, whereas Cunningham et al., (2019) utilized ^{10}Be cosmogenic nuclides to determine that the maximum glacial extension age in Chirripó National Park corresponds with the LGM (~26.5–19 ka). These novel studies agree with previous work that estimated ELA during the LGM were at 3500 m asl around Cerro Chirripó.

Despite the plethora of studies in the region, a detailed glacial geomorphic map for the entire protected area of the Chirripó National Park has not been realized so far, which therefore limits the understanding of the glacial extent and its dynamics during the LGM in one of the least studied regions of the world. In this study, we therefore aim at conducting a geomorphic mapping of the entire Chirripó National Park at a scale of 1: 25,000, with a focus on glacial erosion and deposition landforms, as a basis for further studies of this tropical mountain region and a better understanding of climatic implications of these paleo-landforms in a more regional context.

2. Materials and methods

2.1. Regional setting

The study area is located in the Cordillera de Talamanca, the most prominent mountain system in Central America extending 175 km from the central-southern portion of Costa Rica to the eastern sector of Panama (Marshall, 2007). The Chirripó National Park, established on 19 August 1975, is located in the central part of the Cordillera de Talamanca (Fig. 54).

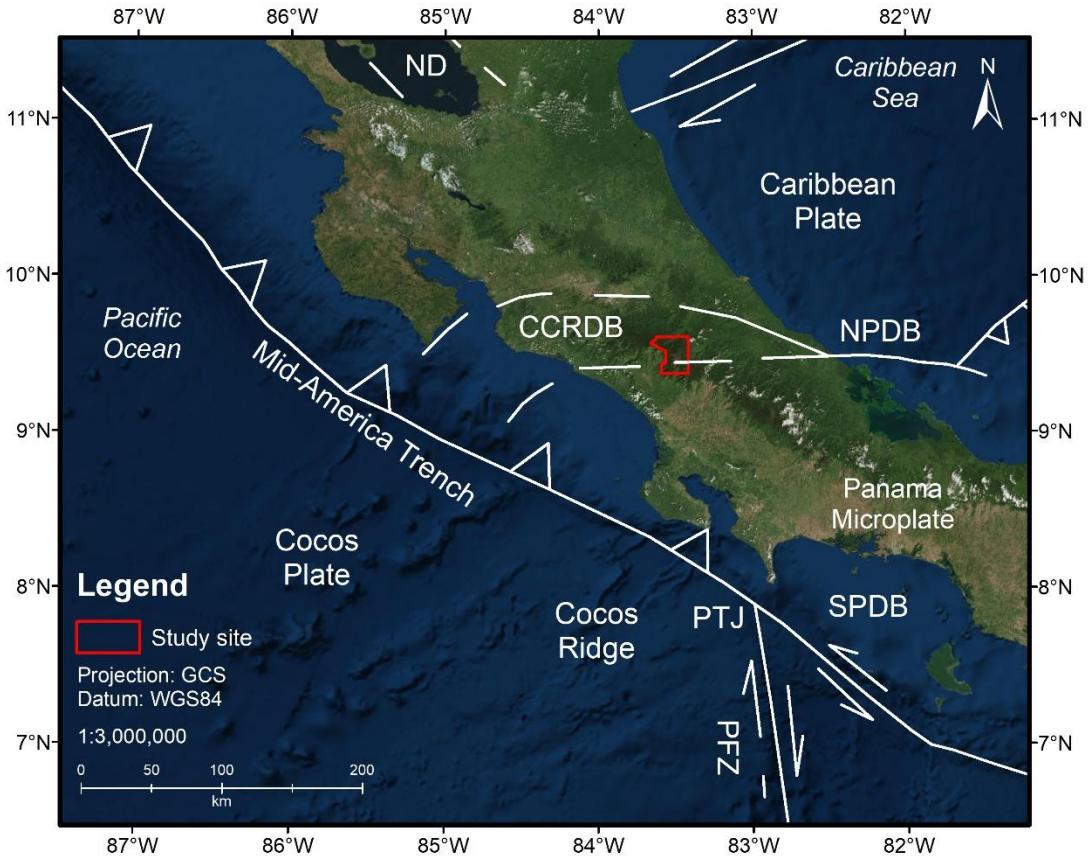

Fig. 54. Location of the Chirripó National Park in a regional tectonic context. ND: Nicaragua Depression; CCRDB: Central Costa Rica Deformed Belt; NPDB: North Panama Depression Belt; SPDB: South Panama Depression Belt; PFZ: Panama Fracture Zone; PTJ: Point Triple Junction (for details see DeMets et al., 2010).

The landscape of the study area is the result of the subduction processes between the Cocos and Caribbean plates, which has implications in terms of regional volcanism and seismicity (DeMets et al., 2010; Alvarado et al., 2017). In SE Costa Rica, the collision of the Cocos Ridge, a sequence of an oceanic crust growth from the Galapagos hotspot, stopped volcanism in the Cordillera de Talamanca some 2 Ma ago (Dzierma et al., 2011; Morellet al., 2012). Consequently, this region has experienced high uplift rates ranging from 1.7 to 8.5 m kyr^{-1} (Gardner et al., 2013). Geology of the national park includes andesitic volcanic rocks of Upper Miocene volcanism (17-11 Ma), granodioritic plutonic rocks of the Mid-Upper Miocene (12.5 – 7.5 Ma), and plutonic alkaline rocks of post-intrusive magmatic pulses from 5 to 2 Ma (Alfaro et al., 2018). Two faulting systems control Chirripó National Park, the first one consists of reverse component faults with NW heading; the second contains sinestral heading displacement faults, towards the NE (Alfaro et al., 2018). Vegetation in the national park includes different types of mountainous forests and peatlands. At elevations exceeding 3000 m, páramo landscapes prevail, a grassy or shrub-dominated ecosystem typical of cool and wet upper hills of tropical mountains, above the tree line (Kappelle and Horn, 2016). Along these landscapes in the higher mountains of Costa Rica, hundreds of palustrine and lacustrine wetlands deliver paramount hydrological and ecological functions (Esquivel-Hernández et al., 2018, Veaset al., 2018; Esquivel-Hernández et al., 2019).

Local climate is controlled by northeastern trade winds, the latitudinal migration of the Intertropical Convergence Zone, cold fronts, and the seasonal influence of Caribbean tropical cyclones (Alfaro et al., 2010; Campos-Durán and Quesada-Román, 2017; Quesada-Román, 2017). These circulation processes produce two rainfall maxima, one in May and one in October, which are interrupted by a relative minimum between July and August known as the Mid-Summer Drought (Zhao et al., 2019). Along these mountains, the active regional and local tectonics, in addition to intense rainfall, favor the occurrence of landslides (Quesada-Román and Zamorano, 2018b).

2.2. Geomorphological mapping

The Main Map (see Supplemental Material in: https://doi.org/10.1080/17445647.2019.1625822) was realized in three phases beginning with pre-mapping aerial photo interpretation (API) followed by fieldwork and finishing with GIS post-mapping (Smith et al., 2011; Chandler et al., 2018). During pre-mapping, the morphogenetic map was generated based on aerial photo interpretation at a 1:25,000 scale from the CARTA project (Costa Rica Airborne Research and Technology Applications), a NASA mission which mapped Costa Rica between 2003 and 2005 (CARTA, 2005). These aerial photographs were georeferenced and processed to accomplish the geomorphic mapping. The method allowed to map the genesis, dynamics, morphology, evolution, and age of the different erosional and depositional glacial landforms (Verstappen et al., 1991) and digital graphic techniques to develop the final cartographic product (Bishop et al., Walsh, 2012). The fieldwork was conducted during four ground truthing missions in July 2016, July 2017, and January 2018 to verify the different landforms dynamics and limits using a preliminary morphogenetic map at a 1:25,000 scale. During the final stage of the post-mapping, the legend and the color election for each landform were genetically chosen (Gustavsson et al., 2006). Finally, the map was edited within a Geographic Information System (ArcGIS 10.3).

3. Results and discussion

3.1. Glacial erosional landforms

The movement of ice masses molded the landscapes in the higher summits of the Cordillera de Talamanca, leaving rounded hills. These surfaces sum 29.7 km^2 over 3500 m asl. We distinguish two types of volcanic slopes modified by glacial action, namely (i) subhorizontal surfaces in the lowest parts of glacial valleys and on mountaintops with slopes <15°, and (ii) edges of the continental divide with steeper morphologies and slope angles of up to 36°. The latter morphologies correspond with the exposed rocky terrains where glaciers left characteristic scars, p-forms, and striations. One such landscape can be found on Cerro Chirripó, the highest peak of Costa Rica with 3820 m asl (Fig. 55a). The different dating procedures applied around Cerro Chirripó indicate that ELA during the LGM were never lower than 3500 m asl.

The volcanic slopes molded by periglacial action represent extensive surfaces located around the glacial molded hillslopes. According to Orvis and Horn (2000) and Lachniet and Seltzer (2002), ~9 °C below present temperatures prevailed during the LGM on the summits of Chirripó National Park. These slopes were presumably affected weathering, frost action, mass movement, nivation, and frozen ground. Periglacial dynamics affected 51.6 km^2 of the area during the LGM or previous glaciations that could not be determined by radiometric dating so far. These surfaces are, however, rarely are located below 3000 m asl. Along these surfaces, rocky terrains are dominant with random presence of whalebacks, striations, p-forms, and scars. Both glacial and periglacial volcanic slopes sum 91 km^2, nowadays covered by páramo vegetation.

Cirques, by contrast, are defined by their amphitheater-like morphology induced by glacial abrasion on those slopes located close to the peaks (Fig. 55b). Cirques alignment have a clear tectonic control by local faulting with NW and NE orientation. The concave geometry is the result of LGM ice pressure on Miocene plutonic rocks and the resultant abrasion of bedrock; frost action and hillslope processes have molded these landforms ever since as Cerro Urán. In Chirripó National Park, two types of cirques can be found, namely continuous and discontinuous cirques. Continuous cirques are limited in extent, occupy small areas (individually), and are elongated or in the shape of arcs. Continuous cirques are well preserved, either because of their recent age or as a result of their altitudinal position. Continuous cirques tend to persist in the landscapes because of a lack of fluvial energy; therefore, they can be recognized without difficulty in the field. Continuous cirques developed between 3500 and 3820 m asl, with a clear majority located on the Caribbean side, probably because rainfall is smaller as compared to the Pacific side (3500 mm/year), which allowed preservation of this type of relief as Cerro Chirripó Grande.

Discontinuous cirques are arcs (typically “boomerang-shaped”) with concave slope geometries. These cirques contain well-developed fluvial systems and significant post-LGM fluvial erosion. The extent to which fluvial erosion has acted explains the discontinuity of these cirques. The fluvial headwaters and their tributaries have reached the basin divides and therefore interrupted or eroded the glacial cirques. Discontinuous cirques are much frequent on the Pacific slope where rainfall exceeds 5000 mm annually as the division between Valle de los Conejos and Laguna Ditkevi. This precipitation regime exacerbates erosion and dismantles original landforms. The position of discontinuous cirques varies from 3450 to 3820 m asl.

Arêtes form when glacial erosion acts on two adjacent cirques, thus resulting in a narrow and sinuous crest, usually constituted by fresh, exposed bedrock with a convex shape or debris. Their existence depends on glacial activity in the first place, but also on bedrock competence (Fig. 55c). At the study site, arêtes can be found at the continental divide and on the Caribbean side of the divide at elevations ranging from 3320 to 3780 m asl, typically on flat (<15°) summits of the Cordillera de Talamanca. Arêtes with sharp (rocky) geometry can, by contrast, be found in positions where two or more peaks join. Vegetation is generally absent on sharp geometry (rocky) arêtes, and this morphology is located on the highest elevations of the national park. Arêtes represent 35 units with variable areas ranging from 2793 to 135028 m^2; over 2840 m asl.

Riegels are large rock barriers sitting across a valley and are usually formed by resistant rock outcrops. In some cases, riegels create natural dams of lakes. They represent broad steps and are slightly inclined. A good example is Laguna Ditkevi, a glacial lake blocked by a riegel shaped by glacial abrasion (Fig. 55d). Glacial valleys are found in riegels and characterized by their steep slope surfaces with a transition toward semi-plane reliefs with inclinations below 15°. The altitude of the riegels varies between 3000 and 3520 m asl and a total of 7 units were recorded in this study, four on the Caribbean and three on the Pacific slope.

Roches moutonnées are present in the valley bottoms, as traces of glacial abrasion that can be found in the form of striations, p-forms, scars and steps. One such example of roches moutonnées is Cerro Terbi with 0.32 km^2 (Fig. 55e). A total of 18 roches moutonnées units (occupied by glacial lakes at present) could be found in Chirripó National Park at altitudes ranging from 3320 to 3680 m asl. These landforms are found on slopes <25° and are located mostly on the Caribbean side, within Miocene plutonic bedrock.

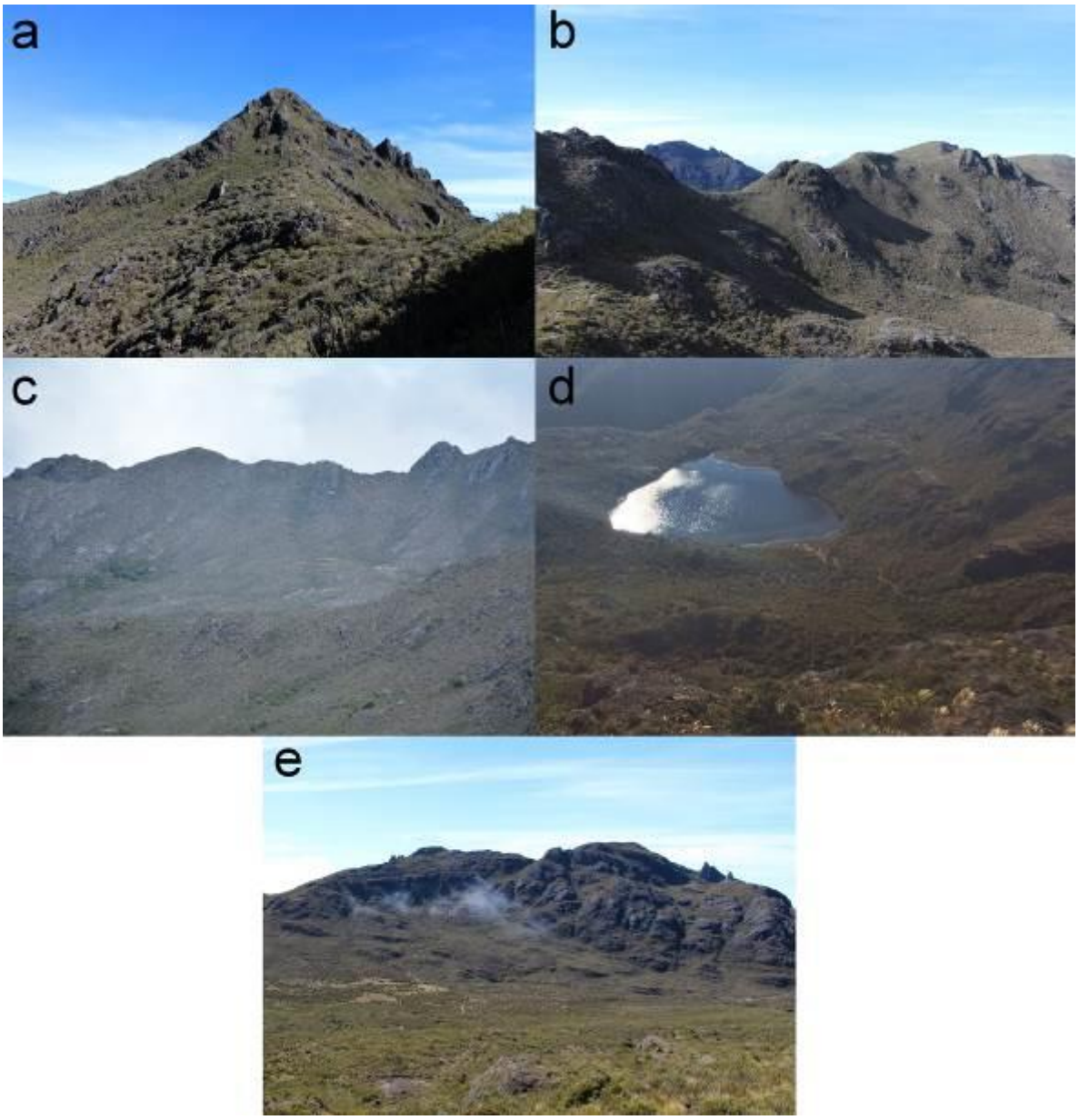

Fig. 55. Glacial erosional landforms: a. Volcanic slopes modified by glacial action (Cerro Chirripó); b. Glacial cirques; c. Arêtes; d. Riegels (Laguna Ditkevi); e. Roches moutonnées (Cerro Terbi).

3.2. Glacial depositional landforms

Morphologies issued by the accumulation of glacial sediments at Chirripó National Park include moraines, till deposits, and glacial lakes. These forms are usually situated on convex slopes with ridge morphologies. Some of these depositional landforms are rather ephemeral, whereas others are also well defined with considerable widths and lengths, especially in the case of lateral moraines.

Lateral moraines are found at the margins of glacial valleys; a vast majority (76%) of these moraines are on the Caribbean slopes (32 of 42). This finding is most likely related to the smaller rainfall totals on the Caribbean side of the summits, which has resulted in less erosion over time and in the preservation of moraines. The best preserved and most obvious moraine is the Valle Talari moraine with a length of 655 m and a width of 70 m (Fig. 56a). In general terms, lateral moraines are located between 3140 and 3660 m asl and occur on slopes ranging from 8° to 35°. Various studies recognized the presence of lateral moraines in Chirripó National Park (Weyl, 1955; Hastenrath, 1973; Orvis & Horn, 2000; Lachniet & Seltzer, 2002; Bergoeing 2017), but with much less detail due to the 1:40,000 or even less detailed aerial photos examined.

Till deposits often consist of poorly sorted debris without stratification, thus pointing to sediment bodies that have lost their original morphology. Indeed, material is arranged as a mantle in the valley bottoms that currently without defined morphology, or with a significant process of dismantling as in Valle d las Morrenas (Fig. 56b) or Valle de los Conejos (Fig. 56c). By contrast, the position within the glacial cirque supports the hypothesis that the small bodies of water found in these poorly distinct environments are indeed relict glacial lakes originating from the impoundment of glacier meltdown waters. A total of 15 till deposits have been identified in the glacial valley bottoms with slopes below 25° at elevations between 3100 to 3600 m asl.

The glacial lakes are interpreted as kettle ponds, cirque lakes, paternoster lakes, or ice-marginal lakes. They originate from glacial scouring processes leaving transversal depressions in the parent material. Twenty-one of these lakes are identified between 3480 and 3660 m asl, in areas with slopes <10° like in Valle de las Morrenas, Lago Chirripó (Fig. 56d), and Laguna Ditkevi. Horn et al. (2005) identified 19 glacial lakes (of which 17 match with the lakes mapped in our work), but with the objective to determine their physical and chemical conditions. Horn and Haberyan (2016) reported about 30 glacial lakes that occupied glacially molded surfaces of the Chirripó National Park.

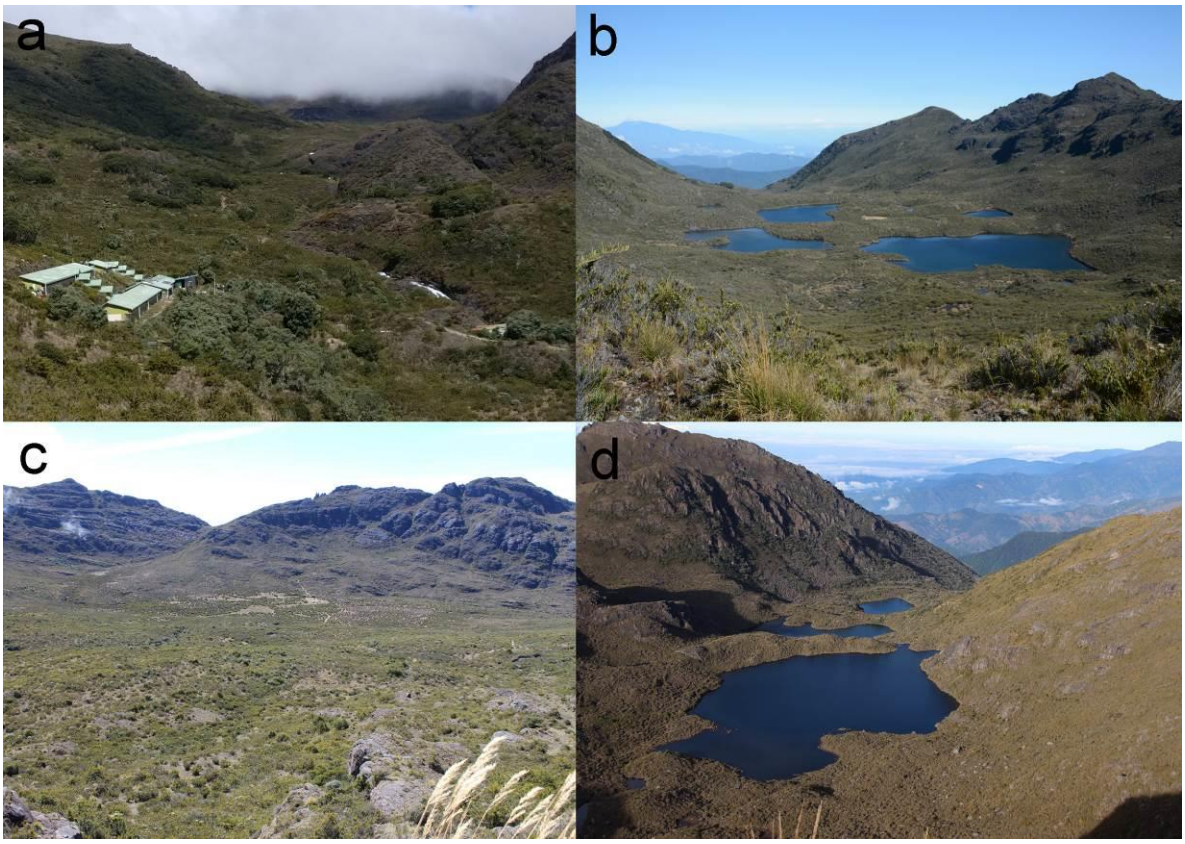

Fig. 56. Glacial depositional landforms: a. Lateral moraines (Valle Talari moraine ridge in the right); b. Till deposits (Valle de las Morrenas); c. Till deposits (Valle de los Conejos); d. Glacial lakes (Lago Chirripó).

4. Conclusions

Different studies of the glacial geomorphology of the Chirripó National Park and surrounding areas have been developed since the 1950s but this study gives, for the first time, a mapped area of ~90 km^2 with detailed information (1:25,000 scale) of glacial and/or periglacial landscapes of the highest summits of Costa Rica was made. The present work also provides a geomorphic analysis of seven erosional landforms (volcanic slopes modified by glacial action and periglacial action, glacial cirques, arêtes, riegels, and roches moutonnées) and three depositional landforms (lateral moraines, till deposits, and glacial lakes). The Main Map (see Supplemental Material in: https://doi.org/10.1080/17445647.2019.1625822) provides new insights into LGM activity in tropical high altitude landscapes of Costa Rica and can also serve as a base map for geographical, ecological, hydrological, climatological and geoheritage studies.